STUDIA UNIVERSITATIS
BABEŞ-BOLYAI

UNIVERSITATEA BABEŞ-BOLYAI
BABEŞ-BOLYAI TUDOMÁNYEGYETEM
BABEŞ-BOLYAI UNIVERSITÄT
BABEŞ-BOLYAI UNIVERSITY
TRADITIO ET EXCELLENTIA

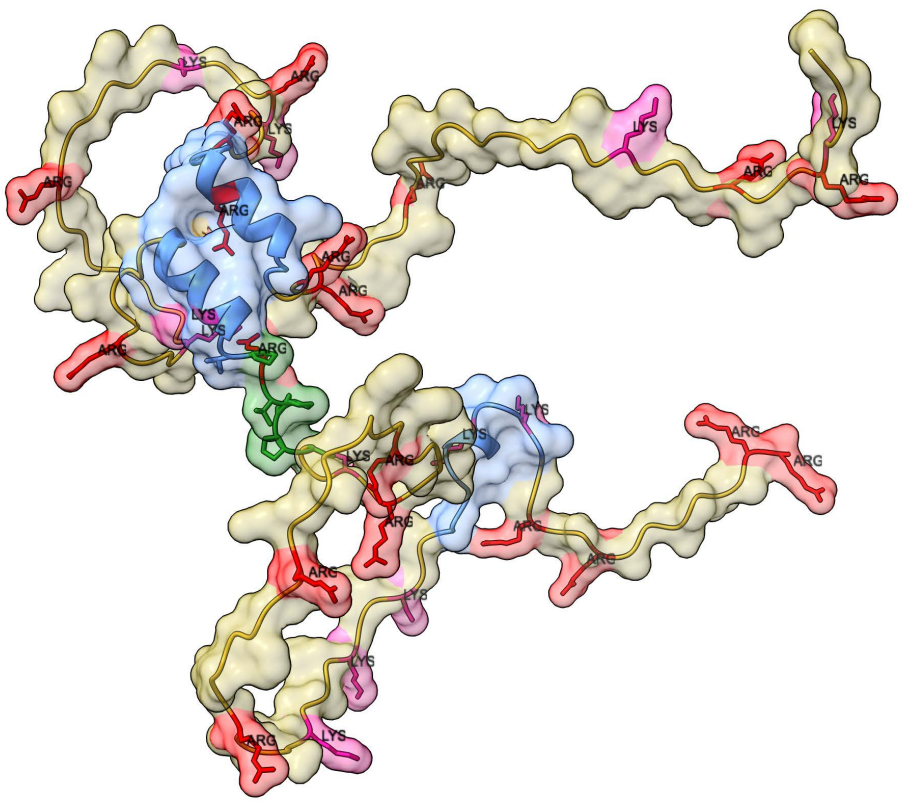

BIOLOGIA

Volume 70 (2025), December, No. 2/2025

STUDIA
UNIVERSITATIS BABEŞ-BOLYAI
BIOLOGIA

2 / 2025
July - December

EDITORIAL BOARD
STUDIA UNIVERSITATIS BABEŞ-BOLYAI BIOLOGIA

YEAR **Volume 70 (LXX), 2025**
MONTH **DECEMBER**
ISSUE **2**

PUBLISHED ONLINE: 2025-12-20
ISSUE DOI: 10.24193/subbbiol.2025.2
ISSN (online): 2065-9512
https://studiabiologia.reviste.ubbcluj.ro/

STUDIA UNIVERSITATIS BABEŞ-BOLYAI

BIOLOGIA

2

SUMAR – CONTENT – SOMMAIRE – INHALT

All authors are responsible for submitting manuscripts in comprehensible US or UK English and ensuring scientific accuracy.

Original picture on front cover: The three-dimensional structure of human myelin basic protein (MBP; UniProt reference: P02686-3), predicted by AlphaFold (AF-P02686-F1-model_v4; https://alphafold.ebi.ac.uk/entry/P02686), and visualized using ChimeraX. The membrane-binding α-helices (α1–α3) are highlighted in blue, arginine residues in red, lysine residues in purple, and the SH3 domain in green. ©Ferencz Kósa

STUDIA UNIVERSITATIS BABEŞ-BOLYAI BIOLOGIA, 70, 2, 2025 (p. 5-13)
doi:10.24193/subbbiol.2025.2.01

Genetic variation of *Lissotriton montandoni* from the eastern part of the Slovak Carpathians

Daniel Mihálik[1,2], Milan Haviar[3], Katarína Ondreičková[1], Marián Janiga[3] and Ján Kraic[1,2,*]

[1]*National Agricultural and Food Center, Research Institute of Plant Production, Bratislavská cesta 122, 92168 Piešťany, Slovakia;*
[2]*University of Ss. Cyril and Methodius in Trnava, Faculty of Natural Sciences, Department of Biotechnology, Nám. J. Herdu 2, 91701 Trnava, Slovakia;*
[3]*University of Žilina, Institute of High Mountain Biology, 05956 Tatranská Javorina 7, Slovakia*
[*] ***Corresponding author, E-mail: jan.kraic@ucm.sk.***

Article history: Received 25 April 2025; Revised 25 August 2025; Accepted 25 August 2025; Available online 20 December 2025

Abstract. This study investigated the extent of genetic variation in *Lissotriton montandoni* individuals collected from three locations in the eastern Slovak Carpathians using microsatellite DNA markers. The genetic characteristics of these microsatellite loci were confirmed to be suitable for molecular genetic studies in *L. montandoni*, as indicated by high polymorphic information content values. Furthermore, a high level of genetic variation was detected in this endemic species of amphibian. The fixation index values suggested minimal differentiation among the three analyzed subpopulations, with only 1% of the total genetic variation occurring between subpopulations, 3% between individuals, and 96% within individuals. The presence of a high number of alleles at the same chromosomal loci contributes to genetic variation across the entire population, which is beneficial and essential for the adaptation of both individuals and the population as a whole to current and future environmental changes.

Keywords: Carpathian Newt, Eastern Carpathians, genetic diversity, microsatellite

Introduction

Genetic diversity is a key component of biodiversity playing a fundamental role in the long-term survival and adaptability of species and in maintaining healthy populations and ecosystems. It is defined as the variation in genes within and between populations of a given species. Diversity needs to be recognised, and its extent and trends described. One of the species for which such a study is necessary is *Lissotriton montandoni* (Boulenger 1880), commonly known as the Carpathian Newt. This species is an endemic amphibian species of the Eastern Carpathians and the easternmost Sudetes. It is found in the Czech Republic, Poland, Romania, Slovakia, and Ukraine and is listed in the International Union for Conservation of Nature (IUCN) Red List of Threatened Species. *L. montandoni* is here classified as "least concern", indicating a stable population and low risk of extinction. However, this does not diminish its conservation importance within the European Union (EU). Under EU legislation, *L. montandoni* is listed in Annex IV of the Habitats Directive (92/43/EEC), which identifies animal and plant species of community interest in need of strict protection. This listing mandates that EU member states implement measures to conserve the species and its habitats. Additionally, the species is included in the Natura 2000 network, a network of protected areas across the EU aimed at conserving biodiversity. The primary regions of its distribution and genetic diversity has been documented in Romania and Ukraine (Zieliński *et al.*, 2014). Genetic variation within populations is crucial for the adaptation of individuals and the survival of the whole population in response to current and upcoming environmental changes. A higher level of genetic variation enhances a population's adaptive capacity. This variation is assessed not only through phenotypic traits but also through genomic diversity in both coding and non-coding DNA sequences. An increasing number of different alleles at the same chromosomal locus contributes to greater genetic variation within the population. In *L. montandoni*, genetic variation is further influenced by sympatry with *Lissotriton vulgaris*. These two species can interbreed, forming hybrids in areas where their ranges overlap (Kotlík and Zavadil, 1999; Gherghel *et al.*, 2012). The assessment of the extent of genetic variation requires highly informative genetic markers, such as microsatellite markers. Previous studies have documented allelic diversity at microsatellite nuclear DNA loci in *L. montandoni* (Johanet *et al.*, 2009; Zieliński *et al.*, 2013). However, the populations of *L. montandoni* in the northwestern Carpathians of Slovakia remains poorly studied. So far, only two populations have been compared from Slovakia, and even then only based on a few morphological features of the newt (Kniha *et al.*, 2013). A study that analyzed the genetic variation in *L. montandoni* populations, also by application of DNA analyses, has not been carried out in Slovakia to date.

The aim of this study was therefore to use specific microsatellite markers to analyze genetic variation within and between subpopulations of this amphibian in areas known to be its habitat.

Materials and methods

Samples of Carpathian newt were collected in two locations of the Eastern Tatras (Tatranská Javorina and Tatranská Kotlina) and one from the Poloniny National Park (Fig. 1).

Figure 1. Sampling localities of *L. montandoni* (red diamonds). Two on the top – Tatranská Javorina and Tatranská Kotlina, one on the right side – Poloniny.

Genomic DNA was extracted from tail samples (1 mm^2) using the Wizard® SV Genomic DNA Purification System (Promega Corp., Madison, USA). The sample sizes were as follows: five individuals from Tatranská Javorina, three from Tatranská Kotlina, and seventeen from Poloniny. Microsatellite loci (Lm_488, Lm_521, Lm_528, Lm_632, Lm_749, and Lm_870) were amplified using primer pairs developed by Nadachowska *et al.* (2010). Forward primers were fluorescently labelled at the 5' end with ATTO550, ATTO565, FAM, or HEX. Polymerase chain reactions (PCR) were performed in 20 µl volumes containing 50 ng of DNA, 10 pmol $µl^{-1}$ of both primers, 10 mM dNTPs, 4 µl of Q-solution (Qiagen N.V., Venlo, The Netherlands), 2 µl of 10x PCR buffer, 2 mM MgCl2, 1 U of HotStar Taq DNA polymerase (Qiagen N.V., Venlo, The Netherlands), and

water to the final volume. The thermal cycling profile of the PCR consisted of an initial denaturation at 95 °C for 15 min, followed by 29 cycles of 94 °C for 30 s, 55 °C (for Lm_521, Lm_528, Lm_632, Lm_749) or 57 °C (for Lm_488, Lm_870) for 60 s. This was followed by a final extension step was performed at 72 °C for 90 s. Subsequently, the PCR products were analyzed by capillary electrophoresis using the automated ABI PRISM® 3100-Avant Genetic Analyzer (Applied Biosystems, Waltham, USA). The fragment sizes were determined using the GeneMapper™ software (Thermo Fisher Scientific, Waltham, USA). The polymorphic information content (PIC) was calculated using Cervus software version 3.0.7 (Kalinowski *et al.*, 2007). The genetic parameters evaluated included the number of alleles per locus (N_a), the number of effective alleles per locus (N_e), observed heterozygosity, expected heterozygosity, and the fixation index (F_{ST}). These were analyzed using GenAIEx v 6.5 software (Peakall and Smouse, 2012). Cluster analysis was conducted using two-way visualisation with UPGMA clustering and Bray-Curtis similarity in Past 4.17c (Hammer *et al.*, 2001).

Results

The first part of the results presents the parameters of the microsatellite markers (loci) used to assess genetic variation in the collected *L. montandoni* samples (Tab. 1).

Table 1. Genetic parameters of six microsatellite loci analyzed.

Locus	N	N_a	N_e	H_o	H_e	F_{ST}	PIC	I
Lm521	25	16	12.500	0.960	0.920	-0.043	0.914	2.637
Lm528	25	12	7.440	0.920	0.866	-0.063	0.854	2.249
Lm749	25	10	4.613	0.640	0.783	0.183	0.759	1.819
Lm632	25	8	4.223	0.840	0.763	-0.101	0.732	1.675
Lm488	23	10	5.038	0.652	0.802	0.186	0.782	1.920
Lm870	25	11	6.906	0.960	0.855	-0.123	0.840	2.111

(N) number of samples; (N_a) number of alleles; (N_e) number of effective alleles; (H_o) observed heterozygosity; (H_e) expected heterozygosity; (F_{ST}) fixation index; (PIC) polymorphic information content; (I) Shannon's information index.

A total of 67 alleles (8-16 per locus) were identified across 25 individuals from the three sampling sites. The number of effective alleles per locus ranged from 4.220 to 12.500, with the highest values at locus Lm521 (16 alleles and 12.50 effective alleles). Expected heterozygosity ranged from 0.763 to 0.920, while observed heterozygosity varied from 0.640 to 0.960. The PIC values

ranged from 0.732 to 0.914 and Shannon's information index (1.675-2.637) indicate the informativeness and high genetic diversity of the microsatellite markers used in this study for analyzing genetic variation. Additionally, these findings underscore a substantial degree of genetic diversity in *L. montandoni*, even when considering the relatively modest sample size from the three Slovakian locations.

The second part of the results compares the genetic variation of *L. montandoni* across the three study locations (Tab. 2).

Table 2. Genetic parameters of analyzed populations of *L. montandoni* from three locations.

Location	Locus	N	N_a	N_e	H_o	H_e	F_{ST}	I
Poloniny	Lm521	17	15.000	11.796	0.941	0.915	-0.028	2.581
	Lm528	17	11.000	7.225	0.941	0.862	-0.092	2.190
	Lm749	17	8.000	4.158	0.529	0.760	0.303	1.693
	Lm632	17	7.000	4.379	0.882	0.772	-0.143	1.658
	Lm488	15	8.000	4.412	0.600	0.773	0.224	1.752
	Lm870	17	9.000	6.568	0.941	0.848	-0.110	2.003
Tatranská Kotlina	Lm521	3	4.000	3.600	1.000	0.722	-0.385	1.330
	Lm528	3	5.000	4.500	1.000	0.778	-0.286	1.561
	Lm749	3	3.000	2.571	0.667	0.611	-0.091	1.011
	Lm632	3	3.000	2.000	0.667	0.500	-0.333	0.868
	Lm488	3	3.000	2.571	0.333	0.611	0.455	1.011
	Lm870	3	5.000	4.500	1.000	0.778	-0.286	1.561
Tatranská Javorina	Lm521	5	7.000	6.250	1.000	0.840	-0.190	1.887
	Lm528	5	6.000	4.167	0.800	0.760	-0.053	1.609
	Lm749	5	5.000	3.125	1.000	0.680	-0.471	1.359
	Lm632	5	6.000	3.333	0.800	0.700	-0.143	1.498
	Lm488	5	7.000	6.250	1.000	0.840	-0.190	1.887
	Lm870	5	7.000	5.556	1.000	0.820	-0.220	1.834

(N) number of samples; (N_a) number of alleles; (N_e) number of effective alleles; (H_o) observed heterozygosity; (H_e) expected heterozygosity; (F_{ST}) fixation index; (I) Shannon's information index.

The mean number of alleles and the number of effective alleles per individual was 16.67 (N_a) and 6.42 (N_e) in Poloniny, 6.33 (N_a) and 4.78 (N_e) in Tatranská Javorina, and 3.83 (N_a) and 3.29 (N_e) in Tatranská Kotlina. The mean expected heterozygosity and observed heterozygosity were 0.822 (H_e) and

0.806 (H_o) in Poloniny, 0.667 (H_e) and 0.778 (H_o) in Tatranská Kotlina, and 0.773 (H_e) and 0.933 (H_o) in Tatranská Javorina. The fixation index (F_{ST}) values ranged from 0.00 to 0.455, indicating minimal differentiation among the three subpopulations and suggesting a high degree of genetic similarity. The analysis of molecular variation revealed that only 1% of the total genetic variation was observed among subpopulations, 3% among individuals, and a significant 96% was within individuals.

The cluster analysis (Fig. 2) generated three key outcomes. Firstly, the *L. montandoni* exhibited a high level of genetic variation, as evidenced by the fact that no two individuals shared an identical microsatellite profile. Secondly, the absence of significant differentiation among the three subpopulations suggests a high degree of genetic overlap among individuals from all three localities (Fig. 2). The relative short geographical distances between the collection sites (approximately 170 kilometers apart by air) do not appear to be sufficient for genetic differentiation. In contrast, differentiation between "southern" and "northern" populations of *L. montandoni* has only been observed when analyzing individuals from localities spanning the entire Carpathian arc, which extends up to approximately 1,000 kilometers (Zieliński *et al.*, 2014). Thirdly, two individuals from Poloniny (marked in red diamond on the right side of Fig. 1) were genetically distinct from all others. This distinction is attributed to the presence of null alleles at the Lm488 locus in a homozygous state.

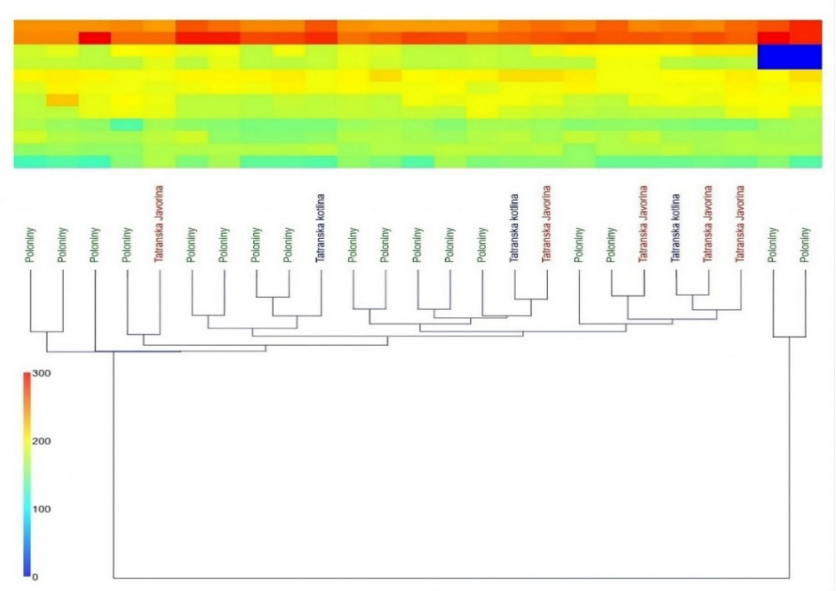

Figure 2. Differentiation of *L. montandoni* individuals and subpopulations by UPGMA clustering.

Discussion

The microsatellite markers used in this study confirmed their effectiveness in detecting high genetic variation in *L. montandoni* populations. The number of alleles per locus (8 – 16) observed in the three studied subpopulations from a relatively small area of the Slovak Eastern Carpathians was comparable to the findings of Nadachowska *et al.* (2010), who analyzed the same microsatellite loci in populations from two geographically distant locations (approximately 540 kilometers apart by air), one in Poland and the other in Romania. However, the Slovak subpopulations exhibited higher observed heterozygosity (H_o) values, ranging from 0.64 to 0.96, compared to 0.20 to 0.87 in the earlier study.

The contrasting mean number of alleles (N_a) and effective alleles (N_e) per individual across the three locations is intriguing. Poloniny displayed considerably lower values compared to Tatranská Javorina and Tatranská Kotlina. This may suggest historical demographic factors, population bottlenecks, or varying levels of gene flow affecting the Poloniny population. Although F_{ST} values indicate minimal differentiation, the slightly higher expected and observed heterozygosity (H_e and H_o) values in Poloniny compared to Tatranská Kotlina are noteworthy, especially considering the lower overall number of alleles. This could reflect a more even allele distribution in Poloniny population, despite reduced overall diversity. The findings that 96% of the genetic variation occurs within individuals underscores the high level of individual genetic diversity in *L. montandoni* across the Slovak populations. This support the idea of significant gene flow or a recent common ancestry among the populations. Additionally, the fact that no two individuals share identical microsatellite profile further emphasized the genetic richness present in this relatively small sample size, allowing insight into the genetic structure of the species in this region.

Of particular interest is the identification of two individuals from Poloniny that were genetically distinct from all others due to homozygosity for null alleles at the Lm488 locus. This highlights the potential impact of technical artifacts, such as null alleles, on genetic analyses and underscores the importance of accounting for such factors during data interpretation.

The absence of clear clustering by sampling site (Figure 2) visually supports the low F_{ST} values and the high degree of genetic overlap among the subpopulations. The relatively short geographical distance (170 km) between the study sites appears insufficient to drive significant genetic differentiation, at least based on the resolution provided by microsatellite markers. A comparison with broader-scale studies, such asthat by Zieliński *et al.* (2014) across the Carpathian arc, provides useful context and suggests that geographical range becomes a more significant barrier to gene flow only over larger spatial scales.

This study provides foundational insights into the genetic diversity and population structure of *Lissotriton montandoni* in three Slovak localities. However, a significant limitation is the very small sample size from the Poloniny population (n = 3), which may reduce the reliability of estimates for allelic diversity and population structure at this site. Small sample sizes can increase the likelihood of sampling bias, underestimate genetic variation, and limit the ability to detect rare alleles. Consequently, the observed lower allelic diversity in Poloniny should be interpreted with caution. Adequate sample size is important in genetic analyses. Although small sample sizes may be considered low for some population genetic analyses, maximizing the number of markers may be beneficial for robust landscape genetic inferences in *L. vulgaris* populations (Zieliński *et al.*, 2014) or observed strenght of spatial genetic patterns (Landguth *et al.*, 2011). Despite this limitation, the dataset offers valuable baseline information that can inform future conservation strategies and serve as a reference for comparative studies across the species' range. Overall, the current study highlights important directions for continued investigation into the population genetics of *L. montandoni* and underscores the need for comprehensive sampling across its distribution.

Conclusions

The study yielded results indicating a high degree of genetic diversity within *L. montandoni* subpopulations from Slovakia and revealed minimal genetic structuring among the three sampled sites. These results have important implications for conservation strategies, suggesting that even relatively small populations can harbor considerable genetic resources and emphasizing the importance of maintaining connectivity among habitats to preserve this diversity.

References

Gherghel, I., Strugariu, A., Ambrosă, I.-M. & Zamfirescu, Ş.R. (2012). Updated distribution of hybrids between *Lissotriton vulgaris* and *Lissotriton montandoni* (Amphibia: Caudata: Salamandridae) in Romania. *Acta Herpetol.* 7, 49-55. https://doi.org/10.13128/Acta_Herpetol-10224

Hammer, Ø., Harper, D.A.T. & Ryan, P.D. (2001). PAST: Paleontological Statistics Software Package for education and data analysis. *Palaeontol. Electron.* 4, 1-9.

Johanet, A., Picard, D., Garner, T.W.J., Dawson, D.A., Morales-Hojas, R., Jehle, R., Peltier, D. & Lemaire, C. (2009). Characterization of microsatellite loci in two closely related *Lissotriton* newt species. *Conserv. Genet.* 10, 1903-1906. https://doi.org/10.1007/s10592-009-9850-z

Kalinowski, S.T., Taper, M.L. & Marshall, T.C. (2007). Revising how the computer program CERVUS accommodates genotyping error increases success in paternity assignment. *Mol. Ecol.* 16, 1099-1106. https://doi.org/10.1111/j.1365-294X.2007.03089.x

Kniha, D., Janiga, M. & Straško, B. (2013). Ecomorphology of *Lissotriton montandoni* from the Eastern and Western Carpathians. *Oecol. Mont.* 22, 1-4.

Kotlík, P. & Zavadil, V. (1999). Natural hybrids between the newts *Triturus montandoni* and *T. vulgaris*: Morphological and allozyme data evidence of recombination between parental genomes. *Folia Zool.* 48, 211-218.

Landguth, E.L., Fedy, B.C., Oyler-McCance, S.J., Garey, A.L., Emel, S.L., Mumma, M., Wagner, H.H., Fortin, M.-J. & Cushman, S.A. (2011). Effects of sample size, number of markers, and allelic richness on the detecion of spatial genetic pattern. *Mol. Ecol. Res.* 12, 276-284. https://doi.org/10.1111/j.1755-0998.2011.03077.x

Nadachowska, K., Flis, I. & Babik, W. (2010). Characterization of microsatellite loci in the Carpathian newt (*Lissotriton montandoni*). *Herpetol. J.* 20, 107-110.

Peakall, R. & Smouse, P.E. (2012): GenAlEx 6.5: genetic analysis in Excel. Population genetic software for teaching and research – an update. *Bioinformatics* 28, 2537-2539. https://doi.org/10.1093/bioinformatics/bts460

Zieliński, P., Dudek, K., Stuglik, M.T., Liana, M. & Babik, W. (2014). Single nucleotide polymorphisms reveal genetic structuring of the Carpathian Newt and provide evidence of interspecific gene flow in the nuclear genome. *PLoS ONE* 9, e97431. https://doi.org/10.1371/journal.pone.0097431

Zieliński, P., Nadachowska-Brzyska, K., Wielstra, B., Szkotak, R., Covaciu-Marcov, S.D., Cogălniceanu, D. & Babik, W. (2013). No evidence for nuclear introgression despite complete mtDNA replacement in the Carpathian newt (*Lissotriton montandoni*). *Mol. Ecol.* 22, 1884-1903. https://doi.org/10.1111/mec.12225

STUDIA UNIVERSITATIS BABEŞ-BOLYAI BIOLOGIA, 70, 2, 2025 (p. 15-25)
doi:10.24193/subbbiol.2025.2.02

Waiting for the train that never came: establishing a new *Podarcis muralis* (Laurenti, 1768) railway population in Romania

Andreea-Maria Lazăr [1, *] and Alina-Florentina Muşet[1]

[1] *University of Oradea, Faculty of Informatics and Sciences, Department of Biology, Oradea, Romania*
[*] ***Corresponding author, E-mail: deealazar99@gmail.com***

Article history: Received 29 August 2025; Revised 27 October 2025; Accepted 1 December 2025; Available online 20 December 2025

Abstract. Nowadays, man-made structures have become surrogate habitats for various species. Among them, lizards are often capable of using railways. In the autumn of 2024, we identified a new *Podarcis muralis* railway population on a railway abandoned for 11 years in southwestern Romania, near Voislova locality. On a 100-meter transect, we observed 13 *P. muralis* and 3 *Lacerta viridis*. Most wall lizards were subadults, indicating a breeding population on the railway. Probably, the lizards were introduced from the nearby marble quarry in Ruşchiţa, where the species is present. Although *P. muralis* was mentioned in the mountains surrounding Voislova, the habitats near the railway are not favorable to it.

Keywords: distribution, lizard, human-modified landscape, quarry, transportation infrastructure.

Introduction

Lizards are known to use different types of artificial or human-modified habitats, as ancient ruins in modern cities (Simbula *et al.*, 2019), town cemeteries (Heltai *et al.*, 2015), remains of fortification (Strijbosch *et al.*, 1980), ports (Iftime, 2005; Santos *et al.*, 2019), road embankments (Gherghel *et al.*, 2009), highway guardrails (Livo, 2025), artificial ditches in agricultural areas (Covaciu-Marcov *et al.,* 2009a), etc. Among artificial habitats, railways play an important role for

lizards, which in many cases populate such structures (e.g., Sá-Sousa, 1995, Graitson, 2006; Covaciu-Marcov *et al.,* 2006; 2009b; Livo, 2025), sometimes even expanding their range along them (Gherghel *et al*., 2009). Abandoned railways have become well-represented elements in the landscape in some regions, thus their possible uses are analyzed nowadays (e.g., Sarmento, 2002; di Ruocco *et al.,* 2017). It appears that abandoned railways could even become green corridors, connecting protected areas with the outskirts of urban areas (see García-Mayor *et al.,* 2020). Recently, abandoned railways have been shown to be important for biodiversity, as they contribute to the maintenance and conservation of certain populations by providing habitats and resources (e.g., Leaney, 1983; Higginson and Dover, 2021; Pop *et al.,* 2021a, b; Dylewski *et al.,* 2022, 2025). Lizards were frequently mentioned on different railways (e.g., Graitson, 2006; Janssen *et al.,* 2025; Kovačević and Tvrtković, 2025), which could even serve as dispersal routes (e.g., Krämer *et al.,* 2025). *Podarcis muralis* (Laurenti, 1768) is a lizard species typically associated with rocky areas, both natural and human-made, in Romania (Fuhn and Vancea, 1961; Covaciu-Marcov *et al.,* 2009b). At its range limit, it is even considered to spread using railways (e.g., Covaciu-Marcov *et al.,* 2006; Gherghel *et al.,* 2009; Dudek, 2014; Gherghel and Tedrow, 2019), as human activities have created useful habitats and colonization routes in regions naturally devoid of suitable habitats (Wirga and Majtyka, 2015). *P. muralis* was frequently mentioned on railways (e.g., Graitson, 2006; Strugariu *et al*., 2008; Dudek, 2014; Niedrist *et al*., 2020; Williams *et al.,* 2021; Petreanu, 2023), as railways are considered major dispersal routes (Schulte *et al.,* 2013). Even where the species is introduced, the wall lizards are advancing through railways (Heden and Heden, 1999). In Romania, this species is primarily found in the southwestern sectors of the Carpathian Mountains (e.g., Cogălniceanu *et al.,* 2013). It is a xero-thermophilic species, present in rocky habitats (Fuhn and Vancea, 1961), although railway *P. muralis* populations were sometimes mentioned in the country in areas outside their ecological preference (Covaciu-Marcov *et al.,* 2005, 2006; Strugariu *et al.,* 2008). Given that railways are usually perceived through their negative impact manifested by fauna road mortality, even in the case of reptiles (e.g., Pop *et al.,* 2021c, 2023; Banerjee *et al.,* 2023; Bhardwaj *et al.,* 2025), this fact indicates a positive facet, confirming that in some cases railways (both active and disused) could have even a conservative value for reptiles (Graitson, 2006). In this context, this note presents information about a new *P. muralis* population on an abandoned railway in south-western Romania, and a possible explanation of the probable causes of its origin.

Materials and methods

The field activity took place on 22 September 2024. The studied region is located in the Bistra River corridor (Fig. 1), in the northwestern part of Caraș-Severin County, at the boundary between the Western Carpathians (Poiana Ruscă Mountains) and the Southern Carpathians (Țarcu Mountains), near the Iron Gate of Transylvania pass (Mândruț, 2006). The region was traversed by a secondary normal gauge railway, which even had a segment with rack (Turnock, 2006). The railway, which connected Caransebeș and Subcetate (C.F.R., 1987; Turnock, 2006), has been without traffic since 2013 (C.F.R., 2012). The analyzed railway segment is situated approximately 1 km east of Voislova locality. The marble quarry in Rușchița is located approximately 19 km from the locality (Todor and Surd, 2013).

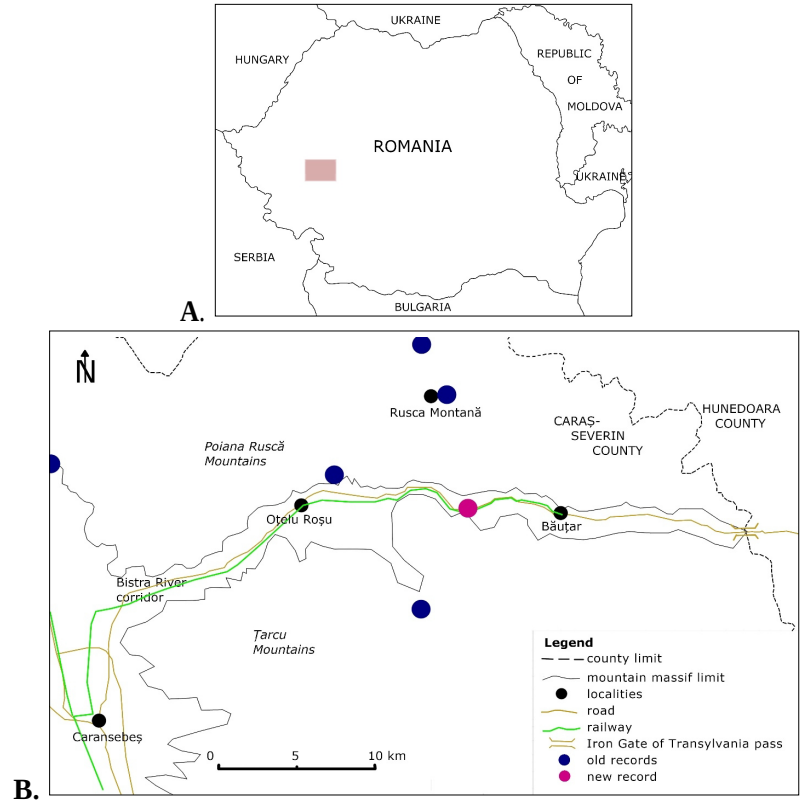

Figure 1. (A) The studied region location in Romania; (B) Detailed map of the Bistra River corridor with the new railway record of *P. muralis* (pink dot) and old records (blue dots, non-railway records according to Bogdan *et al.*, 2011, Iftime and Iftime 2013).

Results

We observed 13 *P. muralis* individuals (Fig. 2) (four adults, nine juveniles and subadults) on the abandoned railway from Voislova (45°31'05''N / 22°28'27''E). The location is situated at an altitude of 341 meters. On the railway, we also observed three juvenile *Lacerta viridis* individuals. The lizards were directly observed, without being captured. They were photographed whenever possible. We spent 30 minutes on the railway and made a 100-meter transect. The wall lizards were very active, running away when we approached and hiding under the tracks or under the railway ballast. This observation was made at 4 pm on a warm, late-autumn day. The railway is partially overgrown with vegetation, particularly by shrubs and trees from neighbouring areas; however, there are also open segments where the railway ballast is exposed (Fig. 3).

Figure 2. *Podarcis muralis* on the abandoned railway from Voislova, Romania.

Figure 3. The abandoned railway from Voislova, Romania.

The location is situated east of Voislova, between this locality and Marga. Surrounding the railways are human-modified areas, including pastures, orchards, and agricultural fields, as well as areas with shrubs and trees interspersed between them.

Discussion

Most *P. muralis* individuals were juveniles and subadults, indicating that a sustainable, reproductive population exists on the abandoned railway from Voislova, as observed in other populations (Jablonski *et al.,* 2025). The railway has been disused for approximately 11 years (C.F.R., 2012), but the wall lizard has also been observed on functional railways (Covaciu-Marcov *et al.,* 2006, 2009b; Niedrist *et al.,* 2020), as well as other lizard species (e.g., Graitson, 2006; Remacle, 2018; Janssen *et al.,* 2025). *P. muralis* is known for its ability to use transportation networks (e.g., Covaciu-Marcov *et al.,* 2006; Graitson, 2006; Gherghel *et al.,* 2009; Dudek, 2014; Petreanu, 2023), but also other artificial habitats with stones, even outside its normal distribution range (e.g., Iftime *et al.,* 2008; Sas-Kovács and Sas-Kovács, 2014; Jablonski *et al.,* 2025). In Romania, the wall lizards were previously identified in human-modified habitats in mountain regions with favourable habitats and distribution records in natural habitats (Covaciu-Marcov *et al.,* 2006, 2009b; Gherghel *et al.,* 2009). Nevertheless, the species was also observed in artificial habitats in plain areas, thus outside the region with favourable habitats (Covaciu-Marcov et al., 2005, 2006; Sas-Kovács and Sas-Kovács, 2014; Ile and Dumbravă, 2020). The record from Voislova is added to other railway populations of this species in Romania (Covaciu-Marcov *et al.,* 2006, 2009b; Gherghel *et al.,* 2009).

The habitats surrounding the railway at Voislova (pastures, orchards, grassy areas, and agricultural cultures to a lesser extent) are not favorable to this species, which in Romania is typically associated with rocky areas, both natural and human-made (Fuhn and Vancea, 1961; Covaciu-Marcov *et al.,* 2009b). Eventually, areas with shrubs and trees situated between agricultural cultures could be favorable for *Lacerta viridis*, a species associated with such habitats (e.g., Fuhn and Vancea, 1961; Sevianu *et al.,* 2022), and which was also observed on the railway, albeit in a smaller number of individuals. Nevertheless, *L. viridis* was not recorded in the neighboring region in the most recent review of Romanian herpetofauna, as it was mentioned only in one location on the other side of the pass and in three older locations in the western parts of the Poiana Ruscă Mountains (Cogălniceanu *et al.,* 2013). Records of *P. muralis* were even scarce, as in the region, there are only four old distribution records in the Poiana Ruscă Mountains (Cogălniceanu *et al.,* 2013). Nevertheless, the two species were previously mentioned in different locations from the Poiana Ruscă Mountains (Bogdan *et al.,* 2011) and Țarcu Mountains (Iftime and Iftime 2013). *L. viridis* was mentioned even at Voislova, and *P. muralis* at about 10 km from the railway population at Voislova, as it is the second most common species in the western sector of the Poiana Ruscă Mountains (Bogdan *et al.,* 2011).

Although the region, in a broad sense, has favorable habitats and wall lizard populations (Bogdan *et al.,* 2011, Iftime and Iftime 2013), the area neighboring the railway did not have favorable habitats, so *P. muralis* could not colonize the railway from its neighboring areas. Thus, this raises the question regarding the range expansion of the railway *P. muralis* population at Voislova. The introduction of this species, as a consequence of railway maintenance works and railway ballast, has been repeatedly indicated in the case of wall lizard railway populations (e.g., Covaciu-Marcov *et al.,* 2006; Gherghel *et al.,* 2009; Dudek, 2014). Nevertheless, at Voislova, another explanation seems more plausible, as a large marble quarry is located in the region (approximately 19 km away) (Todor and Surd, 2013), and *P. muralis* has been mentioned in that locality (Bogdan *et al.,* 2011). Moreover, in the immediate vicinity of the railway, there is a marble warehouse and processing facility. Furthermore, until the late 1970s, a narrow-gauge railway existed between Ruşchiţa and Voislova, used to transport marble to Voislova (Todor and Surd, 2013). Probably through this narrow-gauge railway, *P. muralis* has spread directly or indirectly along the line between Ruşchiţa and Voislova, and from Voislova railway station, it has expanded along the normal-gauge railway. Thus, this would be an introduction related to transportation networks from nearby populations, but this could be verified only with genetic tools, as in other cases (e.g., Oskyrko *et al.,* 2020; Jablonski *et al.,* 2025; Naumov *et al.,* 2025) or by studying the species presence on the line at a wider scale. Nevertheless, the wall lizard was also introduced in other ways, such as through freight transport (Kowalik *et al.,* 2025), building materials (Sas-Kovács and Sas-Kovács, 2014; Ile and Dumbravă, 2020), horticultural trade (Jablonski *et al.,* 2025), and cargo boats (Oskyrko *et al.,* 2020). However, in this case, the marble quarry was an exporter of resources from the area; thus, the introduction of the wall lizard from other regions is less plausible (rather, individuals from Ruşchiţa were introduced in other localities alongside with the marble). The presence of railway populations was previously explained by migrating along railways or by introduction with the railway ballast (Covaciu-Marcov *et al.,* 2006).

Probably, the railway offers the most appropriate habitats for the wall lizard's requirements in the region. This assumption is supported by the aspect of the habitat neighboring the railway, as well as by the fact that the region has a relatively cooler climate (Mândruţ, 2006) compared to other areas populated by *P. muralis* in Romania (Fuhn and Vancea, 1961; Cogălniceanu *et al.,* 2013). Moreover, in the vicinity (approximately 15 km), there is a low-altitude *Zootoca vivipara* population (Bogdan *et al.,* 2011), a cold-adapted species (Fuhn and Vancea, 1961), which suggests that the region and habitats are not particularly favorable for *P. muralis*. In this context, the wall lizard may have been advantaged by increasing temperatures over the past few years (Nagavciuc *et al.,* 2022;

Ionita and Nagavciuc, 2025). Probably, the railway corresponds with the habitat and temperature requirements of *P. muralis*, as in other cases (Covaciu-Marcov *et al.,* 2006). This fact indicates that *P. muralis* is one of the winners of anthropization, as it could adapt to artificial habitats which resemble its natural habitats (e.g., Covaciu-Marcov *et al.,* 2006; Wirga and Majtyka, 2013; Sas-Kovács and Sas-Kovács, 2014; Jablonski *et al.,* 2025). At the same time, this was a secondary railway line (C.F.R., 1987, 2012), which likely did not have a significant negative impact, even during its peak traffic. Additionally, compared to roads, railways appear to have a lesser negative impact on soil quality (Sion *et al.,* 2023). It remains to be seen to what extent the renaturalization of the railway and the development of plant communities will cause the disappearance of this population in the course of time, as it could not beneficiate from the railway closer like other animals (e.g., Leaney, 1983; Higginson and Dover, 2021; Pop *et al.,* 2021a, b; Dylewski *et al.,* 2022, 2025).

Conclusions

The railway *P. muralis* population from Voislova demonstrates the species' capacity to extend its distribution range when corridors with appropriate conditions are available, even if these are represented by anthropogenic structures, such as railways. However, this population, even if it currently seems stable (as evidenced by the presence of juveniles), may be threatened in the future by the advancement of renaturalization along this abandoned railway, which will likely modify at least some of the current habitat conditions.

References

Banerjee, K., Nawani, S., Boruah, B., Habib, B. & Das, A. (2023). A rapid assessment of herpetofaunal diversity and mortality along railway track in Northern Western Ghats, India. *Hamadryad 40,* 11-23.

Bhardwaj, M., Collinson-Jonker, W.J., Thela, S.K., Swanepoel, L.H. & Allin, P. (2025). Mortality on the tracks: spatiotemporal patterns to rail-kill in the Balule Nature Reserve, South Africa. *Wildl. Biol. 2025,* e01167. https://doi.org/10.1002/wlb3.01167

Bogdan, H.V., Ilieş, D., Covaciu-Marcov, S.-D., Cicort-Lucaciu, A.-S. & Sas, I. (2011). Contributions to the study of the herpetofauna of the western region of the Poiana Ruscă Mountains and its surrounding areas. *North-West. J. Zool. 7,* 125-131.

C.F.R. (1987). Mersul trenurilor de călători 31.05.1987 - 28.05.1988. Societatea Națională a Căilor Ferate Române, Serviciul Mersuri de Tren. Societatea Tipografică Filaret SA, București. [in Romanian].

C.F.R. (2012). Mersul trenurilor de călători 11.12.2011 - 8.12.2012. Societatea Națională a Căilor Ferate Române, Serviciul Mersuri de Tren. Societatea Tipografică Filaret SA, Bucureşti. [in Romanian].

Cogălniceanu, D., Rozylowicz, L., Székely, P., Samoilă, C., Stănescu, F., Tudor, M., Székely, D. & Iosif, R. (2013). Diversity and distribution of reptiles in Romania. *ZooKeys 296,* 49-76.

Covaciu-Marcov, S.-D., Cicort-Lucaciu, A.-S., Sas, I., Bredet, A.M. & Bogdan, H. (2005). Herpetofauna from the basin of Mureş river in Arad county, Romania. *Mediul, cercetare, protecţie şi gestiune 5*, 147-152.

Covaciu-Marcov, S.-D., Bogdan, H.-V. & Ferenti, S. (2006). Notes regarding the presence of some *Podarcis muralis* (Laurenti 1768) populations on railroads of western Romania. *North-West. J. Zool. 2,* 126-130.

Covaciu-Marcov, S.-D., Cicort-Lucaciu, A.-S., Gaceu, O., Sas, I., Ferenţi, S., & Bogdan, H.V. (2009a). The herpetofauna of the south-western part of Mehedinţi County. *North-West. J. Zool. 5*(1), *142-164*.

Covaciu-Marcov, S.-D., Cicort-Lucaciu, A.-S., Dobre, F., Ferenţi, S., Birceanu, M., Mihuţ, R. & Strugariu, A. (2009b). The herpetofauna of the Jiului Gorge National Park, Romania. *North-West. J. Zool. 5* (Supplement 1), S1-S78.

di Ruocco, G., Sicignano, E., Fiore, P. & D'Andria, E. (2017). Sustainable reuse of disused railway. *Procedia Eng. 180,* 1643-1652. https://doi.org/10.1016/j.proeng.2017.04.327

Dylewski, Ł., Tobolka, M., Maćkowiak, Ł., Białas, J.T. & Banaszak-Cibicka, W. (2022). Unused railway lines for conservation of pollinators in the intensively managed agricultural landscape. *J. Environ. Manage. 304,* 114186. https://doi.org/10.1016/j.jenvman.2021.114186

Dylewski, Ł., Maćkowiak, Ł. & Dyderski, M.K. (2025). Abandoned railways support greater functional and phylogenetic plant diversity than adjacent grassy meadows in agricultural landscape. *Land Degrad. Dev. 36*, 614–629. https://doi.org/10.1002/ldr.5383

Dudek, K. (2014). Railroads as anthropogenic dispersal corridors. Possible way of the colonization of Poland by a common wall lizard (*Podarcis muralis, Lacertidae*). *Ecol. Quest. 20,* 71-73. https://doi.org/10.12775/EQ.2014.018

Fuhn, I. & Vancea, S. (1961). "Fauna R.P.R.", Volumul XIV, Fascicola II, Reptilia. Bucureşti, Romania, Editura Academiei R.P.R. [in Romanian].

García-Mayor, C., Martí, P., Castaño, M. & Bernabeu-Bautista, Á. (2020). The unexploited potential of converting rail track to greenways: the Spanish *Vías Verdes*. *Sustainability 13,* 881. https://doi.org/10.3390/su12030881

Gherghel, I. & Tedrow, R. (2019). Manmade structures are used by an invasive species to colonize new territory across a fragmented landscape. *Acta Oecol. 101,* 103479. https://doi.org/10.1016/j.actao.2019.103479

Gherghel, I., Strugariu, A., Sahlean, T. & Zamfirescu, O. (2009). Anthropogenic impact or anthropogenic accommodation? Distribution range expansion of the common wall lizard (*Podarcis muralis*) by means of artificial habitats in north-eastern limit of its distribution range. *Acta Herpetol. 4,* 183-189. http://dx.doi.org/10.13128/Acta_Herpetol-3421

Graitson, E. (2006). Répartition et écologie des reptiles sur le réseau ferroviaire en Wallonie. *Bull. Soc. Herp. Fr. 120,* 15-32.

Heltai, B., Sály, P., Hovács, D., & Kiss, I. (2015). Niche segregation of sand lizard (*Lacerta agilis*) and green lizard (*Lacerta viridis*) in an urban semi-natural habitat. *Amphib.-Reptil.* 36, 389-399. https://doi.org/10.1163/15685381-00003018

Heden, S.E. & Heden, D. (1999). Railway-aided dispersal of an introduced *Podarcis muralis* population. *Herpetol. Rev. 30,* 57-58.

Higginson, P. & Dover, J. (2021). Bumblebee abundance and richness along disused railway lines: the impact of track morphology. *J. Insect Conserv. 25,* 481-457. https://doi.org/10.1007/s10841-021-00345-4

Iftime, A. (2005). Herpetological observations in the Danube floodplain sector in the Giurgiu county (Romania). *Trav. Mus. Natl. Hist. Nat. «Grigore Antipa» 48, 339-349.*

Iftime, A., & Iftime, O. (2013). Contribution to the knowledge regarding the distribution and ecology of the ehrpetofauna of Țarcu Massif (Southern Carpathians, Romania). *Trav. Mus. Natl. Hist. Nat. «Grigore Antipa» 56*(1), 81-92.

Iftime, A., Gherghel, I. & Ghiurcă, I. (2008). Contribution to the knowledge of the herpetofauna of Bacău County (Romania). *Trav. Mus. Natl. Hist. Nat. «Grigore Antipa» 51*, 243-253.

Ile, G.A. & Dumbravă, A.-R. (2020). A wall lizard on a Danube island - *Podarcis muralis* (Reptilia) in Moldova Veche island, Iron Gates Natural Park, Romania. *Ecol. Balk. 12*, 191-194.

Ionita, M. & Nagavciuc, V. (2025). 2024: The year with too much summer in the eastern part of Europe. *Weather,* https://doi.org/10.1002/wea.7696

Jablonski, D., Raffaj, M. & Senko, D. (2025). The Balkans in Central Europe: a case of introduced lineage of *Podarcis muralis* in Slovakia highlighting the impact of international trading and climate change. *Herpetozoa 38*, 97-102. https://doi.org/10.3897/herpetozoa.38.e139307

Janssen, A., Staab, M. & Rödel, M.-O. (2025). Home range of Sand Lizards, *Lacerta agilis* (Squamata: Sauria: *Lacertidae*), along railway tracks. *Salamandra 61,* 240-255.

Kovačević, M. & Tvrtković, N. (2025). First evidence of the expansion of *Podarcis siculus* (Reptilia: Squamata: *Lacertidae*) in Pannonian Plain, Croatia. *Nat. Croat. 34*, https://doi.org/10.20302/NC.2025.34.2

Kowalik, C., Skawiński, T., Majtyka, M., Kuśmierek, N., Starzecka, A. & Jablonski, D. (2025). Tracking the origin and current distribution of wall lizards (*Podarcis* spp.) in Poland. *Amphib.-Reptil. 46,* 69-83. https://doi.org/10.1163/15685381-bja10206

Krämer, A., Meyer, H. & Buchholz, S. (2025). Habitat suitability of the Sand Lizard (*Lacerta agilis*) at its distribution limit – an analysis based on citizen science data and machine learning. *J. Biogeogr. 52,* e15099. https://doi.org/10.1111/jbi.15099

Leaney, R. (1983). An ecological and amenity survey of Norfolk's disused railways. *Trans. Norfolk Norwich Nat. Soc. 26*, 112-137.

Livo, L.J. (2025). Widespread use of highway guardrails and other anthropogenic features by the Colorado Checkered Whiptail (*Aspidoscelis neotesselatus*). Western Wildlife 12: 15-18.

Mândruţ, O. (2006). Mic Atlas de Geografie a României. Bucharest, Romania, Editura Corint. [in Romanian].

Nagavciuc, V., Scholz, P. & Ionita, M. (2022). Hotspots of warm and dry summers in Romania. *Nat. Haz. Earth Sys. Sci. 22,* 1347-1369. https://doi.org/10.5194/nhess-22-1347-2022

Naumov, B., Vacheva, E., Borissov, S., Lukanov, S., Dyugmedzhiev, A. & Lazarkevich, I. (2025). On the origin of the easternmost population of *Podarcis erhardii* (Bedriaga, 1876) (Reptilia: Sauria). *North-West. J. Zool. 21,* 43-49.

Niedrist, A., Kaufmann, P., Tribsch, A., Berninger, U.-G., Leeb, C. & Maletzky, A. (2020). Verbreitung und herkunf allochthoner populationen der mauereidechse (*Podarcis muralis*) entlang des bahnliniennetzes im österreichischen Bundesland Salzburg. *Z. Feldherpetol. 27,* 149-166.

Oskyrko, O., Laakkonen, H., Silva-Rocha, I., Jablonski, D., Marushchak, O., Uller, T. & Carretero, M.A. (2020). The possible origin of the common wall lizard, *Podarcis muralis* (Laurenti, 1768) in Ukraine. *Herpetozoa 33,* 87-93. https://doi.org/10.3897/herpetozoa.33.e49683

Petreanu, I.C. (2023). New data regarding the distribution and status of the herpetofauna from urban and peri-urban habitats in the city of Pitești, Argeș County (Romania). *Trav. Mus. Natl. Hist. Nat. «Grigore Antipa» 66,* 307-335. https://doi.org/10.3897/travaux.66.e110472

Pop, D.-R., Ferenţi, S., Maier, A.-R.-M., Cadar, A.-M., Covaciu-Marcov, S.-D. & Cupșa, D. (2021a). A journey on the railway to nowhere: terrestrial isopod assemblages on an abandoned railway in western Romania. *Spixiana 44,* 135-143.

Pop, D.-R., Maier, A.-R.-M., Cadar, A.-M. & Ferenţi, S. (2021b). Preliminary data on terrestrial isopods from some railways in Dobruja, eastern Romania. *Studia UBB Biologia 66*, 85-92. https://doi.org/10.24193/%20subbbiol.2021.1.03

Pop, D.-R., Lucaci, B.-I. & Cupșa, D. (2021c). Preliminary data on fauna railway mortality in Dobruja (Romania) indicate a possible impact on spur-thighed tortoise, *Testudo graeca*. *Oltenia. Studii și Comunicări Științele Naturii 37,* 101-106.

Pop, D.-R., Petruș-Vancea, A., Cicort, A., Moș, A. & Cupșa, D. (2023). Road or railway: which is more deadly for the fauna? A puzzling answer from western Romania. *North-West. J. Zool. 19*, 62-70.

Remacle, A. (2018). Premiers résultats d'une opération de sauvegarde d'une population ferroviare de Lézard des souches, *Lacerta agilis* en Wallonie (Belgique). *Natura Mosana* 71, 21-45.

Santos, J.L., Žagar, A., Drašler, K., Rato, C., Ayres, C., Harris, D.J, Carretero, M., & Salvi, D. (2019). Phylogeographic evidence for multiple long-distance introductions of the common wall lizard associated with human trade and transport. *Amphib.-Reptil. 40*, 121-127.

Sarmento, J. (2002). The geography of "disused" railways: what in happening in Portugal? *Finisterra 37,* 55-71.

Sá-Sousa, P. (1995). The introduced Madeiran lizard, *Lacerta* (*Teira*) *dugesii* in Lisbon. *Amphib.-Reptil. 16*, 211-214.

Sas-Kovács, I. & Sas-Kovács, É.-H. (2014). A non-invasive colonist yet: the presence of *Podarcis muralis* in the lowland course of Crişul Repede River (north-western Romania). *North-West. J. Zool. 10 (Supplement 1),* S141-S145.

Schulte, U., Veith, M., Mingo, V., Modica, C. & Hochkirch, A. (2013). Strong genetic differentiation due to multiple founder events during a recent range expansion of an introduced wall lizard population. *Biol. Invasions 15,* 2639-2649. https://doi.org/10.1007/s10530-013-0480-5

Sevianu, E., Petrişor, M., Maloş, C.-V. & Hartel, T. (2022). Habitat preferences of the European green lizard *Lacerta viridis* (Laurenti 1768) in a protected area, Romania. *Studia UBB Biologia 67,* 165-176. https://doi.org/10.24193/subbbiol.2022.1.09

Simbula, G., Luiselli, L., & Vignoli, L. (2019). Lizards and the city: a community study of *Lacertidae* and *Gekkonidae* from an arheological park in Rome. *Zoologischer Anzeiger 283*, 20-26.

Sion, A., Gîrmacea, A.-C., Ene, A. & Timofti, M. (2023). The effect of road and railway traffic on soil quality from the Public Garden of Galati, Romania. *Ann. Univ. Dunărea de Jos Galaţi 46,* 32-38.

Strijbosch, H., Bonnemayer, J.J.A.M., & Dietvorst, P.J.M. (1980): The northernmost population of *Podarcis muralis* (Lacertilia, *Lacertidae*). *Amphib.-Reptil. 1*, 161-172.

Strugariu, A., Gherghel, I. & Zamfirescu, Ş.R. (2008). Conquering new ground: on the presence of *Podarcis muralis* (Reptilia: *Lacertidae*) in Bucharest, the capital of Romania. *Herpetol. Rom. 2,* 47-50.

Todor, D.-R. & Surd, V. (2013). History and tourist valorization of the Ruşchiţa marble quarry (Caraş-Severin County, Romania). *Studia UBB Geographica 60*, 97-122.

Turnock, D. (2006). Settlement history and sustainability in the Carpathians in the eighteenth and nineteenth centuries. *Rev. Histor. Geogr. Toponomastics 1,* 31-60.

Williams, R.J., Dunn, A.M., da Costa, L.M. & Hassall, C. (2021). Climate and habitat configuration limit range expansion and patterns of dispersal in a non-native lizard. *Ecol. Evol. 11,* 3332-3346. https://doi.org/10.1002/ece3.7284

Wirga, M. & Majtyka, T. (2013). Records of the common wall lizard *Podarcis muralis* (Laurenti, 1768) (Squamata: *Lacertidae*) from Poland. *Herpetol. Notes 6,* 421-423.

Wirga, M. & Majtyka, T. (2015). Do climatic requirements explain the northern range of European reptiles? Common wall lizard *Podarcis muralis* (Laur.) (Squamata, *Lacertidae*) as an example. *North-West. J. Zool. 11*, 296-303.

STUDIA UNIVERSITATIS BABEŞ-BOLYAI BIOLOGIA, 70, 2, 2025 (p. 27-53)
doi:10.24193/subbbiol.2025.2.03

Checklist of the genus *Cortinarius* in Romania: taxonomic and distributional insights

Emerencia Szabó[1], Avar-Lehel Dénes[1,2 *], Róbert Veres[3], Bálint Dima[4] and Lujza Keresztes[1]

[1]Centre 3B, Babeş-Bolyai University, Cluj-Napoca, Romania; [2]Institute of Advanced Studies in Science and Technology (STAR-UBB Institute); Babeş-Bolyai University, Cluj-Napoca, Romania; [3]Hungarian Department of Biology and Ecology, Babeş-Bolyai University, Cluj-Napoca, Romania; [4]Department of Plant Anatomy, Institute of Biology, Eötvös Loránd University, Budapest, Hungary
[*] ***Corresponding author, E-mail:*** avar.lehel@gmail.com

Article history: Received 1 September 2025; Revised 27 November 2025; Accepted 27 November 2025; Available online 20 December 2025

Abstract. The genus *Cortinarius* is one of the most diverse ectomycorrhizal lineages of *Basidiomycota*, yet its diversity in Romania has remained poorly documented. This study presents the first comprehensive checklist of *Cortinarius* sensu lato in the country, integrating historical records, literature data, field surveys, and molecular data. A total of 231 species is confirmed, including 110 supported by DNA sequence evidence and 121 validated solely based on morphology. Spatial analysis of collection sites highlights two major research hotspots in the Apuseni Mountains and the Transylvanian Basin, reflecting uneven sampling effort. Despite its richness and ecological importance, Romanian *Cortinarius* remains underrepresented in global sequence repositories. These findings emphasize the need for broader molecular surveys and systematic biodiversity mapping to resolve species boundaries and better integrate Romanian taxa into European and global frameworks.

Keywords: *Agaricales*, barcoding, *Basidiomycota*, integrative taxonomy, ITS sequences, spatial distribution.

Introduction

General fungal diversity and taxonomy

Fungi are widespread organisms with substantial ecological and economic importance. Despite their global distribution, fungal taxonomy remains incompletely understood. Molecular and evolutionary studies indicate that fungi diverged from a common eukaryotic ancestor shared with *Dermocystidium* and *Ichthyophonus* approximately one billion years ago (Berbee and Taylor 2001). Since then, they have evolved into a distinct eukaryotic lineage, comprising nearly as many species as plants and animals.

The broad application of molecular phylogenetics in fungal systematics has shaped the current classification. Today, fungi are grouped into over 200 orders distributed across 12 phyla, organized into six major groups and two subkingdoms: *Dikarya*, which includes *Ascomycota*, *Basidiomycota*, and *Entorrhizomycota*; and *Chytridiomyceta*, comprising *Chytridiomycota*, *Monoblepharidomycota*, and *Neocallimastigomycota*. Additional lineages include *Mucoromycota*, *Zoopagomycota*, *Blastocladiomycota*, and the *Opisthosporidia* group (*Aphelidiomycota*, *Rozellomycota/ Cryptomycota*, and *Microsporidia*) (Barr 2001; Li *et al.,* 2021).

Taxonomic issues with Cortinarius

The family *Cortinariaceae* is the most species-rich within the phylum *Basidiomycota* (Kirk *et al.,* 2008), comprising more than 3,000 described ectomycorrhizal species with a cosmopolitan distribution (Roskov *et al.,* 2019). Traditionally, this family included eleven genera (Watling *et al.,* 1993). However, morphological taxonomy has undergone major revisions with the implementation of integrative approaches.

Cortinarius species display remarkable morphological variability, ranging from mycenoid to tricholomatoid forms. The pileus varies across species, appearing dry, fibrillose, silky, squamulose, or viscid. Fruiting bodies may be uniformly brown or strikingly colorful, spanning from yellow to purple (Peintner *et al.,* 2004). Despite this variability, some features consistently characterize the genus: spores are typically brownish in print, ornamented (finely to coarsely verrucose), and lack both a germ pore and perisporium. Another universally recognized trait is the presence of an inner veil, the cortina (Singer 1986).

Morphology-based classifications (Fries 1821; Fries 1838; Moser1975; Moser 1983; Moënne-Loccoz *et al.,* 1990; Brandrud *et al.,* 1990, 1992, 1998; Bidaud *et al.,*1994; Brandrud *et al.,* 1995) defined several groups and subdivisions within the genus. Nevertheless, molecular phylogenetics has revealed profound inconsistencies in these frameworks. Since the introduction of molecular methods in fungal taxonomy (Liu *et al.,* 1997; Peintner *et al.,* 2001, 2002; Peintner *et al.,*

2004; Garnica *et al.,* 2005; Soop *et al.,* 2019) , it has become clear that some previously accepted phyla are polyphyletic, and several new clades and sections have been described.

A major taxonomic revision by Liimatainen *et al.* (2022) proposed dividing the family into ten genera, based entirely on molecular evidence: *Aureonarius*, *AustroCortinarius*, *Calonarius*, *Cortinarius*, *Cystinarius*, *Hygronarius*, *Mystinarius*, *Phlegmacium*, *Thaxterogaster*, and *Volvanarius*. Despite intensive research, recent findings suggest that this classification still requires revision (Gallone *et al.,* 2024). In this paper, we use the traditional species names of 231 *Cortinarius*, with the corresponding new names (according to Liimatainen et al.'s revision) provided in parentheses (Tab. 1).

This study focuses on *Cortinarius* species reported from Romania, aiming to synthesize historical records, recent field observations, and available molecular data. While the genus *Cortinarius* has been extensively studied across Europe (e.g., Brandrud 1996; Garnica *et al.,* 2003, 2005, 2009; Frøslev *et al.,* 2007; Niskanen *et al.,* 2008; Suárez-Santiago *et al.,* 2009; Niskanen *et al.,* 2009, 2011; Garnica *et al.,* 2011; Niskanen *et al.,* 2012, 2013, 2016; Liimatainen 2013; Frøslev *et al.,* 2015; Brandrud and Dima 2014; Dima *et al.,* 2014, 2016; Liimatainen *et al.,* 2014, 2020; Garrido-Benavent *et al.*, 2015; Frøslev *et al.,* 2017; Brandrud *et al.,* 2018a, 2018b; Brandrud *et al.,* 2019; Bidaud *et al.,* 2021), Romanian data remain scarce, fragmented, and largely outdated.

Materials and methods

In this review of the genus *Cortinarius* from Romania, we aimed to clarify the national species list using published data. We systematically surveyed 35 literature sources covering the period 1900–2023, including both morphological and molecular studies. These publications comprised regional surveys, ecological assessments, and species checklists. Since the earliest reports from the country were based exclusively on morphological identification, our first step was to compile a comprehensive database of published species records. In the second step, we updated the nomenclature of these taxa according to the most recent taxonomic framework, using Index Fungorum as the primary reference. Finally, we filtered the dataset to eliminate misapplied names, synonyms, and outdated combinations to establish a more accurate and standardized checklist of Romanian *Cortinarius* species.

To assess the geographical distribution of these records, we performed a spatial analysis of collection sites. A Kernel Density Estimate (KDE) of site coordinates was generated in R (v4.4.3) using the packages ggplot2 (v3.5.1),

sf (v1.0-19), and maptiles (v0.9.0), with all coordinates projected in EPSG:3857. The KDE visualization highlights collection hotspots across Romania and allows for the identification of regions that have been studied more intensively.

Results and discussion

Historical Romanian research

Mycological exploration in Transylvania has a long and well-documented tradition, beginning in 1778 when József Benkő first recorded 13 edible fungal species, including representatives of the genera *Agaricus* and *Hydnum* within a floristic framework (Vörösváry 2017), a contribution soon expanded by István Mátyus in this 1787 publication *Új Diaetetica*, which included additional taxa such as *Agaricus* and *Boletus* (Mátyus 1787).

By the late 19th century, important advances were made through the activity of several renowned mycologists: István Schulzer, recognized as a funder of Hungarian mycology, along with Károly Kalchbrenner and Frigyes Hazslinszky, survey regions such as Banat, Băiţa and Oradea, while József Téglási Ercsei provided sporadic data from Cluj County, and Michael Fuss studied the Făgăraş and Rusca Mountains, identifying 160 fungal species around Sibiu (Fuss 1866). Complementary to these contributions, Gyula Istvánffi in 1895 described 40 taxa using vernacular names, thus bridging ethomycological knowledge and scientific taxonomy.

At the begining of the 20th century, László Hollós enriched the regional inventory with records from genera such as *Calvatia*, *Lycoperdon, Bovista,* and *Scleroderma,* while Gusztáv Moesz compiled a list of 76 taxa from Reci and provided a foundation for the study of both macro- and microfungi. Around the same time, Margit Csűrös-Káptalan and István Csűrös initiated the first coecological studies of fungi, later complemented by the work of Kálmán László in collaboration with George Silaghi and Dénes Pázmány (Sántha 1999).

Following 1950, mycological research in Romania intensified considerably, culminating in Bontea's extensive documentation of 8,727 fungal species (Bontea 1985, 1986), which attest to the remarkable richness of Transylvanian mycodiversity. Nevertheless, despite this solid historical and taxonomic foundation, targeted studies on the genus *Cortinarius* remained scarce.

Most Romanian records of *Cortinarius* are based solely on morphological characters. The first such report was published by Pál-Fám (1997) , who, during a survey of macrofungal diversity in the Baraolt Mountains, documented *C. trivialis* from Băile Şugaş in association with tree species of the order Fagales, *C. subfulgens*

from Malnaș Băi, and *C. balaustinus* from the Baraolt Mountains. Bucșa (2007), recorded only *C. olearioides* among 118 taxa from the Breite Natural Reserve, this contribution further expanded the known distribution of the genus in Romania, but like earlier reports, relied exclusively on morphological identification. Chinan *et al.* (2014; 2008) explored the mycobiota of Eastern Carpathian peat bogs, frequently encountering *C. sanguineus* and *C. cinnamomeus*, and later identified nine *Cortinarius* species in *Sphagno-Piceetum* communities, including *C. camphoratus*, *C. collinitus*, *C. evernius*, *C. flexipes*, *C. sanguineus*, *C. scaurus*, and *C. tubarius*.

In the Southern Carpathians Ciortan (2013a, 2013b) documented *C. camphoratus*, *C. caperatus*, *C. cinnabarinus*, *C. cinnamomeus*, *C. multiformis*, *C. orellanus*, and *C. trivialis* using traditional morphological methods. She also surveyed fungal diversity within the Natura 2000 site ROSCI0188, identifying 116 species, including five *Cortinarius* species with potential medicinal or toxicological relevance. Environmental studies by Elekes *et al.* (2010) utilized *Cortinarius* species (*C. largus*, *C. armillatus*) as bioindicators of soil pollution in the Bucegi Mountains due to their known heavy metal accumulation capabilities. Subsequent work (Elekes *et al.*, 2014) extended this to include *C. callisteus* and *C. subfulgens*. Bîrsan *et al.* (2013) examined ectomycorrhizal associations in Eastern Carpathian forests, identifying several *Cortinarius* taxa linked to specific vegetation types, including *C. sanguineus*, *C. semisanguineus*, *C. flexipes*, *C. croceus*, *C. collinitus*, and *C. caperatus* these species are well-known about their ectomycorrhizal connection with species from order *Piceae* .

The Transylvanian region has been extensively studied over the past 10–15 years, thanks to the efforts of mycological associations and the organization of congresses and field camps, primarily in Harghita and Covasna counties. A significant milestone was reached during the 36th J.E.C. Congress (2018, Bálványos), where 74 participants collected samples over a five-day period, mainly from Harghita County (Mohos peat bog, Lake St. Anna, and Lucs peat bog), Covasna County (Bálványos, Băile Șugaș, Veresvíz, Komandó, Ojoz), and Bacău County (Lesenc Valley). In total, 440 taxa were identified based solely on morphological examination, including 19 species reported for the first time in Romania. Within this dataset, 68 species of *Cortinarius* were recorded, of which 29 represented new county records, and several taxa were added to the Romanian mycobiota (Szász *et al*., 2022; Bellù *et al.,* 2019). From the same geological region, Pál-Fám *et al.* (2022) documented 11 additional *Cortinarius* species.

From the territory of Hoghiz, a total of 245 taxa were documented during mycological research conducted by Szász (2022). Among these, seven *Cortinarius* species were recorded: *C. alboviolaceus, C. balteatocumatilis, C. bolaris, C. caperatus, C. melatonus, C. semisanguineus*, and *C. torvus* but none of which represented

new records for Romania. During a mycological camp organized in 2018 by the László Kálmán Society in Harghita County, a total of 105 species were identified using traditional taxonomic methods. Among these, two *Cortinarius* species were recorded: *C. caperatus and C. croceus* (Pál-Fám *et al.*, 2022). From the same camp in 2019, 15 *Cortinarius* species were recorded and later published (Pál-Fám *et al*., 2022). In 2020, the total documented taxa during this camp included 237 from Vărşag and 58 from Harghita, among which seven *Cortinarius* species were recorded (Pál-Fám *et al.,* 2022).

In 2023, Pál-Fám *et al*. published a comprehensive checklist of Transylvanian macrofungi, based on the examination of 119 literature sources spanning 1787–2020. As a result, they compiled a database of 1,477 macrofungal species. Among these, 133 species belonged to the genus *Cortinarius*, including 43 species newly recorded for Romania (Pál-Fám *et al.,* 2023). In contrast, relatively little information is currently available from Maramureş County. During July 2019, Pál-Fám *et al.* (2022a) collected 274 taxa, among which three *Cortinarius* species were recorded: *C. balteatocumatilis*, *C. largus*, and *C. renidens*.

Currently the Red List of Romania includes eight threatened *Cortinarius* species (Tănase and Pop 2005): *C. bulliardii* and *C. orellanus* – Vulnerable; *C. cinnabarinus, C. cotoneus*, *C. dibaphus, C. napus*, *C. percomis*, *C. praestans* – Near Threatened. Despite these listings, most records lack molecular confirmation, precise locality data, or standardized diagnostic criteria. In their study, Szabó *et al*. (2023) aimed to enhance the understanding of *Cortinarius* diversity in the Romanian Carpathians by collecting and analyzing 234 specimens from the Apuseni Mt. region. By applying molecular barcoding of nrDNA ITS sequences, they identified 109 species (Fig. 1), significantly expanding the known diversity in the area. Notably, 66 of these species were new records for Romania, underscoring the region's rich and previously underexplored fungal biodiversity.

An analysis of global genetic repositories further illustrates this underrepresentation of Romanian data. International sequence databases such as NCBI GenBank and BOLD Systems currently contain over 30,200 ITS sequences of *Cortinarius*. In stark contrast, as of 2025, only 246 ITS sequences originated from Romania, reflecting the country's minimal contribution to global molecular data on the genus. This shortfall underscores the need to prioritize molecular tools: DNA barcoding, multilocus phylogenies, and genomic sequencing to achieve reliable species delimitation and integrate Romanian taxa into broader biogeographic frameworks.

Figure 1. Basidiomata of some *Cortinarius* species previously recorded by morphological methods and later confirmed by molecular analyses: A) *C. bergeronii*, B) *C. anomalus*, C) *C. largus*, D) *C. croceus*, E) *C. elegantissimus*, F) *C. subtortus*, G) *C. sulfurinus*, H) *C. talimultiformis*, I) *C. xanthochlorus*, J) *C. balteatus*, K) *C. calochrous*, L) *C. glaucopus*.

List of Cortinarius species documented in Romania

Based on the published literature data, the checklist documents 231 taxa of *Cortinarius* sensu lato in Romania (Tab. 1), all supported by morphological records; 110 of these are additionally confirmed by molecular analyses, while 121 remain morphology-based only.

Table 1. *Cortinarius* species list in Romania

Species name	Morph.	References	Molec.	References
*Cortinarius acutus (*Pers.) Fr. 1838	x	Bellù *et al.* (2019)	NA	
Cortinarius aereus Rob. Henry 1952	x	Pál-Fám *et al.* (2023)	NA	
*Cortinarius alboviolaceus (*Pers.) Fr. 1838	x	Bellù *et al.* (2019)	x	Szabó *et al. (*2023)
Cortinarius allutus Fr. 1838 (*Phlegmacium allutum* (Fr.) M.M. Moser 1960)	x	Bellù *et al. (*2019)	NA	
*Cortinarius alnetorum (*Velen.) M.M. Moser 1967	x	Bellù *et al. (*2019)	NA	
Cortinarius anfractoides Rob. Henry & Trescol 1987	x	Szabó *et al. (*2023)	x	Szabó *et al. (*2023)
Cortinarius angelesianus A.H. Sm. 1944	x	Bellù *et al. (*2019)	NA	
*Cortinarius anomalus (*Fr.) Fr. 1838	x	Bellù *et al. (*2019)	x	Szabó *et al. (*2023)
Cortinarius anfractus Fr. 1838	x	Eliade (1965)	NA	
*Cortinarius anserinus (*Velen.) Rob. Henry 1986 (*Phlegmacium anserinum* Velen. 1920)	x	Bellù *et al. (*2019), Szász *et al. (*2022)	NA	
Cortinarius arcifolius Rob. Henry 1936	x	Pál-Fám *et al.* (2023)	NA	
Cortinarius arcuatorum Rob. Henry 1939 (*Calonarius arcuatorum (*Rob. Henry) Niskanen & Liimat. 2022)	x	Lupoi (1965), as *C. fulvoincarnatus*	NA	
*Cortinarius arcuatus (*Bull.) Quél. 1883	x	Eliade (1965)	NA	
*Cortinarius argentatus (*Pers.) Fr. 1838	x	Chifu *et al.* (1971)	NA	
Cortinarius argutus Fr. 1838 (*Phlegmacium argutum* (Fr.) Niskanen & Liimat., in Liimatainen, Kim, Pokorny, Kirk, Dentinger & Niskanen 2022)	x	Pál-Fám *et al.* (2023)		
*Cortinarius armeniacus (*Schaeff.) Fr. 1838	x	Eliade (1965)	NA	
*Cortinarius armillatus (*Fr.) Fr. 1838	x	Bellù *et al. (*2019)	NA	
Cortinarius atrovirens Kalchbr. 1874	x	Pop *et al.* (1999)	NA	

Species name	Morph.	References	Molec.	References
Cortinarius aureifolius Peck 1885	x	Pál-Fám *et al.* (2023)	NA	
Cortinarius aureopulverulentus M.M. Moser 1952 (*Calonarius aureopulverulentus* (M.M. Moser) Niskanen & Liimat. 2022)	x	Szabó *et al. (*2023)	x	Szabó *et al. (*2023)
Cortinarius balaustinus Fr. 1838	x	Pop *et al.* (1999)	NA	
Cortinarius balteatocumatilis Rob. Henry 1939 (*Phlegmacium balteatocumatile* (Rob. Henry ex P.D. Orton) Niskanen & Liimat. 2022)	x	Szabó *et al. (*2023)	x	Szabó *et al. (*2023)
Cortinarius balteatus Fr. 1838 *(Phlegmacium balteatum (*Fr.) A. Blytt 1905)	x	Eliade (1965)	x	Szabó *et al. (*2023)
Cortinarius bergeronii (Melot) Melot 1992	x	Bellù *et al. (*2019)	x	Szabó *et al. (*2023)
Cortinarius betulinus J. Favre 1948	x	Pop *et al.* (1999)	NA	
*Cortinarius bivelus (*Fr.) Fr. 1838	x	Todorescu (1972)	NA	
*Cortinarius bolaris (*Pers.) Fr. 1835	x	Pál-Fám *et al.* (2023)	NA	
Cortinarius bovinus Fr. 1838	x	Eliade (1965)	NA	
*Cortinarius brunneus (*Pers.) Fr. 1838	x	Szabó *et al. (*2023)	x	Szabó *et al. (*2023)
Cortinarius bulliardii (Pers.) Fr. 1838	x	Eliade (1965)	x	Szabó *et al. (*2023)
*Cortinarius caerulescens (*Schaeff.) Fr. 1838 (*Phlegmacium caerulescens* (Schaeff.) Wünsche 1877)	x	Eliade (1965)	NA	
Cortinarius caesiophylloides Kytöv., Liimat., Niskanen, Brandrud & Frøslev 2014 (*Thaxterogaster caesiophylloides* (Kytöv., Liimat., Niskanen, Brandrud & Frøslev) Niskanen & Liimat. 2022)	x	Szabó *et al. (*2023)	x	Szabó *et al. (*2023)
Cortinarius caesiostramineus Rob. Henry 1939	x	Pál-Fám *et al.* (2023)	NA	
Cortinarius cagei Melot 1990	x	Bellù *et al. (*2019)	NA	
*Cortinarius callisteus (*Fr.) Fr. 1838 (*Aureonarius callisteus* (Fr.) Niskanen & Liimat. 2022)	x	Popovici (1903)	NA	
*Cortinarius calochrous (*Pers.) Gray 1821 (*Calonarius calochrous* (Pers.) Niskanen & Liimat. 2022)	x	Eliade (1965)	x	Szabó *et al. (*2023)
*Cortinarius camphoratus (*Fr.) Fr. 1838	x	Bellù *et al. (*2019)	x	Szabó *et al. (*2023)

Species name	Morph.	References	Molec.	References
*Cortinarius caninus (*Fr.) Fr. 1838	x	Bellù *et al. (*2019)	x	Szabó *et al. (*2023)
*Cortinarius caperatus (*Pers.) Fr. 1838	x	Bellù *et al. (*2019)	x	Szabó *et al. (*2023)
*Cortinarius castaneus (*Bull.) Fr. 1838	x	Pál-Fám *et al.* (2023)	NA	
Cortinarius catharinae Consiglio 1997 (*Calonarius catharinae* (Consiglio) Niskanen & Liimat. 2022)	x	Szabó *et al. (*2023)	x	Szabó *et al. (*2023)
Cortinarius chrysolitus Kauffman 1915	x	Bellù *et al. (*2019)	NA	
Cortinarius cinereobrunneolus Chevassut & Rob. Henry 1982	x	Szabó *et al. (*2023)	x	Szabó *et al. (*2023)
Cortinarius cinnabarinus Fr. 1838	x	Eliade (1965)	NA	
Cortinarius cinnamomeoluteus P.D. Orton 1960	x	Czihac and Szabó (1975)	NA	
*Cortinarius cinnamomeus (*L.) Gray 1821	x	Eliade (1965)	x	Szabó *et al. (*2023)
Cortinarius cinnamoviolaceus M.M. Moser (1968)	x	Bellù *et al. (*2019)	NA	
Cortinarius citrinofulvescens M.M. Moser 1983	x	Pál-Fám *et al.* (2023)	NA	
Cortinarius citrinus J.E. Lange ex P.D. Orton 1960	x	Pál-Fám *et al.* (2023)	NA	
Cortinarius cliduchus Secr. ex Fr. 1838 (*Phlegmacium cliduchum* (Secr. ex Fr.) Ricken 1912)	x	Pál-Fám *et al.* (2023)	NA	
*Cortinarius claricolor (*Fr.) Fr. 1838 (*Phlegmacium claricolor* (Fr.) A. Blytt 1904)	x	Szabó *et al. (*2023)	x	Szabó *et al. (*2023)
*Cortinarius collinitus (*Sowerby) Gray 1821	x	Eliade (1965)	x	Szabó *et al. (*2023)
Cortinarius collocandoides Reumaux 2009 *(Thaxterogaster collocandoides (*Reumaux) Niskanen & Liimat. 2022)	x	Bellù *et al. (*2019)	x	Szabó *et al. (*2023)
Cortinarius colymbadinus Fr. 1838	x	Szabó *et al. (*2023)	x	Szabó *et al. (*2023)
Cortinarius corrosus Fr. 1838 (*Calonarius corrosus* (Fr.) Niskanen & Liimat. 2022)	x	Szabó *et al. (*2023)	x	Szabó *et al. (*2023)
Cortinarius cotoneus Fr. 1838	x	Tănase and Pop (2001)	NA	
Cortinarius crassus Fr. 1838	x	Pál-Fám *et al.* (2023)	NA	
*Cortinarius croceus (*Schaeff.) Gray 1821	x	Eliade (1965), Bellù *et al.* (2019)	x	Szabó *et al. (*2023)

Species name	Morph.	References	Molec.	References
Cortinarius cucumisporus M.M. Moser 1968 *(Cortinarius diasemospermus* var. *leptospermus* H. Lindstr. 1998)	x	Bellù *et al, (*2019), as *C. diasemospermus* var. *leptospermus*	NA	
Cortinarius crystallinus Fr. 1838	x	Pál-Fám *et al.* (2023)	NA	
Cortinarius cumatilis Fr. 1838 (*Phlegmacium cumatile* (Fr.) Ricken 1912)	x	Bellù *et al. (*2019)	NA	
Cortinarius cupreorufus Brandrud 1994 *(Calonarius cupreorufus* (Brandrud) Niskanen & Liimat. 2022)	x	Eliade (1965), as *C. orichalceus*	NA	
*Cortinarius cyaneus (*Bres.) M.M. Moser 1967	x	Pál-Fám *et al.* (2023)	NA	
Cortinarius cyanites Fr. 1838	x	Pál-Fám *et al.* (2023)	NA	
Cortinarius cypriacus Fr. 1838	x	Pál-Fám *et al.* (2023)	NA	
Cortinarius cyanopus Secr. ex Fr. 1838	x	Eliade (1965)	NA	
Cortinarius damascenus Fr. 1838	x	László (1972)	NA	
*Cortinarius daulnoyae (*Quél.) Sacc. 1910 (*Phlegmacium daulnoyae* (Quél.) Niskanen & Liimat. 2022)	x	Szabó *et al. (*2023)	x	Szabó *et al. (*2023)
Cortinarius deceptivus Kauffman 1905	x	Pál-Fám *et al.* (2023)	NA	
*Cortinarius decoloratus (*Fr.) Fr. 1838	x	Eliade (1965)	NA	
*Cortinarius decumbens (*Pers.) Fr. 1838	x	Eliade (1965)	NA	
Cortinarius delibutus Fr. 1838	x	Bellù *et al. (*2019)	x	Szabó *et al. (*2023)
Cortinarius delibutus aff.	x	Szabó *et al. (*2023), as *C. delibutus* 2	x	Szabó *et al. (*2023), as *C. delibutus* 2
Cortinarius diasemospermus Lamoure 1978	x	Pál-Fám *et al.* (2023)	NA	
Cortinarius dibaphus Fr. 1838 (*Calonarius dibaphus* (Fr.) Niskanen & Liimat. 2022)	x	Tănase and Pop (2001)	NA	
Cortinarius duracinus Fr. 1838	x	Pál-Fám *et al.* (2023)	NA	
Cortinarius eburneus (Velen.) Rob. Henry ex Bon 1958	x	Pál-Fám *et al.* (2023)	NA	
Cortinarius elatior Fr. 1838	x	Tănase and Chifu (2000)	x	Szabó *et al. (*2023)
*Cortinarius elegantior (*Fr.) Fr. 1838 (*Calonarius elegantior* (Fr.) Niskanen & Liimat. 2022)	x	Pop *et al.* (1999)	x	Szabó *et al. (*2023)

Species name	Morph.	References	Molec.	References
Cortinarius elegantissimus Rob. Henry 1943 (*Calonarius elegantissimus* (Rob. Henry) Niskanen & Liimat. 2022)	x	Bellù *et al. (*2019)	x	Szabó *et al. (*2023)
Cortinarius eliae Bidaud, Moënne-Locc. & Reumaux 1996 (*Phlegmacium eliae (*Bidaud, Moënne-Locc. & Reumaux) Niskanen & Liimat. 2022)	x	Szabó et *al. (*2023)	x	Szabó *et al. (*2023)
Cortinarius emunctus Fr. 1838	x	Pál-Fám *et al.* (2023)	NA	
Cortinarius erythrinus (Fr.) Fr. 1838	x	Sălăgeanu (1966)	NA	
Cortinarius eufulmineus Rob. Henry 1952	x	Pál-Fám *et al.* (2023)	NA	
*Cortinarius evernius (*Fr.) Fr. 1838	x	Eliade (1965)	NA	
Cortinarius flavovirens Rob. Henry 1939	x	Pál-Fám *et al.* (2023)	NA	
*Cortinarius flexipes (*Pers.) Fr. 1838	x	Bellù *et al.* (2019)	NA	
Cortinarius fraudulosus Britzelm. 1885 (*Phlegmacium fraudulosum* (Britzelm.) Niskanen & Liimat. 2022)	x	Szabó *et al. (*2023)	x	Szabó *et al. (*2023)
Cortinarius fulgens Fr. 1838	x	Eliade (1965)	NA	
Cortinarius fulminoides (M.M. Moser) M.M. Moser 1967	x	Szabó *et al. (*2023)	x	Szabó *et al. (*2023)
Cortinarius fulvescens Fr. 1838	x	Bellù *et al. (*2019)	NA	
Cortinarius fulvo-ochrascens Rob. Henry 1943 (*Thaxterogaster fulvo-ochrascens* (Rob. Henry) Niskanen & Liimat. 2022)	x	Brandrud *et al. (*2018b)	x	Brandrud *et al. (*2018b)
Cortinarius gallurae D. Antonini, M. Antonini & Consiglio 2005	x	Szabó *et al. (*2023)	x	Szabó *et al. (*2023)
Cortinarius geniculatus Bidaud 2014	x	Szabó *et al. (*2023)	x	Szabó *et al. (*2023)
*Cortinarius gentilis (*Fr.) Fr. 1838	x	Eliade (1965)	x	Szabó *et al. (*2023)
Cortinarius glaucoprasinus (M.M. Moser) M.M. Moser 1967	x	Pál-Fám *et al.* (2023)	NA	
Cortinarius glaucopus (Schaeff.) Gray 1821 (*Phlegmacium glaucopus* (Schaeff.) Wünsche 1877)	x	Eliade (1965)	x	Szabó *et al. (*2023)
Cortinarius glaucopus aff.	x	Szabó *et al. (*2023)	x	Szabó *et al. (*2023)
Cortinarius glaucopus var. *olivaceus (*M.M. Moser) Quadr. 1985 (*Phlegmacium glaucopus* var. *olivaceum* M.M. Moser 1960)	x	Bellù *et al.* (2019)	NA	

Species name	Morph.	References	Molec.	References
Cortinarius hadrocroceus Ammirati, Niskanen, Liimat. & Bojantchev 2014	x	Szabó *et al. (*2023)	x	Szabó *et al. (*2023)
*Cortinarius hemitrichus (*Pers.) Fr. 1838	x	Lupoi (1965)	NA	
*Cortinarius hercynicus (*Pers.) M.M. Moser 1967	x	Pál-Fám *et al.* (2023)	NA	
Cortinarius hillieri Rob. Henry 1938	x	Szabó *et al. (*2023)	x	Szabó *et al. (*2023)
Cortinarius hinnuleus Fr. 1838	x	Eliade (1965)	x	Szabó *et al. (*2023)
*Cortinarius holoxanthus (*M.M. Moser & I. Gruber) Nezdojm. 1980	x	Szabó *et al. (*2023)	x	Szabó *et al. (*2023)
*Cortinarius humicola (*Quél.) Maire 1911	x	Eliade (1965)	NA	
Cortinarius huronensis Ammirati & A.H. Sm. 1972	x	Szabó *et al. (*2023)	x	Szabó *et al. (*2023)
Cortinarius turgidoides Rob. Henry 1981	x	Szabó *et al. (*2023), as *C. hydrotelamonioides* ss	x	Szabó *et al. (*2023), as *C. hydrotelamonioides*
Cortinarius iliopodius (Bull.) Fr. 1838	x	Czihac and Szabó (1975)	NA	
Cortinarius illibatus Fr. 1838	x	Pál-Fám *et al.* (2023)	NA	
Cortinarius illuminus Fr. 1838	x	Bellù *et al.* (2019)	NA	
Cortinarius imbutus Fr. 1838	x	Popovici (1903)	NA	
Cortinarius incognitus Ammirati & A.H. Sm. 1972	x	Szabó *et al. (*2023)	x	Szabó *et al. (*2023)
*Cortinarius infractus (*Pers.) Fr. 1838	x	Eliade (1965)	NA	
Cortinarius ionochlorus Maire 1937 (*Calonarius ionochlorus* (Maire) Niskanen & Liimat. 2022)	x	Bohlin (2003)	NA	
Cortinarius inolens (H. Lindstr.) Bidaud 2010	x	Bellù *et al.* (2019)	NA	
*Cortinarius isabellinus (*Batsch) Fr. 1838	x	Pál-Fám *et al.* (2023)	NA	
Cortinarius kristiniae Brandrud 2017 (*Calonarius kristiniae* (Brandrud) Niskanen & Liimat. 2022)	x	Bellù *et al.* (2019)	NA	
Cortinarius lacustris Moënne-Locc. & Reumaux 1997	x	Szabó *et al. (*2023)	x	Szabó *et al. (*2023)
Cortinarius largus Fr. 1838 *(Phlegmacium largum* Fr. 1877)	x	Eliade (1965)	x	Szabó *et al. (*2023)
*Cortinarius latus (*Pers.) Fr. 1838	x	Pál-Fám *et al.* (2023)	NA	
Cortinarius lebretonii Quél. 1880	x	Bellù *et al. (*2019)	NA	

Species name	Morph.	References	Molec.	References
Cortinarius leproleptopus Chevassut & Rob. Henry 1988	x	Szabó *et al. (*2023)	x	Szabó *et al. (*2023)
*Cortinarius leucopus (*Bull.) Fr. 1838	x	Eliade (1965)	NA	
Cortinarius lilacinovelatus Reumaux & Ramm 2001 (*Calonarius lilacinovelatus* (Reumaux & Ramm) Niskanen & Liimat. 2022)	x	Szabó *et al. (*2023)	x	Szabó *et al. (*2023)
*Cortinarius limonius (*Fr.) Fr. 1838 (*Aureonarius limonius (*Fr.) Niskanen & Liimat. 2022)	x	Eliade (1965)	NA	
*Cortinarius lucorum (*Fr.) E. Berger 1846	x	Tănase and Chifu (2000)	NA	
Cortinarius luridus Rob. Henry 1969	x	Szabó *et al. (*2023)	x	Szabó *et al. (*2023)
Cortinarius lustrabilis Moënne-Locc. 2000 (*Mystinarius lustrabilis (*Moënne-Locc.) Niskanen & Liimat. 2022)	x	Bellù *et al. (*2019)	NA	
Cortinarius magicus aff.	x	Szabó *et al. (*2023)	x	Szabó *et al. (*2023)
Cortinarius magicus Eichhorn 1967 (*Phlegmacium magicum (*Eichhorn) Niskanen & Liimat. 2023)	x	Bellù *et al. (*2019)	x	Szabó *et al. (*2023)
Cortinarius malicorius Fr. 1838	x	Bellù *et al. (*2019)	NA	
Cortinarius masseei Bidaud, Moënne-Locc. & Reumaux 1993	x	Szabó *et al. (*2023)	x	Szabó *et al. (*2023)
Cortinarius melanotus Kalchbr. 1874	x	Pál-Fám *et al.* (2023)	NA	
*Cortinarius mucosus (*Bull.) J. Kickx f. 1867	x	Bellù *et al. (*2019)	NA	
Cortinarius multicolor M.M. Moser 1953	x	Pál-Fám *et al.* (2023)	NA	
Cortinarius multiformis Fr. 1838 (*Thaxterogaster multiformis* (Fr.) Niskanen & Liimat. 2022)	x	Eliade (1965)	x	Szabó *et al. (*2023)
Cortinarius napus Fr. 1838 (*Calonarius napus* (Fr.) Niskanen & Liimat. 2022)	x	Eliade (1965)	x	Szabó *et al. (*2023)
Cortinarius neofurvolaesus Kytöv., Niskanen, Liimat. & H. Lindstr. 2005	x	Szabó *et al. (*2023)	x	Szabó *et al. (*2023)
Cortinarius nigrocuspidatus Kauffman 1923	x	Pál-Fám *et al.* (2023)	NA	
Cortinarius occidentalis A.H. Sm. 1939 (*Thaxterogaster occidentalis* (A.H. Sm.) Niskanen & Liimat., in Liimatainen, Kim, Pokorny, Kirk, Dentinger & Niskanen 2022)	x	Pál-Fám *et al.* (2023)	NA	

Species name	Morph.	References	Molec.	References
Cortinarius ochraceopallescens Moënne-Locc. & Reumaux 2001 (*Calonarius ochraceopallescens* (Moënne-Locc. & Reumaux) Niskanen & Liimat. 2022)	x	Szabó *et al. (*2023)	x	Szabó *et al. (*2023)
*Cortinarius ochroleucus (*Schaeff.) Fr. 1838 (*Thaxterogaster ochroleucus* (Schaeff.) Niskanen & Liimat. 2022)	x	Eliade (1965)	NA	
*Cortinarius odoratus (*Joguet ex M.M. Moser) M.M. Moser 1967 (*Calonarius odoratus* (Joguet ex M.M. Moser) Niskanen & Liimat. 2022)	x	Szabó *et al. (*2023)	x	Szabó *et al. (*2023)
Cortinarius odorifer Britzelm. 1885	x	Pál-Fám *et al.* (2023)	NA	
Cortinarius olearioides Rob. Henry 1987 (*Calonarius olearioides* (Rob. Henry) Niskanen & Liimat. 2022)	x	Bucșa (2007)	x	Szabó *et al. (*2023)
Cortinarius olidoamarus A. Favre 1986 (*Phlegmacium olidoamarum (*A. Favre) Niskanen & Liimat. 2022)	x	Szabó *et al. (*2023)	x	Szabó *et al. (*2023)
Cortinarius ominosus Bidaud 1994	x	Szabó *et al. (*2023)	x	Szabó *et al. (*2023)
Cortinarius orellanus Fr. 1838	x	Ciortan (2013b)	NA	
*Cortinarius orichalceus (*Batsch) Fr. 1838	x	Pál-Fám *et al.* (2023)	NA	
Cortinarius pallidostriatus Rob. Henry 1968	x	Szabó *et al. (*2023)	x	Szabó *et al. (*2023)
Cortinarius pelerinii Bellanger, Carteret & Reumaux 2013	x	Szabó *et al. (*2023)	x	Szabó *et al. (*2023)
Cortinarius percomis Fr. 1838 (*Phlegmacium percome* (Fr.) A. Blytt 1905)	x	Tănase and Pop (2001)	NA	
Cortinarius persoonianus Bidaud 2009	x	Szabó *et al. (*2023)	x	Szabó *et al. (*2023)
*Cortinarius pholideus (*Lilj.) Fr. 1838	x	Bellù *et al. (*2019)	NA	
Cortinarius pilatii Svrček 1968	x	Szabó *et al. (*2023)	x	Szabó *et al. (*2023)
*Cortinarius praestans (*Cordier) Gillet 1876 (*Phlegmacium praestans* (Cordier) M.M. Moser 1960)	x	Eliade (1965)	NA	
*Cortinarius prasinus (*Schaeff.) Fr. 1838 (*Calonarius prasinus* (Schaeff.) Niskanen & Liimat. 2022)	x	Eliade (1965)	NA	
Cortinarius pruinatus Bidaud, Moënne-Locc. & Reumaux 1993	x	Szabó *et al. (*2023)	x	Szabó *et al. (*2023)

Species name	Morph.	References	Molec.	References
Cortinarius pseudodaulnoyae Rob. Henry & Ramm 1991 (*Phlegmacium pseudodaulnoyae* (Rob. Henry & Ramm) Niskanen & Liimat. 2022)	x	Szabó *et al. (*2023)	x	Szabó *et al. (*2023)
Cortinarius pseudofervidus Niskanen, Liimat., Ammirati & Kytöv. 2014	x	Szabó *et al. (*2023)	x	Szabó *et al. (*2023)
Cortinarius pseudonaevosus Rob. Henry 1957 (*Phlegmacium pseudonaevosum (*Rob. Henry) Brandrud, Dima, Saar & Schmidt-Stohn 2022)	x	Szabó *et al. (*2023)	x	Szabó *et al. (*2023)
Cortinarius purpurascens Fr. 1838 (*Thaxterogaster purpurascens* (Fr.) Niskanen & Liimat. 2022)	x	Eliade (1965)	x	Szabó *et al. (*2023)
Cortinarius purpureus (Bull.) Bidaud, Moënne-Locc. & Reumaux 1994	x	Bellù *et al. (*2019)	NA	
Cortinarius quarciticus H. Lindstr. 1994	x	Bellù *et al. (*2019)	NA	
Cortinarius radicosissimus Moënne-Locc. 1997	x	Szabó *et al. (*2023)	x	Szabó *et al. (*2023)
Cortinarius renidens Fr. 1838 (*Hygronarius renidens* (Fr.) Niskanen & Liimat. 2022)	x	Szabó *et al. (*2023)	x	Szabó *et al. (*2023)
*Cortinarius riederi (*Weinm.) Fr. 1838 (*Thaxterogaster riederi* (Weinm.) Niskanen & Liimat. 2022)	x	Bellù *et al. (*2019)	NA	
*Cortinarius rigens (*Pers.) Fr. 1838	x	László (1972)	NA	
Cortinarius rubellus Cooke 1887	x	Chinan (2010)	x	Szabó *et al. (*2023)
*Cortinarius rubricosus (*Fr.) Fr. 1838	x	Szabó *et al. (*2023)	x	Szabó *et al. (*2023)
*Cortinarius rubrophyllus (*Moënne-Locc.) Liimat., Niskanen, Ammirati & Dima 2014	x	Szabó *et al. (*2023)	x	Szabó *et al. (*2023)
Cortinarius rufoallutus Rob. Henry ex Bidaud & Reumaux 2006 (*Thaxterogaster rufoallutus* (Rob. Henry ex Bidaud & Reumaux) Niskanen & Liimat. 2022)	x	Szabó *et al. (*2023)	x	Szabó *et al. (*2023)
*Cortinarius rufo-olivaceus (*Pers.) Fr. 1838 (*Calonarius rufo-olivaceus* (Pers.) Niskanen & Liimat 2022)	x	Eliade (1965)	NA	
Cortinarius rusticus P. Karst. 1883	x	Pál-Fám *et al.* (2023)	NA	

Species name	Morph.	References	Molec.	References
*Cortinarius saginus (*Fr.) Fr. 1838 (*Phlegmacium saginum* (Fr.) Ricken 1912)	x	Szabó *et al. (*2023)	x	Szabó *et al. (*2023)
Cortinarius salor Fr. 1838	x	Eliade (1965)	x	Szabó *et al. (*2023)
*Cortinarius sanguineus (*Wulfen) Gray 1821	x	Bellù *et al. (*2019)	NA	
*Cortinarius saniosus (*Fr.) Fr. 1838	x	Pál-Fám *et al.* (2023)	NA	
Cortinarius saporatus Britzelm. 1897 (*Calonarius saporatus* (Britzelm.) Niskanen & Liimat. 2022)	x	Szabó *et al. (*2023)	x	Szabó *et al. (*2023)
Cortinarius scandens Fr. 1838	x	Pál-Fám *et al.* (2023)	NA	
Cortinarius scaurocaninus Chevassut & Rob. Henry 1982 (*Phlegmacium scaurocaninum* (Chevassut & Rob. Henry) Niskanen & Liimat. 2022)	x	Szabó *et al. (*2023)	x	Szabó *et al. (*2023)
*Cortinarius scaurus (*Fr.) Fr. 1838 (*Thaxterogaster scaurus (*Fr.) Niskanen & Liimat. 2022)	x	Eliade (1965)	NA	
Cortinarius semisanguineus (Fr.) Gillet 1876	x	Eliade (1965), Bellù *et al. (*2019)	x	Szabó *et al. (*2023)
Cortinarius semivelatus Rob. Henry 1970	x	Szabó *et al. (*2023)	x	Szabó *et al. (*2023)
Cortinarius sodagnitus Rob. Henry 1935 (*Calonarius sodagnitus* (Rob. Henry) Niskanen & Liimat. 2022)	x	Szabó *et al. (*2023)	x	Szabó *et al. (*2023)
Cortinarius spadicellus Brandrud 1997 (*Phlegmacium spadicellum* M.M. Moser 1960)	x	Szabó *et al. (*2023)	x	Szabó *et al. (*2023)
Cortinarius sphagnophilus Peck 1878 (*Thaxterogaster sphagnophilus* (Peck) Niskanen & Liimat. 2022)	x	Bellù *et al. (*2019)	NA	
Cortinarius splendens Rob. Henry 1936	x	Pál-Fám *et al.* (2023)	NA	
Cortinarius spilomeus (Fr.) Fr. 1863	x	Bellù *et al. (*2019)	x	Szabó *et al. (*2023)
Cortinarius stillatitius Fr. 1838	x	Popovici (1903)	NA	
Cortinarius subargyronotus Niskanen, Liimat. & Kytöv. 2014	x	Szabó *et al. (*2023)	x	Szabó *et al. (*2023)
Cortinarius subdecolorans M. Langl. & Reumaux 2000 (*Phlegmacium subdecolorans* (M. Langl. & Reumaux) Niskanen & Liimat. 2022)	x	Szabó *et al. (*2023)	x	Szabó *et al. (*2023)

Species name	Morph.	References	Molec.	References
Cortinarius suberi Soop 1990	x	Bellù *et al.* (2019)	NA	
Cortinarius subferrugineus (Batsch) Fr. 1838	x	Pál-Fám *et al.* (2023)	NA	
Cortinarius subfoetens M.M. Moser & McKnight 1995 (*Phlegmacium subfoetens* (M.M. Moser & McKnight) Niskanen & Liimat. 2022)	x	Szabó *et al.* (2023)	x	Szabó *et al.* (2023)
Cortinarius subfulgens P.D. Orton 1960	x	Elekes *et al.* (2014)	NA	
Cortinarius sublilacinopes aff.	x	Szabó *et al.* (2023)	x	Szabó *et al.* (2023)
Cortinarius subparvannulatus Moënne-Locc. & Fillion 2010	x	Bellù *et al.* (2019)	x	Szabó *et al.* (2023)
Cortinarius subporphyropus Pilát 1954 (*Thaxterogaster subporphyropus* (Pilát) Niskanen & Liimat. 2022)	x	Szabó *et al.* (2023)	x	Szabó *et al.* (2023)
Cortinarius subpurpurascens (Batsch) E. Berger 1846 (*Thaxterogaster subpurpurascens* (Batsch) Niskanen & Liimat. 2022)	x	Szabó *et al.* (2023)	x	Szabó *et al.* (2023)
Cortinarius subtortus (Pers.) Fr. 1838	x	Bellù *et al.* (2019)	x	Szabó *et al.* (2023)
Cortinarius sulfurinus Quél. 1884 (*Calonarius sulfurinus* (Quél.) Niskanen & Liimat. 2022)	x	Bellù *et al.* (2019)	x	Szabó *et al.* (2023)
Cortinarius tabularis (Fr.) Fr. 1838	x	Tănase and Chifu (2000)	NA	
Cortinarius talimultiformis Kytöv., Liimat., Niskanen, A.F.S. Taylor & Seslı 2014 (*Thaxterogaster talimultiformis* (Kytöv., Liimat., Niskanen, A.F.S. Taylor és Seslı) Niskanen & Liimat. 2022)	x	Bellù *et al.* (2019)	x	Szabó *et al.* (2023)
Cortinarius talus Fr. 1838 (*Thaxterogaster talus* (Fr.) Niskanen & Liimat. 2022)	x	Bellù *et al.* (2019)	NA	
Cortinarius testaceomicaceus Bidaud 2014	x	Szabó *et al.* (2023)	x	Szabó *et al.* (2023)
Cortinarius tirolianus Bidaud, Moënne-Locc. & Reumaux 2005 (*Phlegmacium tirolianum* (Bidaud, Moënne-Locc. & Reumaux) Niskanen & Liimat. 2022)	x	Szabó *et al.* (2023)	x	Szabó *et al.* (2023)
Cortinarius tofaceus Fr. 1838 (*Aureonarius tofaceus* (Fr.) Niskanen & Liimat., in Liimatainen, Kim, Pokorny, Kirk, Dentinger & Niskanen 2022)	x	Pál-Fám *et al.* (2023)	NA	

Species name	Morph.	References	Molec.	References
Cortinarius torvus (Fr.) Fr. 1838	x	Eliade (1965)	x	Szabó *et al.* (2023)
Cortinarius traganus (Fr.) Fr. 1838	x	Eliade (1965)	x	Szabó *et al.* (2023)
Cortinarius triformis Fr. 1838	x	Pál-Fám *et al.* (2023)	NA	
Cortinarius trivialis J.E. Lange 1940	x	Popovici (1903)	NA	
Cortinarius trivialis aff.	x	Szabó *et al.* (2023), as *C. trivialis* 2	x	Szabó *et al.* (2023), as *C.trivialis* 2
Cortinarius tubarius Ammirati & A.H. Sm. 1972	x	Bellù *et al.* (2019)	NA	
Cortinarius turbinatus (Bull.) Fr. 1838	x	Eliade (1965)	NA	
Cortinarius turgidus Fr. 1838	x	Bellù *et al.* (2019)	x	Szabó *et al.* (2023)
Cortinarius turmalis Fr. 1838 (*Thaxterogaster turmalis* (Fr.) Niskanen & Liimat. 2022)	x	Eliade (1965)	x	Szabó *et al.* (2023)
Cortinarius ultrodistortus Rob. Henry & Vagnet 1992	x	Szabó *et al.* (2023)	x	Szabó *et al.* (2023)
Cortinarius uraceus Fr. 1838	x	Pál-Fám *et al.* (2023)	NA	
Cortinarius uraceonemoralis Niskanen, Liimat., Dima, Kytöv., Bojantchev & H. Lindstr. 2014	x	Szabó *et al.* (2023)	x	Szabó *et al.* (2023)
Cortinarius urbicus (Fr.) Fr. 1838	x	Pál-Fám *et al.* (2023)	NA	
Cortinarius variecolor (Pers.) Fr. 1838 (*Phlegmacium variecolor* (Pers.) Wünsche 1877)	x	Eliade (1965)	x	Szabó *et al.* (2023)
Cortinarius varius (Schaeff.) Fr. 1838 (*Phlegmacium varium* (Schaeff.) Wünsche 1877)	x	Eliade (1965)	x	Szabó *et al.* (2023)
Cortinarius venetus (Fr.) Fr. 1838	x	Eliade (1965)	x	Szabó *et al.* (2023)
Cortinarius vibratilis (Fr.) Fr. 1838 (*Thaxterogaster vibratilis* (Fr.) Niskanen & Liimat. 2022)	x	Eliade (1965)	NA	
Cortinarius vibratilis aff.	x	Szabó *et al.* (2023)	x	Szabó *et al.* (2023)
Cortinarius violaceocinereus (Pers.) Fr. 1838	x	Pál-Fám *et al.* (2023)	NA	
Cortinarius violaceus (L.) Gray 1821	x	Eliade (1965)	x	Szabó *et al.* (2023)
Cortinarius vulpinus (Velen.) Rob. Henry 1947 (*Phlegmacium vulpinum* (Velen.) Niskanen & Liimat. 2022)	x	Bellù *et al.* (2019)	NA	
Cortinarius xanthochlorus Rob. Henry 1966 (*Calonarius xanthochlorus* (Rob. Henry) Niskanen & Liimat. 2022)	x	Bellù *et al.* (2019)	x	Szabó *et al.* (2023)

Table legend: x = available; NA = not available.

Cortinarius sample distribution based on literature review

After analyzing the spatial distribution of the recorded samples in Romania using a Kernel Density Estimate (KDE) of site coordinates projected in EPSG:3857, two major hotspots of collection activity become evident (Fig. 2). The KDE is visualized as filled contours, where the color gradient from blue to orange indicates increasing density of sampling sites, while individual locations are marked as black points. The results reveal two dominant clusters: one in the Apuseni Mountains and another in the Transylvanian Basin. These patterns reflect the research focus of previous studies, with the Transylvanian Basin being intensively surveyed during multiple mycological camps and congresses led by Pál-Fám and collaborators, while the Apuseni region was extensively explored by Szabó and her team as part of their molecular taxonomic investigations.

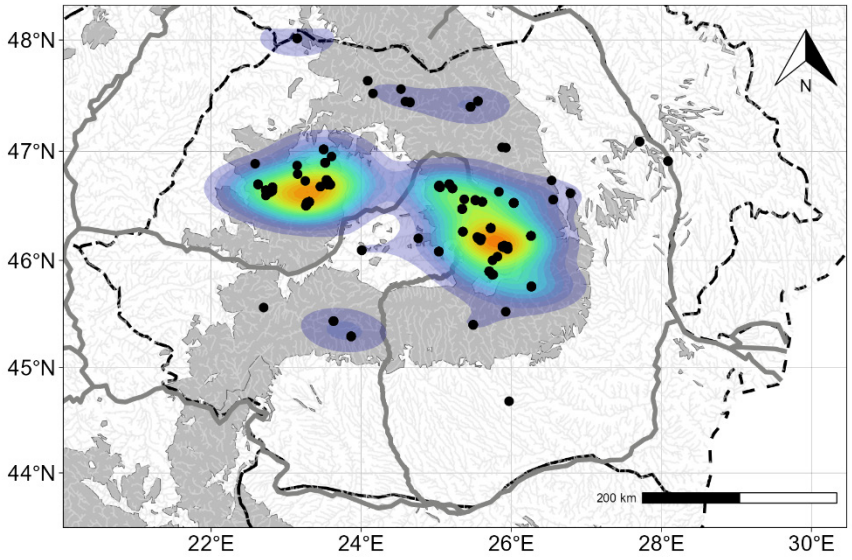

Figure 2. *Cortinarius* sample distribution based on literature review. The map was made in R (v4.4.3) using the ggplot2 (v3.5.1), sf (1.0-19) and maptiles (0.9.0) packages.

Conclusions

This first comprehensive checklist of *Cortinarius* sensu lato in Romania documents 231 taxa. All species are supported by morphological records, with 110 have also confirmed by molecular analyses, reflecting the growing role of DNA-based methods in regional cortinarioid research. The remaining 121 taxa

are still supported exclusively by morphology, underscoring the need for further molecular validation. Several unidentified species were documented: *Cortinarius* aff. *delibutus*, *C.* aff. *glaucopus*, *C.* aff. *magicus*, *C.* aff. *sublilacinopes*, *C.* aff. *trivialis*, and *C.* aff. *vibratilis*. These taxa differ from related species not only in their morphological appearance but also in their molecular characteristics, indicating that further taxonomic and nomenclatural investigations are needed to clarify their taxonomic status and name them properly.

These findings highlight Romania as a region of considerable cortinarioid diversity, though it remains underrepresented in global sequence repositories. The current geographic bias toward the Apuseni Mountains and the Transylvanian Basin emphasizes the need for systematic surveys in underexplored regions. Future research integrating morphology, ecology, and molecular systematics will be essential to refine species boundaries, strengthen conservation assessments, and fully document the ecological role of *Cortinarius* in Romanian forests

Acknowledgements. Grammatical corrections and language polishing were performed with the assistance of ChatGPT (OpenAI, 2025). No content generation or interpretation was carried out by the AI tool.

References

Barr, D.J.S. (2001). Chytridiomycota. *Systematics and Evolution: Part A, Second Edition*, 93–112. http://doi.org/10.1007/978-3-662-10376-0_5

Bellù, F., Zsigmond Gy. & Szász B. (2019). Liste der Cortinarienfunde während den Journées Européennes du Cortinaire in Bálványos. *Journal des JEC 81*, 80.

Berbee, M.L. & Taylor, J.W. (2001). Fungal molecular evolution: gene trees and geologic time. *Systematics and Evolution*, 229–245. http://doi.org/10.1007/978-3-662-10189-6_10

Bidaud, A.P., Moënne-Loccoz,P. & Reumaux, P. (1994). *Atlas des Cortinaires: Clé générale des sous-genres, sections, sous-sections et séries*. Annecy, France: Editions Fédération Mycologique Dauphiné-Savoie.

Bidaud, A., Loizides, M., Armada, F., Reyes, J.D.D., Carteret, X., Corriol, G., Consiglio, G., Reumaux,P., Bellanger, J.M. (2021). *Cortinarius* subgenus Leprocybe in Europe: expanded Sanger and next generation sequencing unveil unexpected diversity in the Mediterranean. *Persoonia. 46,* 188-215 https://doi.org/10.3767/persoonia.2021.46.07

Bîrsan, C., Tănase, C. & Mardari, C. (2013). Variation of macromycetes species composition in two forest habitats from Giumalău Massif (Eastern Carpathians, Romania). *Journal of Plant Development 20(1)*, 79–103.

Bohlin, A., Senn-Irlet, B. (2003). European Council for the Conservation of Fungi 13 – December 2003.

Bontea, V. (1985). Ciuperci parazite şi saprofite din România, vol. 1. *Academia Republicii Socialiste Romania*.

Bontea, V. (1986). Ciuperci parazite şi saprofite din România, vol. 2. *Academia Republicii Socialiste Romania*.

Brandrud, T.E., Lindström, H., Marklund, H., Melot, J. & Muskos, S. (1990). *Cortinarius*, Flora Photographica, vol. 1., *Cortinarius HB*. Matfors, Sweden.

Brandrud, T.E., Lindström, H., Marklund, H., Melot, J. & Muskos, S. (1992). *Cortinarius*, Flora Photographica, vol. 2. *Cortinarius HB*. Matfors, Sweden

Brandrud, T.E., Lindström, H., Marklund, H., Melot, J. & Muskos, S. (1998). *Cortinarius*, Flora Photographica. vol. 4. *Cortinarius HB*. Matfors, Sweden

Brandrud, T.E. (1996). *Cortinarius* subgenus Phlegmacium section Phlegmacium in Europe: descriptive part. *Edinburgh Journal of Botany 53(3)*: 331–400. https://doi.org/10.1017/S0960428600003772

Brandrud, T.E., Schmidt-Stohn, G.& Dima, B. (2019). *Cortinarius hildegardiae* and *C. mariekristinae* spp. nov., two new species in the Phlegmacioid clade Humolentes (Sect. Calochroi s. l.). *Sydowia-Horn 71(115)*, https://doi.org/10.12905/0380.sydowia71-2019-0115

Brandrud, T.E. & Dima, B. (2014). *Cortinarius* subgenus Phlegmacium section Multiformes in Europe. J. *Des J.E.C 16,* 162–199.

Brandrud, T.E., Schmidt-Stohn, G., Liimatainen, K., Niskanen, T., Frøslev, T.G., Soop, K., Bojantechev, D., Kytövuori, I., Stjernegaard Jeppsen, T., Bellù, F., Saar, G., Oertel, B., Ali, T., Thines, M. & Dima, B. (2018a). *Cortinarius* sect. Riederi: taxonomy and phylogeny of the new section with European and North American distribution. *Mycological Progress 17(12)*, 1323–1354. http://dx.doi.org/10.1007/s11557-018-1443-0

Brandrud, T.E., Frøslev, T.G. & Dima, B. (2018b). Rare, whitish–pale ochre *Cortinarius* species of sect. Calochroi from calcareous Tilia forests in South East Norway. *Agarica 38(0349)*, 3–20. https://hdl.handle.net/11250/2503628

Brandrud, T.E., Lindström, H., Marklund, H., Melot, J. & Muskos, S. (1995). *Cortinarius* Flora Photographica. *Ed. R. Watling. Edinburgh:* Royal Botanic Garden.

Bucşa, L. (2007). Macromycetes of the Breite Nature Reserve of ancient oaks (Transylvania, Romania). *Transylv. Rev. Syst. Ecol. Res 4*, 33.

Chifu, T., Toma, M. & Dăscălescu, D. (1971). Contribuţii la cunoaşterea macromicetelor din Moldova*. Iaşi: Com. Şt., Inst. Pedag.*

Chinan, V. (2010). Macrofungi from „Tinovul de la Românești" peat bog (Dornelor Depression, Romania). *AAB Bioflux 2(1)*, 65–70.

Chinan, V. & Manzu, C. (2014). Macrofungal diversity of a peat bog from Dorna Depression (Eastern Carpathians, Romania). *Analele Ştiinţifice ale Universităţii "Al. I. Cuza" Iaşi s. II a Biologie vegetală 60(2),* 43–52.

Chinan, V. & Tănase, C. (2008). Coenological observations referring to macromycetes from peat bogs situated in Eastern Carpathians (Romania). 8th International Scientific Conference on Modern Management of Mine Producing, Geology and Environmental Protection, *SGEM 2*, 83–90.

Ciortan, I. 2013a. Contributions to the mycobiota knowledge of spruce forests from Obârşia Lotrului Health Resort (Romania). *Forestry and Biotechnology 17(4)*, 16–21.

Ciortan, I. (2013b). The taxonomic diversity of the macromycetes from Căpăţânii Mountains (Romania). *Forestry and Biotechnology 17(1)*, 41–50.

Czihac, J. & Szabó, J. (1975). Heil- und Nahrungsmittel, Farbstoffe, Nutz- und Hausgeräte welche Ost-Romänien, Moldauer und Valachen aus dem Pflanzenreiche gewinnen. *Flora oder allgemeine botanische Zeitung* XXI*(20)*, 308–315.

Dima, B., Liimatainen, K., Niskanen, T., Kytövuori, I. & Bojantchev, D. (2014). Two new species of *Cortinarius*, subgenus Telamonia, sections Colymbadini and Uracei, from Europe. *Mycological Progress 13(3),* 867–879. https://doi.org/10.1007/s11557-014-0970-6

Dima, B., Lindström, H., Liimatainen, K., Olson, Å., Soop, K., Kytövuori, I., Dahlberg, A. & Niskanen, T. (2016). Typification of Friesian names in *Cortinarius* sections Anomali, Spilomei, and Bolares, and description of two new species from Northern Europe. *Mycological Progress 15(9),* 903–919. http://dx.doi.org/10.1007/s11557-016-1217-5

Elekes, C.C. & Busuioc, G. (2010). The mycoremediation of metals polluted soils using wild growing species of mushrooms. In: *International Conference on Engineering Education and International Conference on Education and Educational Technologies – Proceedings* 36–39.

Elekes, C.C., Busuioc, G. & Dumitriu, I. (2014). Bioaccumulation and translocation factors of some wild growing mushrooms species of *Cortinarius* genus. 464–468.

Eliade, E. 1965. *Conspectul macromicetelor din România.* Bucureşti: Lucrările Grădinii Botanice din Bucureşti.

Fries, E.M. (1838). Epicrisis Systematis Mycologici seu Synopsis Hymenomycetum, *Typographia Academica.* Uppsala, Sweden.

Fries, E.M. 1821. Systema Mycologicum. *Lundae: Ex Officina Berlingiana*. Uppsala, Sweden.

Frøslev, T. G., Jeppesen, T.S. and B. Dima. 2015. *Cortinarius* koldingensis—a new species of *Cortinarius*, subgenus Phlegmacium related to *Cortinarius* sulfurinus. *Mycological Progress* 14(73).

Frøslev, T. G., Jeppesen, T. S., Læssøe, T. & Kjøller, R. (2007). Molecular phylogenetics and delimitation of species in *Cortinarius* section Calochroi (Basidiomycota, Agaricales) in Europe. *Molecular Phylogenetics and Evolution 44(1),* 217–227. https://doi.org/10.1016/j.ympev.2006.11.013

Frøslev, T.G., Brandrud, T.E. & Dima, B. (2017). *Cortinarius stjernegaardii* and *C. kristinae* (Basidiomycota, Agaricales), two new European species with a mainly northern distribution. *Mycological Progress 16(2)*, 145–153. http://dx.doi.org/10.1007/s11557-016-1264-y

Fuss, M. (1866). Flora Transilvaniei, V. Sibiu*: Typis Haeredum Georgii de Closius,* Sibiu. Gallone, B., Kuyper, T.W. & Nuytinck.J. (2024). The genus *Cortinarius* should not (yet) be split. *IMA Fungus* 15(1). https://doi.org/10.1186/s43008-024-00159-4

Garnica, S., Weiß, M., Oertel, B.,Ammirati, J. & Oberwinkler, F. (2009). Phylogenetic relationships in *Cortinarius*, section Calochroi, inferred from nuclear DNA sequences. *BMC Evolutionary Biology 9(1)*, 1–17. https://doi.org/10.1186/1471-2148-9-1

Garnica, S., Weiß, M., Oertel, B. & Oberwinkler, F. (2003). Phylogenetic relationships of European Phlegmacium species (*Cortinarius*, Agaricales). *Mycologia 95(6)*, 1155–1170. https://doi.org/10.1080/15572536.2004.11833025

Garnica, S., Weiß, M., Oertel, B. & Oberwinkler, F. (2005). A framework for a phylogenetic classification in the genus *Cortinarius* (Basidiomycota, Agaricales) derived from morphological and molecular data. *Canadian Journal of Botany 83(11)*, 1457–1477. https://doi.org/10.1139/b05-107

Garnica, S., Spahn, P., Oertel, B., Ammirati, J. & Oberwinkler, F. (2011). Tracking the evolutionary history of *Cortinarius* species in section Calochroi, with transoceanic disjunct distributions. *BMC Evolutionary Biology 11(1)*, 1–19.

Garrido-Benavent, I., Ballara, J. & Mahiques, R. (2015). New insights into subg. Phlegmacium sect. Calochroi: adding morphological and molecular data from Mediterranean representatives, with special regard to *Cortinarius* prasinus, C. natalis and C. murellensis species complexes. *Journal des JEC 17*, 38–78.

Kirk, P. M., Cannon, P.F., Minter, D.W. & Stalpers, J.A. (2008). Dictionary of the Fungi, *10th edn. CAB International*. Wallingford, UK.

László, K. 1972. Noi contribuţii la cunoaşterea macromicetelor din R.S. România. *Aluta* 41–60.

Li, Y., Steenwyk, J.L., Chang, Y., Wang, Y., James, T.Y., Stajich, J.E., Spatafora, J.W., Groenewald, M., Dunn, C.W., Hittinger, C.T., Shen, X.X. & Rokas, A. (2021). A genome-scale phylogeny of the kingdom Fungi. *Current Biology 31(8)*, 1653–1665.e5. https://doi.org/10.1016/j.cub.2021.01.074

Liimatainen, K. (2013). Towards a better understanding of the systematics and diversity of *Cortinarius*, with an emphasis on species growing in boreal and temperate zones of Europe and North America. *Faculty of Biological and Environmental Sciences Department of Biosciences Plant Biology. University of Helsinki*, Finland

Liimatainen, K., Niskanen, T., Dima, B., Kytövuori, I., Ammirati, J.F. & Frøslev, T. G. (2014). The largest type study of Agaricales species to date: bringing identification and nomenclature of Phlegmacium (*Cortinarius*) into the DNA era. *Persoonia: Molecular Phylogeny and Evolution of Fungi 33*, 98–140. https://doi.org/10.3767/003158514X684681

Liimatainen, K., Niskanen, T., Dima, B., Ammirati, B., Kirk, P.M. & Kytövuori, I. (2020). Mission impossible completed: unlocking the nomenclature of the largest and most complicated subgenus of *Cortinarius*, Telamonia, *Fungal Diversity*. https://doi.org/10.1007/s13225-020-00459-1

Liimatainen, K., Kim, J.T., Pokorny, L., Kirk, P.M., Dentinger, B. & Niskanen, T. (2022). Taming the beast: a revised classification of Cortinariaceae based on genomic data: revised classification of Cortinariaceae based on genomic data. *Fungal Diversity*. https://doi.org/10.1007/s13225-022-00499-9

Liu, Y. J., Rogers, S.O. & Ammirati, J.F. (1997). Phylogenetic relationships in Dermocybe and related *Cortinarius* taxa based on nuclear ribosomal DNA internal transcribed spacers. *Canadian Journal of Botany 75(4)*, 519–532. https://doi.org/10.1139/b97-058

Lupoi, A. (1965). Materiale pentru flora micologică a Munţilor Lăpuş. *Contrib. Bot., Univ. Babeş-Bolyai Cluj-Napoca*: 71–74.

Mátyus, I. (1787). Ó és Új diaetetica az az: az életnek és egésségnek fenn-tartására és gyámolgatására, Istentől adattatott nevezetesebb természeti eszközöknek való elszámlálása. *Landerer,* Pozsony. http://hdl.handle.net/123456789/191

Moënne-Loccoz, P., Reumaux, P. and Bidaud, A. 1990. *Atlas des Cortinaires 1.* Annecy, France: Editions F.

Moser, M. (1983). Die Rőhlinge und Blätterpilze, Band IIb, *Kleine Kryptogamenflora.* Stuttgart, Germany

Moser, M. & Horak, E. (1975). *Cortinarius* Fr. und nahe verwandte Gattungen. *Südamerika. 116*.

Niskanen, T., Liimatainen, K., Kytövuori, I., Lindström, H., Dentinger, B.T.M. & Ammirati, J.F. (2016). *Cortinarius* subgenus Callistei in North America and Europe—type studies, diversity, and distribution of species. *Mycologia 108(5)*,1018–1027. https://doi.org/10.3852/16-033

Niskanen, T., Kytövuori,I. & Liimatainen, K. (2009). *Cortinarius* sect. Brunnei (Basidiomycota, Agaricales) in North Europe. *Mycological Research 113(2)*, 182–206. https://doi.org/10.1016/j.mycres.2008.10.006

Niskanen, T., Kytövuori,I. & Liimatainen, K. (2011). *Cortinarius* sect. Armillati in Northern Europe. *Mycologia 103(5)*, 1080–1101. https://doi.org/10.3852/10-350

Niskanen, T., Kytövuori, I., Liimatainen, K. & Lindström, H. (2013). The species of *Cortinarius*, section Bovini, associated with conifers in Northern Europe. *Mycologia 105(4)*, 977–993. https://doi.org/10.3852/12-320

Niskanen, T., Laine, S., Liimatainen, K. & Kytövuori.I. (2012). *Cortinarius* sanguineus and equally red species in Europe with an emphasis on Northern European material. *Mycologia 104(1)*, 242–253. https://doi.org/10.3852/11-137

Niskanen, T., Liimatainen, K. & Kytövuori, I. (2008). Two new species in *Cortinarius* subgenus Telamonia, *Cortinarius* brunneifolius and C. leiocastaneus, from Fennoscandia (Basidiomycota, Agaricales). *Mycological Progress 7(4)*, 239–24. https://doi.org/10.5852/ejt.2024.970.2747

Pál-Fám, F. (1997). Adatok a Baróti-Hegység Nagygombáinak Ismeretéhez. 2. *Clusiana.*

Pál-Fám, F., Benedek, L., Szász, B. & Szilvásy, E. (2022). "Adatok a Gyergyói-Havasok, Görgényi-Havasok És a Hargita-Hegység Nagygombáinak Ismeretéhez." *Moeszia 11–12,* 53–58.

Pál-Fám, F., Fődi, F., Oross, K. & Benedek, L. (2022). Adatok Bálványos Környéke, a Szent Anna-Tó Környéke És a Lucs Nagygombáinak Ismeretéhez. *Moeszia 11–12*, 60–71.

Pál-Fám, F., Oross, K. & Fedor, I. (2022). Adatok Székelyvarság Környéke És a Hargita Nagygombáinak Ismeretéhez. *Moeszia 11–12*, 89–97.

Pál-Fám, F., Oross, K., Fődi, A. & Benedek, L. (2022a). A Lápos-Vidék (Máramaros) Nagygombáinak Ismeretéhez. *Moeszia 11–12*, 82–89.

Pál-Fám, F., Oross, K., Fődi, A. & Benedek, L. (2022b). Adatok a Görgényi- És a Gyergyói-Havasok Nagygombáinak Ismeretéhez. *Moeszia 11–12*, 71–80.

Pál-Fám, F., Szász, B. & Benedek, L. (2023) Checklist and habitats of macrofungi of Székelyland, Transylvania, Romania. *Moeszia 13-14,* 3-76

Peintner, U., Bougher, N.L., Castellano, M.A., Moncalvo, J.M., Moser, M.M., Trappe, J.M. & Vilgalys, R. (2001). Multiple origins of sequestrate fungi related to *Cortinarius* (Cortinariaceae). *American Journal of Botany 88(12)*, 2168–79. https://doi.org/10.2307/3558378

Peintner, U., Horak, E., Moser, M.M. & Vilgalys, R. (2002). Phylogeny of *Rozites, Cuphocybe* and *Rapacea* inferred from ITS and LSU RDNA sequences. *Mycologia 94(4)*, 620–29. https://doi.org/10.1080/15572536.2003.11833190

Peintner, U., Moncalvo, J.M. & Vilgalys, R. (2004). Toward a better understanding of the infrageneric relationships in *Cortinarius* (Agaricales, Basidiomycota). *Mycologia 96(5)*, 1042–58. https://doi.org/10.1080/15572536.2005.11832904

Pop, A., Tănase, C., Negrean, G., Buscă, L. & Toma, D. Contribuţii la studiul macromicetelor din Masivul Rarău. *Buletinul Grădinii Botanice Iaşi 8*, 37-44

Popovici, A. (1903). Contribution à la flore micologique de la Romanie. *Ann. Sci. Univ. De Jassy 2*, 31–44.

Roskov, Y., Ower, G., Orrell, T., Nicolson, D., Bailly, N., Kirk, P.M., Bourgoin, T., DeWalt, R.E., Decock, W., Nieukerken, E., Zarucchi, J. & Penev, L. (2019). Species 2000 & ITIS Catalogue of Life, 2019 Annual Checklist. *Digital resource at www.catalogueoflife.org/annual-checklist/2019. Species 2000: Naturalis, Leiden, the Netherlands.* (2405-884X).

Sălăgeanu, A. (1966). Macromicete Din Grădina Botanică a Universităţii Din Cluj. *Contribuţii Botanice, Universitatea „Babeş-Bolyai" Cluj-Napoca*: 95–108.

Sántha, T. (1999). A Székelyföld Nagygomba-Világának Kutatása. *ACTA I*, 29–48.

Singer, R. (1986). The Agaricals in Modern Taxonomy. *Seven Koel* 1-478.

Soop, K., Dima, B., Cooper, J.A., Park, D. & Oertel, B. (2019). A Phylogenetic Approach to a Global Supraspecific Taxonomy of *Cortinarius* (Agaricales) with an Emphasis on the Southern Mycota. *Persoonia: Molecular Phylogeny and Evolution of Fungi 42*, 261–90. https://doi.org/10.3767/persoonia.2019.42.10

Suárez-Santiago, V.N., Ortega, A., Peintner, U. & López-Flores, I.. (2009). Study on *Cortinarius* Subgenus Telamonia Section Hydrocybe in Europe, with Especial Emphasis on Mediterranean Taxa. *Mycological Research 113(10)*, 1070–90. https://doi.org/10.1016/j.mycres.2009.07.006

Szász, B. (2022). Újabb adatok Olthévíz és környéke nagygombáinak ismeretéhez II. *Moeszia 11–12*, 34–51.

Szász, B., Benedek, L., Pál-Fám, F. & Zsigmond, Gy. (2022). A Bálványosi Európai *Cortinarius* Kongresszus alkalmával gyűjtött nagygombák jegyzéke. *Moeszia 11–12*, 7–114.

Szabó, E., Dima, B., Dénes, A.L., Papp, V. & Keresztes, L. (2023). DNA barcoding data reveal important overlooked diversity of *Cortinarius* Sensu Lato (Agaricales, Basidiomycota) in the Romanian Carpathians. *Diversity 15*(4), 553. https://doi.org/10.3390/d15040553

Tănase, C. & Chifu, T. 2000. Biodiversitatea speciilor de macromicete în păduri din bazinul superior al râului Jijia. *Buletinul Grădinii Botanice Iaşi 9*, 79–82.

Tănase, C. & Pop, A. 2005. Red List of Romanian macrofungi species. *Bioplatform Romanian National Platform for Biodiversity, Editura Academiei Române* (ISBN 973-27-1211-2), Bucureşti: 101-107.

Todorescu, V. (1972). Macromicetele Din Munţii Ciucaş. *Analele Universităţii Bucureşti, Biologie Vegetală XXI*, 159–66.

Vörösváry, G. (2017). Wild and cultivated plants from Transylvania based on Transsilvania Generalis by Joseph Benkő. *Acta Siculica*: 79–85.

Watling, R., Gregory, N.M. & Orton, P.D. (1993). Cortinariaceae. *Edinburgh: Royal Botanic Garden*.

STUDIA UNIVERSITATIS BABEŞ-BOLYAI BIOLOGIA, 70, 2, 2025 (p. 55-68)
doi:10.24193/subbbiol.2025.2.04

Comparing the effectiveness of honey with *Rubus fruticosus* plant powder from the Algerian farm on wounds and the resultant oxidative stress

Besnaci Sana[1,2,*], Bouacha Mabrouka[2,3], Hamza Malak[4], Heciri Nour-Elhouda[4], Khettache Sarra[4], Khalfallah Sarra[4] and Babouri Yamine[4]

[1]*Laboratory of Cellular Toxicology, Department of Biology, Faculty of Sciences, Badji Mokhtar - Annaba University, Annaba, Algeria;*
[2]*Laboratory of Microbiology and Molecular Biology, Faculty of Sciences, Badji Mokhtar - Annaba University, Annaba, Algeria;*
[3]*Laboratory of Biochemistry and Environmental Toxicology, Department of Biochemistry, Faculty of Sciences, University of Badji Mokhtar, Annaba, Algeria;*
[4]*Department of Biology, Faculty of Sciences, University of Badji Mokhtar, Annaba, Algeria*
[*] ***Corresponding author, E-mails: s.besnaci@yahoo.fr; sana.besnaci@univ-annaba.dz***

Article history: Received 1 October 2024; Revised 2 December 2024; Accepted 11 July 2025; Available online 20 December 2025

Abstract. The use of traditional remedies remains a common therapeutic option for treating burns. In this study, we investigated the healing effect of honey and *Rubus fruticosus* plant powder, and the combination of these two products in burn treatment and accompanied oxidative stress regulation. Over 30 days, Wistar rats with dorsal burns were divided into five groups. Burns were induced on the dorsal region, and treatments were applied topically: honey, blackberry powder, and a honey-plant powder mixture. Two groups served as controls, while treatments were administered daily. Initially, a morphological study was conducted by following the different stages of wound healing and assessing the most effective treatment. At the end of the treatment, histological sections of the wound sites were made, along with an evaluation of oxidative stress by monitoring the activity of Glutathione (GSH), Glutathione-S-Transferase (GST), Glutathione-Peroxydase (GPX), and Catalase (CAT) enzymes, biomarkers at the hepatic level. The results indicate that the natural products used are highly

effective in treating burns compared to those treated with the marketed healing cream. The combination of honey and blackberry powder showed a synergistic effect in burn healing, and the histological observations support the findings from the planimetric study. The study of biomarkers shows a state of oxidative stress in the control rats through a decrease in GSH levels and an increase in the activity of hepatic GST, GPX, and CAT. In conclusion, the natural products used in our study demonstrate significant effectiveness in treating burns and oxidative stress regulation, particularly when used in combination.

Keywords: honey, *Rubus fruticosus*, mixture, oxidative stress, wound healing

Introduction

The quest for new antioxidant, anti-inflammatory, and antimicrobial compounds derived from natural resources has become a significant pursuit in the pharmaceutical, cosmetic, and polymer industries (Bouacha *et al.,* 2024). This interest natural medicine from public perception and the growing demand for naturally derived products, as well as the desire for better resource utilization and lower production costs. Additionally, the need to address pathogens developing resistance to conventional antibiotics and the substitution of synthetic compounds that may pose risks to public health has further driven this interest (Neiva *et al.,* 2020). Dressings provide an environment conducive to wound healing while protecting wounds from damage and infection. However, their absorbency can lead to drying out, causing adhesion to the wound. In addition, some dressings lack antimicrobial agents, antioxidants, and other bioactive compounds (Yasin *et al.,* 2023).

Used for centuries, honey is recognized for its effectiveness in treating skin infections, wounds, burns and ulcers. It creates a moist environment that acts as a protective barrier against infections, while its bioactive components ensure antimicrobial, anti-inflammatory and antioxidant properties (Bouacha *et al.,* 2023). In addition, its acidic pH stimulates the activity of macrophages and fibroblasts at wound sites (Minden-Birkenmaier and Bowlin, 2018). Honey may exert antioxidant effects through the synergistic interactions of various active compounds, particularly phenolic and flavonoid constituents (Boudiar *et al.,* 2022). It is relevant to ensure that a dressing incorporates the properties of honey, or another product known for its effects against infections and inflammations related to burns, and the combined characteristics/properties would enhance the efficacy.

Herbal medicine is a major approach in treatment of burns because of its effectiveness, low cost, limited risk of toxicity, and the great variety offered by the diversity of the plant world. Over 600 species of medicinal and aromatic plants in Algeria are commonly utilized in traditional medicine. However, only a limited number have been studied for their phytochemical compounds and biological activities (Meziti *et al*., 2018). Our ancestors traditionally used bramble leaves for dressing and treating external wounds and injuries (Zia-Ul-Haq *et al*., 2014). Subsequent studies have revealed that they exhibit antibacterial and antifungal properties, as well as significant anti-inflammatory and antioxidant activities (Meziti *et al*., 2018).

This study aims to evaluate the therapeutic capacity of two natural products, honey and blackberry (*Rubus fruticosus*) powder, both individually and in combination, in the treatment of burns and the regulation of associated oxidative stress.

Materials and methods

Sample processing

Our samples (honey and *Rubus fruticosus* leaves) were sourced from an unpolluted forest region (Fig. 1). The honey was of multifloral origin from *Apis mellifera* species. The harvesting location was abundant in *Eucalyptus globulus, Erica arborea* plant species and wild lavender (*Lavandula stoechas*). Immediately after harvesting, the healthy leaves were carefully rinsed with water and subjected to a desiccation process in an environment protected from any light exposure. To preserve the optimal integrity of the molecules, the plant was then rudimentarily ground using an electric mill.

Figure 1. Sampling location in the forest area of the municipality of Berrahal (Djebel El Idough), Annaba Province, Algeria.

For the mixture, we triturated honey and the fine powder of blackberry plant leaves with a spoon in a sterile glass flask. The latter was added in small quantities until a homogeneous and creamy blend was achieved, presenting a texture that is easy to apply.

Experimental animals

Male Wistar rats weighing 220.2g (±10g) were used to create the burns in this study. The experiment was conducted in accordance with the specified ethical guidelines for animal care and use. The study design consisted of five groups (Tab. 1) of five rats each , housed individually and acclimatized in our animal facility for one week before the start of the 30-day experimental period. Anesthesia was administered before the procedures, and the animals were humanely sacrificed at the end of the experiment.

Table 1. Distribution of experimental groups.

Group 01(C-)	Without any treatment
Group 02(C+)	Treated with the commercially available cream (Cicatryl Bio®)
Group 03(H)	Treated with honey
Group 04(P)	Treated with plant powder
Group 05(HP)	Treated with the honey-plant mixture

The experimental study was conducted following previously described methods (Abdullahi et al, 2014), with an experimental protocol adhering to ethical recommendations and good practices according to the Guide for the Care and Use of Animals and the Manual of CCP Guidelines (National Research Council, 2010).

After general anesthesia (1.5 mg/kg acepromazine maleate combined with 100 mg/kg ketamine hydrochloride), burn injuries were induced in the middle of the back of each animal. The burns were created using a sterile round brass piece with a diameter of 22 mm. Our treatments were applied topically once every 24 hours. Immediately following the induction of burns, animals in the treated groups received an application of the product corresponding to each group.

Evaluation of healing through digital planimetry

Photographs were captured using a high-resolution Canon ultraSonic camera every 6 days, starting from Day 0 up to Day 30. Subsequently, the images were processed using ImageJ® (image processing software 2019" General Public License") (Chang *et al.,* 2011), ensuring consistent height and angle parameters at regular intervals for each capture.

The percentage of wound contraction was calculated using the following equation (Bouacha et al, 2024):

$$\text{Contraction percentage} = \frac{(Initial\ Wound\ Size\ (Day\ 0) - Wound\ Size\ at\ Day\ n}{Initial\ Wound\ Size} \times 100$$

Histological study

For each group, two samples from the burn sites were collected and processed accordin previuosly described protocols (Preece, 1972; (Martoja et Martoja, 1967). Tissue sampleswere fixed in 10% formalin for structure preservation and specimen hardening. Following paraffin embedding, 6µm thick sections were cut from using a Leica microtome. Hematoxylin-eosin staining was applied, and as the dyes were in aqueous solution, the slides needed to be deparaffinized before rehydration

Following another dehydration process withtwo baths of 95°C alcohol followed by 100°C, and three baths of toluene), the stained slides were mounted between glass slides and coverslips using synthetic resin. The observation of histological sections of the tissu was conducted with a microscope (Leica DM500) equipped with a camera (Leica ICC50 E) allowing image capture with digital imaging software (Leica LAS EZ).

Biochemical assays

At the end of the experiment, the rats were sacrificed, and liver dissection was performed. One gram of tissue was crushed and homogenized in phosphate buffer (pH 7.4; 0.1 M; stored at 4°C). The tissue homogenates were centrifugated (9000 rpm, 4°C, 15 min), and the resulting supernatant was used for various biochemical assays.

Glutathione (GSH) assay. The GSH assay was performed according to Weckbeker and Cory (1988), which relies on measuring the optical absorbance of 2-nitro-5-mercapturic acid resulting from the reduction of 5,5-dithio-bis-2-nitrobenzoic acid by the (-SH) groups of glutathione, at λ = 412 nm.

Glutathione S-Transferase (GSTs) activity assay. The measurement of GST activity is determined following the method described by Habig *et al.* (1974). The reaction is based on the interaction between GST and 1-Chloro2,4-dinitrobenzene in the presence of glutathione, which leads to the formation of 1-S-Glutathionyl 2-4 Dinitrobenzene molecule, allowing the measurement of GST activity at 340 nm within five minutes.

Glutathione Peroxidase (GPx) activity assay. The enzymatic activity of GPx was measured using the method by Flohe and Gunzler (1984) at 412 nm within five minutes, which is based on the reduction of hydrogen peroxide in the presence of reduced glutathione. Under the influence of GPx, the latter is transformed into the oxidized glutathione (GSSG).

Catalase activity assay. Catalases are tetrameric enzymes, with each unit carrying a heme molecule and an NADPH molecule. These enzymes eliminate reactive species by accelerating the spontaneous reaction of the reactive hydrogen peroxide (H_2O_2) hydrolysis, into water and oxygen at 240 nm within five minutes (Aebi, 1984).

Statistical analysis

Statistical analysis of the data was performed using MINITAB software (Version 16). The results were presented as the mean ± standard deviation (M±SD). The statistical treatment of the results involved a one-way analysis of variance (ANOVA) (AV1) and a two-way analysis of variance (AV2), followed by Fisher's *post hoc* comparison test. Differences were considered significant when $p \leq 0.05$ (*), highly significant when $p \leq 0.01$ (**), and very highly significant when $p \leq 0.001$(***).

Results

Evolution of wound healing

According to the obtained results , the wound size evolution of the treated batches did not record any reduction in their surfaces until the 12th day in case of the groups treated with honey and the mixture and from 24th day for the group treated with the plant powder (Fig. 2a). The statistics confirm these observations (Fig. 2b). According to the percentage of contraction (Fig. 2), we can put the following order of healing of the wounds of the different groups: HP, H, P, C-, C+ (Fig. 3).

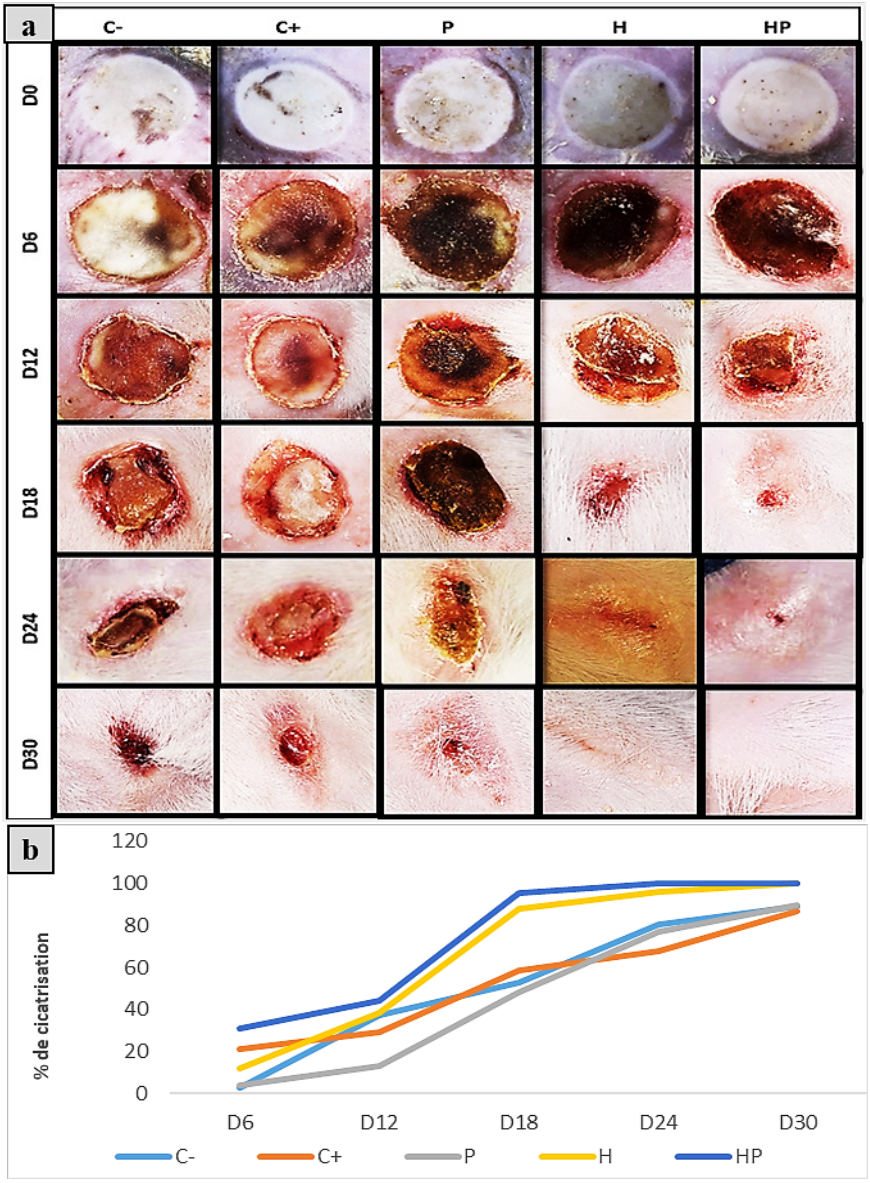

Figure 2. Wound healing effect of the different treatment. (a): Chronology of burn healing with a high-resolution camera (Canon ultra-Sonic), (b): Contraction percentages of wounds in treated and untreated burns. D: day, C-: negative control group, C+: positive control group, P: group treated with plant powder, H: group treated with honey, HP: group treated with honey-plant powder mixture.

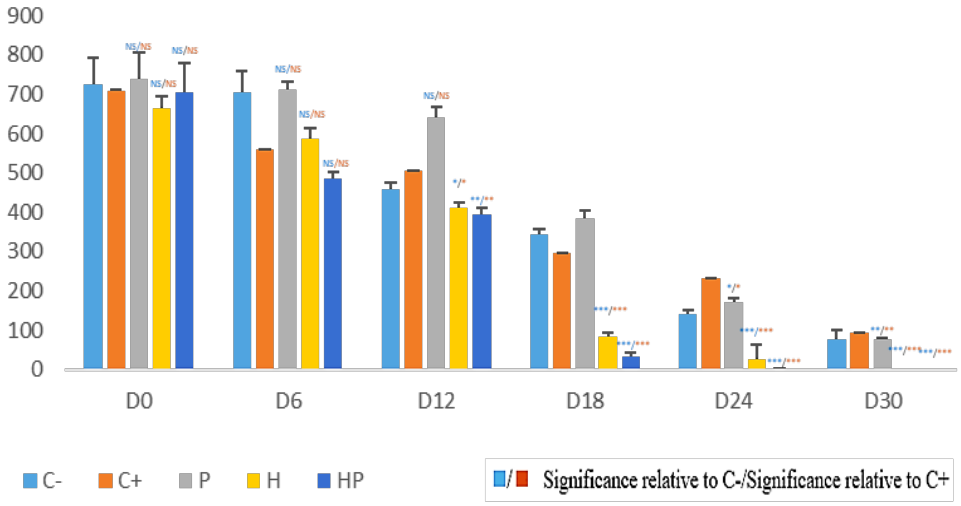

Figure 3. Evolution of the average burn surfaces of the five groups during the experimental period (30 days). D: day, C-: negative control group, C+: positive control group, P: group treated with plant powder, H: group treated with honey, HP: group treated with honey-plant powder mixture. (*)Differences were considered significant, (**) highly significant, and (***) very highly significant.

Histological sections

In general, the processes of inflammation and repair were observed in all examined sections, but to varying degrees among the batches. The inflammatory process was particularly pronounced in the control batches, while the intensity of inflammation decreased to become very low, almost absent, in the batches treated with honey and the mixture, and moderate reduction of inflammation(?) in the batch treated with the plant powder. The repair process, assessed by the intensity of fibrosis, was moderate in the control batches, while the batches treated with natural products (honey, plant powder and mixture) showed a higher intensity of fibrosis (Fig. 4).

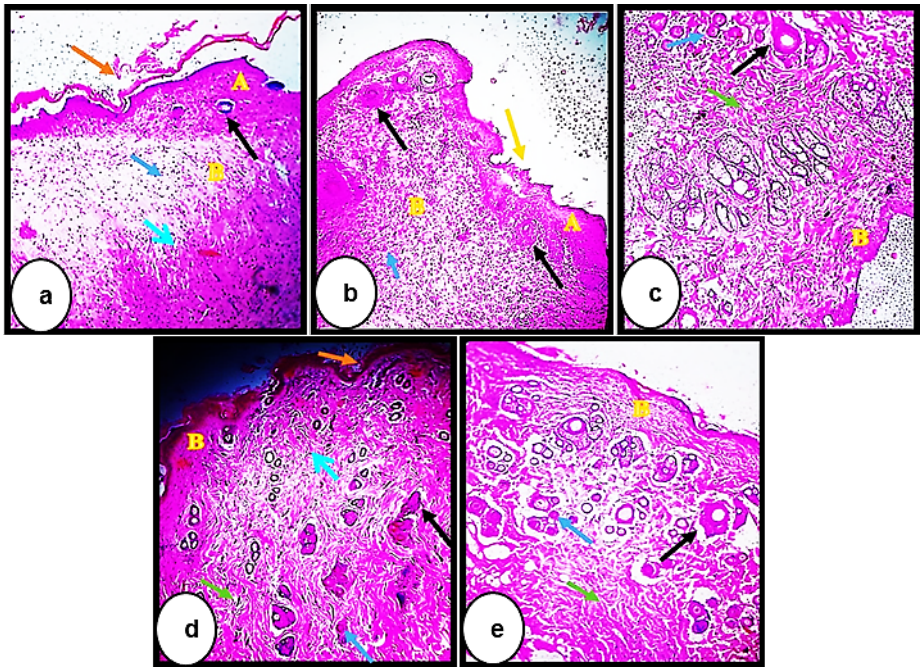

Figure 4. Histological sections of wound tissue (GX400). a: untreated control group (C-), b: treated control group (C+); c: group treated with honey (H), d: group treated with plant powder (P), e: group treated with mixture (HP). A: young fibroblasts with dense inflammation, B: a high number of fibroblasts with simple inflammation, Dark blue arrow: Vessel full of inflammatory elements, orange arrow**:** Debris cell, Light blue arrow: newly formed vessels "Slightly dense fibrosis", Green arrow: Normal dermis, Black arrow: tissue necrosis

Oxidative stress parameters

An significant increase of GSH, GST, GPX and CAT levels/expression was observed in the positive control and the treated groups compared to the untreated control (Fig. 5).

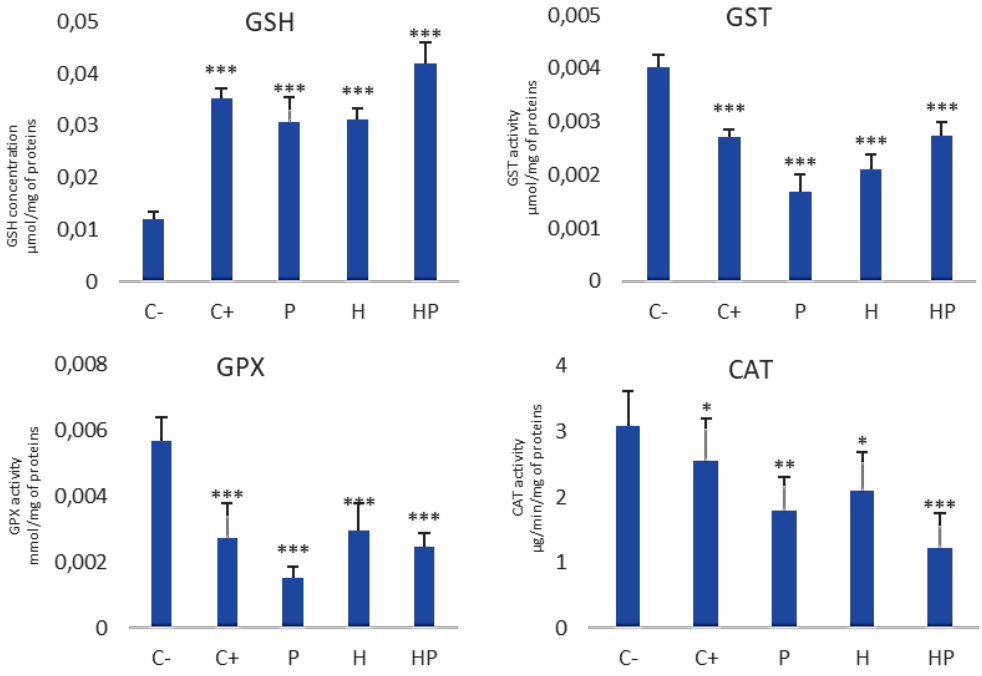

Figure 5. Hepatic enzymatic levels and activities of the oxidative stress parameters of the experimental groups. (*)Differences were considered significant, (**) highly significant, and (***) very highly significant.

Discussion

To replace synthetic molecules, the healing of burns is achieved through the use of conventional products made from natural ingredients. These products have been used in traditional medicine since times to treat various pathologies, as they are considered safer compared to pharmaceuticals (Markiewicz-Gospodarek *et al.,* 2022). They also offer significant advantages in terms of availability, safety, and reduced costs (Jayakumar, 2015). The use of honey as a treatment for burns is well-documented in several scientific studies that have reported its ability to protect wounds, reduce infections, alleviate pain, debride necrotic tissue, and promote granulation tissue formation (Bouacha *et al.,* 2022; Naik *et al.,* 2022; Bouacha *et al.,* 2024). The application of honey to a wound creates a favorable moist environment due to its hygroscopic properties and optimal pH (Tashkandi, 2021),which facilitates faster healing compared to a dry

dressing, as it prevents damage to newly formed epithelial tissues. Furthermore, its hyperosmolarity absorbs exudates and promotes a reduction in tissue edema, thereby indirectly improving local microcirculation (Benhanifia *et al.,* 2011).

Phytotherapy is the oldest method of healing in the world, found in all civilizations through various preparations using fresh or dried plants. Phenolic compounds and flavonoids have the ability to inhibit the production of pro-inflammatory mediators such as leukotrienes and prostaglandins (Tangney and Rasmussen, 2013). The richness of the *Rubus fruticosus* extract in these compounds contributes to its anti-inflammatory effect.

Honey is very rich in anti-inflammatory molecules (Saikaly and Khachemoune, 2017), as is blackberry (Tangney and Rasmussen, 2013).

In our study, the natural treatments we selected resulted in complete wound healing, albeit to varying healing degrees, allowing us to compare the healing effects of the products used.

According to the results obtained, wounds treated with the honey-R. fruticosus powder mixture showed better healing progress (Fig. 2 “a and b”). This outcome can be explained not only by the richness and chemical composition of honey but also by the properties of the blackberry. Furthermore, a synergistic effect may exist between honey and *Rubus fruticosus* powder. According to Spoială *et al.,* (2022), the efficacy of a mixture may be related to the synergy of the anti-inflammatory, antioxidant, and antibacterial activities of its components (honey and blackberry in our case).

The effects of our products were manifested in the histological sections, thereby confirming the morphological results and indicating the efficacy of these products at the tissue level. It was observed that the inflammatory process was still present in the negative control group, with an early formation of vessels, while in the treated control group, there was an increase in the number of these vessels, along with cleansing inflammatory vesicles. The treated groups show good re-epithelialization due to the significant formation of neovessels, promoting the emergence of healthy tissue. However, the combination of these two natural products yielded excellent outcomes for wound healing compared to controls, by eliminating inflammation and promoting the renewal of skin cells (fibroblasts). This confirms the biological activities and, especially, the healing properties present in these natural products.

Morphological and physiological changes always subject living organisms to a state of stress (Lagadic *et al.,* 1997). Glutathione is a non-enzymatic antioxidant that also plays a protective role for the skin by participating in the metabolic synthesis of several vitamins, such as vitamin D and vitamin A. The low GSH level observed in the negative control group indicated the mostlyintensified oxidative stress levels during the treatment period, which

may explain the absence of wound healing. GST is an essential enzyme for the detoxification process. Our results show a decrease in GST activity across all treated groups. A high level of GSH requires low GST activity, as the enzyme is responsible for the transformation of GSH(Besnaci *et al.,* 2019; 2022). In the antioxidant system, GPX and CAT hydrolyze hydrogen peroxide into water and subsequently reduce the levels of free radicals. The high activities of GPX and CAT indicate elevated levels of H_2O_2 and free radicals, which explains the increased stress state in the control group, while oxidative markers were alleviated/reduced in the treated groups. The observed variations in oxidative stress markers suggested that the body was undergoing metabolic adaptation in reaction to the burn injuries. This process involved an enhanced antioxidant response, reflecting the activation of repair and recovery mechanisms aimed at restoring homeostasis and promoting tissue healing.

Conclusion

In conclusion, we find that the efficacy of these products encourages the use of natural remedies, which represent a better solution for the treatment of burns and wound healing. Honey and blackberry exhibit good anti-inflammatory properties and an excellent antioxidant effect, while their combination provides optimal results due to the synergy between the bioactive molecules of the two products.

References

Abdullahi, A., Amini-Nik, S., Jeschke, M.G. (2014). Animal models in burn research. *Cell. Mol. Life Sci*. 71, 3241-3255. https://doi.org/10.1007%2Fs00018-014-1612-5

Aebi H. 1984. Catalase *in vitro*. *Methods Enzymol.* 1984; 105: 121–126. https://doi.org/10.1016/S0076-6879(84)05016-3

Benhanifia, M.B., Boukraâ, L., Hammoudi, S.M., Sulaiman, S.A., Manivannan, L. (2011). Recent patents on topical application of honey in wound and burn management. *Recent Pat. Inflamm. Allergy Drug Discov*. 5(1), 81-6. https://doi.org/10.2174/187221311794474847

Besnaci, S., Bensoltane, S., Djekoun, M. (2019). Oxidative stress and histological changes induced by the nano-Fe_2O_3 in *Helix aspersa*. *Sci. Stud. Res. Chem. Chem. Eng. Biotechnol. Food Ind.* 20(2), 119-133.

Besnaci, S., Bouacha, M., Chaker, A., Babouri, Y., Bensoltane, S. (2022). Impact des nanoparticules de silice fumée SiO_2 sur des indicateurs du stress oxydatif chez *Helix aspersa*. *Bull. Soc. R. Sci. Liège*. 91(1), 11-22. https://doi.org/10.25518/0037-9565.10781

Bouacha, M., Besnaci, S., Boudiar, I. AlKafaween, M. A. (2022). Impact of storage on honey antibacterial and antioxidant activities and their correlation with polyphenolic content. *Trop. J. Nat. Prod. Res.* 6(1), 34-39. https://doi.org/10.26538/tjnpr/v6i1.7

Bouacha, M., Besnaci, S., Boudiar, I. (2023). An overview of the most used methods to determine the *in vitro* antibacterial activity of honey. *Acta Microbiol Hell. 39*(1), 23-30.

Bouacha, M., Besnaci, S., Tigha-Bouaziz, N., Boudiar, I. (2024). Evaluation of antibacterial, anti-inflammatory, antioxidant, and wound-healing properties of multifloral honey. *Int. Food Res. J.* 31(5), 1094 -1106. https://doi.org/10.47836/ifrj.31.5.02

Boudiar, I., Bouacha, M., Besnaci, S., Khallef, M., Abdi, A. (2022). Evaluation of the antibacterial and antimutagenic effects of multiflora honeys produced by the Apis mellifera bee and their correlation with polyphenolic content, flavonoids and color. *J. Entomol. Res.* 46(3), 607-614. https://doi.org/10.5958/0974-4576.2022.00105.0

Chang, A.C., Dearman, B., Greenwood, J.E. (2O11). A comparison of wound area measurement techniques: Visitrak versus photography. *Eplasty*. 2; 11.

Flohé, L., Günzler, W.A. (1984). Assays of glutathione peroxidase. *Methods Enzymol.* 105,114–120. https://doi.org/10.1016/S0076-6879(84)05015-1

Habig, W.H., Pabst, M.J., Fleischner, G., Gatmaitan, Z., Arias, I.M. (1974). The identity of glutathione S-transferase B with ligandin, a major binding protein of liver. *Proc. Natl. Acad. Sci. USA.* 71(10), 3879–3882. https://doi.org/10.1073/pnas.71.10.387

Jayakumar, K. (2015). Ethno medicinal value of plants in thanjavur district, tamil nadu, India. *Int. Lett. Nat. Sci*. 29,(2), 33-42. https://doi.org/10.18052/www.scipress.com/ILNS.29.33

Lagadic, L., Caquet, T., Amiard, J.C. (1997). Biomarqueurs en écotoxicologie : principes et définitions. In Biomarqueurs en écotoxicologie : aspects fondamentaux .*Eds Masson*, Paris. France, pp 1-9.

Markiewicz-Gospodarek, A., Kozioł, M., Tobiasz, M., Baj, J., Radzikowska-Büchner, E., & Przekora, A. (2022). Burn wound healing: clinical complications, medical care, treatment, and dressing types: the current state of knowledge for clinical practice. *Int. J. Environ. Res. Public Health*. *19*(3), 1338. https://doi.org/10.3390/ijerph19031338

Martoja, R., Martoja, P.M. (1967). Initiation aux techniques de l'histologie animale. *Eds Masson et Cie*, Paris VI, pp 345.

Meziti, A., Bouriche, H., Meziti, H., Seoussen, K., & Dimertas, I. (2018). Antioxidant and anti-inflammatory activities of *Rubus fruticosus* and *Zizyphus vulgaris* methanol extracts. *Int. J. Pharm. Pharm. Sci.* 9(2), 69-76.

Minden-Birkenmaier, B.A.; Bowlin, G.L. (2018). Honey-based templates in wound healing and tissue engineering. *Bioengineering*. 5(2), 46. https://doi.org/10.3390/bioengineering5020046

Naik, P.P., Chrysostomou, D., Cinteza, M., Pokorná, A., Cremers, N.A. (2022). When time does not heal all wounds—The use of medical grade honey in wound healing: A case series. *J. Wound Care*. 31(7), 548-558. https://doi.org/10.12968/jowc.2022.31.7.548

National Research Council. 2010. Guide for the care and use of laboratory animals. United States: The National Academic Press.

Neiva, D.M., Luís, Â., Gominho, J., Domingues, F., Duarte, A.P., Pereira, H. (2020). Bark residues valorization potential regarding antioxidant and antimicrobial extracts. *Wood Sci. Technol*. 54, 559-585. https://doi.org/10.1007/s00226-020-01168-3

Preece, A. (1972). A manual for histologic technicians.Little, *Ed Brown and Company*, Boston.

Saikaly, S.K., Khachemoune, A. (2017). Honey and wound healing: an update. *Am. J. Clin. Dermatol*. 18, 237-251. https://doi.org/10.1007/s40257-016-0247-8

Spoială, A., Ilie, C.I., Ficai, D., Ficai, A., Andronescu, E. (2022). Synergic effect of honey with other natural agents in developing efficient wound dressings. *Antioxidants*. *12*(1), 34. https://doi.org/10.3390/antiox12010034

Tangney, C.C., Rasmussen, H.E. (2013). Polyphenols, inflammation, and cardiovascular disease. *Curr Atheroscler Rep*. 15(324), 2-10. https://doi.org/10.1007/s11883-013-0324-x

Tashkandi, H. (2021). Honey in wound healing: An updated review. *Open Life Sci*. 16(1), 1091-1100. https://doi.org/10.1515/biol-2021-0084

Weckbecker, G., Cory, J.G. (1988). Ribonucleotide reductase activity and growth of glutathione-depleted mouse leukemia L1210 cells *in vitro*. *Cancer Lett*. 40(3), 257–264. https://doi.org/10.1016/0304-3835(88)90084-5

Yasin, S.N.N., Said, Z., Halib, N., Rahman, Z.A., Mokhzani, N.I. (2023). Polymer-based hydrogel loaded with honey in drug delivery system for wound healing applications. *Polymers*. *15*(14), 3085. https://doi.org/10.3390/polym15143085

Zia-Ul-Haq, M., Riaz, M., De-Feo, V., Jaafar, H.Z., Moga, M. (2014). *Rubus fruticosus* L.: constituents, biological activities and health related uses. *Molecules*. 19(8), 10998-1029. https://doi.org/10.3390/molecules190810998

STUDIA UNIVERSITATIS BABEŞ-BOLYAI BIOLOGIA, 70, 2, 2025 (p. 69-82)
doi:10.24193/subbbiol.2025.2.05

Photoperiodic influence of light-emitting diode (LED) on vegetative parameters of *Spinacia oleracea* L. (Spinach)

Musa Saheed Ibrahim[1,2], Beckley Ikhajiagbe[2] and Kingsley Erhons Enerijiofi[3] *

[1]*Department of Biology and Forensic Science, Admiralty University of Nigeria, Delta State Nigeria;*
[2]*Department of Plant Biology and Biotechnology, University of Benin, Edo State Nigeria;*
[3]*Department of Biological Sciences, College of Basic, Applied and Health Sciences, Glorious Vision University, Ogwa, Edo State Nigeria.*
* **Corresponding author Email:** kingsleyenerijiofi@gmail.com

Article history: Received 05 October 2025; Revised 09 December 2025; Accepted 11 December 2025; Available online 20 December 2025

Abstract. This research aims to determine sustainable strategies to optimize crop growth and yield, by testing the possibilities of using light-emitting diode (LED) technique to influence the vegetative parameters of spinach. A speed-breeding chamber was constructed using LEDs as a light source under varying photoperiods (19, 17, 15, and 13 hours). The control was established to be the normal light duration of 11 hours during the study period. Spinach vegetative parameters involving morphological parameters such as stem length, root length, and leaf area as well as physiological parameters such as plant weight and percentage necrosis and chlorosis were investigated for 30 days after transplanting. The results showed a significant ($p < 0.05$) increase in morphological parameters of spinach with increasing photoperiod. The spinach plant under the long photoperiod was observed to show the highest morphological and physiological properties. About a 30% increase in root length was observed in the speed-breeding chamber with the longest photoperiod duration compared to the control conditions. Significantly improved spinach plant weight was observed for 19-hour photoperiod compared to the shorter exposure ($p < 0.05$). A lower percentage of necrosis and chlorosis was observed in spinach with longer LED exposure. This research indicated that LED-induced speed breeding is very effective in improving the vegetative properties of spinach. It can be argued that

a 19-hour LED-induced photoperiod is the optimum photo duration required by spinach to improve vegetative growth. Future research should be conducted to investigate the influence of similar LED-induced photoperiods on other species of vegetables.

Keywords: breeding chambers, light-emitting diode, photoduration, photoperiodic influence.

Introduction

Over the years, the global population has increased and it is expected to continue to do so in the next years. Mathematically, it has been estimated that the world population will expand by 75 % by 2050 **(**Ray *et al*., 2013). This poses a serious concern on food security and availability for the growing population. For this purpose, several strategies have been considered on how to improve food productivity to meet up with the ever-increasing food demand (Musa and Ikhajiagbe, 2021; Moses *et al.,* 2023). Previously, local farmers relied on traditional methods of breeding, which can no longer meet the food requirements of the ever-increasing population. Consequently, farmers are under constant pressure to optimize crop production and improve yield in less time, with higher nutritional value (Enerijiofi *et al*., 2024). It has been documented that temperature, light duration and humidity are important abiotic conditions that determine plant growth and development (Rouphael *et al*., 2012; Rahman *et al*., 2019). Research has further proved that plant yield and cultivation time can be easily influenced by the normal light conditions using speed breeding techniques. Since plants has several photoreceptors that can be used in signaling and regulation of photomorphogenesis in them (Galvão and Fankhauser, 2015; Musa and Ikhajiagbe, 2024a).

Speed breeding technique involves several strategies where abiotic features like temperature and light are manipulated in order to speed up vegetation, flowering and seed development (Hussain *et al***.,** 2018). Speed breeding is a very important strategy that was initiated by the US National Aeronautics and Space Administration (NASA). It has helped farmers in fast cultivation of crops (NASA, 2016). African researchers are using speed breeding to generate new kinds of crops more quickly. The speed breeding technique involved artificially allowing plants to have a continuous light for 20–22 hours. Since plants can undergo photosynthesis for long period in order to bring about increased yield. In a normal condition where a plant takes 6 months to grow, speed breeding may reduce this long period to about 50% per year.

Previous researchers have employed the speed breeding technique to influence the photoperiod and temperature of various important crops to optimize its yield (Rouphael *et al*., 2012; Rahman *et al*., 2019). However, researchers are skeptical regarding photoperiod manipulation due to the various sources and forms of artificial lights. Among many artificial light sources, light-emitting diode (LED) has been proven to have the highest colour rendering index (CRI), indicating its high photoelectrons, which may be the best in plant growth optimization (Khan *et al*., 2017). Light sources with high CRI can easily adjust the light quality, light intensity, and photoperiod of plants (Chiuruywi *et al*., 2018). However, previous studies used the blue and red illumination in improving the growth of basil microgreens (Collard *et al*., 2017). Even though, these lights have been proven to have less CRI than the white LED light (Rahman *et al*., 2019). According to Monostori *et al.* (2018), speed breeding research, especially on light manipulation can best be studied using light-specific plants. For this purpose, the current research focuses on spinach plant as a test plant. The study was aimed at using speed breeding technique specifically the white LED in optimizing vegetative properties of *Spinacia oleracea* to meet up with the global rising demand for food, as the global population increases.

Materials and methods

Sample collection

A composite soil sample was collected from the Admiralty University of Nigeria farm (6.16471 ^{o}N, 6.57544 ^{o}E), located in the University campus at Ibusa-Ogwashi-Uku expressway, Delta State. About 4 kg of soil was measured and distributed into 15 polyether bags; some of the soil was also used for the nursery bed.

Collection of Spinacia oleracea seed

Seeds of *S. oleracea* (No. 21-38135/979100042077) were obtained from Songhai Delta at Amukpe in Sapele, Delta State, on 10th of July 2022.

Preparation of the nursery bed

About 150 seeds were dispersed in the prepared nursery bed and allowed to germinate for 4 days. After 4 days, seedlings of similar height were picked and transplanted.

Seedling transplantation

About 10 seedlings of *S. oleracea* were transferred into each of the 15 experimental polythene bags. It was ensured that all seedlings transplanted were ranging between 1.9 cm and 2.0 cm in height and were all transplanted at same time into the 15 experimental polythene bags following the Randomized Block Design (RBD) in three replicates as described by Musa *et al*., 2017.

Construction of the speed breeding chamber

Transparent rubbers of 50 X 50 cm were used as the breeding chamber. Five speed breeding chambers were constructed using the transparent plastic rubber. White LED bulbs were attached at the extreme end of each chamber (Fig. 1). Each speed-breeding chamber was made to have a unique photoperiod duration as described in Tab. 1. The experiment was conducted in Asaba during its wet season (0.04 inches precipitation) according to Wolter *et al.,* (2019) with an average of 11 hours sunlight duration. The speed-breeding chamber also served as a screen house that shielded the plants from pests, but not from rainfall. The experimental polyether bags were then situated in the speed-breeding chamber with three experimental polythene bags per speed breeding chamber as replicates. The soils in all the polyether bags were stirred once every week to enhance aeration and no chemicals was used during the study. The experimental pots were weeded every two days following Musa and Ikhajiagbe (2021). The experiments lasted for 30days (August 12th – October 10th), the spinach was harvested on the 30th day.

Table 1. LED-induced photoperiod duration.

Speed breeding chamber code	Light duration
A	19 hours
B	17 hours
C	15 hours
D	13 hours
E (Control)	11 hours

Figure 1. Constructed speed breeding chamber.

Morphological parameters

Morphological parameters that are analytical of vegetative growth and yield of *S. oleracea* were examined. The morphological parameters were divided into two. The above ground parameters include the number of leaves, stem length, leaf area and leaf length, while the below ground parameters were root length and secondary root number. The leaf number were calculated by counting at every six (6) days intervals from the transplanting date to 30th day. The stem length was measured in (cm) at six (6) days intervals from day 1 after transplanting to day 30. Leaf area (cm^2) was calculated using an android application (Leaf-IT) using the method of Julian *et al.,* (2017) at six (6) days interval from transplanting day to day 30. Leaf length was calculated in (cm) at interval of six (6) days. The number of leaves were calculated by counting at an interval six (6) days from the day of transplanting to the 30th day. The length of fresh root was measured in (cm) at 20th and 30th day after transplanting. Also, the number of secondary roots were accurately detected and calculated at 20th and 30th day after transplanting.

Physiological parameters

To analyze the effect of LED on the vegetative parameters of *S. oleracea*, physiological parameters were investigated. Leaf tip chlorosis and necrosis was measured at 10, 20 and 30 days after transplanting as follows:

$$\text{Leaf tip necrosis/chlorosis (\%)} = \frac{\text{Number of spinach leaf with signs of necrosis or chlorosis}}{\text{Number of spinach leaf}} \times 100$$

Weight of fresh leaf (g) was measured using an analytical weighing balance at day 10, 20 and 30 after transplanting. The chlorophyll *a* and *b* levels at 10 and 30 days after transplanting were calculated as seen in Arnon *et al.*, (1949); Maxwell and Johnson (2000).

Statistical analysis:

The recorded data were presented as means and standard errors of three replicates and subjected to statistical analysis. A One-Way Analysis of Variance (ANOVA) at a significance level of p=0.05 was used throughout the study to determine if there were significant differences in the values recorded values.

Results

Effect of photoperiod on spinach morphological parameters

The influence of LED-induced photoperiod on spinach plant was evaluated using morphological parameters. The morphological parameters that were assayed in this research were divided into; the above ground parameters and below ground parameters.

The above ground parameters

The number of spinach leaves was observed to be highest (5.9) at 30 DAT in the speed-breeding chamber A, while the lowest leaf number (3.7) at 30 DAT was observed in the control (E). At 6 DAT, three (3) leaves were observed in the speed breeding chamber A, B and C, while in the speed breeding chamber D and the control (E), only two (2) leaves were observed. Furthermore, at 30 DAT, there was a significant increase ($p<0.05$) in leaf number was observed in the speed breeding chamber A compared to the other speed breeding chambers (B, C, D and control) (Tab. 2).

Table 2. Response of spinach photoperiod on leaf number.

Sample	Leaf number				
	6 DAT	12 DAT	18 DAT	24 DAT	30 DAT
A	3.0 ± 0.23^{a}	3.0 ± 0.12^{a}	4.9 ± 0.11^{a}	5.2 ± 0.01^{a}	5.9 ± 0.22^{a}
B	3.0 ± 0.13^{a}	3.0 ± 0.34^{a}	4.0 ± 0.25^{b}	4.0 ± 0.11^{b}	4.0 ± 0.22^{b}
C	3.0 ± 0.54^{a}	3.0 ± 0.32^{a}	3.6 ± 0.43^{c}	3.7 ± 0.21^{c}	4.0 ± 0.12^{b}
D	2.3 ± 0.55^{b}	2.3 ± 0.22^{b}	3.6 ± 0.11^{c}	4.3 ± 0.11^{d}	4.3 ± 0.12^{c}
E	2.0 ± 0.01^{b}	2.0 ± 0.32^{c}	3.0 ± 0.76^{d}	3.6 ± 0.21^{e}	3.7 ± 0.32^{d}

Results with same alphabetic superscripts on same column did not show significant difference from each other ($p > 0.05$). Results were recorded in mean and standard error of three replicates. DAT = Days after transplant. A = 19 hours photoperiod, B = 17 hours photoperiod, C = 15 hours photoperiod, D = 13 hours photoperiod and E = 11 hours photoperiod (control).

The stem length (cm) is one of the important parameters in growth studies. The spinach under speed breeding chamber A was observed to show the highest stem length at all the assayed days. Also, at 30 DAT, it was observed that the spinach under the control (E) showed the least (2.4 cm) stem length. Furthermore, significant difference ($p < 0.05$) was observed in the stem length between all the speed breeding chambers (A, B, C and) and the control (E). In addition, significant increase ($p < 0.05$) in stem length were observed as the days progress, except for the control (E), where no significant ($p>0.05$) increase in stem length was observed from 18 DAT to 30 DAT. Furthermore, leaf length observed, range from 2.3 – 5.3 cm throughout the 30-day study. At 30 DAT, speed breeding chamber A was observed to show the highest (5.3 cm) leaf length, while the control (E) showed the lowest (2.5 cm) leaf length (Tab. 3). Since leaf area is a major indicator of plants ability to utilize light, the spinach under the speed breeding chamber A had the highest (7.7 cm^2) leaf area at 30 DAT, compared to other speed breeding chambers (B, C and D). The spinach under the

control condition (E) was observed to show the lowest (2.2 cm^2). There was a significant difference ($p<0.05$) in leaf area of spinach under all the assayed speed breeding conditions at 30 DAT. Delayed increases in leaf area was observed in the spinach under the control condition (E) and (D) (Tab. 4).

Table 3. Response of spinach photoperiod on stem length and leaf length.

Sample	Stem length (cm)					Leaf length (cm)				
	6 DAT	12 DAT	18 DAT	24 DAT	30 DAT	6 DAT	12 DAT	18 DAT	24 DAT	30 DAT
A	2.6 ± 0.3^a	3.2 ± 0.2^a	3.5 ± 0.2^a	3.7 ± 0.3^a	4.4 ± 0.1^a	2.1 ± 0.2^a	2.9 ± 0.2^a	4.6 ± 0.1^a	4.8 ± 0.2^a	5.3 ± 0.1^a
B	3.0 ± 0.2^b	3.0 ± 0.4^b	3.1 ± 0.2^b	3.2 ± 0.3^b	3.5 ± 0.1^b	2.0 ± 0.3^a	3.3 ± 0.3^b	3.8 ± 0.2^b	4.1 ± 0.2^b	4.5 ± 0.3^b
C	2.0 ± 0.5^c	2.3 ± 0.3^c	2.5 ± 0.3^c	2.6 ± 0.2^c	2.9 ± 0.1^c	2.0 ± 0.4^a	2.0 ± 0.5^c	2.3 ± 0.1^c	2.5 ± 0.1^c	2.8 ± 0.2^c
D	1.7 ± 0.3^c	1.7 ± 0.2^d	2.0 ± 0.4^d	2.2 ± 0.1^d	2.5 ± 0.1^d	1.6 ± 0.3^b	2.5 ± 0.4^d	2.6 ± 0.1^d	2.7 ± 0.3^c	2.7 ± 0.2^c
E	2.0 ± 0.3^c	2.0 ± 0.4^e	2.3 ± 0.4^e	2.4 ± 0.6^e	2.4 ± 0.1^e	2.0 ± 0.3^a	2.5 ± 0.2^d	2.5 ± 0.1^c	2.5 ± 0.3^c	2.5 ± 0.3^c

Results with same alphabetic superscripts on same column did not show significant difference from each other ($p > 0.05$). Results were recorded in mean and standard error of three replicates. DAT = Days after transplant. A = 19 hours photoperiod, B = 17 hours photoperiod, C = 15 hours photoperiod, D = 13 hours photoperiod and E = 11 hours photoperiod (control).

Table 4. Response of spinach photoperiod on leaf area.

Sample	Leaf area (cm^2)				
	6 DAT	12 DAT	18 DAT	24 DAT	30 DAT
A	5.0 ± 0.2^a	5.6 ± 0.5^a	6.3 ± 0.1^a	7.1 ± 0.2^a	7.7 ± 0.3^a
B	3.3 ± 0.4^b	3.6 ± 0.1^b	3.8 ± 0.1^b	4.1 ± 0.1^b	4.4 ± 0.1^b
C	3.5 ± 0.2^c	3.6 ± 0.4^b	3.6 ± 0.2^c	3.8 ± 0.1^c	3.9 ± 0.2^c
D	2.3 ± 0.1^d	2.4 ± 0.2^c	2.4 ± 0.1^d	2.4 ± 0.1^d	2.7 ± 0.1^d
E	2.0 ± 0.5^e	2.1 ± 0.1^d	2.1 ± 0.1^e	2.2 ± 0.1^e	2.2 ± 0.1^e

Results with same alphabetic superscripts on same column did not show significant difference from each other ($p > 0.05$). Results were recorded in mean and standard error of three replicates. DAT = Days after transplant. A = 19 hours photoperiod, B = 17 hours photoperiod, C = 15 hours photoperiod, D = 13 hours photoperiod and E = 11 hours photoperiod (control).

The below ground parameters

The result of the below ground parameters of spinach plant showed that spinach root length increased significantly ($p > 0.05$) with continuous photoperiod. Spinach plant from the speed-breeding chamber A was observed to have the longest (16.0 cm) root length at 30 DAT, while the shortest root length (6.4 cm) was observed in the spinach plant from the control condition (E). There was statistically significant difference ($p < 0.05$) in the root length of the spinach plant under all the photoperiod condition at all the assayed days (Tab. 5). At 20 DAT, it was observed that spinach root length in the speed breeding chamber C and D showed no significant difference ($p > 0.05$) (Fig. 2).

Table 5. Response of spinach photoperiod on root length and number of secondary roots.

Sample	Root length (cm)		Number of secondary roots	
	20 DAT	30 DAT	20 DAT	30 DAT
A	11.0 ± 0.1^{a}	16.0 ± 0.2^{a}	30 ± 0.4^{a}	38 ± 0.1^{a}
B	8.0 ± 0.2^{b}	11.0 ± 0.2^{b}	21 ± 0.2^{b}	26 ± 0.1^{b}
C	3.8 ± 0.2^{c}	7.0 ± 0.1^{c}	15 ± 0.1^{c}	19 ± 0.1^{c}
D	3.7 ± 0.2^{c}	6.8 ± 0.3^{d}	12 ± 0.2^{d}	16 ± 0.1^{d}
E	3.4 ± 0.2^{d}	6.4 ± 0.2^{e}	10 ± 0.1^{d}	13 ± 0.1^{e}

Results with same alphabetic superscripts on same column did not show significant difference from each other ($p > 0.05$). Results were recorded in mean and standard error of three replicates. DAT = Days after transplant. A = 19 hours photoperiod, B = 17 hours photoperiod, C = 15 hours photoperiod, D = 13 hours photoperiod and E = 11 hours photoperiod (control).

Figure 2. Root length parameters. DAT=Days after transplant. A= 19 hours photoperiod, B= 17 hours photoperiod, C= 15 hours photoperiod, D= 13 hours photoperiod and E= 11 hours photoperiod (control).

Effect of photoperiod on Spinach physiological parameters

Greater percentage (35%) of the spinach leaves under the control (E) condition showed visible signs of leaf tip necrosis and chlorosis, while lower (15 %) of the spinach leaves from the speed breeding chamber C showed visible signs of leaf tip necrosis and chlorosis at 30 DAT. No visible signs of chlorosis and necrosis were observed in the spinach leaf under the speed-breeding chamber A and B throughout the 30 DAT period of study. However, at 10 DAT, lower leaf necrosis and chlorosis were observed on the spinach plant under the speed breeding chamber D and the control (Tab. 6). Furthermore, it was observed that the spinach plants under the speed breeding chamber A had the highest weight (4.2 g) at 30 DAT which showed a significant difference ($p < 0.05$) when compared to the weight of other spinach plant from B, C and D speed breeding chambers. The lowest spinach weight (2.2 g) was observed in the control (E). However, there was no significant difference ($p > 0.05$) between the weight of spinach plant under C and D speed breeding chamber, as well as the control (E) (Fig. 3). Chlorophyll-a and Chlorophyll-b content of spinach leaves at day 10 and 30 after transplanting also showed a significant increase between spinach leaves in speed breeding chamber A and others (B, C, D and Control). The control speed breeding chamber showed the least chlorophyll-a and chlorophyll-b content (Tab. 7).

Table 6. Response of spinach photoperiod on leaf tip necrosis and chlorosis.

Sample	LTNC (%)		
	10 DAT	20 DAT	30 DAT
A	No sign	No sign	No sign
B	No sign	No sign	No sign
C	No sign	10	15
D	20	25	25
E	30	30	35

Results with similar alphabetic superscripts on same column did not differ from each other ($p > 0.05$). Results were in mean and standard error of three replicates. DAT = Days after transplant. A = 19 hours photoperiod, B = 17 hours photoperiod, C = 15 hours photoperiod, D = 13 hours photoperiod and E = 11 hours photoperiod (control). LTNC = Leaf tip necrosis and chlorosis.

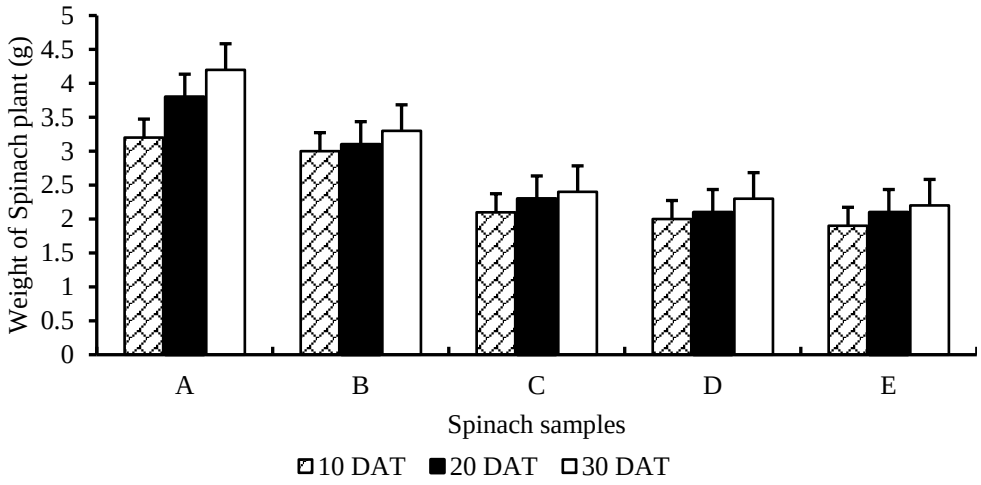

Figure 3. Response of spinach photoperiod on plant weight.

Table 7. Response of spinach photoperiod on chlorophyll-a and b.

Sample	Chlorophyll-a (mg/cm^2) FW on		Chlorophyll-b (mg/cm^2) FW on	
	10 DAT	30 DAT	10 DAT	30 DAT
A	6.4	8.9	2.9	3.6
B	6.1	8.1	2.6	3.2
C	6.1	8.0	2.6	3.0
D	4.8	5.2	3.1	3.6
E	4.1	5.0	2.8	3.3

DAT = Days after transplanting, FW =fresh weight, A = 19 hours photoperiod, B = 17 hours photoperiod, C = 15 hours photoperiod, D = 13 hours photoperiod and E = 11 hours photoperiod (control).

Discussion

LED-induced speed breeding technique has been widely used in improving algal breed in recent times. This research aimed at using the LED-induced speed breeding technique under different photoperiod to improve vegetative parameters of spinach plant. Since spinach plant is known to be a long day plant, allowing spinach to achieve its required photoperiod may be essential in improving the growth of spinach plant. Plant morphology and physiology can easily be influenced

by environmental photoperiods, majorly due to some plant photoreceptors that are sensitive to LED (Wolter *et al.,* 2019). From the current study, the increased number of spinach leaf observed in the speed-breeding chamber A (19 hours LED-induced photoperiod) may be linked to the effectiveness of the LED in improving vegetative parameters of spinach. This suggests that the LED level in the present study must have signal plant photoreceptors, leading to increase in growth parameters of the test plant. Similar results were found in Piovene *et al.,* (2015) experiment, where strawberry plant blooming was influenced with blue ratio lightening than the normal blooming period. In addition, blooming of Azalea was also improved using white ratio lightening source (Wolter *et al.,* 2019; Musa and Ikhajiagbe, 2024b). This research is in agreement with a study by Wolter *et al.,* (2019) where he discovered that extra plant leaf was observed in *Amaranthus hybridus* after 40 days red light induced photoperiod.

At elevated LED intensity, the increased stem length, leaf length and leaf area that was witnessed in the current study may be due to the increased plant photosynthetic activities. In this study, it can be concluded that due to the high LED light intensity, plants were able to optimize nutrient assimilation, bringing about increased growth of vegetative parameters. According to Piovene *et al.,* (2015), about 40% increase in plant biomass and 60% increase in plant yield properties were recorded using LED in comparison with organic fertilizers (Collard *et al*., 2017; Musa and Ikhajiagbe, 2023). However, the reduced spinach vegetative properties observed in the control can be linked to the reduce photoperiod witnessed in the control set up.

Root morphology is a good indicator of a plant's health since strong roots may help a plant grow correctly by supplying it with enough water and nutrients. In our experiment, the improved root parameters observed at increasing photoperiod may be due to the improved vegetative properties, leading to more nutrient intake and water usage. Research by Hogewoning *et al.,* (2010) explained that light photoperiod can induce the activation of phloem and xylem receptors, leading to more nutrient and water suction for plants during translocation, bring about root elongation as well as increased number of secondary roots. This result is in agreement with the work of Dong *et al.,* (2014) who observed increased root parameters. Furthermore, improved light intensity to a minimum level have been documented to bring about rapid cell growth and development (Musa and Ikhajiagbe, 2021).

Physiological parameters are significant in understanding the response of vegetables to photoperiod. For this purpose, physiological parameters such as leaf tip necrosis and chlorosis were studied. The higher signs of necrosis and chlorosis observed with reduced photoperiod indicated that the plant leaf is not receiving required duration of photoperiod, which may be the reason why

vegetative decline in spinach has been directly proportional to reduced photoperiod. According to Musa and Ikhajiagbe (2021), photosynthetic parameters are known to improve root properties of vegetables. Furthermore, the high photosynthetic pigments observed from the result of chlorophyll-a and chlorophyll-b in the 19 hours LED induced treatment (A) compared to the control indicated the positive effect of the increased LED photoperiod on plant photosynthesis. Since good light source can improve plant photosynthesis and improve exchange of stomatal gas (Collard *et al*., 2017), this may be reason that makes the spinach in the speed breeding chambers with high LED photoperiod had higher plant morphological, as well as physiological parameters.

Conclusion

The outcomes demonstrated that white LED light could be utilized in altering the growth, yield and metabolism for spinach plant. The 19 hours LED-induced photoperiod proved to be the most effective and optimum light level for spinach plant. For the optimal light combinations to be achieved, it is important that the white LED lightening source be used. Based on the findings, it appears that spinach may develop to its peak quality in 6 weeks under white LED induced photoperiod with continuous 19 hours duration per day.

Conflict of interest. None exist among the authors

References

Alika, J. (2006). Statistics and research methods. 2nd Ed. *Ambik Press*, Benin City, Nigeria. pp. 369. https://doi.org/10.1101/2020.09.30.320952

Arnon, D. (1949). Copper enzymes in isolated chloroplast Polyphenol Oxidase in *Beta vulgaris. Plant Physiology*. 24, 1-15. https://doi.org/10.1104/pp.24.1.1

Chiurugwi, T., Kemp, S., Powell, W., Hickey, L.T & Powell, W. (2018). Speed breeding orphan crops. *Theory of Applied Genetics*. 2(2), 12-19. https://doi.org/10.1007/s00122-018-3202-7

Collard, B. C., Beredo, J. C., Lenaerts, B., Mendoza, R., Santelices, R., Lopena, V., Verdeprado, H., Raghavan, C., Gregorio, G. B. & Vial, L. (2017). Revisiting rice-breeding methods evaluating the use of rapid generation advance (RGA) for routine rice breeding. *Plant Product of Science*. 20, 337–352. https://doi.org/10.1080/1343943x.2017.1391705

Dong, C., Fu, Y., Liu, G. and Liu & H. (2014). Growth, photosynthetic characteristics, antioxidant capacity and biomass yield and quality of wheat (*Triticum aestivum* L.) exposed to LED light sources with different spectra combinations. *Journal of Agronomy and Crop Science*. 200, 219–230. https://doi.org/10.1111/jac.12059

Enerijiofi, K. E., Musa, S. I., Igiebor, F. A., Lawani, M., Chuka, N. E. Odozi, E. B. & Ikhajiagbe, B. (2024). Nanotechnological approaches for enhanced microbial activities, sustainable agriculture and the environment. In: *Sustainable Agriculture Nanotechnology and Biotechnology for Crop Production and Protection,* Rajput, V. D., Singh, A., Ghazaryan, K. and Minkina, T. M. (eds), Walter de Gruyter, Berlin, Germany, pp. 153-183. https://doi.org/101515/978311123494-009

Galvão, V.C. & Fankhauser, C. (2015). Sensing the light environment in plants: Photoreceptors and early signaling steps. *Current Opinions in Neurobiology* 34, 46-53. https://doi.org/10.1016/j.conb.2015.01.013

Hogewoning, S. W., Trouwburst, G., Maljaars, T. & Pooter, H. (2010). Blue light dose responses of leaf photosynthesis morphology and chemical composition of *Cucunis sativus* grown under different combinations of red and blue light. *Journal of African Breeding*. 23(2), 12-23. https://doi.org/10.1093/jxb/erq132

Hussain, H. A., Hussain, S., Khaliq, A., Ashraf, U., Anjum, S. A., Men, S. & Wang, L. (2018). Chilling and drought stresses in crop plants: Implications, crosstalk, and potential management opportunities. *Frontiers in Plant Science*. 9, 393-394. https://doi.org/10.3389/fpls.2018.00393

Ikhajiagbe, B., Edokpolor, Geoffrey O., Gloria O. & Thomas, U. (2017) Investigating plant growth and physiological response to soil wetting with grey water under different shade regimes: A case of fluted pumpkin (*Telfairia occidentalis*). *Electronic Journal of Polish Agricultural Universities* 20 (4), 44-49. https://doi.org/10.30825/5.ejpau.31.2017.20.4

Khan, A., Najeeb, U., Wang, L., Tan, D. K. Y., Yang, G., Munsif, F., Ali, S. & Hafeez, A. (2017). Planting density and sowing date strongly influence growth and lint yield of cotton crops. *Field Crops Research*. 209, 129–135. https://doi.org/10.1016/j.fcr.2017.04.019

Maxwell, K. & Johnson, G, (2000). Chlorophyll fluorescence - A practical guide, *Journal of Experimental Botany.* 51, 659-668. https://doi.org/10.1093/jexbot/51.345.659

Monostori, I., Heilmann, M., Kocsy, G., Rakszegi, M., Ahres, M., Altenbach, S. B., Szalai, G., Pál, M., Toldi, D., Simon-Sarkadi, L., Harnos, N., Galiba, G., & Darko, É. (2018). LED lighting - Modification of growth, metabolism, yield and flour composition in wheat by spectral quality and intensity. *Frontiers in Plant Science, 9*, 605. https://doi.org/10.3389/fpls.2018.00605

Moses Nathan, Ezenwata, I.S. and Musa, S.I. (2023). Some physicochemical properties and heavy metals in water from Oboshi rivee, Ibusa in Delta State, Nigeria. *Journal of Applied Sciences and Environmental Management*. 27(6), 91-98. https://doi.org/10.4314/jasem.v27i6.33

Musa, S. I. & Ikhajiagbe, B. (2021). The growth response of rice (*Oryza sativa* L. var. FARO 44) *in vitro* after inoculation with bacterial isolates from a typical ferruginous ultisol. *Bulletin of the National Research Centre.* 2(3), 23-29. https://doi.org/10.1186/s42269-021-00528-8

Musa, S.I. and Beckley Ikhajiagbe (2024a). Evaluation of previously isolated and characterized phosphate solubilizing bacteria with plant growth promoting potentials for Rice grown in ferruginous ultisol soil in Benin City, Edo State, Nigeria. *J. Appl. Science. Envion. Management*. 28, 4393-4407. https://doi.org/10.4314/jasem.v28i12.55

Musa, S.I. and Beckley Ikhajiagbe (2024b). Effects of plant growth promoting bacteria (PGPB) rhizo-inoculation on soil physico-chemical, bacterial community structure and root colonization of rice (*Oryza sativa* L. var. FARO 44) grown in ferruginous ultisol conditions. *Science World Journal*. 19(3), 894-899. https://dx.doi.org/10.4314/swj.v19i3.38

Musa, S.I. and Ikhajiagbe B. (2023). Seed bio-priming with phosphate solubilizing bacteria strains to improve rice (*Oryza sativa* L. var. FARO 44) growth under ferruginous ultisol conditions. *BioTechnologia*. 27, 33-51. https://doi.org/10.5114/bta.2023.125084

National Research Council. (2006). Assessment of NASA's Mars architecture. The National Academies Press, Washington DC.

Piovene, C., Orsini, F., Bosi, S. & Sanourser, R. (2015). Optimal red: blue ration in led lighting for nutraceutical indoor horticulture. *Scientific Horticulture*. 193, 202-208. https://doi.org/10.1016/j.scienta.2015.07.015

Priyadarshan, P. M. (2019). Breeding self-pollinated crops. Plant breeding: *Classical to Modern*. Springer. 23, 12-23.https://doi.org/10.1007/978981-13-7095-3

Rahman, M. A., Quddus, M. R., Jahan, N., Rahman, A., Hossain, M. R. A. S. H. & Iftekharuddaula, K. M. (2019). Field rapid generation advance: An effective technique for industrial scale rice breeding program. *The Experiment*. 47(2), 2659 2670.https://doi.org/10.1080/1343943X.2017.1391705

Ray, D. K., Mueller, N. D., West, P. C. & Foley, J. A. (2013). Yield trends are insufficient to double global crop production by 2050. *Journal of Agricultural Sciences.* 12, 23-29. https://doi.org/10.1371/journal.pone.0066428

Rouphael, Y., Cardarelli, M., Schwarz, D., Franken, P. & Colla, G. (2012). Effects of drought on nutrient uptake and assimilation in vegetable crops: In: *Plant responses to drought stress, from morphological to molecular features*, Aroca R. (ed.), Springer, Berlin, Heidelberg. https://doi.org/10.1007/978-3-642-32653-0_7

Wolter, F., Schindele, P. & Puchta, H. (2019). Plant breeding at the speed of light: The power of CRISPR/Cas to generate directed genetic diversity at multiple sites. *BMC Plant Biol*ogy. 19, 1–8.https://doi.org/10.1186/s12870-019-1775-1

STUDIA UNIVERSITATIS BABEŞ-BOLYAI BIOLOGIA, 70, 2, 2025 (p. 83-99)
doi:10.24193/subbbiol.2025.2.06

Antifungal activity of lactic acid bacteria against *Aspergillus niger* and *Fusarium oxysporum*

Houda Ouazzani[1 *], Anas Mami[2] and Nour Elhouda Madjidi[3]

[1] Department of Life and Environment, University of Science and Technology of Oran Mohamed-Boudiaf USTOMB, Algeria; [2] Laboratory of Applied Microbiology, Faculty of Sciences, University of Oran, Oran, Algeria; [3] University of Adrar - Saharan Natural Resources Laboratory - Flocculator. Adrar, Algeria

[*] Corresponding author, E-mail: houda.ouazzani@univ-usto.dz

Article history: Received 15 January 2025; Revised 28 October 2025; Accepted 28 October 2025; Available online 20 December 2025

Abstract. Many fungi are viewed as contaminants in nearly all food products. This contamination can be affected by various pollutants, including natural toxins. Among these toxins are mycotoxins produced by mold pathogens that affect plants. Combating these pathogens is essential in the agri-food industry, and the development of innovative strategies like biopreservation presents a promising solution. This study aims to isolate lactic acid bacteria (LAB) from fermented cow's milk and examine their antifungal properties against *Aspergillus niger* and *Fusarium oxysporum*. The LAB were identified through morphological, biochemical, and MALDI-Tof analyses. Five strains of LAB sourced from fermented cow's milk were evaluated for their antifungal activity using both the streak method and the double-layer method. The LAB isolates displayed inhibitory effects against *Aspergillus niger* and *Fusarium oxysporum*, showing a significant reduction in mean fungal diameter in comparison to the control, with these isolates categorizing under the *Lactobacillus* genus. The *Fusarium oxysporum* strain exhibited greater sensitivity to LAB compared to the *Aspergillus niger* strain. No decrease in antifungal activity was noted after subjecting the inhibitory metabolites in LAB supernatants to temperature treatments (4°C, 45°C, 60°C, and 100°C). After treatment with the proteolytic enzyme (chymotrypsin), no alterations in inhibition zones were observed. Inhibition was noted at an acidic pH for all strains. Investigating the nature of the inhibitory metabolites

of LAB through thin-layer chromatography (TLC) and following their characterization allowed us to conclude that the antifungal properties of this LAB are attributed to the production of lactic and acetic acids.

Keywords: antifungal activity, biopreservation, lactic acid bacteria, MALDI-Tof, thin layer chromatography

Introduction

Microorganisms, especially lactic acid bacteria (LAB), are extensively employed in the food sector for fermentation procedures (Bourdichon *et al*., 2012). These bacteria play a crucial role in improving the quality of fermented items by creating distinct organoleptic features, such as flavor and texture, while maintaining the original taste and aroma of the product (Ledenbach, 2009).

Biopreservation entails the introduction of selected bacterial strains into a product to inhibit the growth of undesirable microbes, without affecting the product's organoleptic and health aspects. LAB are particularly ideal for this approach, as they often produce various inhibitory substances, including organic acids, hydrogen peroxide, diacetyl, bacteriocins, and reuterin, which exhibit antagonistic microbiological properties that hinder the proliferation of unwanted microbiota (Leyva *et al*., 2017), while preserving the organoleptic and health characteristics of the product.

Nonetheless, microbial contamination in food can trigger considerable physical and biochemical alterations, including the generation of mycotoxins, which pose significant health hazards and economic repercussions. To tackle this issue, biological control techniques utilizing natural compounds sourced from bacteria, fungi, or plants are being explored as eco-friendly methods to thwart mold proliferation and guarantee food safety (Heydari and Pessarakli, 2010). To combat microbial spoilage, food preservation strategies are primarily employed to avoid spoilage during storage and distribution, extending to consumer usage (Prokopov and Tanchev, 2007). These methods help to ensure that the anticipated shelf-life durations are upheld (Russell and Gould, 2003). Moreover, they inhibit the growth of bacteria and fungi in food, delay fat oxidation to minimize rancidity, and sustain the quality, such as color, texture, flavor, and nutritional content of food products. Some of the most prevalent techniques include drying (Rahman and Perera, 2007), cooling (Fennema, 1966), smoking (Lingbeck *et al*., 2014), vacuum packaging (Goulas and Kontominas, 2007), pasteurization (Steele, 2000), irradiation (Abdulmumeen *et al.,* 2012), and ultra-high temperature (UHT) treatment (De Alcântara *et al.,* 2022).

Various biological control techniques utilizing natural substances from bacteria, fungi, or plants are being explored as eco-friendly approaches to inhibit mold proliferation and guarantee food safety (Calpice and Fitzgerald, 1999). Among these techniques, LAB have been utilized in a range of food items, such as dairy (Erem *et al*., 2024; Jaafar *et al*., 2024), vegetables (Nemati *et al.,* 2023), and seafood (Elidrissi *et al.,* 2023), where they significantly contribute to prolonging shelf life. This application aligns with the growing consumer preference for minimally processed foods that do not contain chemical preservatives. In the dairy sector, LAB have been historically employed in the creation of fermented milk products and are classified as Generally Recognized as Safe (Amenu *et al*., 2023), underscoring their recognized safety and effectiveness. Numerous studies have been conducted to formulate antifungal cultures for the Bio preservation of dairy products (Batish *et al*., 1997).

The presence of mycotoxin-producing fungi in food not only presents a quality challenge for the global food industry but also leads to significant health risks due to the generation of various mycotoxins, some of which can be quite hazardous for food safety. In current large-scale food production systems, which encompass numerous processing stages and a variety of ingredients, fungal contamination is frequently unavoidable, even with adherence to good manufacturing practices (Sadiq *et al*., 2019). In today's society, health-conscious consumers prefer fresh and natural foods that do not contain synthetic preservatives or stabilizers. Mycotoxins are a major health hazard for consumers, making the search for effective methods to prevent or eliminate them a primary goal. LAB show promising potential in this area due to their resistance and functional capabilities. This work is organized based on that premise, aiming to underscore the antifungal properties of LAB (Siedler *et al*., 2019).

Molds present in food can be classified into two groups: beneficial molds, which are involved in fermentation and antibiotic production (such as *Penicillium roqueforti* and *Penicillium camemberti*), and harmful molds that lead to food spoilage. Mycotoxins, produced by the secondary metabolism of filamentous fungi or molds, result in mycotoxicosis when consumed by humans or animals (Bhatnagar *et al*., 2004). Although these toxic substances are generated by fungi, they are not critical for their growth. They may, however, function as a defense mechanism against other microorganisms in their surroundings. The primary mold genera implicated in mycotoxin production comprise *Aspergillus, Claviceps, Penicillium,* and *Fusarium* (Le Bars, 1998).

Various factors, including fungal species, climatic conditions, and agricultural practices for growing and storing products, affect mycotoxin levels in food (Castegnaro and Pofhl-Leszkowicz, 2002). The objective of the study was to explore the antifungal properties of LAB and to identify and characterize the

inhibitory metabolites contributing to this antifungal effect. The findings support the ongoing efforts to establish LAB as dependable bio-preservation agents in the food industry.

Materials and methods

Biological material

Lactic acid bacteria (LAB). LAB were isolated from fermented cow's mbarefoot ilk samples. These samples were collected directly from a farm located in Oran (western Algeria). Successive decimal dilutions were made in 9 ml of sterile physiological saline up to a dilution of about 10^{-6}, from which 1 ml was taken from the 10^{-4}, 10^{-5}, and 10^{-6} dilutions and inoculated into Petri dishes filled with MRS (deMan, Rogosa, and Sharpe) culture medium supplemented with $CaCO_3$ at 5 g/l. The cultures were incubated at 37°C for a period of 48 to 72 hours. After the incubation period, 10% of the various types of colonies that formed and had a clear halo were selected and purified on MRS, followed by further tests, including the catalase test and Gram staining. The identification of the LAB isolates was conducted using conventional analytical methods that relied on morphological examination, physiological and biochemical criteria, and were compared against the identification table (Carr *et al.,* 2002). Additionally, identification was performed through the MALDI-ToF method.

Phytopathogenic fungi. The fungal strains used in this study were primarily provided by the Saharan Natural Resources Laboratory at Adrar University, Algeria. The fungal species included: *Aspergillus niger* and *Fusarium oxysporum*. These fungal strains were subcultured on Potato Dextrose Agar (PDA) medium and incubated at 37°C for five days.

Identification of bacterial isolates using the Bioÿper Sirius GP MALDI system. The identification of bacterial isolates took place at the Genomics Technology Platform of the Oran School of Biological Sciences (Algeria) utilizing the MALDI Biotyper Sirius GP system from Bruker Daltonics, Germany.

Antifungal activity research. The antifungal activity of LAB against *Aspergillus niger* and *Fusarium oxysporum* was first evaluated through a qualitative test (Wang *et al*., 2012; Gerbaldo *et al.,* 2012), followed by a quantitative assessment (Barefoot and Klaenhammer, 1983).

Qualitative ("confrontation") test: Initially, two streaks of each lactic culture were applied on Petri dishes containing the MRS culture medium and incubated at 37°C for 48 hours. Subsequently, a 5mm disc of each fungus was positioned in the same dish, which was then incubated again at 30°C for three

days. After the incubation, the fungal growth diameter was measured and compared against a control, which consisted of an uninhibited fungal strain placed in the center of the dish containing PDA medium without LAB. The percentage inhibition of growth of the phytopathogenic fungus (I) was calculated using the following formula: $I = (Rw - Rt / Rw) \times 100$, where Rw represents the maximum radial distance of growth for the phytopathogenic fungus in the non-LAB control and Rt denotes the radial distance of growth for the phytopathogenic fungus towards the antagonist (measured in centimeters). All experiments were conducted in triplicate and repeated three times.

Quantitative (well) test: Wells were created in the agar surface of a Petri dish filled with MRS medium that had been inoculated with fungi, using a sterile tip. Subsequently, 100 µl of the supernatant from each culture was placed in the wells. The wells were formed with a cookie cutter on a Petri dish containing 10 ml of MRS, which was then overlaid with 10 ml of PDA medium that had a monosporal suspension (10^3 spores/ml); after this, 100 µl of the lactic bacteria supernatant was added to the wells. LAB strains were grown in MRS broth at 37°C, and after 18 hours of incubation, the cells were centrifuged at 4000 rpm for 15 minutes at 4°C. It's important to filter the supernatant through a 0.22 µm Millipore filter to inhibit bacterial cell growth. A negative control with no inoculated culture medium was established. After a 72-hour incubation at 37°C, the zones of inhibition around each well were evaluated.

Antifungal metabolite characterization

The temperature effect. The thermal influence on the crude active supernatant of LAB was examined at varying temperatures (4°C, 45°C, 60°C, 100°C) for a duration of 20 minutes (Teubeur, 1993; Stiles, 1996). Heating was performed in a water bath. This investigation was conducted using the Well Method (Barefoot and Klaenhammer, 1983).

The pH effect. Antifungal efficacy was evaluated in liquid MRS (medium deMan, Rogosa, and Sharpe) at pH levels of 2, 4, 6, and 8, followed by an 18-hour incubation at 37°C utilizing the well method described by Barefoot and Klaenhammer (1983).

Proteolytic enzyme effect. The influence of proteolytic enzymes was determined according to the methodology outlined by Hirsch, 1979. Accordingly, 10 µl of chymotrypsin enzyme (1 mg ml^{-1}, prepared in a buffer solution of 50 mM Tris-HCl, pH 8.0) was mixed with the active crude supernatant. The study utilized the previously mentioned well method (Barefoot and Klaenhammer, 1983). Zones of inhibition were evaluated after three days of incubation at 30°C and compared to the untreated control.

Identification of inhibiting metabolites

Thin layer chromatography (TLC). This method, which is based on adsorption, enables the initial separation and identification of metabolites in the supernatant, according to the approach described by Lee et al. (2001). The frontal ratio (Rf) is calculated as the ratio of the distance migrated by the sample (L1) to the distance traveled by the mobile phase (L2), serving as a comparative measure of metabolite migration. (Rf = L1/L2), where L1 represents the distance of the spot formation and L2 signifies the migration distance of the mobile phase.

Results

Identification of LAB

Following the purification of the various isolates on MRS agar medium, the LAB colonies appeared small, with a whitish or yellowish hue, transparent and smooth textures, and distinct lenticular shapes. The macroscopic observations after purifying the LAB isolates in liquid MRS medium displayed a clear halo on the surface, which signifies the microaerophilic characteristics of our strains. All test outcomes, determined by physiological and biochemical traits, are summarized (Tab. 1).

Table 1. Morphological, physiological and biochemical characteristics of lactic acid bacteria isolated from fermented cow's milk.

Properties	LAB1	LAB2	LAB3	LAB4	LAB5
Gram strain	+	+	+	+	+
Spores formation	-	-	-	-	-
Catalase activity	-	-	-	-	-
Fermentation type	Hetero-	Hetero-	Hetero-	Hetero-	Hetero-
Exopolysaccharide production	+/-	+/-	+/-	+/-	+/-
Use of citrates	-	-	-	-	-
Gelatin degradation	+	+	+	+	+
Acetoin degradation	-	-	-	-	-
Mannitol-mobility	-	-	-	-	-
Fermentation of D-fructose	+	+	+	+	+
D-Mannose	+	+	+	+	+
D-Raffinose	+	+	+	+	+
Saccharose	+	+	+	+	+
Ribose	+	+	+	+	+

Properties	LAB1	LAB2	LAB3	LAB4	LAB5
Gluconate	+	+	+	+	+
Lactose	+	+	+	+	+
Galactose	+	+	+	+	+
Esculine	+	+	+	+	+
D-Glucose	+	+	+	+	+
Maltose	+	+	+	+	+
D-tagatose	+	+	+	+	+
Growth at 15°C	-	-	-	-	-
Growth at 45°C	+	+	+	+	+
ADH degradation	-	-	-	-	-

Identification of bacterial isolates using the MALDI-TOF Biotyper Sirius GP system

Following a series of triplicate analyses conducted on the samples utilizing the MALDI-TOF BIOTYPER Sirius GP system, all five strains were identified as *Limosilactobacillus fermentum*, achieving a high overall confidence score (Tab. 2). The findings suggest that *Limosilactobacillus fermentum* is predominant in the ecological niche from which the samples were isolated. Additionally, there is a potential for redundancy of the same strain. To validate this assumption, further investigations, such as REP-PCR and 16S rRNA sequencing, should be performed.

Table 2. Identification of isolated strains by the MALDI-TOF/BS GP method with the log value of similarities.

Strain code	Matched pattern	Score
LAB1	*Limosilactobacillus fermentum* DSM 20391 DSM-2	2.16
LAB2	*Limosilactobacillus fermentum* 21 –PG -1 ZZMK	2.05
LAB3	*Limosilactobacillus fermentum* 21 –PG -1 ZZMK	2.10
LAB4	*Limosilactobacillus fermentum* 21 –PG -1 ZZMK	2.08
LAB5	*Limosilactobacillus fermentum* 21 –PG -1 ZZMK	1.86

Study of the antifungal activity of LAB

The study examined the production of antifungal agents targeting *Aspergillus niger* and *Fusarium oxysporum* using the streak method outlined by Magnusson *et al.* (2003), which facilitated an initial selection of LAB with anti-*Aspergillus* and anti-*Fusarium* properties. The direct confrontation tests between LAB and phytopathogenic fungi indicated a significant decrease in fungal diameter in the presence of LAB compared to the control group.

The inhibition effects appeared to vary by strain, with the *Fusarium* strain demonstrating greater sensitivity to the LAB supernatant than the *Aspergillus* strain. The assessment disclosed a range of antifungal effectiveness among the bacterial strains, with fungal growth inhibition rates varying from 33% to 100%. LAB2 exhibited low antifungal efficacy against *Aspergillus niger*, while LAB1 and LAB5 showed moderate inhibitory effects, stopping the fungus's growth, in contrast to LAB3 and LAB4, which demonstrated strong activity against *Aspergillus*. The findings indicate that certain strains of LAB possess significant inhibitory action against *Fusarium*, leading to a total lack of fungal growth (Fig. 1, 2).

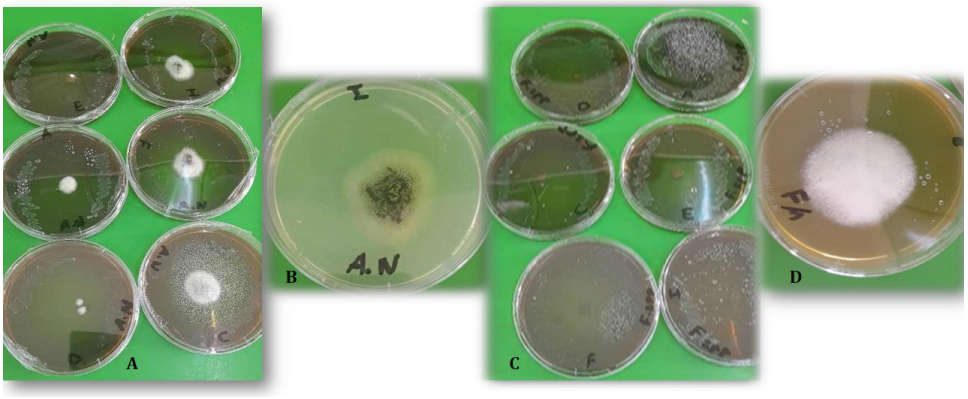

Figure 1. A: Antifungal activity of strains of LAB against *Aspergillus niger* by the streak method. B: *Aspergillus niger* control. C: Antifungal activity of strains of LAB against *Fusarium oxysporum* by the streak method. D: *Fusarium oxysporum* control.

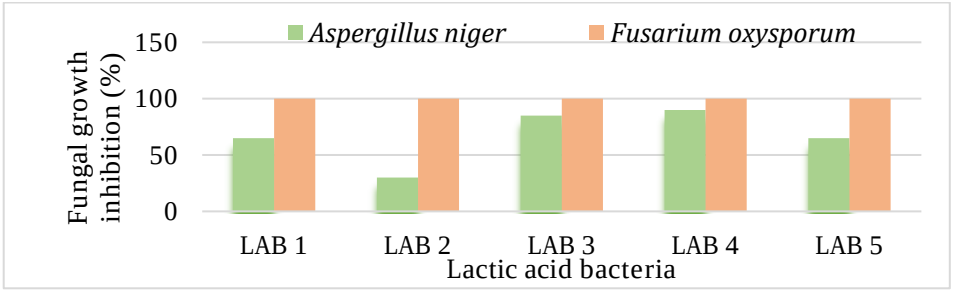

Figure 2. Inhibition of two phytopathogenic strains (*Aspergillus niger* and *Fusarium oxysporum*) by 05 strains of lactic bacteria. LAB1: *Limosilactobacillus fermentum* DSM 20391 DSM-2(2.16), LAB2: *Limosilactobacillus fermentum* 21-PG-1 ZZMK 2.05, LAB3: *Limosilactobacillus fermentum* 21-PG-1 ZZMK 2.10, LAB4: *Limosilactobacillus fermentum* 21-PG-1 ZZMK 2.08, LAB5: *Limosilactobacillus fermentum* 21-PG-1 ZZMK 1.86

Characterization of antifungal metabolites

The areas of inhibition differ based on how the inhibiting metabolites in the supernatants are treated.

The temperature effect. No decrease in antifungal effectiveness was noted after exposing LAB metabolites to temperatures of 4, 45, 60, and 100 °C for 20 minutes. This compound was observed to maintain its stability for 20 minutes across the temperature range of 4°C to 100°C. The inhibitory compound generated by lactic isolates is regarded as thermally stable (Fig. 3, 4).

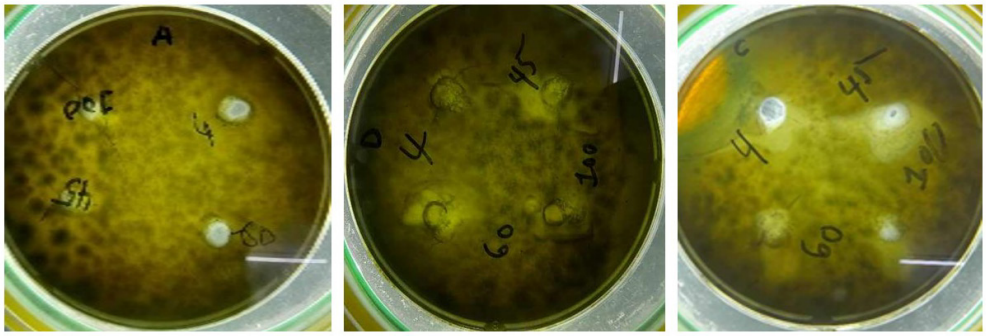

Figure 3. The effect of different temperatures on antifungal substances produced by LAB against *Fusarium oxysporum*.

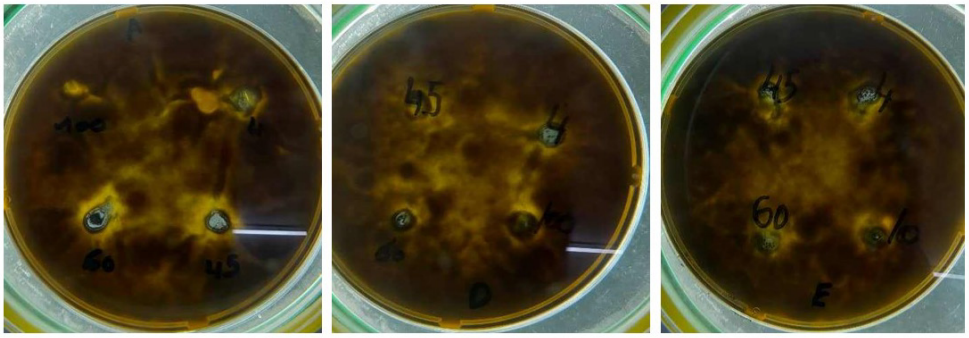

Figure 4. The effect of different temperatures on antifungal substances produced by against *Aspergillus niger*.

The pH effect. The findings indicated that the antifungal effectiveness of the supernatant diminishes as the pH increases, while a drop in pH corresponds with an enhancement in this activity, peaking at pH 2, 4, and 6 against *Aspergillus*

niger and *Fusarium oxysporum*, decreasing once pH reaches 8 (Fig. 5). This trend is frequently seen in antifungal agents, where pH significantly impacts the stability and effectiveness of the active ingredients. Additionally, we tested an SRM medium buffered to pH 7 to determine if there would be any suppression of fungal growth, with the results showing antifungal activity at neutral pH.

Proteolytic enzyme effect. Treatment of antifungal substances with the proteolytic enzyme (Chymotrypsin) does not appear to alter their inhibitory activity. This finding suggests that the enzyme's action on these compounds does not compromise their ability to inhibit fungal growth, offering a promising new avenue in the development of potential antifungal treatment methods, which suggests that the antifungal activity may be due to compounds other than proteins.

Research of the nature of antifungal substances. This initial study regarding the biochemical properties of the metabolites generated by LAB indicated that these substances are resistant to heat, maintain their efficacy when exposed to chymotrypsin treatment, and are more potent at acidic pH levels, implying a significant role of organic acids in their antifungal action.

Thin layer chromatography (TLC)

The retention factors (Rf) determined with a mobile phase migration distance (L2) of 7 cm show that acetic organic acids have a better migration performance, while lactic acid exhibits a shorter migration distance (Tab. 3, Fig. 5).

Table 3. Frontal ratios of organic acid revelation spots.

Depots	L2	RF=L1/L2
Lactic acid	0.5	0.071
Acetic acid	2.5	0.35
Citric acid	3.5	0.5
Limosilactobacillus fermentum DSM 20391 DSM-2 (2.16)	2.5	0.35
Limosilactobacillus fermentum 21-PG-1 ZZMK 2.05	2.5	0.35
Limosilactobacillus fermentum 21-PG-1 ZZMK 2.10	2.5	0.35
Limosilactobacillus fermentum 21-PG-1 ZZMK 2.08	2.5	0.35
Limosilactobacillus fermentum 21-PG-1 ZZMK 1.86	0.5	0.071

Figure 5. Separation of organic acids by thin-layer chromatography (TLC). AL: lactic acid, AC: citric acid, AA: acetic acid, LAB1: *Limosilactobacillus fermentum* DSM 20391 DSM-2(2.16), LAB2*: Limosilactobacillus fermentum* 21-PG-1 ZZMK 2.05, LAB3: *Limosilactobacillus fermentum* 21-PG-1 ZZMK 2.10, LAB4: *Limosilactobacillus fermentum* 21-PG-1 ZZMK 2.08, LAB5: *Limosilactobacillus fermentum* 21-PG-1 ZZMK 1.86.

The supernatant from most of the strains exhibited an Rf value of 0.35, which corresponds precisely to that of acetic acid; thus, we can conclude that in the various strains where inhibition was observed, acetic acid is the predominant organic acid present. Conversely, one specific strain's supernatant showed an Rf value of 0.071, matching that of lactic acid. This study reinforces the notion that the antifungal properties of LAB against *Aspergillus niger* and *Fusarium oxysporum* are attributed to the organic acids: acetic and lactic.

Discussion

LAB isolates were characterized through two different stages. The initial stage involves Gram staining, catalase activity testing, and spore identification. The second stage focuses on both macroscopic and microscopic morphological examinations, alongside fermentation type analysis. Based on identification using the MALDI-Tof method, all lactic bacteria from fermented cow's milk selected from the Oran region are classified under the genus *Limosilactobacillus*. As noted by Sudeepa and Bhavini (2020), *Lactobacillus fermentum* is a species within the *Lactobacillus* genus known for its wide-ranging probiotic and antimicrobial characteristics, as well as its straightforward cultivation and characterization. Exploiting this bacterium for meaningful applications that could benefit humanity offers a valuable opportunity.

LAB demonstrate significant antagonistic properties against various microorganisms, including pathogens and organisms that cause food spoilage. To address the germs linked to food poisoning, eight strains of *lactobacilli* were isolated and identified from raw goat milk in western Algeria, primarily belonging to the following dominant species*: Lb. plantarum* (*Lb.*58), *Lb. plantarum* (*Lb.*68), *Lb. casei* (*Lb.*13), *Lb. rhamnosus (Lb.*54 and *Lb.*52), *Lb. paracasei* subsp. *paracasei* (*Lb.*55), *Lb. sakei* subsp. *sakei* (*Lb.*21), and *Lb. plantarum* (*Lb.*22) (Mami, 2013).

The findings of this research indicate that the antifungal properties of strains of *Lactobacillus* spp exhibit varying levels of antifungal efficacy against *Aspergillus niger* and *Fusarium oxysporum*. Additionally, although all five strains belong to the same genus, their zones of inhibition differ. The inhibitory effects are strain-dependent, with *Fusarium* strains appearing to be more susceptible to the effects of LAB supernatant compared to *Aspergillus* strains. Comparable findings were reported by Nazareth *et al.* (2019), who observed that *L. plantarum* CECT 748 and *L. plantarum* CECT 749 were the only ones demonstrating antifungal activity against all *Fusarium* and *Aspergillus* strains. Further investigations conducted by Guo *et al.* (2012) revealed that various *Lactobacillus* strains exhibit strong antifungal effects against *A. fumigatus* and *A. niger.*

Additional studies by Dalie *et al.* (2010) indicated a correlation between cell growth, pH levels, and the generation of antifungal metabolites. These metabolites retain their antifungal properties even after being subjected to 120°C for 20 minutes. However, research by Hansal *et al.* (2024) indicated that *Leuconostoc* selected against Gram-positive indicator bacteria showed a decrease after heat treatments (60°C/30 min, 80°C/15 min, 100°C/15 min), with most strains completely vanishing after 120°C for 10 minutes. Batish *et al.* (1997) and Sathe *et al.* (2007) proposed that pH is a critical factor in the synthesis of antifungal metabolites, with optimal production seen in *Lc. lactis* subsp. *diacetylactis* at pH levels of 6 and 8. Research has demonstrated that pH fluctuations can affect solubility, bioavailability, and the interaction between antifungal compounds and fungal cell membranes, thereby influencing their overall effectiveness. The application of proteolytic enzyme (Chymotrypsin) to antifungal substances does not seem to impact their inhibitory performance. Similar findings were reported by Laref (2014).

The current study validates that LAB exhibit antifungal properties against *Aspergillus niger* and *Fusarium oxysporum* due to the presence of acetic and lactic acids. As noted by Riley and Wertz (2002), the primary factor behind the inhibitory action of LAB is organic acids. Moreover, Sadiq *et al.* (2019) indicate that lactic, acetic, and propionic acids can slow the growth of *Aspergillus niger*, *Penicillium corylophilum*, and *Eurotium repens.* These acids interact with the cytoplasmic membrane, leading to the disruption of the membrane potential

and hindering active transport mechanisms. *Lactobacillus* species are well established for their production of organic acids in culture environments and for their capacity to generate hydrogen peroxide and other antimicrobial substances (Barefoot and Klaenhammer, 1983). The inhibitory effects of *Lactobacilli* may stem from the production of lactic and/or acetic acid; indeed, lactobacilli are recognized for their notable resistance to acidic conditions (Wilson *et al.,* 2005; Benthin and Villadsen, 1995), in addition to the synthesis of bacteriocins (Lrsen *et al*., 1993; Avila *et al.,* 2005).

Conclusions

The objective of the current study was to explore the antifungal properties of lactic bacteria in relation to *Aspergillus niger and Fusarium oxysporum*, as well as to identify the inhibitory metabolites involved. Five bacterial isolates were obtained from fermented cow's milk and underwent additional analysis. These isolates were recognized as LAB through morphological, biochemical, and physiological assessments, along with MALDI-Tof identification.

Following the qualitative and quantitative assessment of the inhibitory effects of the lactic isolates, it was observed that these strains exhibited significant fungal inhibition. It seems that the inhibitory activity differs among the various strains. The strains of *Fusarium oxysporum* demonstrated greater sensitivity to the impacts of the supernatants from lactic bacteria compared to *Aspergillus niger* strains.

The compounds produced by LAB are stable against temperature changes and proteolytic enzymes, exhibiting strong antifungal properties at acidic pH levels. The use of thin-layer chromatography (TLC) has confirmed that the antifungal action of LAB against *Aspergillus niger* and *Fusarium oxysporum* is attributed to the production of organic acids like acetic and lactic acids. The inhibitory mechanism of LAB is intricate, necessitating further investigation to conclusively establish their antifungal effectiveness, safety, and biocompatibility.

References

Abdulmumeen, H. A., Risikat, A. N., & Sururah, A. R. (2012). Food: Its preservatives, additives and applications. International *J. Chem. Biochem Sciences*, 1, 36-47. https://doi.org/10.13140/2.1.1623.5208

Amenu, D., & Bacha, K. (2023). Probiotic potential and safety analysis of lactic acid bacteria isolated from Ethiopian traditional fermented foods and beverages. *Ann. Microbiol.*, 73(1), 37. https://doi.org/10.1186/s13213-023-01740-9

Avila, M., Garde, S., Medina, M., & Nunez, M. (2005). Effect of milk inoculation with bacteriocin producing lactic acid bacteria on a *Lactobacillus helveticus* adjunct cheese culture. *J. Food Prot.* 68, 1023-1033. https://doi.org/10.4315/0362-028x-68.5.1026

Barefoot, S.F, & Klaenhammer, T.R. (1983). Detection and activity of lactacin B, a bacteriocin produced by *Lactobacillus acidophilus*. *Appl. Environ. Microbiol.*, 45(6),1808- 1815. https://doi.org/10.1128/aem.45.6.1808-1815.1983

Batish, V.K., Roy, U., Lal, R., & Grower, S. (1997). Antifungal attributes of lactic acid bacteria - a review. *Crit. Rev. Biotechnol*., 17(3), 209-225. https://doi.org/10.3109/07388559709146614

Benthin, S., & Villadsen, J. (1995). Different inhibition of *Lactobacillus delbruckii subsp. bulgaricus* by D- and L- lactic acid: effects on lag phase, gowth rate and cell yield. *J. Appl. Bacteriol*., 78, 647-654. https://doi.org/10.1111/j.1365-2672.1995.tb03111.x

Bhatnagar, D., Payne, G.A., Cleveland, T.E. & Robens, J.F. (2004). Mycotoxins: current issue in USA. In H. Barug, H.P. van Egmond, R. Lopez-Garcia, W.A. van Osenbruggen and A. Visconti (eds). Meeting the mycotoxin menace, pp. 17–47. Wageningen, the Netherlands, Wageningen Academic Publisher.

Bourdichon, F., Casaregola, S., Farrokh, C., Frisvad, J.C., Gerds, M.L., Hammes, W.P., Harnett, J., Huys, G., Laulund, S., Ouwehand, A., Powell, I.B., Prajapati, J.B., Seto, Y., Ter Schure, E., Van Boven, A., Vankerckhoven, V., Zgoda, A., Tuijtelaars, S., Hansen, E.B. (2012). Food fermentations: microorganisms with technological beneficial use. *Int. J. Food Microbiol*., 2012 Mar 15;154(3), 87-97. https://doi.org/10.1016/j.ijfoodmicro.2011.12.030

Calpice, E., & Fitzgerald, G.F. (1999). Food fermentation: role of microorganisms in food production and preservation. *Int. J. Food Microbiol*., 50(1-2), 131-149. https://doi.org/10.1016/s0168-1605(99)00082-3

Carr, F.J., Chill, D., & Maida, N. (2002), The lactic acid bacteria: a literature survey, *Crit. Rev. Microbiol.*, 28(4), 281-370. https://doi.org/10.1080/1040-840291046759

Castegnaro, M., Pfolhl-Leszkowicz, A. (2002) Les mycotoxines: contaminants omniprésents dans l'alimentation animale et humaine. Moll. & Moll. (Eds). La sécurité alimentaire du consommateur. Lavoisier, Tec doc.

Dalie, D. K. D., Deschamps, A.M., Atanasova-Penichon, V., & Richard-Forget. F. (2010). Potential of *Pediococcus pentosaceus* (L006) isolated from maize leaf to suppress fumonisin-producing fungal growth. *J. Food Prot.,* 73(6), 1129-1137. https://doi.org/10.4315/0362-028x-73.6.1129

de Alcântara, N. E., Castro, J.S.M., Tavares Filho, E.R., Pagani, M.M., da Cruz, A.G., Máralém, E. T., & Esmerino, É. A. (2022). Use of stabilizers in UHT milk: technological and regulatory aspects. *J. Engineer. Exact Sci*., 8(8), 14846–01e. https://doi.org/10.18540/jcecvl8iss8pp14846-01e

Elidrissi, A., Ezzaky, Y., Boussif, K., & Achemchem, F. (2023). Isolation and characterization of bioprotective lactic acid bacteria from Moroccan fish and seafood. *Braz. J. Microbiol*., 54(3), 2117-2127. https://doi.org/10.1007/s42770-023-01077-0

Erem, E., & Kilic-Akyilmaz, M. (2024). The role of fermentation with lactic acid bacteria in quality and health effects of plant-based dairy analogues. *Compr. Rev. Food Sci. Food Saf.*, 23(4), e13402. https://doi.org/10.1111/1541-4337.13402

Fennema, O. (1966). An over-all view of low temperature food preservation. *Cryobiology*, 3(3), 197-213. https://doi.org/10.1016/S0011-2240(66)80013-5

Gerbaldo, G.A, Barberisa, C, Pascuala, L, Dalceroa, A, & Barberisa, L. (2012), Antifungal activity of two *Lactobacillus* strains with potential probiotic properties, *FEMS Microbiol. Lett.*, 332, 27-33. https://doi.org/10.1111/j.1574-6968.2012.02570.x

Goulas, A. E. & Kontominas, M. G. (2007). Effect of modified atmosphere packaging and vacuum packaging on the shelf-life of refrigerated chub mackerel (*Scomber japonicus*): biochemical and sensory attributes. *Eur. Food Res. Technol.,* 224, 545–553. https://doi.org/10.1007/s00217-006-0316-y

Guo, J., Brosnan, B., Furey, A., Arendt, E., Murphy, P., & Coffey, A. (2012). Antifungal activity of *Lactobacillus* against *Microsporum canis*, *Microsporum gypseum* and *Epidermophyton floccosum*, *Bioeng. Bugs*, 3, 2, 104-113. https://doi.org/10.4161/bbug.19624

Hansal, N., Benmchernene, Z., & Mebrouk, K. (2024). Antibacterial activity of *Leuconostoc mesonteroides* isolated from raw goat milk. *J. Appl. Biol. Sci.*, 18(1), 14-32. https://doi.org/10.71336/jabs.1261

Heydari, A., & Pessarakli, M. (2010). A review on biological control of fungal plant pathogens using microbial antagonists. *J. Biol. Sci.*, 10(4), 273-290. https://doi.org/10.3923/jbs.2010.273.290

Jaafar, M. H., Xu, P., Mageswaran, U. M., Balasubramaniam, S. D., Solayappan, M., Woon, J. J., The, C.S., Todorov, S.D., Park, Y.H., Liu, G., & Liong, M. T. (2024). Constipation anti-aging effects by dairy-based lactic acid bacteria. *J. Anim. Sci. Technol.*, 66(1), 178-203. https://doi.org/10.5187/jast.2023.e93

Laref, N. (2014). L'étude de l'activité antifongique des lactobacilles et leur effet sur la croissance d'*Aspergillus sp*. Thèse de doctorat, Université Oran.

Le Bars, J., & Le Bars, P. (1998) Strategy for safe use of fungi and fungal derivatives in food processing in Mycotoxins in Food chain, (Le Bars, J., Galtier, P., eds), *Revue Méditerranéene Vétérinaire*. 149, 493-500.

Ledenbach, L.H., & Marshall, R.T. (2009). Microbiological spoilage of dairy products. Compendium of the microbiological spoilage of foods and beverages, 41-67.

Lee, K.Y., So, J.S. & Heo, T.R. (2001). Thin layer chromathographic determination of organic acids for rapid identification of *Bifidobacteria* at genus level. *J. Microbiol. Methods*, 45(1), 1-6. https://doi.org/10.1016/s0167-7012(01)00214-7

Leyva Salas, M., Mounier, J., Valence, F., Coton, M., Thierry, A., & Coton, E. (2017). Antifungal microbial agents for food biopreservation-A review. *Microorganisms*, 5(3), 37. https://doi.org/10.3390/microorganisms5030037

Lingbeck, J. M., Cordero, P., O'Bryan, C.A., Johnson, M.G., Ricke, S.C., Crandall, P.G. (2014). Functionality of liquid smoke as an all-natural antimicrobial in food preservation. *Meat Sci.*, 97(2), 197-206. https://doi.org/10.1016/j.meatsci.2014.02.003

Lrsen, A.G., Vagensen, F.K., & Josephsen, J. (1993). Antimicrobial activity of lactic acid bacteria isolated from sour doughs: purification and characterization of bavaricin A, a bacteriocine produced by *Lactobacillus bavaricus* MI401. *J. Appl. Bacteriol.* 75(2), 113-122. https://doi.org/10.1111/j.1365-2672.1993.tb02755.x

Magnusson, J., Ström, K., Roos, S., Sjogren, J., & Schnürer, J. (2003), Broad and complex antifungal activity among environmental isolates of lactic acid bacteria. *FEMS Microbiol.* Letters, 219, 129-135. https://doi.org/10.1016/S0378-1097(02)01207-7

Mami, A. (2013). Recherche des bacteries lactiques productrices de bactérioicines à large spectre d'action vis à vis des germes impliqués dans les intoxications alimentaires (Doctoral dissertation, Université Mohamed Boudiaf des Sciences et de la Technologie-Mohamed Boudiaf d'Oran).

Nazareth, T.M., Luz, C., Torrijos, R., Quiles, J.M., Luciano, F.B., Mañes, J., & Meca, G. (2019). Potential Application of Lactic Acid Bacteria to Reduce Aflatoxin B1 and Fumonisin B1 Occurrence on Corn Kernels and Corn Ears. *Toxins (Basel),* 12(1), 21. https://doi.org/10.3390/toxins12010021

Nemati, V., Hashempour-baltork, F., Alizadeh, A. M., & Varzakas, T. (2023). Production of traditional torba yogurt using lactic acid bacteria isolated from fermented vegetables: Microbiological, physicochemical and sensory properties. *J. Agric. Food Research*, 14, 100850. https://doi.org/10.1016/j.jafr.2023.100850

Prokopov, T., & Tanchev, S. (2007). Methods of food preservation. Food safety: a practical and case study approach, Springer.

Rahman, M. S., & Perera, C. O. (2007). Drying and food preservation. Handbook of food preservation, CRC Press, 421-450.

Riley, M.A. & Wertz, J.E. (2002). Bacteriocins: evolution, ecology, and application. *Ann. Rev. Microbiol.*, 56(1), 117-137. https://doi.org/10.1146/annurev.micro.56.012302.161024

Russell, N. J., & Gould, G.W. (2003). Food preservatives, Springer Science & Business Media.

Sadiq, F.A., Yan, B., Tian, F., Zhao, J., Zhang, H., & Chen, W. (2019). Lactic acid bacteria as antifungal and anti-mycotoxigenic agents: A comprehensive review. *Compr. Rev. Food Sci. Food Saf.* 18 (5), 1403-1436. https://doi.org/10.1111/1541-4337.12481

Sathe, S.J., Nawani, N. N., Dhakephalkar, P.K., & Kapadnis, B.P.(2007). Antifungal lactic acid bacteria with potential to prolong shelf-life of fresh vegetables. *J. Appl. Microbiol.,* 103, 2622–2628. https://doi.org/10.1111/j.1365-2672.2007.03525.x

Siedler, S., Balti, R., & Neves, A.R. (2019). Bioprotective mechanisms of lactic acid bacteria against fungal spoilage of food. *Curr. Opin. Biotechnol.*, 56, 138-146. https://doi.org/10.1016/j.copbio.2018.11.015

Steele, J. H. (2000). History, trends, and extent of pasteurization. *J. Am. Vet. Med. Assoc.*, 217(2), 175-178. https://doi.org/10.2460/javma.2000.217.175

Stiles, M. E. (1996). Biopreservation by lactic acid bacteria. *Antonie van Leeuwenhoek*, 70, 331-345. https://doi.org/10.1007/BF00395940

Sudeepa, E.S., & Bhavini, K. (2020), Review on *Lactobacillus fermentum*. 6, 3. *IJARIIE*-ISSN(O)-2395-4396, 719- 726.

Teubeur, M. (1993). L'actic acid bacteria. In rahm. J., Reed., Puhller A., Stadller P (Eds.), *Biotechnology* , 2Ed., Verlag chemie, Weinheim 1, 325-366.

Wang, H, Yan, Y., Wang, J., Zhang, H., & Qi, W. (2012), Production and characterization of antifungal compounds produced by *Lactobacillus plantarum* IMAU10014, *PLoS ONE*, 7, e29452. https://doi.org/10.1371/journal.pone.0029452

Wilson, A.R., Signee, D. & Epton, H.A.S. (2005). Anti-bacterial activity of *Lactobacillus plantarum* strain SK1 against *Listeria monocytogenes* due to lactic acid production. *J. Appl. Microbiol*., 99, 1516-1522. https://doi.org/10.1111/j.1365-2672.2005.02725.x

STUDIA UNIVERSITATIS BABEŞ-BOLYAI BIOLOGIA, 70, 2, 2025 (p. 101-114)
doi:10.24193/subbbiol.2025.2.07

Overexpression of *HSFA4A* and *RAP2.12* transcription factors in *Arabidopsis thaliana* confers tolerance to various abiotic stresses

Norbert Andrási[1 *], Gábor Rigó[1], Laura Zsigmond[1] and László Szabados[1]

[1] *Institute of Plant Biology, Biological Research Centre, Szeged, Hungary*
[*] ***Corresponding author, E-mail: andrasinorbi@gmail.com.***

Article history: Received 18 February 2025; Revised 11 November 2025; Accepted 15 November 2025; Available online 20 December 2025

Abstract. Transcription factors are part of stress-signaling pathways, controlling activation of stress-responsive target genes. Heat shock factors and ethylene response factors can regulate responses to extreme temperature, salinity, drought, heavy metals, oxidative damage and anoxia. *Arabidopsis* HEAT SHOCK FACTOR A4A (HSFA4A) is part of the mitogen-activated protein kinase signaling pathway and was previously shown to regulate responses to salt, oxidative and heat stresses as well as their combinations. The RELATED TO APETALA2.12 (RAP2.12) factor was shown to be involved in anoxia, oxidative and osmotic stresses, and to modulate sensitivity to abscisic acid (ABA). Here we show that overexpression of *HSFA4A* and *RAP2.12* can increase the survival rate of *Arabidopsis* plants exposed to heat, salt or osmotic stresses and combinations of high temperature with salt or osmotic stresses. Moreover, overexpression of these factors improved photosynthetic activity in such adverse conditions. Photosynthetic performance of the *hsfa4a* and *rap2.12-2* mutants was variable in plantlets stressed in sterile conditions and less affected in soil-grown mutants when exposed to drought stress. Our data clearly indicate that these factors are implicated in stress response control, although their precise function remains to be elucidated.

Keywords: abiotic stress tolerance, *Arabidopsis*, combined stress, heat shock factor, RAP

Introduction

Extreme environmental conditions can considerably hinder plant growth and development. Plants evolved various mechanism to cope with such challenges, including a number of physiological, transcriptional, biochemical and molecular responses (Nawaz *et al.*, 2023). Effect of and responses to individual abiotic stresses, such as high temperature, drought, osmotic and salinity stress, are well documented (Mareri *et al.*, 2022; Zhang *et al.*, 2022). In natural environments such stress conditions often act simultaneously, resulting in a more dramatic and distinctive impact on plants. Combined stresses lead to novel and unique transcriptome and metabolome profiles, suggesting that simultaneous effects generate more complex responses (Rasmussen *et al.*, 2013; Rivero *et al.*, 2014; Sewelam *et al.*, 2014; Suzuki *et al.*, 2014; Barah *et al.*, 2016; Georgii *et al.*, 2017).

The success to adapt to extreme environmental conditions depends on cascades of molecular networks, stress-signaling pathways. Transcription factors (TFs) play a pivotal role in these pathways, regulating the activation of specific stress-related target genes by recognizing and binding to their *cis*-regulatory elements located in their promoter regions (Gujjar *et al.*, 2014; Khan *et al.*, 2018). TFs are essential components of the signal transduction networks, often regulated by various types of protein kinases, such as mitogen-activated protein kinase (MAPK) cascades, CBL-interacting protein kinases (CIPK) or calcium-dependent protein kinases (CDPKs). Based on genome wide analyses we can distinguish a large number of TFs belonging to different TF families, like HSF, AP2/ERF, MYB, bHLH, WRKY, bZIP, NAC and others (Lindemose *et al.*, 2013; Khan *et al.*, 2018).

Heat shock factors (HSFs) have been identified first as essential regulators of responses to high temperatures, but were found later to be implicated in salt, heavy metal, high light and other abiotic and biotic stresses (Andrási *et al.*, 2021). HSFs share a well conserved domain structure, consisting of DNA binding domain, oligomerization domain and nuclear localization signal. Heat shock factors activate target genes by recognizing and binding special regulatory elements in their promoters, called heat shock elements (HSEs). HSEs consist of palindromic cis-regulatory binding domains, 5′-AGAAnnTTCT-3′ (Nover *et al.*, 2001; Akerfelt *et al.*, 2010; Anckar and Sistonen, 2011). *Arabidopsis* HEAT SHOCK FACTOR A4A (HSFA4A) was identified in a salt screen using a special genetic tool, allowing controlled cDNA overexpression (COS system). HSFA4A confers tolerance to salt, oxidative, high irradiance and combined stress and it is phosphorylated by MPK3, MPK4 and MPK6 protein kinases. In response to individual or combined stresses HSFA4A can activate other TFs such as *WRKY30* and *ZAT12* or molecular chaperons such as heat shock protein 17.6A (*HSP17.6A)* by directly binding their HSE-containing promoter regions (Papdi *et al.,* 2008; Pérez-Salamó *et al.*, 2014; Huang *et al.*, 2018; Andrási *et al.*, 2019).

The ethylene response factor (ERF) family is a plant-specific group of TFs, which regulates hormone response, development, and tolerance to biotic and abiotic stresses (Licausi *et al.*, 2013; Dey and Vlot, 2015). The members of RAP-type ERF-VII TFs are involved in oxygen sensing, and they are distinguished by their conserved APETALA2 (AP2) domain that plays an essential role in protein–DNA interactions (Gibbs *et al.*, 2011; Licausi *et al.*, 2013). RELATED TO APETALA2.12 (RAP2.12) is a member of the ethylene response factor VII (ERF-VII) protein family. RAP2.12 was identified in *Arabidopsis* plants in a screen using the COS system and the *ADH1 promoter::luciferase* (*ADH1-LUC*) reporter (Papdi *et al*., 2008, Papdi *et al*., 2015). RAP2.12 confers tolerance to anoxia, oxidative and osmotic stress and enhances abscisic acid (ABA) sensitivity (Papdi *et al*., 2015).

Although HSFA4A and RAP2.12 belong to distinct transcription factor families, both have been reported to participate in various stress responses (Pérez-Salamó *et al.*, 2014; Papdi *et al.*, 2015; Andrási *et al.*, 2019). Therefore, we selected these two genes to compare and characterize their role in response to heat, salt, osmotic and combined stresses.

Materials and methods

Plant material and growth conditions

Arabidopsis Col-0 ecotype was used in all experiment. The overexpressing *Arabidopsis* lines, HSFA4Aox and RAP2.12ox, were generated in our lab (Papdi *et al.,* 2008; Pérez-Salamó *et al.*, 2014). The *hsfa4a* (GK-181H12) mutant line was a kind gift of prof. Wu (Huang *et al.,* 2018) and the *rap2.12-2* (SAIL-1215-H10) mutant line was identified and deposited in our lab collection by Papdi *et al.,* (2015).

Arabidopsis plants were grown in sterile conditions in growth chambers with the following settings: 8 h light–16 h dark light cycle at 22 °C and 100 µE m^{-2} s^{-1} light intensity (control condition). Seedlings were grown on half-strength Murashige and Skoog (½MS) medium. To control the transcription of *HSFA4A* and *RAP2*.12 in overexpressing *Arabidopsis* lines, the culture medium was supplemented with 5 µM estradiol at the beginning and during stress treatments (Pérez-Salamó *et al.*, 2014; Andrási *et al.,* 2019).

Stress conditions

Stress treatments were carried out *in vitro* in growth chamber, with the same light/dark cycle and light intensity as indicated above. Conditions for stress treatments were optimized on wild-type *Arabidopsis* plants (Col-0). A nylon mesh (SEFAR 07-20/13) was placed on the surface of agar-solidified

standard ½MS medium. Col-0 seeds were germinated, and seedlings were grown on this nylon mesh for 12 days and then placed to ½MS medium, containing 0.5% agar and the following supplements: 150mM or 200mM NaCl (salt stress), 300mM or 400mM Sorbitol (osmotic stress). Heat stress was implemented as incubation of seedlings on high temperature: 37 °C in light and 30 °C in dark (Andrási *et al.,* 2019).

Stress combinations were implemented by simultaneous application of salt or osmotic stress with high temperature. All treatments were carried out for 2-4 days. 40 wild-type plants were used for each stress treatment to optimize the treatments. In case of scoring plant survival, photosynthetic activity measurements and plant phenotyping, we used 70, 15 and 20 plants for each genotype (including the wild-type) in every treatment, respectively.

Scoring plant survival

Sensitivity to individual or combined stresses was evaluated by counting the percentage of recovered or dead plants after the treatments. Plants were subjected to different doses of stress and subsequently transferred to standard growth conditions for 7 days. Following the recovery period, we recorded the percentages of three groups: healthy plants, with several new green leaves, damaged plants, with decreased growth and possibly chlorotic leaves, and dead plants (Andrási *et al.,* 2019). 70 plants were assessed for each genotype in every treatment, divided into seven Petri dishes/treatment and 10 plants/genotypes in a Petri dish (13 cm diameter).

Photosynthetic activity

To assess the photosynthetic performance of control and stressed plants, we measured the PSII maximum quantum efficiencies (Imaging-PAM MAXI, M-Series, Heinz Walz GmbH, Germany; Baker 2008) using the same stress conditions as described above, except the treatments were carried out for three days and there was no recovery period. Fv/Fm values were measured on dark-adapted plants (incubation in dark for 15 minutes, 15 plants were used for each genotype in every treatment, divided into 3 Petri dishes as 5 plants/genotype in a Petri dish).

Plant phenotyping (drought stress)

Phenotypic traits of Col-0, *rap2.12-2* and *hsfa4a* mutants were recorded in controlled environmental conditions with the PlantScreen™ Compact Phenotyping System as described by Faragó *et al.,* (2022). Briefly, after germination plants were grown in soil filled pots for 21 days, in well-watered condition, then subjected to drought stress by suspending watering for 15 days. RGB and chlorophyll fluorescence (ChlF) images were obtained daily during the drought period. ChlF imaging was

performed after dark-adaptation (15 minutes) with specific intermittent light pulses, as described by Kant *et al.,* (2024). 20 plants/genotype/treatment were used in the experiment, planted individually in soil filled pots.

Results

Stress treatment optimization using wild-type Arabidopsis plants

Treatments were optimized with *Arabidopsis* wild-type (Col-0) plants. When heat stress was applied alone, all wild type plants survived, although more damaged plants recorded (30%). Salt stress had time- and concentration-dependent effect on wild type plants. After 2 days of 150-200mM NaCl treatment, 70% and 50% of the plants recovered, respectively. 54% and 23% of the plants survived when 150mM or 200 mM NaCl was used for 4 days. Consequently, higher doses of salt stress increased plant lethality (Fig. 1).

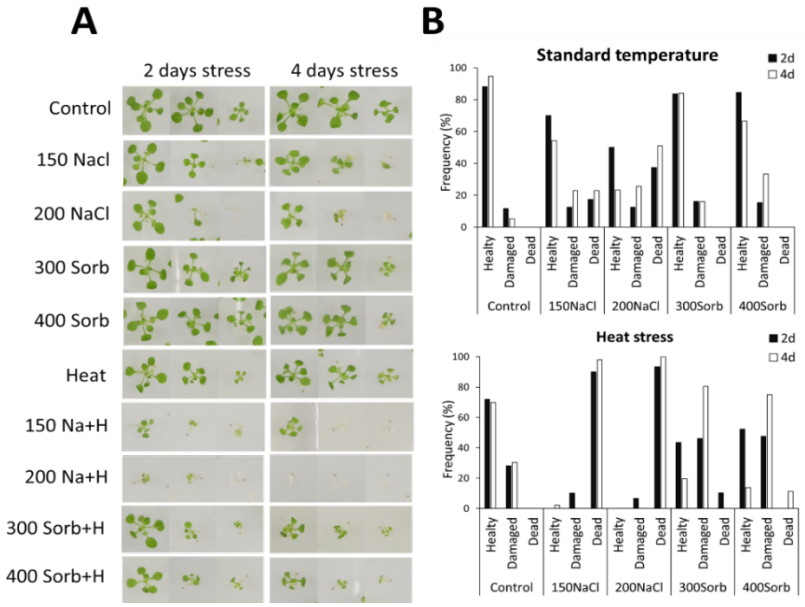

Figure 1. Stress response of wild-type *Arabidopsis* plants. Plants were grown *in-vitro* for twelve days, then exposed to different stress conditions. After 2 or 4 days of treatments plants were placed to standard culture conditions for recovery. Survival was scored by imaging the plants 7 days later. (A) Growth of wild-type (Col-0), after individual and combined stress treatments and recovery period. Treatments: 150 NaCl – 150mM NaCl; 200 NaCl – 200mM NaCl; 300 Sorb – 300mM Sorbitol; 400 Sorb – 400mM Sorbitol; 150 Na+H – 150mM NaCl+37°C Heat; 200 Na+H – 200mM NaCl+Heat; 300 Sorb+H – 300mM Sorbitol+Heat; 400 Sorb+H – 400mM Sorbitol+Heat. (B) Percentages of healthy, damaged, and dead plants after control, heat, salt, osmotic and combined stresses applied for 2 or 4 days.

Combination of salt stress with high temperature led to more severe damage: 90 to 93% of the plants died after 2 days, while nearly all of them was dead after 4 days of salt and heat stress. Surviving plants were heavily damaged after both 2 and 4 days of such treatments, regardless of salt concentration used (Fig. 1).

Effect of osmotic stress was slightly different. 300 and 400mM sorbitol concentration had similar effect, almost 85% of plants survived and were healthy after 2 days treatment, and around 15% of them were damaged. 4-days of 400mM sorbitol treatment had a bit more drastic effect, as it resulted in 34% damaged plants. Combination of osmotic and heat stress increased the ratio of damaged plants, although most of them still survived the treatments. When plants were simultaneously exposed to sorbitol and heat, 50% and 80% of the plants became damaged after 2 and 4 days of stress, respectively (Fig. 1B).

Based on the results of our trial experiment the following treatments were used to test the tolerance of the overexpressing and mutant *Arabidopsis* lines to various stresses: 125mM NaCl, 300mM Sorbitol, 37°C (heat), 125mM NaCl+heat and 300mM Sorbitol+heat for 4 days.

HSFA4A and RAP2.12 can alleviate the adverse effect of certain individual and combined stresses

Transcription factors HSFA4A and RAP2.12 were reported to regulate responses to different adverse conditions including salt, osmotic, anoxic or oxidative stress (Pérez-Salamó *et al.*, 2014; Papdi *et al.,* 2015; Andrási *et al.,* 2019). Their role in different stress combination and drought condition is not well known. To study the effects of HSFA4A and RAP2.12 factors on stress tolerance, responses of overexpressing lines and knockout mutants to salt and heat or osmotic and heat stresses and their combinations were tested. Due to the high degree of lethality of 150mM NaCl and heat stress combination (Fig. 1), 125mM of NaCl was used in combination with 37°C in subsequent experiments. Number of damaged plants increased moderately when heat stress (10-20%), sorbitol (15-35%) or combination of heat and sorbitol treatment (17-27%) was applied. No differences in survival rates between the overexpressing lines and mutants were observed compared to wild type, when sorbitol and heat treatment was applied alone or in combination (Fig. 2). However, overexpression of *HSFA4A* and *RAP2.12* significantly increased the number of healthy plants (from 65% to 85%) after salt treatment. When salt and heat treatment was applied in combination, *HSFA4A* overexpression had significantly positive effect on survival: while 19% of Col-0 plants survived this stress combination, 46% of HSFA4Aox plants recovered completely. Survival frequencies of the *hsfa4a* and *rap2.12* mutants were similar to wild type plants under these conditions (Fig. 2A, B).

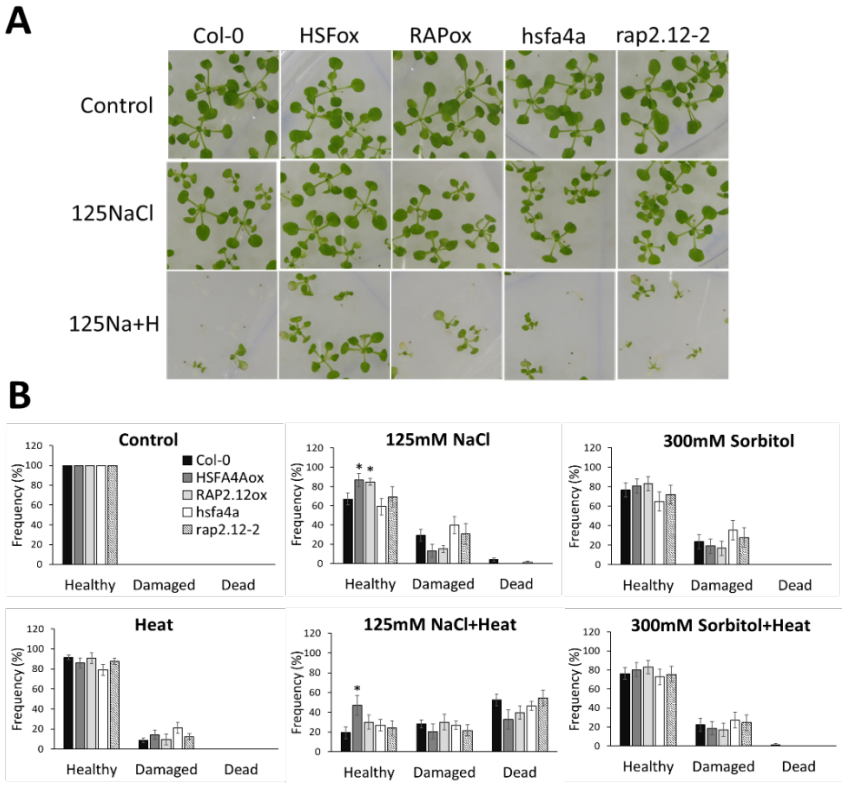

Figure 2. Survival of Col-0, transgenic overexpressing and mutant plants in salt, osmotic, heat stresses and their combinations. Survival rate was recorded after 7-day recovery. (A) Images of recovered Col-0, HSFA4Aox (HSFox), RAP2.12ox (RAPox), *hsfa4a* and *rap2.12-2* plants subjected to 125mM NaCl (125Na) and 125mM NaCl+Heat (125Na+H) treatments. (B) Percentages of established categories (healthy, damaged, and dead plants) after different stress conditions applied for 4 days. Standard errors are shown; overexpressing and mutant plants were compered to Col-0 plants (Student's *t*-test, **P*<0.05; n=7).

Photosynthetic parameters are known to be affected by environmental stresses. To find out how the studied TFs could influence photosynthetic efficiency in stress conditions, the maximum quantum yield of PSII photochemistry (Fv/Fm) was determined in mutant and overexpressing plants exposed to different stresses. *Arabidopsis* lines were exposed to the same stress conditions as described above, except that treatments were applied for 3 days, to get statistically more reliable results. In control condition the RAP2.12ox, *hsfa4a* and *rap2.12-2* had similar or

slightly higher Fv/Fm values than Col-0 plants. 300mM sorbitol treatment slightly reduced Fv/Fm values of all plants, but the differences between the genotypes remained similar to control. Col-0 and HSFA4Aox had Fv/Fm 0.65 to 0.67, while the other overexpressing and mutant lines displayed Fv/Fm 0.70. Heat stress reduced the Fv/Fm values of Col-0, HSFA4Aox and *hsfa4a* mutant lines to similar degree, while *RAP2.12* overexpressing and mutant lines had slightly higher Fv/Fm values. When osmotic stress was combined with high temperature, PSII maximum yield of HSFA4Aox, RAP2.12ox and *rap2.12-2* mutants were significantly higher when compared to Col-0 plants. Salt stress imposed by 125mM NaCl lead to considerable reduction of Fv/Fm while combination of salt and heat stress reduced even more these values. There were no significant differences between photosynthetic activities of the studied lines when they were exposed to combined salt and heat stress (Fig. 3).

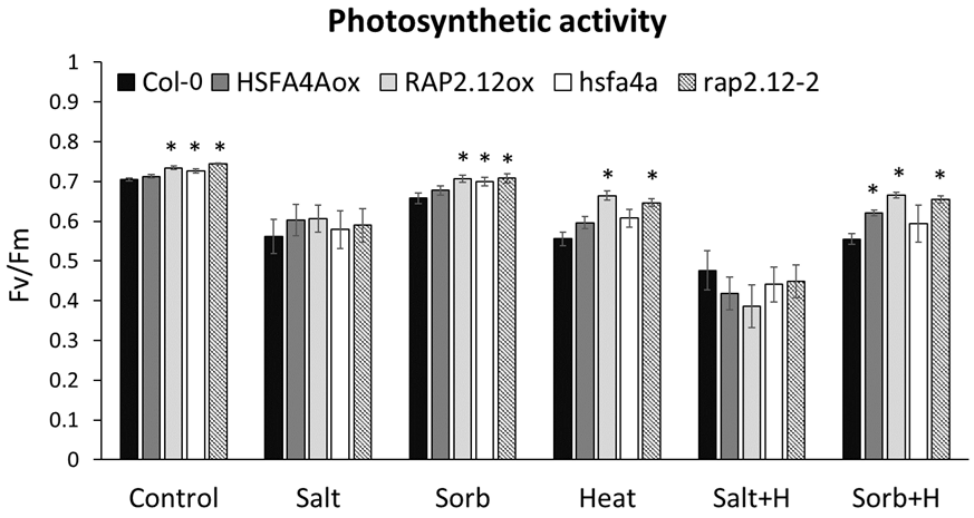

Figure 3. Photosynthetic activities of wild-type, HSFA4Aox, RAP2.12ox, *hsfa4a* and *rap2.12-2* plants after 72-hour of stress treatments (Salt: 125mM NaCl; Sorb: 300mM Sorbitol; Salt+H: 125mM NaCl+Heat; Sorb+H: 300mM Sorbitol+Heat). PSII maximum yields are shown. Standard errors are shown (n=3); significant differences to Col-0 wild-type plants were shown with statistical analyses, Student's *t*-test (*P<0.05).

To further characterize the role of HSFA4A and RAP2.12 in stress tolerance, we conducted an image-based phenotyping experiment analyzing growth and photosynthetic performance of soil grown Col-0 wild type, *hsfa4a* and *rap2.12-2* mutant plants in water-limited conditions. The rosette growth of *hsfa4a* mutant

in well-watered control condition was smaller than that of Col-0, throughout the whole experiment, while growth of *rap2.12-2* mutant was similar to Col-0 plants with the exception of last few days when its growth lagged behind the wild type. Water stress reduced growth of all lines to similar degree, with the exception of the *hsfa4a* mutant, which was less affected in the last few days of water limitation (Fig. 4A). The photosynthetic activity was monitored by chlorophyll fluorescence imaging. Fv/Fm values of all lines were similar in well-watered condition and were similar up to 9 days after watering was stopped. More severe water depletion has less deleterious effect on Fv/Fm of the studied mutants than Col-0 *Arabidopsis* plants (Fig. 4B).

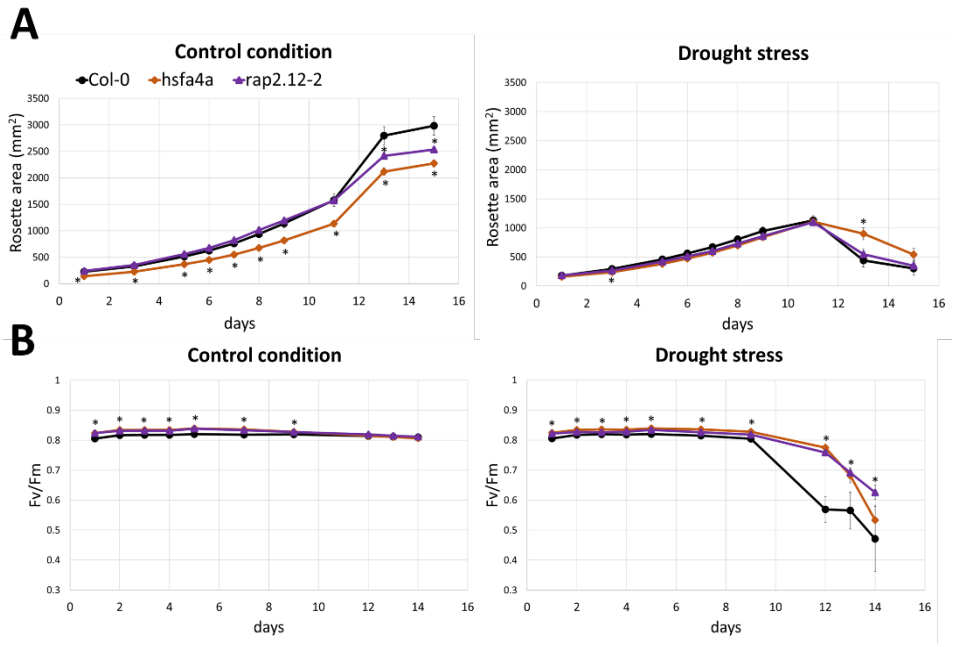

Figure 4. Image-based phenotyping of plants subjected to water deprivation. Plants were grown for 3 weeks in well-watered conditions, then watering was suspended to generate drought stress. RGB and chlorophyll fluorescence imaging was subsequently initiated and performed on daily intervals. (A) Rosette size and (B) photosynthetic activity of Col-0, *hsfa4a* and *rap2.12-2* mutant plants in control and drought conditions. Error bars represent standard error; **P*<0.05 represent significant differences compared to Col-0 (Student's *t*-test, n=20, individual plants).

Discussion

Transcription factors are essential components of stress-signaling pathways and stress responses (Khan *et al.*, 2018). Barah *et al*., (2016) identified 294 TFs, including *HSFA1A* and *RAP2.7*, whose expression was differentially regulated by individual and combined stresses, including heat, salinity and cold. Many of these TFs controlled the activity of more than 1500 target genes, highlighting the importance of TFs in stress responses (Barah *et al*., 2016). Heat shock factors are key regulators of stress-responsive signaling networks, with varying degrees of impact (Akerfelt *et al.*, 2010; Scharf *et al.*, 2012). HSFA4A is activated by various abiotic stress, including salt, oxidative, heavy metal, high irradiance, high temperature and combined salt and heat stress (Pérez-Salamó *et al.*, 2014; Huang *et al*., 2018; Lin *et al.*, 2018 Andrási *et al*., 2019). HSFA4A regulates a set of TFs and chaperon proteins, and its overexpression can reduce oxidative damages and enhance growth in salt, heat and combined stress (Pérez-Salamó *et al.*, 2014; Andrási *et al*., 2019). Ethylene response factors (ERFs) are one of the largest transcription factor families in plants and plays indispensable role in plant growth, development and in responses to various stresses (Wu *et al*., 2022). Several members of ERF-VII subfamily function in perception and transmission of low oxygen signals (Giuntoli & Perata, 2018). RAP2.12 modulates anoxic, oxidative and osmotic stress responses, acts as an oxygen sensor and was shown to be implicated in ABA signaling (Licausi et al., 2011; Kosmacz *et al*., 2015; Papdi *et al*., 2015).

Simultaneously acting stress conditions impacts plants growth, development and survival more severely than individual stresses. The particular effect of stress combinations on transcript profiles demonstrated that plant responses are characterized by special signatures, not observed in conditions imposed by individual stresses (Rasmussen *et al.*, 2013; Shaar-Moshe et al., 2017; Zandalinas *et al*., 2021; Jiang *et al*., 2024). Withstand such conditions require special regulatory mechanisms with particular factors. Overexpression of *Arabidopsis HSFA2* can improve PSII activity and alleviate rosette wilting in short-lasting heat stress combined with high-light stress and methylviologen treatment (Nishizawa *et al*., 2006). Transgenic *Arabidopsis* plants overexpressing *HSFA7b* have increased tolerance to salt and heat stresses, characterized by greater fresh weight and chlorophyll content, and longer roots, while *hsfa7a* mutant plants showed salt and heat hypersensitivity (Zang *et al*., 2019). Zang *et al*., (2019) identified 193 TFs, whose expression was positively regulated by HSFA7a, several of them with the capacity to improve salt tolerance, including *RAP2.6*, *WRKY38* and *ZFP3*. Overexpression of *Arabidopsis ERF1* and wheat *ERF3* enhanced tolerance to salt and drought stress, manifested in increased

survival and growth rates, while stress tolerance of *erf1* and *erf3* mutants was considerably inferior to wild-type plants (Cheng *et al*., 2013; Rong *et al*., 2014). A recent study showed that *Arabidopsis* ERF95 and ERF97 factors are interacting with each other in heat-dependent manner, and overexpression of them can increase thermotolerance, by directly upregulating various heat responsive target genes including *HSFA2* (Huang *et al*., 2021). Our results show that overexpression of *HSFA4A* and *RAP2.12* improves survival and may play a role in rosette growth in salt and combined heat and salt stresses, suggesting an important role in plant growth and development during stress response (Fig. 2). We also showed that overexpression of these TFs protects photosynthetic performance by maintaining PSII activity during osmotic, high temperature and combined osmotic and heat stresses. Interestingly photosynthetic activity of *hsfa4a* and *rap2.12* mutants was similar to wild type during osmotic and drought stresses, while *rap2.12-2* mutant plants displayed slightly higher PSII activity when plants were exposed to heat and combined osmotic and heat stresses (Fig. 3). It is not uncommon, that individual gene mutations result in stress tolerance comparable to wild-type plants, and only multiple mutations leads to decreased stress tolerance, due to complementing function of TFs (Cheng *et al*., 2013; Rong *et al*., 2014, Papdi *et al*., 2015; Huang *et al*., 2021). Further research is required to decipher the precise molecular mechanisms which are controlled by these factors and the way they determine responses to stress combinations.

Conclusions

This study allowed us to understand better the role of two transcription factors in controlling tolerance to individual and combined stresses. We demonstrated that overexpression of *HSFA4A* and *RAP2.12* can enhance the tolerance of *Arabidopsis* plants to heat, salt, osmotic and combined stresses. Our knowledge could be extended to decipher the function of HSFA4A and RAP2.12 in stress signaling. However, to elucidate the role of these transcription factor in drought stress needs more research.

Acknowledgements. We would like to thank to Annamária Király for the excellent technical assistance. Research was supported by NKFI KH-129510 grant. Norbert Andrási was supported by Young Scientist Fellowship of Hungarian Academy of Sciences.

References

Åkerfelt, M., Morimoto, R. & Sistonen, L. (2010). Heat shock factors: integrators of cell stress, development and lifespan. *Nat Rev Mol Cell Biol. 11*, 545–555. https://doi.org/10.1038/nrm2938

Anckar, J. & Sistonen, L. (2011). Regulation of HSF1 function in the heat stress response: implications in aging and disease. *Annu Rev Biochem. 80*, 1 1089-1115. https://doi.org/10.1146/annurev-biochem-060809-095203

Andrási, N., Pettkó-Szandtner, A. & Szabados, L. (2021). Diversity of plant heat shock factors: regulation, interactions, and functions, *J Exp Bot. 72*, 5:1558–1575, https://doi.org/10.1093/jxb/eraa576

Andrási, N., Rigó, G., Zsigmond, L., Pérez-Salamó, I., Papdi, Cs., Klement, E., Pettkó-Szandtner, A., Baba, A. I., Ayaydin, F., Dasari, R., Cséplő, Á. & Szabados, L. (2019). The mitogen-activated protein kinase 4-phosphorylated heat shock factor A4A regulates responses to combined salt and heat stresses. *J Exp Bot. 70*, 18:4903–4918, https://doi.org/10.1093/jxb/erz217

Baker, N.R. (2008). Chlorophyll fluorescence: A probe of photosynthesis in vivo. *Annu Rev Plant Biol. 59*, 89–113. https://doi.org/10.1146/annurev.arplant.59.032607.092759

Barah, P., Naika, M.B.N., Jayavelu, N.D., Sowdhamini, R., Shameer, K. & Bones, A.M. (2016). Transcriptional regulatory networks in *Arabidopsis thaliana* during single and combined stresses. *Nucleic Acids Res. 44*, 7:3147–3164. https://doi.org/10.1093/nar/gkv1463

Cheng,M.C., Liao, PM., Kuo, WW. & Lin, TP. (2013). The Arabidopsis ETHYLENE RESPONSE FACTOR1 regulates abiotic stress-responsive gene expression by binding to different cis-acting elements in response to different stress signals. *Plant Physiol. 162*, 3, 1566–1582. https://doi.org/10.1104/pp.113.221911

Dey, S. & Vlot, A.C. (2015). Ethylene responsive factors in the orchestration of stress responses in monocotyledonous plants. *Front. Plant Sci. 6*, 640. https://doi.org/10.3389/fpls.2015.00640

Faragó, D., Zsigmond, L., Benyó, D., Alcazar, R., Rigó, G., Ayaydin, F. & Szabados, L. (2022). Small paraquat resistance proteins modulate paraquat and ABA responses and confer drought tolerance to overexpressing *Arabidopsis* plants. *Plant, Cell & Environ. 45*, 1985–2003. https://doi.org/10.1111/pce.14338

Georgii, E., Jin, M., Zhao, J. *et al.* (2017). Relationships between drought, heat and air humidity responses revealed by transcriptome-metabolome co-analysis. *BMC Plant Biol. 17*, 120. https://doi.org/10.1186/s12870-017-1062-y

Gibbs, D. J., Lee, S. C., Md Isa, N., Gramuglia, S., Fukao, T., Bassel, G. W., et al. (2011). Homeostatic response to hypoxia is regulated by the N-end rule pathway in plants. *Nature 479*, 415–418. https://doi.org/10.1038/nature10534

Giuntoli, B., & Perata, P. (2018). Group VII ethylene response factors in *Arabidopsis*: regulation and physiological roles. *Plant Physiol. 176*, 1143-1155. https://doi.org/10.1104/pp.17.01225

Gujjar, R.S., Akhtar, M. & Singh, M. (2014). Transcription factors in abiotic stress tolerance. *Ind J Plant Physiol. 19*, 306–316. https://doi.org/10.1007/s40502-014-0121-8

Huang, HY., Chang, KY. & Wu, SJ. (2018). High irradiance sensitive phenotype of *Arabidopsis hit2/xpo1a* mutant is caused in part by nuclear confinement of AtHsfA4a. *Biol Plant. 62*, 69–79. https://doi.org/10.1007/s10535-017-0753-4

Huang, J., Zhao, X., Bürger, M., Wang, Y. & Chory, J. (2021). Two interacting ethylene response factors regulate heat stress response. *The Plant Cell 33*, 2, 338–357. https://doi.org/10.1093/plcell/koaa026

Jiang, Z., Verhoeven, A., Li, Y., Geertsma, R., Sasidharan, R. & van Zanten, M. (2024). Deciphering acclimation to sublethal combined and sequential abiotic stresses in *Arabidopsis thaliana*. *Plant Physiol.* kiae581. https://doi.org/10.1093/plphys/kiae581

Kant, K., Rigó, G., Faragó, D. *et al.* (2024). Mutation in *Arabidopsis* mitochondrial pentatricopeptide repeat 40 gene affects tolerance to water deficit. *Planta* 259, 78. https://doi.org/10.1007/s00425-024-04354-w

Khan, S.A., Li, M.Z., Wang, S.M., & Yin, H.J. (2018). Revisiting the role of plant transcription factors in the battle against abiotic stress. *Int J Mol Sci. 19,* (6), 1634. https://doi.org/10.3390/ijms19061634

Kosmacz, M., Parlanti, S., Schwarzländer, M., Kragler, F., Licausi, F. And Van Dongen, J.T. (2015). The stability and nuclear localization of the transcription factor RAP2.12 are dynamically regulated by oxygen concentration. *Plant Cell Environ. 38*, 1094-1103. https://doi.org/10.1111/pce.12493

Licausi, F., Kosmacz, M., Weits, D. *et al.* (2011). Oxygen sensing in plants is mediated by an N-end rule pathway for protein destabilization. *Nature 479*, 419–422 https://doi.org/10.1038/nature10536

Licausi, F., Ohme-Takagi, M. & Perata, P. (2013). APETALA2/Ethylene responsive factor (AP2/ERF) transcription factors: mediators of stress responses and developmental programs. *New Phytol. 199*, 639-649. https://doi.org/10.1111/nph.12291

Lin, KF., Tsai, MY., Lu, CA. *et al.* (2018). The roles of *Arabidopsis HSFA2*, *HSFA4a*, and *HSFA7a* in the heat shock response and cytosolic protein response. *Bot Stud. 59*, 15. https://doi.org/10.1186/s40529-018-0231-0

Lindemose, S., O'Shea, C., Jensen, M. K., & Skriver, K. (2013). Structure, function and networks of transcription factors involved in abiotic stress responses. *Int J Mol Sci. 14,* (3), 5842-5878. https://doi.org/10.3390/ijms14035842

Mareri, L., Parrotta, L. & Cai, G. (2022). Environmental stress and plants. *Int. J. Mol. Sci. 23*, 5416. https://doi.org/10.3390/ijms23105416

Nawaz, M., Sun, J., Shabbir, S., Khattak, W. A., Ren, G., Nie, X., Bo, Y., Javed, Q., Du, D. & Sonne, C. (2023). A review of plants strategies to resist biotic and abiotic environmental stressors, *Sci Total Environ. 900*, 165832, https://doi.org/10.1016/j.scitotenv.2023.165832.

Nishizawa, A., Yabuta, Y., Yoshida, E., Maruta, T., Yoshimura, K. and Shigeoka, S. (2006), Arabidopsis heat shock transcription factor A2 as a key regulator in response to several types of environmental stress. *Plant J. 48*, 535-547. https://doi.org/10.1111/j.1365-313X.2006.02889.x

Nover, L., Bharti, K., Döring, P., Mishra, SK., Ganguli, A. & Scharf, KL. (2001). *Arabidopsis* and the heat stress transcription factor world: How many heat stress transcription factors do we need? *Cell Stress & Chaperon* 6, 3,177. https://doi.org/10.1379/1466-1268(2001)006<0177:aathst>2.0.co;2

Papdi, C., Pérez-Salamó, I., Joseph, M.P., Giuntoli, B., Bögre, L., Koncz, C. & Szabados, L. (2015). The low oxygen, oxidative and osmotic stress responses synergistically act through the ethylene response factor VII genes *RAP2.12*, *RAP2.2* and *RAP2.3*. *Plant J. 82*, 772-784. https://doi.org/10.1111/tpj.12848

Papdi, Cs., Ábrahám, E., Joseph, MP., Popescu, C., Koncz, Cs. & Szabados, L. (2008). Functional identification of *Arabidopsis* stress regulatory genes using the controlled cDNA overexpression system. *Plant Physiol. 147*, 528–542. https://doi.org/10.1104/pp.108.116897

Pérez-Salamó, I., Papdi, Cs., Rigó, G., Zsigmond, L., Vilela, B., Lumbreras,V., Nagy, I., Horváth, B., Domoki, M., Zsuzsa Darula, Medzihradszky, K., Bögre, L., Koncz, Cs. & Szabados, L. (2014). The heat shock factor A4A confers salt tolerance and is regulated by oxidative stress and the mitogen-activated protein kinases MPK3 and MPK6. *Plant Physiol. 165*, 319–334. https://doi.org/10.1104/pp.114.237891

Rasmussen, S., Barah, P., Suarez-Rodriguez, M.C., Bressendorff, S., Friis, P., Costantino, P., Bones, A.M., Nielsen, H.B. & Mundy, J. (2013). Transcriptome responses to combinations of stresses in *Arabidopsis*. *Plant Physiol. 161*, 1783–1794. https://doi.org/10.1104/pp.112.210773

Rivero, R.M., Mestre, T.C., Mittler, R., Rubio, F., Garcia-Sanchez, F. & Martinez, V. (2014). Stress combination in tomato plants. *Plant Cell Environ. 37*, 1059-1073. https://doi.org/10.1111/pce.12199

Rong, W., Qi, L., Wang, A., Ye, X., Du, L., Liang, H., Xin, Z. and Zhang, Z. (2014). The ERF transcription factor TaERF3 promotes tolerance to salt and drought stresses in wheat. *Plant Biotechnol J. 12*: 468-479. https://doi.org/10.1111/pbi.12153

Scharf, K. D., Berberich, T., Ebersberger, I., & Nover, L. (2012). The plant heat stress transcription factor (Hsf) family: structure, function and evolution. *BBA-Gene Regul Mech. 1819*, 104-119. https://doi.org/10.1016/j.bbagrm.2011.10.002

Sewelam, N., Oshima, Y., Mitsuda, N. & Ohme-Takagi, M. (2014). Plant responses to multiple abiotic stresses. *Plant Cell Environ. 37*, 2024-2035. https://doi.org/10.1111/pce.12274

Shaar-Moshe, L., Blumwald, E. & Peleg, Z. (2017). Unique physiological and transcriptional shifts under combinations of salinity, drought, and heat. *Plant Physiol. 174*, 421–434. https://doi.org/10.1104/pp.17.00030

Suzuki, N., Rivero, R.M., Shulaev, V., Blumwald, E. and Mittler, R. (2014). Abiotic and biotic stress combinations. *New Phytol. 203*, 32-43. https://doi.org/10.1111/nph.12797

Wu, Y., Li, X., Zhang, J., Zhao, H., Tan, S., Xu, W., Pan, J., Yang, F. & Pi, E. (2022). ERF subfamily transcription factors and their function in plant responses to abiotic stresses. *Front. Plant Sci. 13*, 1042084. https://doi.org/10.3389/fpls.2022.1042084

Zandalinas, S.I., Sengupta, S., Fritschi, F.B., Azad, R.K., Nechushtai, R. and Mittler, R. (2021), The impact of multifactorial stress combination on plant growth and survival. *New Phytol*. 230, 1034-1048. https://doi.org/10.1111/nph.17232

Zang, D., Wang,J., Zhang, X., Liu, Z., & Wang, Y. (2019). *Arabidopsis* heat shock transcription factor HSFA7b positively mediates salt stress tolerance by binding to an E-box-like motif to regulate gene expression, *J Exp Bot. 70*, 19, 5355–5374. https://doi.org/10.1093/jxb/erz261

Zhang, H., Zhu, J., Gong, Z. *et al.* (2022). Abiotic stress responses in plants. *Nat Rev Genet. 23*, 104–119. https://doi.org/10.1038/s41576-021-00413-0

STUDIA UNIVERSITATIS BABEŞ-BOLYAI BIOLOGIA, 70, 2, 2025 (p. 115-150)
doi:10.24193/subbbiol.2025.2.08

Evolutionary patterns of structural disorder and post-translational modifications in the 18.5 kDa myelin basic protein

Ilka Koszorus[1 *] and Ferencz Kósa[1,2]

[1]*Affiliation: Babeş-Bolyai University, Hungarian Department of Biology and Ecology, Cluj-Napoca, Romania;*
[2]*Babeş-Bolyai University, Center for Systems Biology, Biodiversity and Bioresources, Sociobiology and Insect Ecology Lab, Cluj-Napoca, Romania;*
[*] ***Corresponding author, E-mail: koszorusilka@gmail.com.***

Article history: Received 31 August 2025; Revised 4 December 2025; Accepted 05 December 2025; Available online 20 December 2025

Abstract. Myelin basic protein (MBP, 18.5 kDa isoform) is a key structural component of the myelin sheath, where it drives multilayer compaction through electrostatic interactions and dynamic conformational transitions. Despite its functional importance, a comprehensive understanding of MBP's evolutionary patterns of intrinsic disorder, post-translational modifications (PTMs), and sequence-derived properties across vertebrates have been lacking. Here, we analyzed MBP consensus sequences from six major vertebrate clades (*Chondrichthyes, Teleostei, Amphibia, Reptilia, Aves, Mammalia*) using an integrated bioinformatic framework combining intrinsic disorder predictions, Shannon entropy-based complexity profiling, hydrophobic moment (μH) analyses, net charge per residue (NCPR) patterns, and experimentally supported PTM mapping.

Our results reveal that MBP maintains a highly conserved intrinsically disordered architecture characterized by long N- and C-terminal IDRs and several clade-specific central IDRs. Teleosts exhibit a truncated N-terminal, lacking the first 15 residues, but compensate through additional positively charged residues downstream, preserving membrane-binding potential. Amphibians show unique insertions enriched in basic residues, leading to the longest MBPs and potentially enhanced lipid interactions. Shannon entropy and μH profiles demonstrate alternating conserved

α-helices and flexible IDRs that overlap with PTM hotspots, particularly phosphorylation and citrullination sites, suggesting dynamic regulatory roles. NCPR analyses highlight a conserved electrostatic topology composed of alternating basic clusters and acidic/neutral dips, balancing reversible membrane adhesion with controlled aggregation. Together, these findings demonstrate that MBP combines strong structural conservation with lineage-specific adaptations in intrinsic disorder, charge distribution, and PTM patterning. This evolutionary flexibility likely underpins MBP's ability to support functional diversity in myelin architecture while maintaining its essential role in vertebrate nervous system evolution.

Keywords: hydrophobic moment, internally disordered region, myelin basic protein, net charge per residue, sequence complexity.

Introduction

The prevailing paradigm in molecular biophysics and structural biology states that a protein's amino acid sequence determines its three-dimensional structure, and that structure dictates its function - the *one sequence–one structure–one function* model. This view has been challenged by the discovery of intrinsically disordered proteins (IDPs) and intrinsically disordered regions (IDRs). IDPs lack a stable three-dimensional structure under physiological conditions, whereas IDRs are unstructured segments within otherwise folded proteins (Uversky *et al*., 2013). Rather than adopting a fixed conformation, these proteins exist as dynamic ensembles of rapidly interconverting states, allowing them to remain functional in multiple cellular contexts (Oldfield *et al.*, 2019). Some proteins are entirely disordered, while others contain one or more discrete IDRs, often referred to as multi-IDR proteins (Lobley *et al.*, 2005).

IDPs and IDRs are widespread across all domains of life. According to the latest version (2025) of the DisProt database (https://disprot.org), 3,200 IDPs and 9,365 IDRs have been annotated, encompassing 38 distinct biological functions. In eukaryotic genomes, disordered segments are particularly common: for example, 44% of human protein-coding genes contain disordered regions longer than 30 amino acids (van der Lee *et al*., 2014). Computational analyses indicate that 45–50% of eukaryotic proteins possess long disordered segments, whereas in archaea and bacteria, only 7–30% of proteins contain such regions (Xue *et al*., 2013).

The functional significance of intrinsic disorder lies in its ability to expose large and adaptable interaction surfaces that enable recognition of diverse

ligands (Lobley *et al.,* 2005). Consequently, many IDPs are multifunctional and play central roles in molecular recognition, signaling, and regulation (Wright and Dyson, 2014) and they participate in essential cellular processes such as transcriptional and translational control, cell-cycle regulation, and signal transduction (Xue *et al., 2013*).

IDRs are characterized by a high net charge and low overall hydrophobicity, as well as low sequence complexity compared with folded proteins (van der Lee *et al*., 2014). They are strongly depleted in bulky hydrophobic and aromatic residues (tryptophan, tyrosine, phenylalanine) and large aliphatic residues such as valine, while being enriched in charged and polar residues including lysine, arginine, glutamate, glutamine, and serine (Oldfield *et al.,* 2019).

IDPs are also strongly linked to disease, including cancer, cardiovascular disorders, amyloidoses, neurodegenerative diseases, and diabetes (Babu, 2011; Xue *et al*., 2013).

Myelin basic protein (MBP) is the second most abundant component of central nervous system (CNS) myelin, accounting for approximately 30% of its dry protein mass (Kister and Kister, 2023). Its best-established function is to promote adhesion of myelin membrane layers, driving the formation of compact sheaths (Raasakka and Kursula, 2020). Beyond its structural role, MBP has been implicated in the pathogenesis of multiple sclerosis (MS), where increased deimination (citrullination) contributes to myelin destabilization, and MBP may also act as a candidate self-antigen in the autoimmune response (Libich and Harauz, 2008). MBP is generated by alternative splicing of a single mRNA transcript, giving rise to four major isoforms in humans, with molecular masses of 21.5, 20.2, 18.5, and 17.2 kDa (Harauz *et al*., 2004). The classic 18.5 kDa isoform is the predominant form in adult CNS myelin and plays an essential role in maintaining sheath stability (De Avila *et al.*, 2014).

Spectroscopic and sequence-based analyses classify all known MBP isoforms as intrinsically disordered proteins (Libich and Harauz, 2008). This disorder underlies MBP's interactions with a range of partners, including Fyn kinase, cytoskeletal proteins such as actin and tubulin, calmodulin in a Ca^{2+}-dependent manner, and proteins containing SH3 domains (De Avila *et al.,* 2014; Raasakka and Kursula, 2020;). MBP function is further modulated by extensive post-translational modifications (PTMs). Among these, serine/threonine phosphorylation is reversible, whereas arginine deimination is irreversible and can critically alter MBP's stability and interactions (Raasakka and Kursula, 2020).

MBP family members are broadly distributed among vertebrates (Xue *et al.* 2013), and MBP itself is highly conserved across species (Raasakka and Kursula, 2020). Yet, despite intensive research, the relationship between MBP's intrinsic disorder and its strong sequence conservation remains unclear.

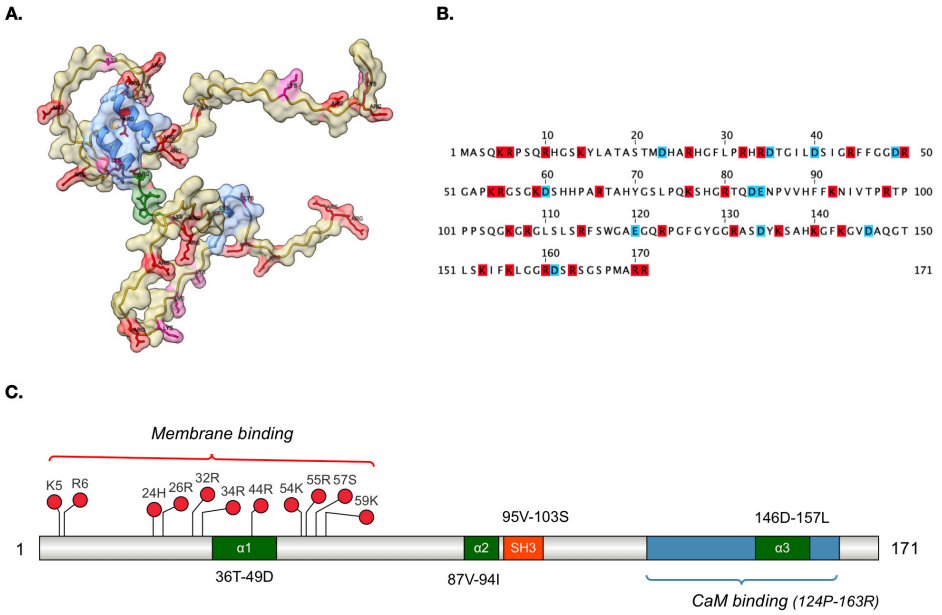

Figure 1. Structural and functional features of the human 18.5 kDa myelin basic protein (MBP, UniProt ID: P02686.3). The 18.5 kDa MBP isoform is depicted in all panels (A–C). (A) Three-dimensional structure predicted by AlphaFold (AF-P02686-F1-model_v4; https://alphafold.ebi.ac.uk/entry/P02686) and visualized with ChimeraX (Pettersen *et al.,* 2021). The α-helices involved in membrane binding (α1–3) are highlighted in blue, arginine residues in red, lysines in purple, and the SH3 domain (Polverini *et al*., 2008) in green. (B) Amino acid sequence of the 18.5 kDa MBP isoform (UniProt ID: P02686.3), with positively charged residues (Arg, Lys) marked in red and negatively charged residues (Asp, Glu) in blue. (C) Schematic representation of the 18.5 kDa MBP isoform sequence with annotated functional regions. Membrane-binding residues are indicated above the sequence, α-helices (α1–3) are marked in green (De Avila, 2014), the SH3-binding motif is shown in orange, and the calmodulin (CaM)-binding region is highlighted in blue (Libich and Harauz, 2008).

Despite numerous proteome-wide studies investigating the overall degree and evolutionary dynamics of intrinsic disorder across species (Ward *et al.*, 2004; Schad *et al.*, 2011; Necci *et al.*, 2016; Zarin *et al*., 2019; Kastano *et al.,* 2020; Singleton and Eisen, 2024; Mughal *et al.*, 2025), relatively few have addressed how the intrinsic disorder of a specific intrinsically disordered protein (IDP) and the parameters governing it have evolved (Siltberg-Liberles, 2011; Xue *et al*., 2013; Siddiqui *et al.*, 2016). In this study, we systematically examine the 18.5 kDa isoform of myelin basic protein (MBP) to explore evolutionary changes

in its disorder-related features, including the degree and extent of intrinsic disorder, the distribution, length, and number of intrinsically disordered regions (IDRs), and key structural characteristics such as sequence complexity, net charge per residue (NCPR), and hydrophobic moment profiles across vertebrates. Additionally, we investigate potential associations between evolutionary shifts in these disorder-related parameters and the distributional and numerical patterns of functionally critical post-translational modifications (PTMs), particularly citrullination and phosphorylation.

Matrials and methods

Retrieval of myelin basic protein amino acid sequence

MBP protein sequences were obtained via BLASTp searches against the non-redundant (nr) protein database using the NCBI BLAST tool (https://blast.ncbi.nlm.nih.gov), with the 18.5 kDa isoform as the query. The search was specifically aimed at identifying orthologous sequences. To ensure lineage-specific coverage, we used distinct representative query sequences for each major vertebrate clade: *Danio rerio* (UniProt ID: XP_005157892.1) for bony fish (*Teleostei*), selecting only mbpa sequences and excluding mbpb isoforms due to their distinct functional roles; *Leucoraja erinacea* (UniProt ID: AAA96756.1) for cartilaginous fish (*Chondrichthyes*), *Xenopus laevis* (UniProt ID: P87346) for amphibians, *Gekko japonicus* (UniProt ID: Q5I1E1) for reptiles, *Gallus gallus* (UniProt ID: P15720-1) for birds, and *Homo sapiens* (UniProt ID: P02686) for mammals. BLASTp searches were performed with the following parameters: maximum number of target sequences: 250, expect threshold (E-value): 0.05, and the BLOSUM62 substitution matrix. Retrieved sequences were filtered based on the following homology criteria: E-value $<10^{-5}$and 100% query coverage (Riley *et al*., 2023). To ensure broad phylogenetic representation, sequences were selected from all major taxonomic orders within each vertebrate group. In total, 199 MBP sequences were curated, with clade-specific distribution (cartilaginous fishes: 15, teleosts: 36, amphibians: 18, reptiles: 31, birds: 49, mammals: 50).

Sequence alignment and consensus sequence determination

Multiple sequence alignments (MSAs) were performed separately for each clade using Clustal Omega (https://www.ebi.ac.uk/Tools/msa/clustalo/) with default parameters (Madeira *et al.,* 2024). Sequences with alignment issues were manually removed. Aligned sequences were visualized and analyzed in

Jalview (version 2.11.2.5), and consensus sequences were generated using a 0.5 conservation threshold (Waterhouse *et al.,* 2009). These consensus sequences were then used for downstream analyses, including the prediction of conserved post-translational modification (PTM) motifs and intrinsically disordered regions (IDRs), calculation of Shannon entropy, generation of linear net charge per residue (NCPR) profiles, and hydrophobic moment (μH) analysis. The number of sequences used per clade ranged from 15 to 50. Although most clades met the recommended threshold of 20–50 sequences for high-quality MSAs, some included fewer due to the limited availability of homologous, full-length sequences. Nonetheless, alignments were manually curated to ensure accuracy before consensus generation.

Conservation scores displayed beneath the alignments (Fig. 3) in Jalview were also generated within the software, using the AMAS method of multiple sequence alignment analysis, which quantifies the conservation of physico-chemical properties for each alignment column (Livingstone and Barton, 1993).

A phylogenetic tree was generated using the neighbor-joining (NJ) method in MEGA version 12 for reference purposes: the protein alignment yielded a tree that reflects the known relationships among vertebrates. The tree was not used for subsequent analyses and is provided in the supplementary materials for completeness (see supplementary files: Fig. S1).

Assessment of protein disorder and identification of intrinsically disordered regions

To systematically analyze the intrinsic disorder propensity of MBP sequences across lineages, we applied several disorder prediction tools, each of which rely on distinct principles and vary in their outputs, being optimized for identifying IDRs of different lengths (Liu *et al.*, 2019). Given the difficulty in precisely defining IDR boundaries - even with experimental methods (Jensen *et al*., 2013) - and observed variability in IDR detection across predictors (Yruela *et al.*, 2017), we selected and combined tools to maximize sensitivity across a broad range of disordered features. Current prediction accuracy for IDRs up to 30 residues is estimated at roughly 70% (Monastyrskyy *et al*., 2014).

Our primary analysis was performed using the CAID Prediction Portal (https://caid.idpcentral.org/portal), which runs standardized, benchmarked intrinsic disorder predictors on the input FASTA amino acid sequences (Del Conte *et al.*, 2023). Specifically, we selected a set of complementary predictors from the CAID suite, including AUCpreD (Wang *et al*., 2016), ESpritz-N, ESpritz-X and ESpritz-D (Walsh *et al.,* 2012), IUPred3 (Erdős and Dosztányi, 2020), MobiDB Lite (Necci *et al.,* 2017), PredIDR long and PredIDR short (Xie *et al.,* 2022), to ensure the detection of both short and long intrinsically disordered

regions (IDRs). The CAID portal also generated a consensus annotation of disordered region boundaries, which we used to define the number and extent of disordered regions across the MBP clade-specific consensus sequences. To complement the CAID results, we additionally used the PONDR VLXT predictor (https://www.pondr.com), which is particularly sensitive to short disordered regions and terminal flexibility (Xue *et al.,* 2010). All algorithms output a number between 0 and 1 for each amino acid residue. If the predicted value exceeds or equals 0.5, this residue is considered disordered. All predictions were performed using default parameters, and the output scores were integrated to identify conserved disordered segments across MBP orthologs.

Furthermore, we calculated the predicted percent of disorder, defined as the ratio of disordered residues to the total number of residues, expressed as a percentage (van Bibber *et al.*, 2020).

Sequence complexity profile (Shannon entropy score profile)

Sequence complexity profile (Shannon entropy) for the clade specific consensus sequences was calculated according to Sen *et al.,* 2019 using a custom R script. Then Shannon entropy was computed for each MBP sequence within the six vertebrate clades. Calculations were performed in R 4.5.1 (R Core Team, 2024) using RStudio (Posit Software, 2024) and the seqinr package for sequence handling. A sliding window of 15 residues was applied, and the mean entropy value per sequence was obtained. Resulting Shannon entropy profiles were visualized using custom scripts with the ggplot2 package (Wickham, 2016).

Hydrophobic moment profile

The hydrophobic moment (μH) was calculated to quantify the amphipathic potential of the sequences using the hmoment site from EMBOSS Explorer with the default parameters (https://www.bioinformatics.nl/cgi-bin/emboss/hmoment) (Eisenberg *et al.,* 1984). This initial analysis was performed on representative consensus MBP sequences from each clade. Hydrophobic moment profiles were visualized in R (R Core Team, 2024) using custom scripts and the ggplot2 package (Wickham, 2016).

To complement the hydrophobic moment (μH) calculations we developed a custom R script to analyze a larger dataset of MBP sequences from all available representatives within each clade. FASTA sequences were imported and processed using the seqinr package (Charif & Lobry, 2007) in R version 4.5.1 (R Core Team, 2024) running in RStudio (Posit Software, 2024). The hydrophobic moment was calculated with a sliding window approach, employing a window size of 10 residues and the Eisenberg hydrophobicity scale as reference values (Eisenberg

et al., 1984). Angular periodicities of 100° and 160° per residue were analyzed to capture α-helical and β-strand segment tendencies, respectively. Hydrophobic moments were calculated for each sliding window by vectorially summing hydrophobicity values weighted by their angular positions, then averaged per sequence for statistical analysis.

Net charge per residue (NCPR) profiles

Net charge per residue (NCPR) was calculated for each MBP sequence within each vertebrate clade using R (R Core Team, 2024) in RStudio (Posit Software, 2024). Amino acids were assigned charges at physiological pH (Asp, Glu: –1; Lys, Arg: +1; His: +0.1), and NCPR was computed using a sliding window of five residues (Das and Pappu, 2013). Average NCPR per sequence was subsequently determined.

Prediction of phosphorylation sites

To predict conserved phosphorylation sites in MBP across vertebrate clades, we analyzed the clade-specific consensus sequences using three independent phosphorylation site predictors: DEPP, Musite, and NetPhos (Wang *et al.*, 2017). All predictions focused on serine, threonine, and tyrosine residues, and only sites scoring ≥0.5 in at least two of the three tools were retained.

In addition to *in silico* predictions, we also reviewed the literature for experimentally validated phosphosites in human 18.5 kDa MBP (Kishimoto *et al.* 1985; Harauz *et al.*, 2004). Using these datasets, we tested the performance of our three prediction methods in identifying experimentally confirmed phosphorylation sites. The integration of multiple prediction methods and empirical data allowed for high-confidence identification of functionally relevant phosphorylation motifs.

Prediction of citrullination sites

Although several citrullination site predictors such as ModPred, iCitr-PseAAC, and CKSAAP_CitrSite exist, at the time of writing this manuscript (July 2025), none of these tools were available or functional for our analyses. Citrullinated arginine residues in human MBP were collected from published experimental studies (Harauz and Musse, 2006; Polverini *et al.,* 2010). The human sequence was aligned to clade-specific consensus sequences, and citrullination sites were mapped across clades based on positional correspondence within the multiple sequence alignment. Only aligned arginine residues corresponding to modified positions in human MBP were considered.

Statistical analyses

All sequence-derived features (hydrophobic moment, Shannon entropy, and NCPR) were analyzed in R version 4.5.1 (R Core Team, 2024) using RStudio (Posit Software, 2024). FASTA sequences were processed with the seqinr package (Charif and Lobry, 2007), and data manipulation employed dplyr (Yarberry, 2021). Calculations were performed at both the sequence level (averaging per sequence within each clade) and at the consensus level (using clade-specific consensus sequences). Clade-wise mean values were compared using Welch's one-way ANOVA, appropriate for unequal variances and non-normal distributions (Welch, 1951). When global effects were significant, pairwise post hoc comparisons were carried out with Welch's t-tests and multiple-testing corrections. Data visualization was performed with custom R scripts using *ggplot2* (Wickham, 2016).

Domain structure visualization

Schematic representations of protein domain structures, post-translational modifications (PTMs) and intrinsically disordered regions (IDRs) were created using the IBS 2.0 (Illustrator for Biological Sequences) tool (Liu *et al.*, 2022; https://ibs.renlab.org).

Results and Discussion

Sequence-based analysis of disorder propensity

Disorder propensity profiles (Fig. 2) were predicted using clade-specific consensus sequences derived from multiple sequence alignments of 18.5 kDa myelin basic protein (MBP) orthologs. A total of nine complementary disorder prediction algorithms were employed, and their outputs were integrated based on predictor consensus: a residue was classified as disordered if more than 62.5% of the algorithms consistently identified it as disordered at that position. The combined use of multiple prediction algorithms enabled estimation of the predicted percent disorder per sequence, as well as the prediction of the number, boundaries, lengths, and distribution of conserved intrinsically disordered regions (IDRs) within each clade-specific consensus sequence (Figs. 2 and 3).

The predicted percent disorder was calculated as the ratio of disordered residues to the total number of residues, expressed as a percentage (van Bibber *et al.*, 2020). Across clades, this metric ranged from 52.22% to 86.11% (Table 1). To assess potential evolutionary trends, Spearman rank correlation analyses were conducted and complemented by permutation-based significance testing. While the analysis revealed a negative trend ($\rho = -0.54$), the correlation did not reach statistical significance ($p = 0.30$).

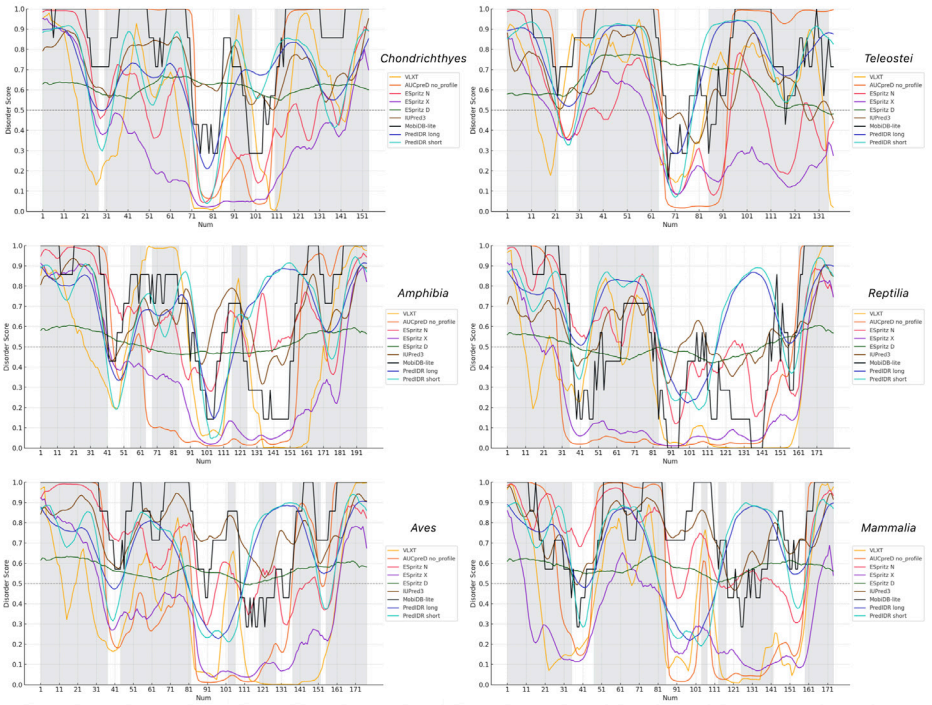

Figure 2. Intrinsically disordered region (IDR) predictions for clade-specific consensus MBP sequences. Disorder propensity was calculated for consensus MBP sequences of six major vertebrate lineages (*Chondrichthyes, Teleostei, Amphibia, Reptilia, Aves,* and *Mammalia*). Per-residue disorder scores (0–1) were obtained using complementary prediction tools from the CAID portal (AUCpreD, ESpritz-N/X/D, IUPred3, MobiDB Lite, PredIDR-long, PredIDR-short) and the PONDR VLXT predictor. A disorder threshold of 0.5 (horizontal reference) was applied to define disordered residues. Shaded background areas indicate regions of consensus disorder (IDRs) across predictors.

The predicted percent disorder has been reported to depend on protein chain length (Xie *et al.*, 2007; Mughal and Caetano-Anollés, 2025), except in viral proteomes, where it decreases with increasing chain length (Xie *et al.*, 2007). In the case of vertebrate MBPs, however, we found no significant correlation between chain length variation and predicted percent disorder values: fishes, which possess the shortest MBP isoforms, exhibited the highest disorder levels. Although the predicted percent disorder generally increases during evolution (Kastano *et al.*, 2020; Mughal and Caetano-Anollés, 2025) and tends to rise with organismal complexity — commonly measured by the number of cell types or overall proteome size (Schad *et al.*, 2011; Kastano *et al.*, 2020) — no such relationships were observed for vertebrate MBPs, likely because the previously reported

correlations were derived from analyses encompassing a much broader taxonomic spectrum.

Following the classification system proposed by Gsponer *et al. (2008) and* Rajagopalan *et al.* (2011), which distinguishes between highly ordered (0–10% disordered), moderately disordered (11–30%), and highly disordered (31–100%) proteins, our results show that all MBP consensus sequences across vertebrate clades fall into the highly disordered category. Given that MBP exhibited a high degree of disorder even in the earliest vertebrate lineages, these findings support the hypothesis that extensive intrinsic disorder is functionally important for MBP activity.

Identification and distribution of intrinsically disordered regions

Analysis of the intra-sequence distribution patterns of predicted disordered regions (Figs. 2 and 3) revealed a consistent architecture across all vertebrate clades: both an N-terminal and a C-terminal intrinsically disordered region (IDR) were invariably present. This terminal disorder pattern mirrors that of other intrinsically disordered proteins (IDPs) (van der Lee *et al.*, 2014; Necci *et al.*, 2016; de Vries *et al.*, 2024). Additionally, every MBP contains a variable number of internal IDRs, typically ranging from three to six per consensus sequence (Table 1, Fig. 2, 3 and 7).

Table 1. Intrinsic Disorder, Sequence Complexity, Net Charge Per Residue and Post-Translational Modification Predictions for the MBP 18.5 kDa Isoform in Vertebrate Lineages.

	Chondrich-thyes	***Teleostei***	***Amphibia***	***Reptilia***	***Aves***	***Mammalia***
Consensus sequence lenght (aa)	147	137	197	180	177	174
Predicted percent of disorder (%)	86.11	78.83	63.45	52.22	73.44	67.24
Nr of disordered regions (IDR)	4	3	5	3	6	6
Mean length of disordered regions (aa)	31	36	25	31.3	21.66	19.5
Mean hydrophobic moment (μH) at 100°)	0.253	0.264	0.256	0.253	0.248	0.239
Mean hydrophobic moment (μH) at 160°	0.160	0.239	0.183	0.203	0.208	0.198
Mean Shannon entropy	3.067	2.867	2.988	2.977	2.959	3.077
Mean net charge per residue (NCPR)	0.108	0.184	0.114	0.127	0.122	0.118

	Chondrich-thyes	*Teleostei*	*Amphibia*	*Reptilia*	*Aves*	*Mammalia*
Nr. of phosphorylation sites	24	26	35	26	28	22
Nr. of phosphorylation sites in disordered regions	21	22	26	16	21	16
Percent of phospho-rylation sites in disordered regions (%)	87.5	84.61	74.28	61.53	75	72.72
Nr. of citrullination sites	4	4	12	14	14	17
Nr. of citrullination sites in disordered regions	4	3	8	11	11	15
Percent of citrullination sites in disordered regions (%)	100	75	66.66	78.57	78.57	88.23
Consensus sequence lenght (aa)	147	137	197	180	177	174
Predicted percent of disorder (%)	86.11	78.83	63.45	52.22	73.44	67.24
Nr of disordered regions (IDR)	4	3	5	3	6	6

Following Necci *et al.* (2016), IDRs were classified by length into short IDRs (at least five disordered residues) and long IDRs (>20 disordered residues) categories. With the exception of the C-terminal region in mammals, the terminal IDRs of all clade-specific consensus sequences corresponded to long disordered regions, while all short IDRs were located in the central portion of the sequence. While a comprehensive analysis of proteins in the UniProt database demonstrated that long intrinsically disordered regions (IDRs) are predominantly located in central parts of proteins, whereas short IDRs are mostly positioned at the termini (Necci *et al.*, 2016), the opposite pattern is observed for all MBPs. This inversion is likely explained by the fact that several functionally important regions relevant to MBP activity (Fig. 1C) are located within these terminal segments.

According to Necci *et al.*, 2016, proteins with long IDRs are enriched in eukaryotes and short IDRs seem to be uniformly distributed among all domains of life. Notably, short IDRs were more frequent in tetrapods (excluding *Reptilia*) myelin basic proteins, whereas long IDRs predominated in fishes.

While the number of predicted IDRs showed a positive evolutionary trend ($\rho = 0.65$), it was not statistically significant ($p = 0.19$). Conversely, the average IDR length displayed a stronger negative correlation ($\rho = -0.71$) with a lower p-value ($p = 0.13$), though still below the threshold for statistical significance.

To investigate the relationship between intrinsic disorder and amino acid conservation, we analyzed the aligned clade-specific consensus sequences (Fig. 3). We first identified conserved disordered regions (CDRs) as segments consisting of at least four consecutive residues that were predicted to be disordered in >66.66% of the aligned sequences. These CDRs were further categorised based on the framework of Bellay *et al.* (2011), with modifications to distinguish between flexible and constrained disorder. In regions of flexible disorder, positions are disordered in more than 66.66% of sequences, but the mean conservation score of the segment is less than 5. In regions of constrained disorder, positions are disordered in more than 66.66% of sequences, and the mean conservation score exceeds 5.

Most conserved disordered regions, both flexible and constrained, partially overlapped with known functional elements, including α1–α3 helices, lipid membrane binding regions, calmodulin-binding sites, and serine/threonine phosphorylation sites (Figs. 1C, 3, and 7).

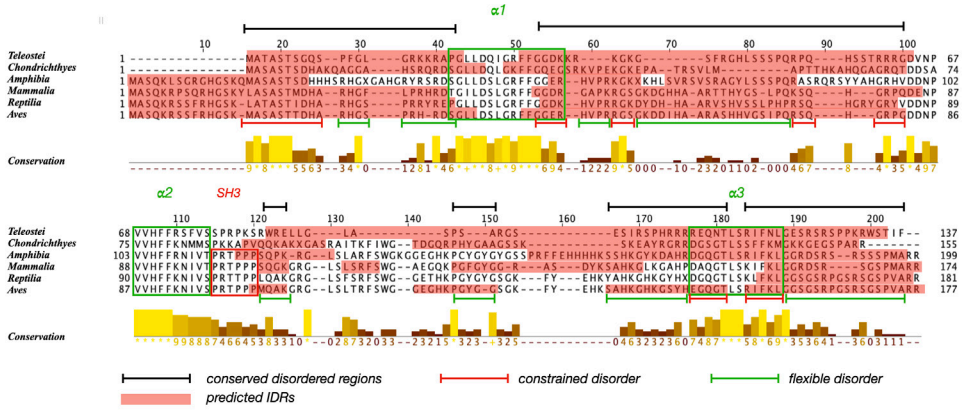

Figure 3. Classification of conserved intrinsically disordered regions (IDRs) in MBP. Multiple sequence alignment of clade-specific MBP consensus sequences with predicted IDRs (brick color) for every sequence. Conserved disordered segments (black) were defined as alignment columns where at least four sequences have a disordered residue. Conserved IDRs were further subdivided into flexible disorder (green) and constrained disorder (red) according to conservation scores, following Bellay *et al.* (2011): segments with an average conservation score ≤5 were classified as flexible disorder, while those with scores >5 were classified as constrained disorder. α-helices are indicated by green rectangles, the SH3-binding motif by a red rectangle. The yellow plot below the alignment shows per-position conservation scores (0–11 scale).

Sequence complexity (Shannon entropy)

The Shannon entropy metric, computed on a sliding 15-amino acid window, reflects the variability and compositional complexity of a sequence (Romero *et al.*, 2001).

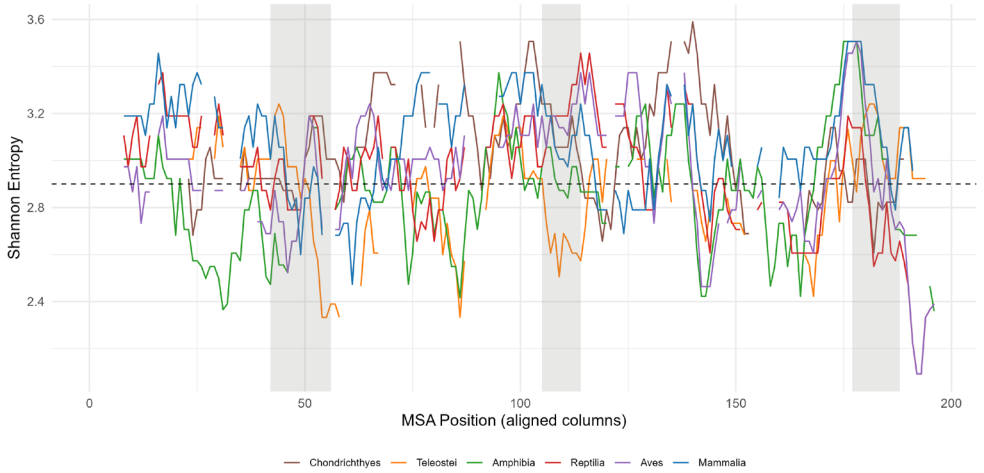

Figure 4. Residue-level aligned profiles of Shannon entropy, with a sliding window of 15 residues, threshold at 2.9. Each plot shows six overlaid lines corresponding to clade-specific MBP consensus sequences: *Chondrichthyes* (brown), *Teleostei* (orange), *Amphibia* (green), *Reptilia* (red), *Aves* (purple), and *Mammalia* (blue). Grey shaded areas in all panels indicate the positions of the three α-helices.

The calculated mean values of the Shannon entropy ranged from 2.287 (*Teleostei*) to 3.077 (*Chondrichthye*s and *Mammalia*) (Table 1, see supplementary files: Fig. S2A). Welch's ANOVA demonstrated that the mean Shannon entropy of MBP differed significantly across vertebrate clades [$F(5, 38.7) \approx 228$, $p < 0.001$, $\eta^2 \approx 0.82$, 96% CI (0.79, 1.00)]. Post-hoc tests revealed clade-specific patterns: cartilaginous fishes (*Chondrichthyes*) differed significantly from all groups except mammals ($p = 0.19$). *Teleosts* (bony fishes) were distinct from all other clades ($p < 0.001$ in all cases). Amphibians did not differ significantly from reptiles ($p = 0.52$), but differed from all others. Reptiles overlapped with amphibians ($p = 0.52$) and birds ($p = 0.16$), but differed from remaining groups. Birds differed from all other clades except reptiles ($p = 0.16$). Mammals differed from all clades except cartilaginous fishes ($p = 0.19$). Overall, entropy displayed strong clade-specific patterns: teleosts consistently had the lowest mean entropy values, cartilaginous fishes the highest, and they overlapped only with mammals.

Figure 4 shows the aligned Shannon entropy profiles of MBP (18.5 kDa isoform) across six vertebrate clades. Entropy values above 2.9 indicate high sequence complexity, strong variability, typical of intrinsically disordered regions (IDRs), while lower values reflect compositional bias or repeats and indicates conservation, often corresponding to structural or functional motifs (e.g., membrane binding) (Romero *et al.*, 2001). The selected entropy value 2.9 threshold is often used in protein disorder and complexity studies as it approximates the point at which variability shifts from constrained to highly flexible (Sen *et al.*, 2019).

Aligned Shannon entropy profiles across *Chondrichthyes, Teleostei, Amphibia, Reptilia, Aves, and Mammalia* reveal both conserved low-complexity domains (entropy values < 2.9) and variable, high-complexity stretches (Fig. 4).

In all clades, three positionally conserved entropy minima can be distinguished, located within the 42–56, 105–114, and 177–188 regions. These correspond to experimentally confirmed α-helices, representing conserved, low-complexity sequence segments (Libich and Harauz, 2008). The N-terminal region (positions 1–15, Fig.3), which is absent in fishes, is characterized by consistently high entropy values, indicative of intrinsic disorder. The entropy profile of this segment shows a gradual increase across vertebrates: it is lowest in amphibians, increases in reptiles and birds, and reaches its highest values in mammals. The elevated intrinsic disorder in this region likely facilitates post-translational modifications, as supported by experimental evidence demonstrating two citrullination sites, two phosphorylation sites, and two membrane-binding residues within this segment in mammals (Harauz *et al.*, 2004). Similarly, the adjacent N-terminal conserved disordered region (positions 16–42, Fig.3), partially overlapping with the α1 helix, exhibits entropy values exceeding 2.9 in all clades except amphibians and *Chondrichthyes* (Fig. 4). The disordered nature of this region suggests an important regulatory role in MBP function, consistent with experimental identification of four phosphorylation sites, three citrullination sites, and four membrane-binding residues in this segment in mammals (Harauz *et al.*, 2004). The conserved disordered region located between the α1 and α2 helices (Fig. 3) shows clade-specific variability in entropy and sequence complexity (Fig. 4): the lowest values are observed in amphibians and teleosts, the highest in *Chondrichthyes* and mammals, whereas birds and reptiles exhibit intermediate levels. This region also contains several post-translational modifications associated with structural flexibility, including four citrullination and three phosphorylation sites, as well as three membrane-binding motifs (Harauz *et al.*, 2004). The 114–140 region (Fig.3), which overlaps with the SH3 motif and contains four phosphorylation and four citrullination sites in mammals (Harauz *et al.*, 2004), is generally characterized by high entropy values (Fig. 4) and a pronounced degree of intrinsic disorder. In contrast, the adjacent 141–170 segment, with the exception of *Chondrichthyes* and mammals, displays relatively

low entropy values on average (Fig. 4), suggesting a tendency toward structural stabilization. Finally, the C-terminal tail (positions 189–200), in contrast to the N-terminal end, shows lower entropy values, indicative of a higher degree of structural order.

The entropy-based complexity analysis reveals evolutionary stratification of MBP disorder across vertebrates. *Mammalia*, *Aves*, *Reptilia* consistently exhibit higher mean entropy values across the protein, suggesting increased sequence variability and functional adaptability compared to amphibians and *Teleostei*. Evolutionarily, the diversification of entropy patterns supports the hypothesis that MBP underwent clade-specific functional tuning to accommodate differences in myelin architecture.

Hydrophobic moment profiles across vertebrate clades

Because protein disorder scores show the strongest correlations with overall polarity and hydrophobicity (Singleton and Eisen, 2024), we analyzed the aligned hydrophobic moment (μH) profiles (Fig. 5 A, B) of the 18.5 kDa myelin basic protein (MBP) across six vertebrate clades (*Chondrichthyes*, *Teleostei, Amphibia, Reptilia, Aves,* and *Mammalia*) at helical angles of 100° and 160° (Eisenberg *et al.*, 1984). The hydrophobic moment quantifies the amphipathicity of a sequence segment: a high μH indicates clustering of hydrophobic side chains on one face of an α-helix or β-strand (Eisenberg *et al.*, 1982; Phoenix and Harris, 2002). Such amphipathic segments frequently correspond to membrane-interacting domains (Gulsevin and Meiler, 2021).

The calculated mean hydrophobic moment (μH) values for amphipathic α-helices (100°) ranged from 0.323 to 0.369, and for amphipathic β-sheets (160°) from 0.219 to 0.342 (Table 1, see supplementary files: Fig. S 2C, D). The hydrophobic moment profiles exhibited clear clade-specific differences. For amphipathic α-helices (100°), Welch's ANOVA revealed a large effect [$F(5, 38.1) = 81.62$, $p < 0.001$, $\eta^2 \approx 0.52$, 95% CI (0.44, 1)]. *Teleostei* (mean = 0.264) had significantly higher α-helical μH values than all other clades ($p \leq 0.01$). Mammals (0.239) exhibited the lowest values, significantly lower than every other clade ($p < 0.001$). *Chondrichthyes* (0.253) did not differ significantly from *Amphibia* (0.256, $p = 0.42$) or *Reptilia* (0.253, $p = 0.44$), but differed from *Aves* (0.248, $p = 0.010$) and *Mammalia* ($p < 0.001$). *Amphibia* overlapped with *Reptilia* and *Chondrichthyes* (both $p > 0.1$), but differed from *Aves* and *Mammalia* (both $p < 0.001$). *Reptilia* overlapped with *Amphibia* ($p = 0.14$) and *Aves* ($p = 0.057$), but were significantly different from *Mammalia* ($p < 0.001$). Aves differed significantly from *Teleostei*, *Chondrichthyes*, *Amphibia*, and *Mammalia* (all $p \leq 0.01$), but not from *Reptilia* ($p = 0.057$). Overall, *Teleostei* exhibited the highest α-helical μH values, *Mammalia* the lowest, and the remaining clades formed an intermediate but partially overlapping group.

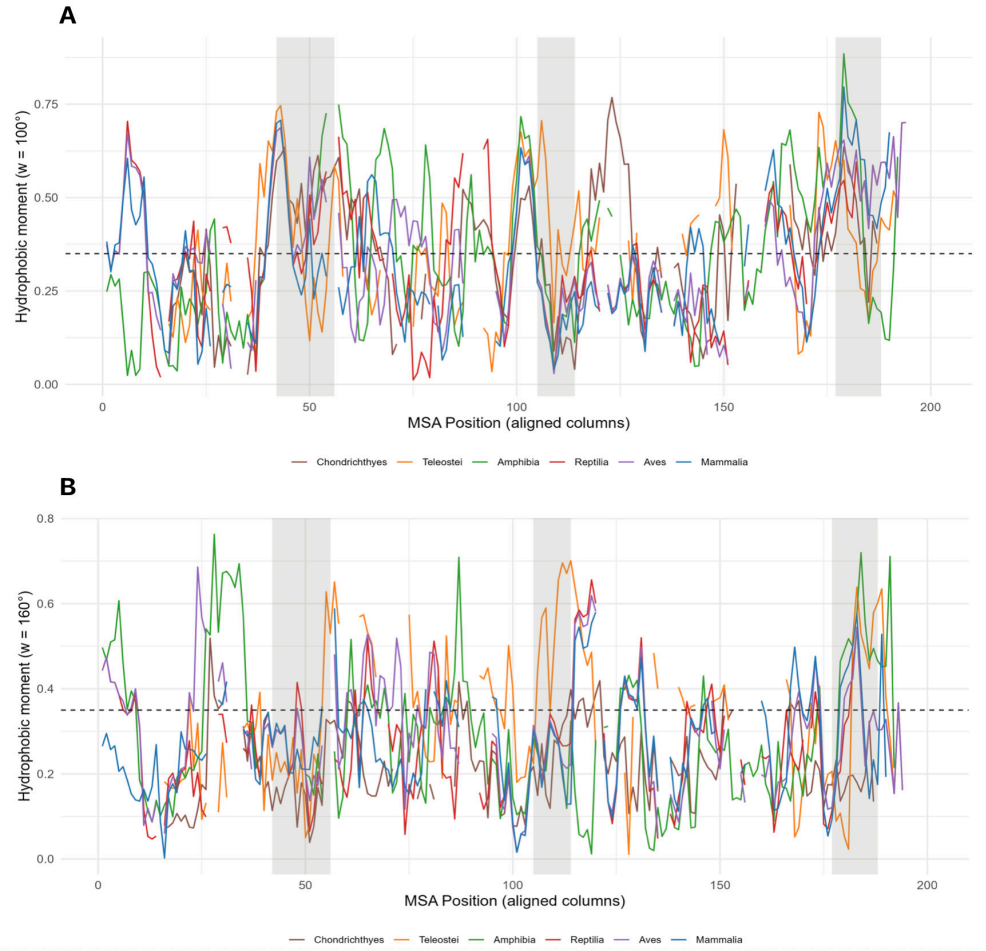

Figure 5. Residue-level aligned profiles of hydrophobic moment. The plots show in order: (A) Hydrophobic moment at 100° (α-helical periodicity), with a sliding window of 10 residues, threshold at 0.35. (B) Hydrophobic moment at 160° (β-strand periodicity), with a sliding window of 10 residues, threshold at 0.35. Each plot shows six overlaid lines corresponding to clade-specific MBP consensus sequences: *Chondrichthyes* (brown), *Teleostei* (orange), *Amphibia* (green), *Reptilia* (red), *Aves* (purple), and *Mammalia* (blue). Grey shaded areas in all panels indicate the positions of the three α-helices.

For amphipathic β-sheets (160°), the differences were even stronger [$F(5, 40.5) = 502.70$, $p < 0.001$, $\eta^2 \approx 0.88$, 95% CI (0.86, 1.00)]. All clades differed significantly ($p < 0.01$), with *Chondrichthyes* showing the lowest and *Teleostei* the highest μH means.

Thus, hydrophobic moment analyses reveal robust clade-specific variation: α-helical values indicate partial overlaps among intermediate clades (*Amphibia, Reptilia, Chondrichthyes*), β-sheet values demonstrate complete separation between all groups.

In addition to comparing clade-specific μH means, comparative hydrophobic moment profiling offers deeper structural insights. Several studies have proposed threshold ranges for μH values, enabling structure-dependent interpretations (Eisenberg *et al.*, 1989; Segrest *et al.*, 1990; Phoenix and Harris, 2002): low μH (< 0.35) values are indicative of weak amphipathicity, typically associated with disordered or flexible regions unlikely to form stable helices, intermediate μH (0.35–0.5) values represents transient or interfacial helices, which may dynamically interact with membranes or partner proteins, and high μH (> 0.5) values are characteristic of strongly amphipathic membrane-binding helices.

Examining hydrophobic moment (μH) profiles (Fig. 5A, B) corresponding to conserved disordered regions (CDRs) (Fig. 3) revealed notable evolutionary differences among clades. In the segment 1–10 of the N-terminal IDR (positions 1–42, Fig. 3) *Reptilia*, *Aves*, and *Mammalia* exhibit μH profiles indicative of a propensity for amphipathic α-helix formation (high 100°, low 160°, Fig. 5A, B). By contrast, *Amphibia* display a preference for β-sheet formation at the same region, likely due to the presence of three adjacent glycines, which may destabilize α-helices. Similar cases where the same conserved disordered region favors different secondary structures across taxa have been reported for other proteins (Siltberg-Liberles, 2011).

Chondrichthyes and *Teleostei* lack the first 15 N-terminal residues (Fig, 3). In mammals, this missing segment contains two experimentally confirmed membrane-binding residues, two citrullination sites and two phosphorylation sites (Harauz *et al.*, 2004). Region 11–25 partially overlapping a constrained CDR (Fig. 3), shows low μH for both angles in all clades (Fig. 5A, B), consistent with disordered character. In region 26–35 in *Chondrichthyes*, *Amphibia*, and *Aves*, the profile shows low 100° but high 160° values (Fig. 5A, B), suggesting a β-sheet propensity. Other clades exhibit low μH at both angles, indicative of disorder.

The central conserved region (positions 53–100, Fig. 3) overlapping the α1 helix, alternates between high 100° and high 160° peaks, implying structural plasticity. It can adopt both shallowly membrane-inserting α-helices and amphipathic β-sheets (Fig. 5A, B). Disorder predictors uniformly classify this region as disordered across all clade consensus sequences (Fig. 2). Amphibians exhibit higher μH values here than other tetrapods, suggesting a possible adaptive increase in membrane-binding capacity during the transition from aquatic to terrestrial environments. In mammals, this region includes four experimentally confirmed membrane-binding residues, three phosphorylation sites, and four

citrullination sites (Harauz *et al.*, 2004). Amphibians possess an inserted sequence segment here that contains multiple positively charged residues, which likely enhance the protein's membrane-binding affinity.

In the C-terminal IDRs region 120–130, partially overlapping a flexible conserved region (positions 121–124, Fig. 3), exhibits high α-helical μH only in *Reptilia*, whereas all other clades show μH values consistent with disorder (Fig. 5A). In region 131–160, all clades generally exhibit low μH values (indicative of disorder), except for *Teleostei*, which display a localized high 100° μH peak near position 150, suggesting potential amphipathic α-helix formation. The short C-terminal tail (positions 181–184) overlapping the α3 helix exhibits simultaneously high 100° and 160° μH values, indicating marked structural plasticity (Fig. 5A, B).

Together, these findings reveal that MBP conserved disordered regions exhibit clade-specific amphipathic profiles, with structural adaptability likely linked to membrane interactions, post-translational regulation, and functional diversification across vertebrate evolution.

Net charge per residue (NCPR) across vertebrate MBP 18.5 kDa orthologs

The net charge per residue (NCPR) differed significantly among vertebrate clades ($F(5, 34.3) = 971.46$, $p < 0.001$), with an exceptionally large effect size ($\eta^2 \approx 0.97$, 95% CI [0.96, 1.00]). Post-hoc comparisons revealed distinct clade-specific patterns: teleosts showed the highest NCPR (mean ≈ 0.184), significantly greater than all others ($p < 0.001$). At the other extreme, cartilaginous fishes exhibited the lowest values (mean ≈ 0.108), while amphibians (mean ≈ 0.114), mammals (mean ≈ 0.118), birds (mean ≈ 0.122), and reptiles (mean ≈ 0.127) formed an intermediate cluster with modest but statistically significant pairwise differences (e.g., amphibians vs. mammals, $p = 0.037$; chondrichthyans vs. amphibians, $p = 0.030$; chondrichthyans vs. mammals, $p < 0.001$). Thus, the NCPR rank order was: cartilaginous fishes (lowest) < amphibians < mammals < birds < reptiles < teleosts (highest) (see supplementary files: Fig. S2B).

Aligned NCPR (net charge per residue) profiles of clade-specific consensus sequences (Fig. 6) revealed an electrostatic architecture that is largely conserved across vertebrates: positively charged peaks — reflecting lysine- and arginine-rich segments — occur predominantly at the N- and C-terminal IDRs, whereas negative troughs correspond to central conserved disordered regions (CDRs) (Fig. 3). These positively charged segments are known to mediate electrostatic binding to the negatively charged cytoplasmic leaflet of myelin, thereby promoting multilayer compaction (Raasakka *et al.*, 2017). In contrast, neutral or acidic regions appear mainly at conserved positions. The alternating pattern of

strongly positive peaks and neutral/acidic dips in MBP's NCPR profile reflects the characteristic electrostatic signature of intrinsically disordered proteins.

The N-terminal portion of the NCPR profile (residues 1–42; Fig. 3) largely overlaps with the N-terminal conserved disordered region (CDR) and is characterized by moderately to strongly positive net charge values (approximately +0.25 to +0.80). In teleost fishes, this segment is truncated by about 15 amino acids compared to tetrapod MBPs. *Teleostei* appear to compensate for the loss of lipid-binding, positively charged residues within positions 1–15 by featuring two additional positively charged residues near the end of the N-terminus, which accounts for the pronounced positive peak observed between positions 31 and 41.

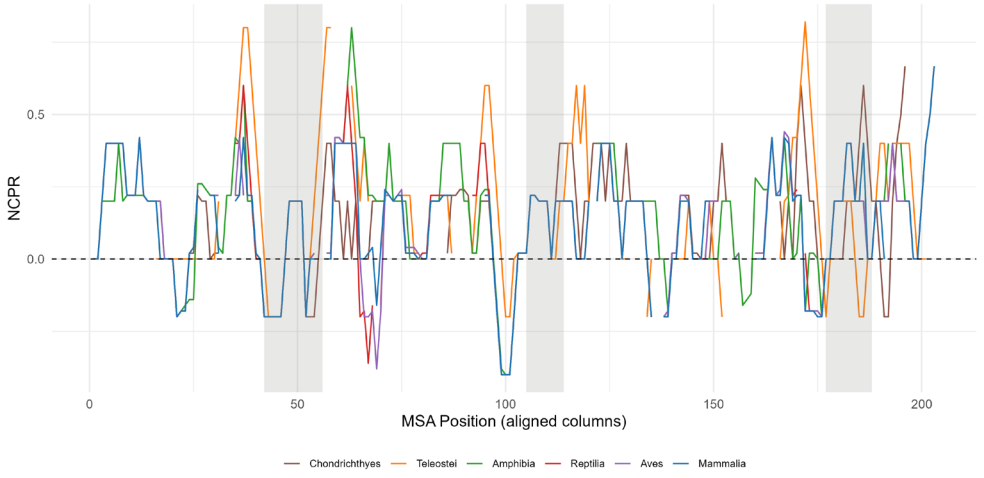

Figure 6. Aligned profiles of net charge per residue (NCPR), with a sliding window of 5 residues, threshold at 0. Each plot shows six overlaid lines corresponding to clade-specific MBP consensus sequences: *Chondrichthyes* (brown), *Teleostei* (orange), *Amphibia* (green), *Reptilia* (red), *Aves* (purple), and *Mammalia* (blue). Grey shaded areas in all panels indicate the positions of the three α-helices.

The central region of MBP (residues 60–119, Fig. 3) exhibits fluctuating net charge — from approximately −0.4 to +0.8 — with a generally positive bias, which mitigates but does not fully eliminate electrostatic repulsion, thereby creating transient windows for intermolecular contact. Notably, this charge variability coincides with an amyloid-prone segment shown to mediate the formation of amyloid fibrils in myelin sheaths (Sysoev *et al.*, 2025), where transient reduction in repulsion could facilitate adhesive MBP stacking, yet also increase the risk of aggregation under altered conditions.

The C-terminal half (residues 124-184, Fig. 3) shows oscillating charge (Fig. 6) and several conserved disordered regions. The segment spanning residues 161–164 contains a histidine-rich insertion in amphibians, introducing a pH-sensitive motif that may fine-tune MBP assembly under variable environmental conditions (Alibardi, 2002; Buchko *et al.*, 2022). The segment spanning residues 166–181, overlapping partially with α3, remains strongly basic until residue 174, where most clades insert an acidic residue; teleosts diverge with consecutive arginines (171–173), raising NCPR above +0.8. Residues 191–184 (Thr, Ser, Arg) are conserved as potential phosphorylation/citrullination sites regulating assembly (Harauz and Boggs, 2013; Smirnova *et al*., 2021).

The extended C-terminal tail (residues 184–204) adds further regulatory capacity. Lys188 is widely conserved but missing in teleosts, Arg194 remains conserved across clades, except cartilaginous fishes, reinforcing positive charge. Overall, the tail balances strong positive clusters with acidic sites, ensuring both adhesion and regulatory potential (Homchaudhuri *et al*., 2010; Raasakka and Kursula, 2022).

Despite this conserved alternating topology, clade-specific adaptations are evident. Mammals and birds share nearly identical high-charge profiles at both termini, consistent with tightly compacted myelin and fast conduction (Müller *et al*., 2013; Sysoev *et al*., 2025). Reptiles largely retain this pattern but with subtle charge reductions and neutral extensions, reflecting conservation with minor adaptation to ectothermy (Müller-Späth *et al.*, 2010; Li and Buck, 2022). Amphibians modify the central region with histidine insertions, creating pH-sensitive motifs that allow environmental responsiveness (Alibardi, 2002). Teleosts markedly intensify terminal charge through dense arginine clusters, likely compensating for lower temperatures by enhancing electrostatics (Aponte-Santamaría *et al*., 2017; Dreier *et al*., 2018). Cartilaginous fish retain lower overall charge intensity, consistent with early marine environments where extreme polycationicity was unnecessary (Tai *et al*., 1985; Bellard, 2016).

Thus, MBP's electrostatic architecture appears both conserved and adaptable. MBP emerged alongside the evolution of myelin in early vertebrates (Nawaz et al., 2013) and has retained its characteristic alternating charge topology under strong selective pressure. In teleosts, the amplification of MBP isoforms may reflect adaptive responses following whole-genome duplication events (Glasauer and Neuhauss, 2014). Amphibians and reptiles appear to have introduced more flexible modifications, whereas birds and mammals have converged on high-charge conservation to optimize saltatory conduction (Stämpfli, 1954). By contrast, cartilaginous fishes retain a more ancestral electrostatic configuration (Bellard, 2016). Overall, the NCPR landscape highlights MBP's dual nature: intrinsically disordered yet functionally encoded through

finely tuned charge distribution. Conserved basic clusters, interspersed with acidic and neutral dips, enable reversible membrane adhesion and provide platforms for post-translational regulation (Bianchi *et al.,* 2022). This tunable electrostatic framework underpins MBP's central role in myelin compaction, balancing deep evolutionary stability with lineage-specific adaptations.

Distribution of predicted phosphorylation and citrullination sites

As previous studies have identified a notable correlation between the distribution of post-translational modifications (PTMs) and intrinsically disordered regions (IDRs) (Iakoucheva *et al.*, 2004; Kurotani *et al.*, 2014; Zarin *et al.*, 2019,), we aimed to investigate whether vertebrate evolution has influenced the number of functionally critical PTMs (specifically, phosphorylation and citrullination) within MBP, and whether their distribution correlates with predicted IDRs. Because experimentally validated phospho- and citrullination sites in MBP are limited to only a few species (Zand *et al.*, 2001; Kim *et al.*, 2009; Zang *et al.*, 2012), we supplemented these data with predictive methods.

We used computational predictors to identify phosphorylation sites for each clade (Figure 7, see supplementary files: Table S1), which revealed a high but variable proportion of sites located in disordered regions: 87.5% in cartilaginous fish, 84.6% in bony fish, 74.3% in amphibians, 61.5% in reptiles, 75.0% in birds, and 72.2% in mammals (Table 1).

Separately, using experimentally determined human MBP phosphorylation sites (n = 20), we examined the aligned consensus sequences across the six vertebrate clades (*Chondrichthyes, Teleostei, Amphibia, Reptilia, Aves,* and *Mammalia*) (Fig. 3). Six of these sites were conserved across all clades (18S/T, 20S, 21T, 114S/T, 181T, 183S). Additional positions were retained only in subsets of lineages: 8S, 13S, 42S/T, 65S, 79Y, 81S, 117T, 121S, 136S, 159S/Y, 166S/Y, 193S, 199S, and 201S. 11 of the 20 sites were located within conserved disordered regions. According to this predictions phosphorylation sites accumulated gradually, with six positions conserved across all vertebrates and numerous additional sites appearing in amphibians and higher lineages. Under normal conditions, MBP functions as a phosphoprotein in the myelin sheath (Turner *et al.,* 1982). Phosphorylation is critical for regulating protein function, localization, and protein–protein interactions. By partially neutralizing MBP's charge, phosphorylation modulates membrane-binding affinity and participation in intracellular signaling pathways (Harauz and Boggs, 2013). According to our data, across vertebrates, predicted phosphorylation sites are generally associated with intrinsically disordered regions, although the strength of this association varied among clades. This suggests that in early vertebrates, phosphorylation

was already tightly linked to disorder, but over evolutionary time, it expanded into more structured regions, particularly in reptiles.

In dogfish, experimental methods identified six phosphorylation sites (Zand *et al.*, 2001), whereas our combined predictive approach estimated 24 sites across the consensus MBP sequence for cartilaginous fishes, and the alignment-based method predicted seven. These apparent discrepancies likely arise both from differences between predictive methodologies and from limitations in the available experimental data.

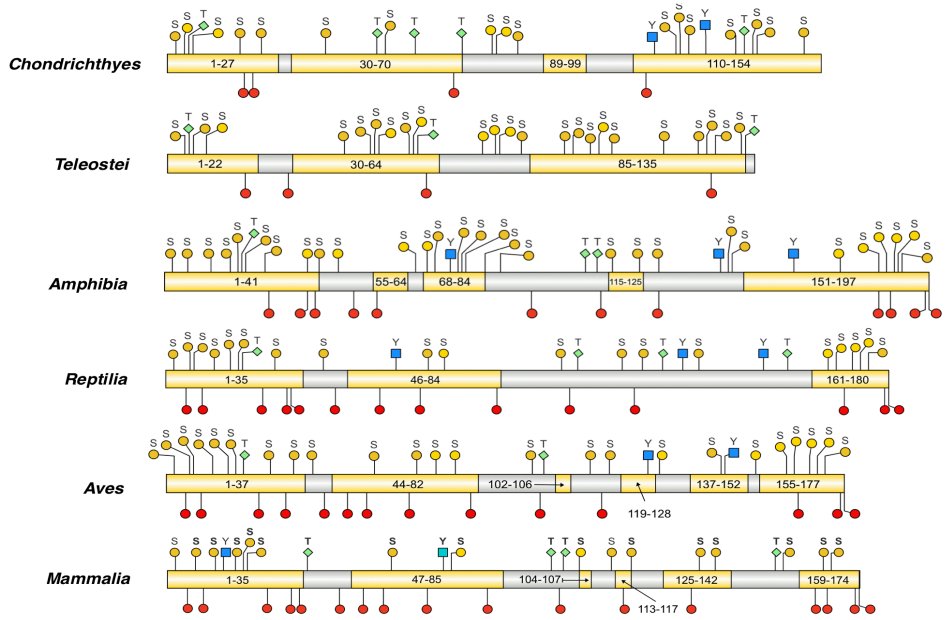

Figure 7. Predicted post-translational modifications (PTMs) of MBP consensus sequences across vertebrate lineages. For each of the six vertebrate clades (*Chondrichthyes, Teleostei, Amphibia, Reptilia, Aves, Mammalia*), the consensus MBP sequence is shown with annotated PTM sites. Phosphorylation sites were identified using three independent predictors (DEPP, NetPhos, MusiteDeep) and are indicated only when supported by at least two predictors: yellow circles (serine), green diamonds (threonine), and blue squares (tyrosine). In the *Mammalia* panel, phosphorylation sites that are bolded have been experimentally confirmed (Harauz and Boggs, 2013). Citrullination sites (red circles) were compiled from published experimental studies (Harauz *et al.*, 2004; Kishimoto *et al.,* 1985). Intrinsically disordered regions are highlighted in yellow along the sequences (numbers indicate the start and end positions of each disordered region within the sequence).

The number of predicted citrullination sites gradually increased across vertebrate clades, from 4 sites in cartilaginous and bony fishes to a maximum of 17 sites in mammals (Table 1, and see supplementary files: Table S2). Several positions were highly conserved across clades (e.g., R6, R40, R50, R63, R98) and include residues also implicated in membrane binding, notably R40 and R63. Eleven of these sites in the aligned sequences were located within conserved disordered regions. On the individual consensus sequences (Figure 7), the proportion of citrullination sites in disordered regions varied (Table 1.): 100% in cartilaginous fish, 75% in bony fish, 66.66% in amphibians, 78.57% in reptiles, 78.57% in birds, and 88.23% in mammals.

In early vertebrates, almost all predicted citrullination sites were located in disordered regions (Fig. 7), but they were few in number (four in cartilaginous fish and four in bony fish). In amphibians, their number increased, with a majority expected to fall within disordered regions. Reptiles and birds had more predicted sites, most of which were predicted to be in disordered regions, and mammals carried the highest number, many within disordered segments. This pattern shows that even though the proportion of predicted disordered residues dropped from 100% in cartilaginous fish to ~67–88% in tetrapods, the absolute number of predicted disorder-associated citrullination sites more than tripled. Many of these residues coincide with membrane-binding arginines, highlighting an increasing potential for regulatory conflict between citrullination and membrane adhesion as MBP diversified (Gogól, 2013). The trajectory of citrullination differs from phosphorylation by combining strong disorder association with numerical expansion. Citrullination modifies specific arginine residues in MBP, converting them to citrulline via calcium-dependent PAD (peptidylarginine deiminase) enzymes. This reduces MBP's positive charge, weakening its electrostatic binding to negative membrane lipids and potentially disrupting myelin structure (Moscarello *et al*., 2006). It may also reduce interactions with other proteins, affecting myelin organization (Carrillo-Vico *et al.*, 2010).

Together, these findings suggest that MBP evolution was shaped by a progressive accumulation of PTMs within disordered regions, which not only expanded the number of modification sites, but also increased the dynamic potential of the protein. Phosphorylation acts as a flexible, conserved regulatory mechanism, partially neutralizing MBP charge to fine-tune membrane binding and signaling, while citrullination selectively targets membrane-binding arginines, potentially disrupting MBP-membrane interactions and protein-protein contacts. By localizing within intrinsically disordered regions, these PTMs likely create a "regulatory code," enabling switch-like modulation of interactions, scaffold assembly, and fuzzy binding without requiring rigid structural changes (Bah and Forman-Kay, 2016; Darling and Uversky, 2018).

Conclusion

This study presents an integrative evolutionary analysis of the 18.5 kDa myelin basic protein (MBP) isoform across major vertebrate clades, combining sequence-based intrinsic disorder predictions, hydrophobic moment and net charge per residue (NCPR) profiling, and post-translational modification (PTM) mapping. By employing consensus sequence alignments and multi-predictor computational approaches, we identified both deeply conserved and lineage-specific features that contribute to the structural and functional versatility of MBP.

Our results demonstrate that MBP exhibits an intrinsically disordered architecture across all vertebrate groups, with predicted disorder percentages ranging from 52.22% to 86.11%. The spatial distribution of intrinsically disordered regions (IDRs) follows a conserved pattern: long N- and C-terminal IDRs are universally present, while the number and length of central IDRs vary among clades. Short IDRs dominate in tetrapods, whereas teleost fishes exhibit longer, more extended disordered segments. These conserved disordered regions (CDRs) overlap with functional elements such as membrane-binding regions, α-helices, and PTM motifs, underscoring their dual role as structural scaffolds and regulatory platforms.

Shannon entropy profiles and hydrophobic moment distributions reveal that MBP's low-complexity segments are closely associated with structural motifs. Three conserved entropy minima correspond to experimentally verified α-helical segments, likely serving as structural anchors within otherwise flexible regions. In contrast, high-entropy segments align with disordered zones enriched in phosphorylation and citrullination sites, supporting the hypothesis that intrinsic disorder enhances regulatory plasticity. Despite overarching conservation, our analyses reveal lineage-specific fine-tuning. Hydrophobic moment profiles show that reptiles, birds, and mammals display a tendency toward amphipathic α-helix formation in the N-terminal CDR, whereas amphibians favor β-sheet formation. Central disordered regions alternate between α-helical and β-sheet propensities, reflecting structural plasticity, while teleosts and reptiles uniquely exhibit C-terminal helical propensity, absent in other clades.

Although the overall electrostatic topology of MBP — alternating basic clusters and neutral or acidic dips that facilitate reversible membrane adhesion — has remained stable since the emergence of myelin in early vertebrates, subtle inter-clade differences reflect functional divergence. Mammals and birds exhibit enhanced conservation of positively charged domains, consistent with the requirements of rapid saltatory conduction, while amphibians and reptiles display greater flexibility in their electrostatic architecture. Teleost MBPs, which lack the first 15 N-terminal residues, exhibit compensatory enrichment

of positively charged residues nearby, partially restoring membrane-binding potential. Amphibians show unique insertions that extend the protein and introduce additional basic residues, likely enhancing membrane affinity and supporting clade-specific adaptations in myelin organization.

Mapping experimentally validated and computationally predicted PTMs onto aligned consensus sequences revealed a strong association between phosphorylation and citrullination sites and disordered regions, although the strength of this association varied across clades. In early vertebrates, PTMs were primarily localized within IDRs, while in reptiles and birds their distribution expanded into more ordered regions, suggesting evolutionary broadening of regulatory control. PTMs were frequently co-located with conserved helices and membrane-binding sites, indicating a synergistic relationship between structural flexibility and post-translational regulation.

In summary, MBP exemplifies the dual nature of an intrinsically disordered protein: highly conserved in its core architecture yet dynamically adaptable through clade-specific modifications. The preservation of structural and electrostatic features across vertebrate evolution underscores strong selective pressure to maintain MBP's essential role in myelin compaction and stability. Simultaneously, adaptive changes in disorder profiles, sequence complexity, secondary structure, charge distribution, and PTM positioning reflect evolutionary tuning to diverse myelin architectures and functional requirements. Extending this comparative framework to other intrinsically disordered proteins may deepen our understanding of how disorder-mediated regulation shapes protein evolution and cellular plasticity.

References

Alibardi, L., 2002. Immunocytochemical localization of keratins, associated proteins and uptake of histidine in the epidermis of fish and amphibians. *Acta Histochem. 104,* 297–310. https://doi.org/10.1078/0065-1281-00651

Aponte-Santamaría, C., Fischer, G., Båth, P., Neutze, R. & De Groot, B.L., 2017. Temperature dependence of protein-water interactions in a gated yeast aquaporin. *Sci. Rep. 7*, 4016. https://doi.org/10.1038/s41598-017-04180-z

Babu, M.M., Van Der Lee, R. & De Groot, N.S., Gsponer, J., 2011. Intrinsically disordered proteins: regulation and disease. *Curr. Opin. Struct. Biol. 21,* 432–440. https://doi.org/10.1016/j.sbi.2011.03.011

Bah, A & Forman-Kay, J.D., 2016. Modulation of intrinsically disordered protein function by post-translational modifications. J. *Biol. Chem. 291,* 6696–6705. https://doi.org/10.1074/jbc.R115.695056

Bates, I.R., Feix, J.B., Boggs, J.M. & Harauz, G., 2004. An immunodominant epitope of myelin basic protein is an amphipathic α-helix. *J. Biol. Chem. 279,* 5757–5764. https://doi.org/10.1074/jbc.M311504200

Bedja-Iacona, L., Richard, E., Marouillat, S., Brulard, C., Alouane, T., Beltran, S., Andres, C.R., Blasco, H., Corcia, P., Veyrat-Durebex, C. & Vourc'h, P., 2024. Post-translational variants of major proteins in amyotrophic lateral sclerosis provide new insights into the pathophysiology of the disease. *IJMS 25,* 8664. https://doi.org/10.3390/ijms25168664

Bellay, J., Han, S., Michaut, M., Kim, T., Costanzo, M., Andrews, B.J., Boone, C., Bader, G.D., Myers, C.L. & Kim, P.M., 2011. Bringing order to protein disorder through comparative genomics and genetic interactions. *Genome Biol. 12,* R14. https://doi.org/10.1186/gb-2011-12-2-r14

Bianchi, G., Mangiagalli, M., Barbiroli, A., Longhi, S., Grandori, R., Santambrogio, C. & Brocca, S., 2022. Distribution of charged residues affects the average size and shape of intrinsically disordered proteins. *Biomolecules 12,* 561. https://doi.org/10.3390/biom12040561

Buchko, G.W., Mergelsberg, S.T., Tarasevich, B.J. & Shaw, W.J., 2022. Residue-specific insights into the intermolecular protein–protein interfaces driving amelogenin self-assembly in solution. *Biochemistry 61,* 2909–2921. https://doi.org/10.1021/acs.biochem.2c00522

Carrillo-Vico, A., Leech, M.D. & Anderton, S.M., 2010. Contribution of myelin autoantigen citrullination to t cell autoaggression in the central nervous system. *J. Immunol. 184,* 2839–2846. https://doi.org/10.4049/jimmunol.0903639

Charif, D. & Lobry, J.R., 2007. Seqinr 1.0-2: a contributed package to the R project for statistical computing devoted to biological sequences retrieval and analysis, in: bastolla, u., Porto, M., Roman, H.E., Vendruscolo, M. (Eds.), structural approaches to sequence evolution, biological and medical physics, biomedical engineering. Springer Berlin Heidelberg, Berlin, Heidelberg, pp. 207–232. https://doi.org/10.1007/978-3-540-35306-5_10

Darling, A.L. & Uversky, V.N., 2018. Intrinsic disorder and posttranslational modifications: the darker side of the biological dark matter. *Front. Genet. 9,* 158. https://doi.org/10.3389/fgene.2018.00158

Das, R.K. & Pappu, R.V., 2013. Conformations of intrinsically disordered proteins are influenced by linear sequence distributions of oppositely charged residues. *Proc. Natl. Acad. Sci. U.S.A. 110,* 13392–13397. https://doi.org/10.1073/pnas.1304749110

De Avila, M. & Vassall, K.A., Smith, G.S.T., Bamm, V.V., Harauz, G., 2014. The proline-rich region of 18.5 kDa myelin basic protein binds to the SH3-domain of Fyn tyrosine kinase with the aid of an upstream segment to form a dynamic complex *in vitro*. *Biosci. Rep. 34,* e00157. https://doi.org/10.1042/BSR20140149

De Bellard, M.E., 2016. Myelin in cartilaginous fish. *Brain Res. 1641,* 34–42. https://doi.org/10.1016/j.brainres.2016.01.013

De Vries, I., Bak, J., Salmoral, D.Á., Xie, R., Borza, R., Konijnenberg, M. & Perrakis, A., 2024. Disentangling the CHAOS of intrinsic disorder in human proteins. *bioRxiv* https://doi.org/10.1101/2024.10.26.620428

Del Conte, A., Bouhraoua, A., Mehdiabadi, M., Clementel, D., Monzon, A.M., CAID predictors, Holehouse, A.S., Griffith, D., Emenecker, R.J., Patil, A., Sharma, R., Tsunoda, T., Sharma, A., Tang, Y.J., Liu, B., Mirabello, C., Wallner, B., Rost, B., Ilzhöfer, D., Littmann, M., Heinzinger, M., Krautheimer, L.I.M., Bernhofer, M., McGuffin, L.J., Callebaut, I., Feildel, T.B., Liu, J., Cheng, J., Guo, Z., Xu, J., Wang, S., Malhis, N., Gsponer, J., Kim, C.-S., Han, K.-S., Ma, M.-C., Kurgan, L., Ghadermarzi, S., Katuwawala, A., Zhao, B., Peng, Z., Wu, Z., Hu, G., Wang, K., Hoque, M.T., Kabir, M.W.U., Vendruscolo, M., Sormanni, P., Li, M., Zhang, F., Jia, P., Wang, Y., Lobanov, M.Y., Galzitskaya, O.V., Vranken, W., Díaz, A., Litfin, T., Zhou, Y., Hanson, J., Paliwal, K., Dosztányi, Z., Erdős, G., Tosatto, S.C.E. & Piovesan, D., 2023. CAID prediction portal: a comprehensive service for predicting intrinsic disorder and binding regions in proteins. *Nucleic Acids Res.* 51, W62–W69. https://doi.org/10.1093/nar/gkad430

Dreier, L.B., Nagata, Y., Lutz, H., Gonella, G., Hunger, J., Backus, E.H.G. & Bonn, M., 2018. Saturation of charge-induced water alignment at model membrane surfaces. *Sci. Adv. 4,* eaap7415. https://doi.org/10.1126/sciadv.aap7415

Eisenberg, D., Weiss, R.M. & Terwilliger, T.C., 1984. The hydrophobic moment detects periodicity in protein hydrophobicity. *Proc. Natl. Acad. Sci. U.S.A. 81,* 140–144. https://doi.org/10.1073/pnas.81.1.140

Eisenberg, D., Weiss, R.M., Terwilliger, T.C. & Wilcox, W., 1982. Hydrophobic moments and protein structure. Faraday Symp. *Chem. Soc. 17,* 109. https://doi.org/10.1039/fs9821700109

Eisenberg, D., Wesson, M. & Wilcox, W., 1989. Hydrophobic moments as tools for analyzing protein sequences and structures, in: fasman, g.d. (Ed.), prediction of protein structure and the principles of protein conformation. Springer US, Boston, MA, pp. 635–646. https://doi.org/10.1007/978-1-4613-1571-1_16

Erdős, G. & Dosztányi, Z., 2020. Analyzing protein disorder with IUPred2A. *Curr. Protoc. Bioinform. 70,* e99. https://doi.org/10.1002/cpbi.99

Glasauer, S.M.K. & Neuhauss, S.C.F., 2014. Whole-genome duplication in teleost fishes and its evolutionary consequences. *Mol. Genet. Genomics 289,* 1045–1060. https://doi.org/10.1007/s00438-014-0889-2

Gogól, M., 2013. Citrullination – small change with a great consequence. *Acta Universitatis Lodziensis. Folia Biologica Et Ecologica 9,* 17–25. https://doi.org/10.2478/fobio-2013-0003

Gsponer, J., Futschik, M.E., Teichmann, S.A. & Babu, M.M., 2008. Tight regulation of unstructured proteins: from transcript synthesis to protein degradation. *Science 322,* 1365–1368. https://doi.org/10.1126/science.1163581

Gulsevin, A. & Meiler, J., 2021. Prediction of amphipathic helix—membrane interactions with Rosetta. *PLoS. Comput. Biol. 17,* e1008818. https://doi.org/10.1371/journal.pcbi.1008818

Harauz, G. & Boggs, J.M., 2013. Myelin management by the 18.5-kDa and 21.5-kDa classic myelin basic protein isoforms. *J. Neurochem. 125,* 334–361. https://doi.org/10.1111/jnc.12195

Harauz, G., Ishiyama, N., Hill, C.M.D., Bates, I.R., Libich, D.S. & Farès, C., 2004. Myelin basic protein—diverse conformational states of an intrinsically unstructured protein and its roles in myelin assembly and multiple sclerosis. *Micron 35,* 503–542. https://doi.org/10.1016/j.micron.2004.04.005

Harauz, G. & Musse, A.A., 2007. A tale of two citrullines—structural and functional aspects of myelin basic protein deimination in health and disease. *Neurochem. Res. 32,* 137–158. https://doi.org/10.1007/s11064-006-9108-9

Holehouse, A.S., Das, R.K., Ahad, J.N., Richardson, M.O.G. & Pappu, R.V., 2017. Cider: resources to analyze sequence-ensemble relationships of intrinsically disordered proteins. *Biophys. J. 112,* 16–21. https://doi.org/10.1016/j.bpj.2016.11.3200

Homchaudhuri, L., De Avila, M., Nilsson, S.B., Bessonov, K., Smith, G.S.T., Bamm, V.V., Musse, A.A., Harauz, G. & Boggs, J.M., 2010. Secondary structure and solvent accessibility of a calmodulin-binding c-terminal segment of membrane-associated myelin basic protein. *Biochemistry 49,* 8955–8966. https://doi.org/10.1021/bi100988p

Houben, B., Michiels, E., Ramakers, M., Konstantoulea, K., Louros, N., Verniers, J., Van Der Kant, R., De Vleeschouwer, M., Chicória, N., Vanpoucke, T., Gallardo, R., Schymkowitz, J. & Rousseau, F., 2020. Autonomous aggregation suppression by acidic residues explains why chaperones favour basic residues. *EMBO J. 39,* e102864. https://doi.org/10.15252/embj.2019102864

Iakoucheva, L.M., 2004. The importance of intrinsic disorder for protein phosphorylation. *Nucleic Acids Res. 32,* 1037–1049. https://doi.org/10.1093/nar/gkh253

Jensen, M.R., Ruigrok, R.W. & Blackledge, M., 2013. Describing intrinsically disordered proteins at atomic resolution by NMR. *Cur. Opin. Struct. Biol. 23,* 426–435. https://doi.org/10.1016/j.sbi.2013.02.007

Kastano, K., Erdős, G., Mier, P., Alanis-Lobato, G., Promponas, V.J., Dosztányi, Z. & Andrade-Navarro, M.A., 2020. Evolutionary study of disorder in protein sequences. *Biomolecules 10,* 1413. https://doi.org/10.3390/biom10101413

Kim, J., Zhang, R., Strittmatter, E.F., Smith, R.D. & Zand, R., 2009. Post-translational modifications of chicken myelin basic protein charge components. *Neurochem. Res. 34,* 360–372. https://doi.org/10.1007/s11064-008-9788-4

Kishimoto, A., Nishiyama, K., Nakanishi, H., Uratsuji, Y., Nomura, H., Takeyama, Y. & Nishizuka, Y., 1985. Studies on the phosphorylation of myelin basic protein by protein kinase C and adenosine 3‘:5‘-monophosphate-dependent protein kinase. *J. Biol. Chem. 260,* 12492–12499. https://doi.org/10.1016/S0021-9258(17)38898-1

Kister, A. & Kister, I., 2023. Overview of myelin, major myelin lipids, and myelin-associated proteins. *Front. Chem. 10,* 1041961. https://doi.org/10.3389/fchem.2022.1041961

Kurotani, A., Tokmakov, A.A., Kuroda, Y., Fukami, Y., Shinozaki, K. & Sakurai, T., 2014. Correlations between predicted protein disorder and post-translational modifications in plants. *Bioinformatics 30,* 1095–1103. https://doi.org/10.1093/bioinformatics/btt762

Li, Z. & Buck, M., 2023. A proteome-scale analysis of vertebrate protein amino acid occurrence: Thermoadaptation shows a correlation with protein solvation but less so with dynamics. *Proteins 91,* 3–15. https://doi.org/10.1002/prot.26404

Libich, D.S. & Harauz, G., 2008. Backbone dynamics of the 18.5kDa isoform of myelin basic protein reveals transient α-helices and a calmodulin-binding site. *Biophys. J. 94,* 4847–4866. https://doi.org/10.1529/biophysj.107.125823

Liu, Y., Wang, X. & Liu, B., 2019. A comprehensive review and comparison of existing computational methods for intrinsically disordered protein and region prediction. *Brief. Bioinform. 20,* 330–346. https://doi.org/10.1093/bib/bbx126

Livingstone, C.D. & Barton, G.J., 1993. Protein sequence alignments: a strategy for the hierarchical analysis of residue conservation. *Bioinformatics 9,* 745–756. https://doi.org/10.1093/bioinformatics/9.6.745

Lobley, A., Orengo, C.A., Swindells, M.B. & Jones, D., 2005. Inferring function using patterns of native disorder in proteins. *PLoS. Comput. Biol. preprint,* e162. https://doi.org/10.1371/journal.pcbi.0030162.eor

Madeira, F., Madhusoodanan, N., Lee, J., Eusebi, A., Niewielska, A., Tivey, A.R.N., Lopez, R. & Butcher, S., 2024. The EMBL-EBI Job Dispatcher sequence analysis tools framework in 2024. *Nucleic Acids Res. 52,* W521–W525. https://doi.org/10.1093/nar/gkae241

Monastyrskyy, B., Kryshtafovych, A., Moult, J., Tramontano, A. & Fidelis, K., 2014. Assessment of protein disorder region predictions in CASP10. *Proteins 82,* 127–137. https://doi.org/10.1002/prot.24391

Moscarello, M.A., Mastronardi, F.G. & Wood, D.D., 2007. The role of citrullinated proteins suggests a novel mechanism in the pathogenesis of multiple sclerosis. *Neurochem. Res. 32,* 251–256. https://doi.org/10.1007/s11064-006-9144-5

Mughal, F. & Caetano-Anollés, G., 2025. Evolution of intrinsic disorder in the structural domains of viral and cellular proteomes. *Sci. Rep. 15,* 2878. https://doi.org/10.1038/s41598-025-86045-4

Müller, C., Bauer, N.M., Schäfer, I. & White, R., 2013. Making myelin basic protein -from mRNA transport to localized translation. *Front. Cell. Neurosci. 7,* 1-7. https://doi.org/10.3389/fncel.2013.00169

Müller-Späth, S., Soranno, A., Hirschfeld, V., Hofmann, H., Rüegger, S., Reymond, L., Nettels, D. & Schuler, B., 2010. Charge interactions can dominate the dimensions of intrinsically disordered proteins. *Proc. Natl. Acad. Sci. U.S.A. 107,* 14609–14614. https://doi.org/10.1073/pnas.1001743107

Nawaz, S., Schweitzer, J., Jahn, O. & Werner, H.B., 2013. Molecular evolution of myelin basic protein, an abundant structural myelin component: phylogeny of myelin basic protein. *Glia 61,* 1364–1377. https://doi.org/10.1002/glia.22520

Necci, M., Piovesan, D., Dosztányi, Z. & Tosatto, S.C.E., 2017. MobiDB-lite: fast and highly specific consensus prediction of intrinsic disorder in proteins. *Bioinformatics 33,* 1402–1404. https://doi.org/10.1093/bioinformatics/btx015

Necci, M., Piovesan, D. & Tosatto, S.C.E., 2016. Large-scale analysis of intrinsic disorder flavors and associated functions in the protein sequence universe. *Prot. Sci 25,* 2164–2174. https://doi.org/10.1002/pro.3041

Oldfield, C.J., Uversky, V.N., Dunker, A.K. & Kurgan, L., 2019. Introduction to intrinsically disordered proteins and regions, in: Intrinsically Disordered Proteins. *Elsevier,* pp. 1–34. https://doi.org/10.1016/B978-0-12-816348-1.00001-6

Phoenix, D.A. & Harris, F., 2002. The hydrophobic moment and its use in the classification of amphiphilic structures (Review). *Mol. Membr. Biol. 19,* 1–10. https://doi.org/10.1080/09687680110103631

Polverini, E., Coll, E.P., Tieleman, D.P. & Harauz, G., 2011. Conformational choreography of a molecular switch region in myelin basic protein — Molecular dynamics shows induced folding and secondary structure type conversion upon threonyl phosphorylation in both aqueous and membrane-associated environments. *Biochim. Biophys. Acta Biomembr. 1808,* 674–683. https://doi.org/10.1016/j.bbamem.2010.11.030

Raasakka, A. & Kursula, P., 2020. Flexible players within the sheaths: the intrinsically disordered proteins of myelin in health and disease. *Cells 9,* 470. https://doi.org/10.3390/cells9020470

Raasakka, A., Ruskamo, S., Kowal, J., Barker, R., Baumann, A., Martel, A., Tuusa, J., Myllykoski, M., Bürck, J., Ulrich, A.S., Stahlberg, H. & Kursula, P., 2017. Membrane Association Landscape of Myelin Basic Protein Portrays Formation of the Myelin Major Dense Line. *Sci. Rep. 7,* 4974. https://doi.org/10.1038/s41598-017-05364-3

Rajagopalan, K., Mooney, S.M., Parekh, N., Getzenberg, R.H. & Kulkarni, P., 2011. A majority of the cancer/testis antigens are intrinsically disordered proteins. *J. Cell. Biochem. 112,* 3256–3267. https://doi.org/10.1002/jcb.23252

Riley, A.C., Ashlock, D.A. & Graether, S.P., 2023. The difficulty of aligning intrinsically disordered protein sequences as assessed by conservation and phylogeny. *PLoS. ONE 18,* e0288388. https://doi.org/10.1371/journal.pone.0288388

Romero, P., Obradovic, Z., Li, X., Garner, E.C., Brown, C.J. & Dunker, A.K., 2001. Sequence complexity of disordered protein. *Proteins 42,* 38–48. https://doi.org/10.1002/1097-0134(20010101)42:1<38::AID-PROT50>3.0.CO;2-3

Schad, E., Tompa, P. & Hegyi, H., 2011. The relationship between proteome size, structural disorder and organism complexity. *Genome Biol. 12,* R120. https://doi.org/10.1186/gb-2011-12-12-r120

Segrest, J.P., De Loof, H., Dohlman, J.G., Brouillette, C.G. & Anantharamaiah, G.M., 1990. Amphipathic helix motif: classes and properties. *Proteins 8,* 103–117. https://doi.org/10.1002/prot.340080202

Sen, S., Dey, A., Chowdhury, S., Maulik, U. & Chattopadhyay, K., 2019. Understanding the evolutionary trend of intrinsically structural disorders in cancer relevant proteins as probed by Shannon entropy scoring and structure network analysis. *BMC Bioinformatics 19,* 549. https://doi.org/10.1186/s12859-018-2552-0

Siddiqui, I.J., Pervaiz, N. & Abbasi, A.A., 2016. The Parkinson disease gene SNCA: evolutionary and structural insights with pathological implication. *Sci. Rep. 6,* 24475. https://doi.org/10.1038/srep24475

Siltberg-Liberles, J., 2011. Evolution of structurally disordered proteins promotes neostructuralization. *Mol. Biol. Evol. 28*, 59–62. https://doi.org/10.1093/molbev/msq291

Singleton, M.D. & Eisen, M.B., 2024. Evolutionary analyses of intrinsically disordered regions reveal widespread signals of conservation. *PLoS. Comput. Biol. 20,* e1012028. https://doi.org/10.1371/journal.pcbi.1012028

Smirnova, E.V., Rakitina, T.V., Ziganshin, R.H., Arapidi, G.P., Saratov, G.A., Kudriaeva, A.A. & Belogurov, A.A., 2021. Comprehensive atlas of the myelin basic protein interaction landscape. *Biomolecules 11,* 1628. https://doi.org/10.3390/biom11111628

Stämpfli, R., 1954. Saltatory conduction in nerve. *Phy. Rev.* https://journals.physiology.org/doi/abs/10.1152/physrev.1954.34.1.101?journalCode=physrev

Sysoev, E.I., Shenfeld, A.A., Belashova, T.A., Valina, A.A., Zadorsky, S.P. & Galkin, A.P., 2025. Amyloid fibrils of the myelin basic protein are an integral component of myelin in the vertebrate brain. *Sci. Rep. 15,* 29053. https://doi.org/10.1038/s41598-025-13524-z

Tai, F.L., Smith, R., Bernard, C.C.A. & Hearn, M.W.T., 1986. Evolutionary divergence in the structure of myelin basic protein: comparison of chondrichthye basic proteins with those from higher vertebrates. *J. Neurochem. 46,* 1050–1057. https://doi.org/10.1111/j.1471-4159.1986.tb00617.x

Turner, R.S., Chou, C. -H. J., Kibler, R.F. & Kuo, J.F., 1982. Basic protein in brain myelin is phosphorylated by endogenous phospholipid-sensitive Ca^{2+} -dependent protein kinase. *J. Neurochem. 39,* 1397–1404. https://doi.org/10.1111/j.1471-4159.1982.tb12583.x

Uversky, V.N., 2019. Intrinsically disordered proteins and their “mysterious” (meta)physics. *Front. Phys. 7,* 10. https://doi.org/10.3389/fphy.2019.00010

Van Bibber, N.W., Haerle, C., Khalife, R., Xue, B. & Uversky, V.N., 2020. Intrinsic disorder in tetratricopeptide repeat proteins. *IJMS 21,* 3709. https://doi.org/10.3390/ijms21103709

Van Der Lee, R., Buljan, M., Lang, B., Weatheritt, R.J., Daughdrill, G.W., Dunker, A.K., Fuxreiter, M., Gough, J., Gsponer, J., Jones, D.T., Kim, P.M., Kriwacki, R.W., Oldfield, C.J., Pappu, R.V., Tompa, P., Uversky, V.N., Wright, P.E. & Babu, M.M., 2014. Classification of intrinsically disordered regions and proteins. *Chem. Rev. 114,* 6589–6631. https://doi.org/10.1021/cr400525m

Walsh, I., Martin, A.J.M., Di Domenico, T. & Tosatto, S.C.E., 2012. ESpritz: accurate and fast prediction of protein disorder. *Bioinformatics 28,* 503–509. https://doi.org/10.1093/bioinformatics/btr682

Wang, D., Zeng, S., Xu, C., Qiu, W., Liang, Y., Joshi, T. & Xu, D., 2017. MusiteDeep: a deep-learning framework for general and kinase-specific phosphorylation site prediction. *Bioinformatics 33,* 3909–3916. https://doi.org/10.1093/bioinformatics/btx496

Wang, S., Ma, J. & Xu, J., 2016. AUCpreD: proteome-level protein disorder prediction by AUC-maximized deep convolutional neural fields. *Bioinformatics 32,* i672–i679. https://doi.org/10.1093/bioinformatics/btw446

Ward, J.J., Sodhi, J.S., McGuffin, L.J., Buxton, B.F. & Jones, D.T., 2004. Prediction and functional analysis of native disorder in proteins from the three kingdoms of life. *J. Mol. Biol. 337,* 635–645. https://doi.org/10.1016/j.jmb.2004.02.002

Waterhouse, A.M., Procter, J.B., Martin, D.M.A., Clamp, M. & Barton, G.J., 2009. Jalview Version 2—a multiple sequence alignment editor and analysis workbench. *Bioinformatics 25,* 1189–1191. https://doi.org/10.1093/bioinformatics/btp033

Welch, B.L., 1951. On the comparison of several mean values: an alternative approach. *Biometrika 38,* 330. https://doi.org/10.2307/2332579

Wickham, H., 2016. Programming with ggplot2, in: ggplot2, use R! *Springer International Publishing, Cham,* pp. 241–253. https://doi.org/10.1007/978-3-319-24277-4_12

Wright, P.E. & Dyson, H.J., 2015. Intrinsically disordered proteins in cellular signalling and regulation. *Nat. Rev. Mol. Cell Biol. 16,* 18–29. https://doi.org/10.1038/nrm3920

Xie, H., Vucetic, S., Iakoucheva, L.M., Oldfield, C.J., Dunker, A.K., Uversky, V.N. & Obradovic, Z., 2007. Functional Anthology of Intrinsic Disorder. 1. Biological Processes and Functions of Proteins with Long Disordered Regions. *J. Proteome Res. 6,* 1882–1898. https://doi.org/10.1021/pr060392u

Xie, Y., Li, Huiqin, Luo, X., Li, Hongyu, Gao, Q., Zhang, L., Teng, Y., Zhao, Q., Zuo, Z. & Ren, J., 2022. IBS 2.0: an upgraded illustrator for the visualization of biological sequences. *Nucleic Acids Res. 50,* W420–W426. https://doi.org/10.1093/nar/gkac373

Xue, B., Brown, C.J., Dunker, A.K. & Uversky, V.N., 2013. Intrinsically disordered regions of p53 family are highly diversified in evolution. *Biochim. Biophys. Acta Proteins and Proteomics*, *1834,* 725–738. https://doi.org/10.1016/j.bbapap.2013.01.012

Xue, B., Dunbrack, R.L., Williams, R.W., Dunker, A.K. & Uversky, V.N., 2010. PONDR-FIT: A meta-predictor of intrinsically disordered amino acids. *Biochim. Biophys. Acta Proteins and Proteomics*, *1804,* 996–1010. https://doi.org/10.1016/j.bbapap.2010.01.011

Yarberry, W., 2021. *CRAN Recipes: DPLYR, Stringr, Lubridate, and RegEx in R.* Apress, Berkeley, CA. https://doi.org/10.1007/978-1-4842-6876-6

Yruela, I., Oldfield, C.J., Niklas, K.J. & Dunker, A.K., 2017. Evidence for a strong correlation between transcription factor protein disorder and organismic complexity. *Genome Biol. Evol. 9,* 1248–1265. https://doi.org/10.1093/gbe/evx073

Zand, R., Jin, X., Kim, J., Wall, D.B., Gould, R. & Lubman, D.M., 2001. Studies of posttranslational modifications in spiny dogfish myelin basic protein. *J. Neurosci.* https://link.springer.com/article/10.1023/A:1010921230859

Zarin, T., Strome, B., Nguyen Ba, A.N., Alberti, S., Forman-Kay, J.D. & Moses, A.M., 2019. Proteome-wide signatures of function in highly diverged intrinsically disordered regions. *eLife 8,* e46883. https://doi.org/10.7554/eLife.46883

Zavialova, M.G., Zgoda, V.G. & Nikolaev, E.N., 2017. Analysis of the role of protein phosphorylation in the development of diseases. *Biochem. Moscow Suppl. Ser. B 11,* 203–218. https://doi.org/10.1134/S1990750817030118

Zhang, C., Walker, A.K., Zand, R., Moscarello, M.A., Yan, J.M. & Andrews, P.C., 2012. Myelin basic protein undergoes a broader range of modifications in mammals than in lower vertebrates. *J. Proteome Res. 11,* 4791–4802. https://doi.org/10.1021/pr201196e

Supplementary materials

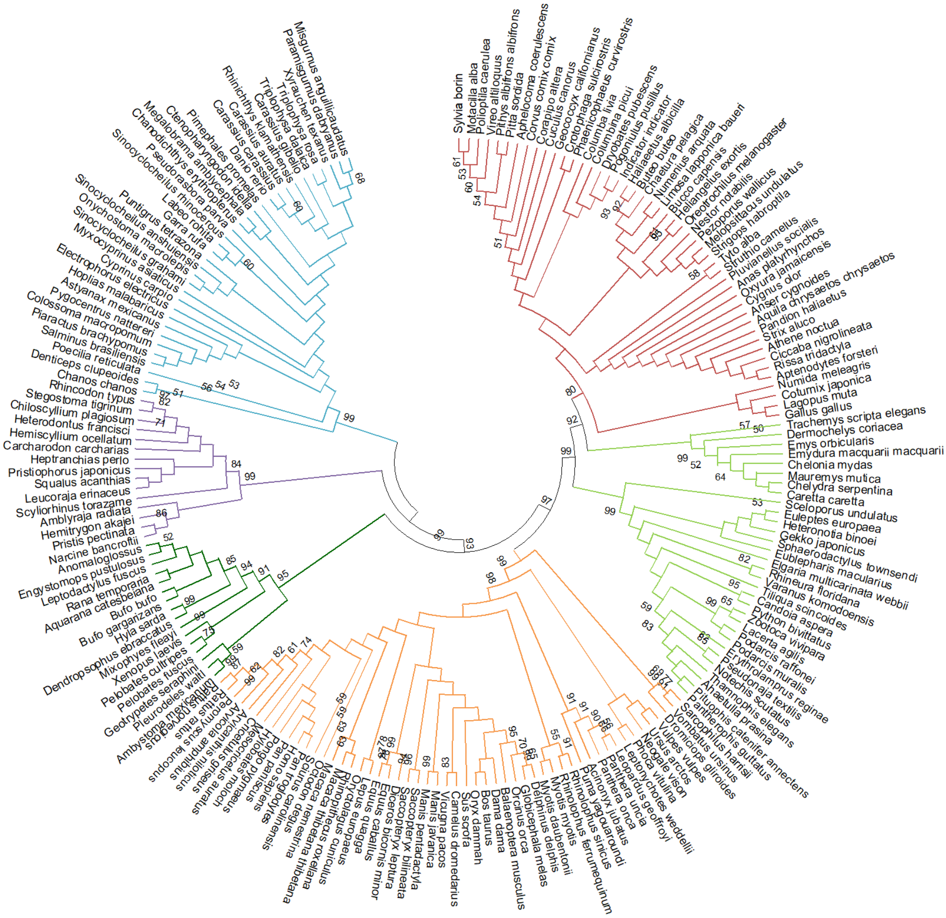

Figure S1. Neighbor-joining phylogenetic tree of representative vertebrate species based on protein sequence alignment. The tree was constructed using the Neighbor-Joining (NJ) method in MEGA version 12. Support for each node was assessed with 500 bootstrap replicates, with values shown at key nodes. Clades are color-coded as follows: purple – *Chondrichthyes*, blue – *Teleostei*, dark green – *Amphibia*, light green – *Reptilia*, red – *Aves*, orange – *Mammalia*.

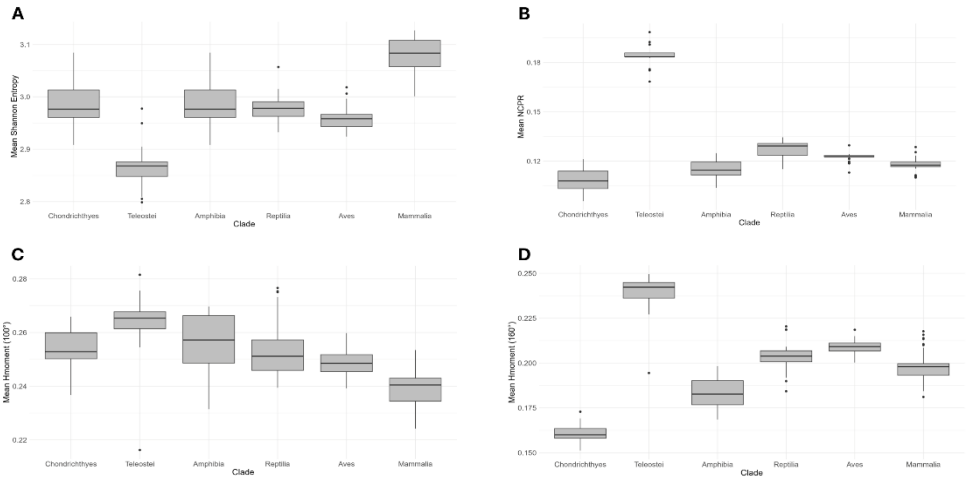

Figure S2. Comparison of biophysical properties of the 18.5 kDa MBP across six vertebrate clades (*Chondrichthyes, Teleostei, Amphibia, Reptilia, Aves,* and *Mammalia*). Boxplots show (A) mean Shannon entropy, (B) net charge per residue (NCPR), (C) mean hydrophobic moment at 100°, and (D) mean hydrophobic moment at 160°.

Table S1. Predicted phosphorylation sites of the MBP 18.5 kDa isoform across vertebrate clades (confirmed by ≥2 predictors: PONDR DEPP, Musite, NetPhos). In the table, letters represent amino acid one-letter codes, while numbers indicate the position within the consensus sequence.

Chondrichthyes	***Teleostei***	***Amphibia***	***Reptilia***	***Aves***	***Mammalia***
3S	5S	3S	3S	3S	3S
5S	6T	5S	7S	7S	8S
6T	7S	6T	8S	8S	13S
7S	10S	7S	13S	13S	15Y
18S	42S	18S	17T	17S	18S
23S	48S	23S	19S	19S	20S
38S	49S	38S	20T	21T	21S
50T	50S	41S	28S	28S	36T
52S	57S	46S	40S	34S	57S
59T	58S	66S	58Y	39S	70Y
70T	59T	69S	66S	55S	72S
115Y	74S	71S	70S	66S	97T
120S	77S	75Y	99S	71S	100T
123S	78S	77S	103T	76S	104S
127Y	83S	78S	114S	96S	112S
134S	93S	79S	119S	99T	117S
136T	95S	84S	124T	111S	134S

Chondrichthyes	*Teleostei*	*Amphibia*	*Reptilia*	*Aves*	*Mammalia*
138S	99S	88S	129Y	116S	138S
139S	101S	110T	133S	126Y	153T
150S	104S	113T	149Y	129S	155S
	116S	117S	155T	145S	165S
	124S	124S	165S	146Y	167S
	126S	129S	167S	154S	169S
	128S	145Y	171S	162S	
	134S	147S	173S	164S	
	135T	148S	175S	168S	
		164Y		170S	
		176S		172S	
		186S			
		188S			

Table S2. Conservation of experimentally identified citrullination sites of the human MBP 18.5 kDa isoform across aligned vertebrate consensus sequences. In the table, letters represent amino acid one-letter codes, while numbers indicate the position within the consensus sequence. Conserved residues are shown in bold, and substitutions that remain positively charged are highlighted in red.

Homo sapiens	*Chondrich-thyes*	*Teleostei*	*Amphibia*	*Reptilia*	*Aves*	*Mammalia*
R6	0	0	L6	**R6**	**R6**	**R6**
R10	0	0	G10	**R10**	**R10**	**R10**
R26	A13	P11	**R28**	**R25**	**R25**	**R26**
R32	**R19**	K17	**R38**	**R31**	H31	**R32**
R34	**R21**	**R19**	**R40**	**R32**	**R32**	**R34**
R44	K31	**R29**	**R50**	**R43**	**R42**	**R44**
R50	G37	K35	**R56**	K49	**R48**	**R50**
R55	K44	K38	K61	**R54**	**R53**	**R55**
R66	L54	S42	S73	**R64**	**R64**	**R66**
R80	**R68**	**R61**	**R96**	**R83**	**R80**	**R81**
R98	K86	P79	**R114**	**R101**	**R98**	**R99**
R114	K104	0	**R129**	**R117**	**R114**	**R115**
R123	**R113**	S93	K140	K126	K123	K124
R131	S122	S99	S149	K135	K131	**R132**
R160	K147	S124	**R186**	S166	S162	**R163**
R163	G150	**R127**	**R189**	**R169**	**R165**	**R166**
R170	0	0	**R198**	**R180**	**R176**	**R173**
R171	0	0	**R199**	**R181**	**R177**	**R174**

STUDIA UNIVERSITATIS BABEŞ-BOLYAI BIOLOGIA, 70, 2, 2025 (p. 151-161)
doi:10.24193/subbbiol.2025.2.09

From instinct to experience: understanding feeding behaviour in *Python regius* (Shaw, 1802)

Octavian Craioveanu[1], Vlad Stoicescu[2], and Cristina Craioveanu[2,3] *

[1]Academic Cultural Heritage Department – Vivarium, Babeş-Bolyai University, Cluj-Napoca, Romania; [2]Department of Taxonomy and Ecology, Faculty for Biology and Geology, Babeş-Bolyai University, Cluj-Napoca, Romania; [3]Sociobiology and Insect Ecology Lab, Centre 3 B, Babeş-Bolyai University, Cluj-Napoca, Romania
Corresponding author, E-mail: cristina.craioveanu@ubbcluj.ro.

Article history: Received 08 September 2025; Revised 18 December 2025; Accepted 18 December 2025; Available online 20 December 2025

Abstract. Research on the cognitive abilities and behaviour of reptiles is quite limited, largely due to the challenges in accurately quantifying and interpreting observations made in both natural and controlled settings. This limitation is particularly notable in the study of snakes, where investigations into the cognitive skills of this suborder are scarce.
In this study, we focused on the feeding behaviour of young *Python regius* specimens to explore whether these behaviours are purely instinctual or if they involve learning and/or using previously acquired knowledge. We observed eight naive juvenile individuals to analyse their feeding behaviour. Our hypothesis proposed that as these snakes gained experience in the first month of their lives, their feeding efficiency would improve. We recorded and analysed the time allocated to various stages of their feeding behaviours during their initial four feedings.
The findings we obtained were unexpected and partially contradicted our initial assumptions. Ultimately, we concluded that the feeding efficiency in these reptiles presents a complex interplay of instinct, past experiences, and certain factors that remain challenging to explain within the framework of existing specialised literature.

Keywords: Ball pythons, feeding behaviour, feeding efficiency, snake learning, time budget.

Introduction

Historically, reptiles were regarded as a stimulus-bound, slow-learning group with a limited behavioural repertoire (Burghart, 1977). As they have a relatively small and simple brain compared to endotherms (Burghart, 1977), they were labelled as ”reflex machines” (Jerison, 1973), ”intellectual dwarfs" (Turner, 1892), or even completely inferior (Sagan, 1977; MacLean, 1985). However, new research into the cognitive abilities of reptiles is increasingly challenging these labels, as they reveal an impressive range of problem-solving, learning, and social skills (De Meester and Baeckens, 2021).

In their natural element, reptiles are actually far more than underperforming, pre-programmed robots. They show a high propensity for experience-based learning in areas such as homing behaviour, territoriality, formation of food preferences, and social dominance relationships (Burghart, 1973). Studying cognition under these natural conditions would be the preferred approach, as it makes the results more relevant, but reptiles are poorly suited to this type of experiment (Whiting and Noble, 2018). This seemingly rich behavioural palette may be responsible for the upsurge in reptile cognition research over the last decade (Wilkinson and Huber, 2012; Burghardt, 2013, Matsubara *et al*., 2017, De Meester and Baeckens, 2021); however, little experimental research has been conducted compared to other taxa in vertebrate phylogeny, particularly mammals and birds (Szabo *et al*., 2021).

The main reason for this, apart from the traditional reputation mentioned above, is the difficulty in designing a meaningful study, due to the lack of efficient reinforcers and motivators (e.g., food, which is commonly used as a motivator for cognitive tasks, is not very attractive to reptiles compared to other vertebrates - Burghart, 1977). In cognitive studies performed on snakes, these design difficulties become even greater. Their sedentary lifestyle in captivity, the difficulty of using food as a reinforcer, and the lack of limbs to press levers mean that this reptilian suborder is generally avoided.

Additionally, the total absence of parental care, which requires newborn snakes to find and capture prey without prior experience, suggests that instincts play a crucial role in their feeding behaviour. Newborn individuals can perform their tasks accurately without previous experience, but there is also evidence in the literature that the predisposition for a particular behaviour is not necessarily genetically determined (Suboski, 1992; Nafus *et al*., 2021).

Regarding the relationship between cognition and feeding, the literature is sparse and somewhat contradictory.

As far as initial chemosensory feeding responses are concerned, the reaction to a favoured prey item can be modified by experience (*Thamnophis sirtalis* to

Eisenia foetida and *Poecilia reticulata,* and *Drymarchon couperi* to mice), whereas in other cases it appears to be completely unaffected (*Thamnophis sirtalis* to tadpoles and frogs) (Fuchs and Burghardt, 1971; Arnold, 1978, Goetz *et al.* 2018).

The prey capture tactics described in the literature also appear to be prone to some experience-based learning. In a study on *Coleognathus helena*, concerning the response to different prey sizes, Mehta (2009) found that experience led to a better capture technique (forebody capture), a more complex prey restraint method, and an increase in the ingestion of dead prey versus still live prey. However, Mori (1993) found no effect of recent experience with large or small prey on subsequent capture and restraint behaviour in *Elaphe climacophora*. And, Ryerson (2020) found a decline in strike performance of *Python regius* over a three year time period.

Given this diversity of behavioural expressions, we were interested in testing whether neonate naïve constrictor snakes are able to improve the effectiveness of their feeding technique throughout their first four feeding sessions. More specifically, does experience promote an improvement in detection, constriction, and ingestion? We considered feeding behaviour to be more efficient if it led to a shorter duration of the time required for it (Bealor and Saviola, 2007). Based on the existing literature and anecdotal observation, we tried to answer the above question by formulating two starting hypotheses:

1. Feeding is not purely an instinct-driven behaviour.

2. There will be an improvement in the efficiency of feeding behaviour in the form of reduced time.

Materials and methods

The study was conducted in May 2024 at the herpetology laboratory of Babeş-Bolyai University's Vivarium. The experimental group consisted of eight neonate, naive *Python regius* (Shaw, 1802) (IUCN near threatened, number P1-P8), a constrictor species native to West and Central Africa (D'Cruze, 2020), obtained by captive breeding. Animal husbandry, management, and experiments were conducted in accordance with the ethical standards established by the World Association of Zoos and Aquariums (WAZA, 2023).

To have a more compact experimental group, we used only females with no significant variation in size and weight (initial measurements: 528.50 mm ± 12.78 mm SD average length, and 64.12 g ± 1.96 g SD average mass) and across experiment-time. The prey size used was approximately 15% of the snake's body weight. The animals were housed separately, in opaque Tupperware plastic containers (27 cm x 17 cm x 8 cm), which were equipped with bark mulch

substrate, a hiding place, and a water bowl, illuminated with indirect sunlight, and had a temperature difference between day and night of 20/27 °C (Westhoff, 2005).

During the three-week experiment, we carried out four test feedings at one-week intervals. The first test feeding coincided with the very first feeding of the snakes and took place at the age of 2 weeks. To minimise handling stress in the snakes and obtain the best possible quality data, all test feedings were conducted directly in the housing containers. Preparations for the experiment began by replacing the opaque lid of the Tupperware container with a clear glass panel and positioning the container under the tripod-mounted camera. The experiments were filmed with a GoPro 7 camera placed 40 cm above the container. Playing back the videos (Windows Media Player), we measured the time budget (Brockman, 1994) of the following behavioural variables: 1) time to first strike, 2) constriction time, and 3) ingestion time.

The variables were measured in seconds and are defined as follows:

1) time to strike (S) was defined as the time between the insertion of the mouse in the housing container and the snake's strike.

2) constriction time (C) was defined as an interval starting with the strike and lasting until the experimental animal releases the initial bite or dislodges.

3) ingestion time (I) starts at the end of the constriction and also includes vomeronasal sniffing and adjustment of prey after constriction, not just the actual swallowing.

We also measured the total feeding time (T) that starts with the strike and is defined as a sum of the constriction time (C) and the ingestion time (I); and additionally, the time of the experiment in days after the start, with the first day of the experiment considered day 1, and the last, day 28.

To analyse the data, we first checked the distributions for each variable using a Shapiro-Wilk test (shapiro.test in RStudio, RStudio Team, 2025). Because the test results showed a non-normal distribution of the data in all cases ($P < 0.01$), we further used non-parametric tests to check for differences between trials accounting for repeated measures on individuals. For each variable (S, C, I, and T), we applied a Friedman test, treating individual identity as a blocking factor and feeding occasion as the within-subject factor. To maintain a complete block design, individuals that did not feed during the first trial, were excluded from these analyses. When the Friedman test indicated a significant effect of feeding occasion, post-hoc pairwise comparisons between trials were performed using Wilcoxon signed-rank tests with Holm correction for multiple comparisons. All analyses were conducted in R (RStudio Team, 2025). We also computed a correlation test with the method "Spearman's rank correlation" between the time of experiment in days and each variable (cor.test in RStudio, RStudio team, 2025).

Results

There were significant differences only between the trials regarding the time to strike – S (Tab. 1). The first trial had a higher value of S, which declined with time (Fig. 1). However, post-hoc pairwise comparisons using Wilcoxon signed-rank tests with Holm correction did not identify significant differences between individual feeding occasions (all adjusted $p \geq 0.19$).

Constriction time (C) varied slightly between trials, but had an overall lower median value on the fourth occasion (Fig. 2).

In the case of ingestion time, we can observe the tendency for a longer time in trial 3, and a similar median time with less variability in trial 4 (Fig. 3).

The median values of the total feeding time showed a tendency to increase, showing in the third and fourth trials longer and slightly longer times than those in the first two trials (Fig. 4).

Table 1. Results of the Friedman test comparisons between trials for all four variables measured (S – time to strike, C – constriction time, I – ingestion time, T – total feeding time). Significant values are underlined.

Parameters	chi squared	df	P value
S	9.600	3	0.022
C	4.627	3	0.201
I	5.000	3	0.172
T	3.800	3	0.284

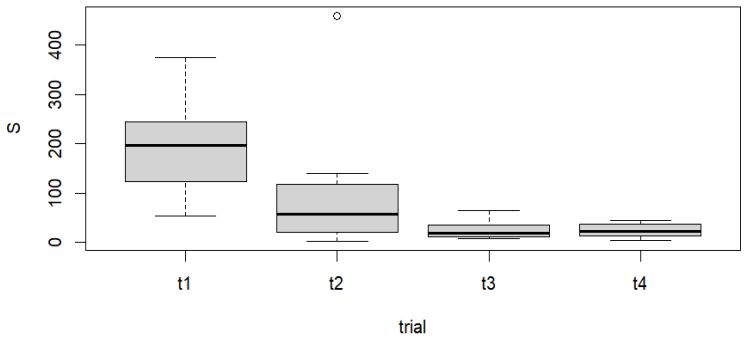

Figure 1. Time to strike values (S measured in seconds) for all *Python* juvenile individuals in the four feeding trials. Boxplots represent median values (thick line inside the box), interquartile range (the box), maximum and minimum values (whiskers), and outliers (empty circles).

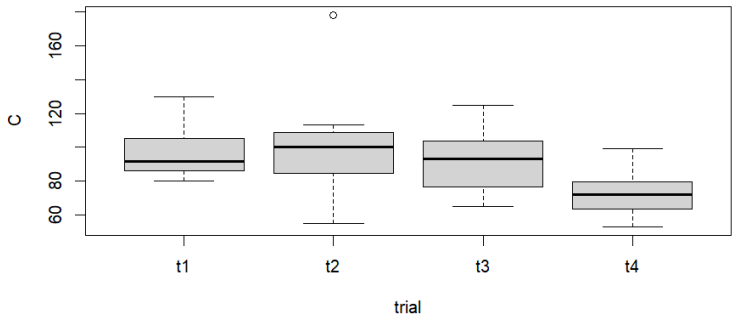

Figure 2. Constriction time (C measured in seconds) for all *Python* juvenile individuals in the four feeding trials. Boxplots represent median values (thick line inside the box), interquartile range (the box), maximum and minimum values (whiskers), and outliers (empty circles).

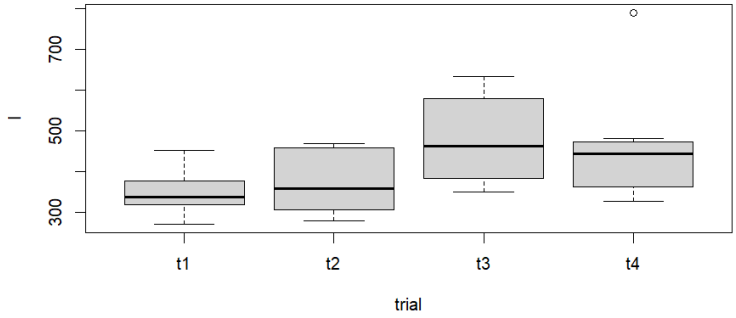

Figure 3. Ingestion time (I measured in seconds) for all *Python* juvenile individuals in the four feeding trials. Boxplots represent median values (thick line inside the box), interquartile range (the box), maximum and minimum values (whiskers), and outliers (empty circles).

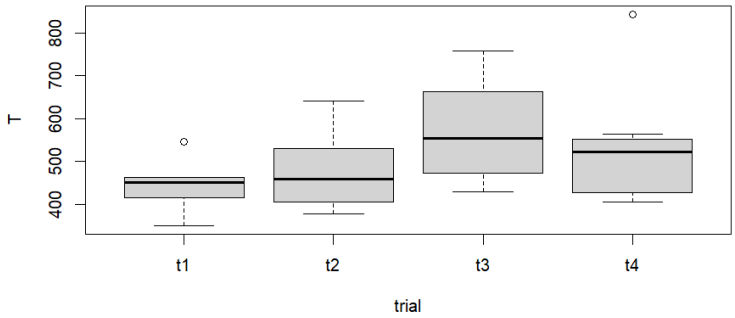

Figure 4. Total feeding time (T measured in seconds) for all *Python* juvenile individuals in the four feeding trials. Boxplots represent median values (thick line inside the box), interquartile range (the box), maximum and minimum values (whiskers), and outliers (empty circles).

The correlation analysis showed a strong negative correlation between time to strike (S) and time, and a more moderate negative correlation between constriction time (C) and time (Tab. 2). Another significant but only moderate positive correlation was between ingestion time (I) and time (Tab. 2). Total feeding time was not significantly correlated with time of the experiment (Tab. 2).

Table 2. Spearman rank correlation results for each variable (S – time to strike, C – constriction time, I – ingestion time, T – total feeding time) with experiment time.

S	C	I	T
Rho = -0.616, P < 0.001	Rho = -0.489, P = 0.006	Rho = 0.439, P = 0.015	Rho = 0.307, P = 0.099

Discussion

In this study, we tested whether the feeding behaviour of the Ball python is completely driven by instinct or whether it is subject to improvement in time and with experience. For this purpose, we measured the time budget invested in time to strike (S), constriction (C), ingestion time (I) and total feeding time (T) of a cohort of 8 newborn naive animals, throughout their first four feedings.

The results show a clear and linear improvement in some of these parameters, which is evidence of behaviour altered by experience. However, in the case of our second hypothesis regarding the decrease of the total feeding time, the result is quite different than expected, and suggests that there are other factors besides feeding efficiency that determine feeding time management.

The first parameter we measured was the time to strike. Here, our analysis showed a significant reduction in time, even though no particular pair of feeding occasions showed a dramatic contrast. This can be explained by the gradual trend this parameter displayed during all trials, rather than a steep change. The behavioural dynamics of the snakes were very close to what we hypothesised for this stage, namely, there was a clear, chronological improvement in the time budget as the prey was progressively more quickly and more eagerly attacked (Fig. 1, Tab. 1, Tab. 2).

We view these decreasing attack latencies as a form of associative learning in which the naive animals learn to associate two cues through positive reinforcement. More specifically, they have learned to associate the visual and chemical stimuli of the prey (conditioned stimulus) with the reward (unconditioned stimulus, the taste of the prey and post-feeding satiation).

The three other measured parameters (constriction time, ingestion time, and total feeding time) are interconnected and mutually dependent, i.e. total feeding time is the sum of the other two, so we will discuss the results accordingly.

In our experiment, we found that the animals showed a tendency to improve the ability to constrict the prey, expressed in a progressively shortened constriction time (Fig. 2, Tab. 2). Increased muscle efficiency could improve constriction patterns (Moon, 2000), but, at the same time, the snakes did not show significant dimensional gains during the three-week experiment. Consequently, we consider this progress as evidence of learning ability and subsequent utilisation of the acquired knowledge, and also a confirmation of our two initial hypotheses.

In contrast with our initial assumption, the ingestion time has shown a tendency to increase throughout the experiment (Fig. 3, Tab. 2). Despite an accelerated constriction rate, this caused the total feeding time to also increase from t1 to t4 (Fig. 4).

Thus, there was a clear difference in the overall feeding duration, with a linear relationship between time spent feeding and experience, which, however, proceeded in a direction contrary to our initial hypothesis. This outcome was not anticipated. The most obvious explanation was that the snakes at t4 were less skilled at ingesting their prey than at t1. However, such a circumstance is extremely unlikely, and the opposite is the most credible alternative. If we consider the first feeding as pure instinctual and the last feeding as the effect of a learning curve, it can be inferred that the protracted ingestion period must confer a certain benefit to the animals.

The biggest problem with the lengthened ingestion time is the unnecessary exposure to predation (Garland and Arnold, 1983). But what if the animals were never exposed to the smell or sight of a predator, and simply reacted to the consistent absence of stressors that overwrote their instinctual fearfulness, through learning? And, if so, is a longer ingestion time even beneficial for the animal? Does it increase ingestion efficiency? Why would they do it, anyway? The truth is that we found no mention of such a behaviour in the existing literature, so this takes us into the realm of speculation and educated guesswork. Nevertheless, we will attempt to make some inferences. Sometimes the snakes may exhibit more cautious or meticulous feeding behaviours, which can slow down the ingestion process. This could include repositioning the prey, adjusting its position, or needing more time to secure the prey within their jaws. If the snake is not fully hungry, it may take longer to swallow because it is not overly eager to consume its prey, or it simply has a lower energetic cost and a better energetic return. A slower swallowing process may reduce oesophageal abrasion by producing more saliva, and it could help with the kinematics of the jaw apparatus during prey handling and ingestion.

To summarise, our study highlighted a circumstance in which instinct, learning, and ecology interplay during the feeding process of the Ball python, with the unexpected outcome that the time spent ingesting prey tended to increase with gaining experience.

Furthermore, we hope that we have succeeded in debunking the stereotype that reptiles are merely "reflex machines" and confirming that cognition sometimes takes the road less travelled.

Authors contributions: Conceptualization, methodology, writing, and supervision was realised by Octavian Craioveanu; investigation, data collection and writing was realised by Vlad Stoicescu; data curation, data analysis, and writing was realised by Cristina Craioveanu. All authors have read and agreed the published version of the manuscript.

References

Arnold, S.J. (1978). Some effects of early experience on feeding responses in the common garter snake, *Thamnophis sirtalis. Anim. Behav. 26* (2), 455-462. https://doi.org/10.1016/0003-3472(78)90062-3

Bealor, M.T. & Saviola, A.J. (2007). Behavioural complexity and prey-handling ability in snakes: Gauging the benefits of constriction. *Behav. 144*(8), 907–929. https://doi.org/10.1163/156853907781492690

Brockmann, H.J. (1994). Measuring behaviour: *Ethograms, kinematic diagrams, and time budgets.* Technical document, Department of Biology, University of Florida, USA.

Burghardt, G.M. (1973). Instinct and innate behavior: Toward an ethological psychology. In J. A. Nevin & G. S. Reynolds, *The study of behavior: Learning, motivation, emotion, and instinct*. Scott, Foresman.

Burghardt, G.M. (1977). Learning processes in reptiles. In: *Biology of the Reptilia: Ecology and behaviour* (Gans, C. & Tinkle, D.W., eds). Academic Press, London. 555-681.

Burghardt, G.M. (2013). Environmental enrichment and cognitive complexity in reptiles and amphibians: concepts, review, and implications for captive populations. *Appl. Anim. Behav. Sci. 147*, 286–298. https://doi.org/10.1016/j.applanim.2013.04.013

D'Cruze, N., Harrington, L.A., Assou, D., Green, J., Macdonald, D.W., Ronfot, D., Segniagbeto, G.H. & Auliya, M. (2020). Betting the farm: A review of ball python and other reptile trade from Togo, West Africa. *Nat. Conserv*. 40, 65–91. https://doi.org/10.3897/natureconservation.40.48046

De Meester, G. & Baeckens, S. (2021). Reinstating reptiles: from clueless creatures to esteemed models of cognitive biology. *Behaviour. 158*(12-13), 1057-1076. https://doi.org/10.1163/1568539X-00003718

Fuchs, J.L. & Burghardt, G.M. (1971). Effects of early feeding experience on the responses of garter snakes to food chemicals. *Learn. Motivat. 2*, 271-279. https://doi.org/10.1016/0023-9690(71)90027-0

Garland, T. & Arnold, S.J. (1983). Effects of full stomach on locomotory performance of juvenile garter snakes (*Thamnophis elegans*). *Copeia. 4,* 1092-1096. https://doi.org/10.2307/1445117

Goetz, S.M., Godwin, J.C., Hoffman, M., Antonio, F. & Steen, D.A. (2018). Eastern indigo snakes exhibit an innate response to pit viper scent and an ontogenetic shift in their response to mouse scent. *Herpetologica 74*(2), 152-158. https://doi.org/10.1655/Herpetologica-D-17-00070.1

Jerison, H.J. (1973). Evolution of the brain and intelligence. *Academic Press*, New York, NY. https://doi.org/10.1126/science.184.4137.677

MacLean, P.D. (1985). Brain evolution relating to family, play and the separation call. *Arch. Gen. Psychiatry. 42*, 405-417. https://doi.org/10.1001/archpsyc.1985.01790270095011

Matsubara, S., Deeming, D.C. & Wilkinson, A. (2017). Cold-blooded cognition: New directions in reptile cognition. *Curr. Opin. Behav. Sci. 16*, 126-130. https://doi.org/10.1016/j.cobeha.2017.06.006

Mehta, R.S. (2009). Early experience shapes the development of behavioral repertoires of hatchling snakes. *J. Ethol. 27*, 143–151. https://doi.org/10.1007/s10164-008-0097-9

Moon, B. (2000). The mechanics and muscular control of constriction in gopher snakes (*Pituophis melanoleucus*) and a king snake (*Lampropeltis getula*). *J. Zool. 252*, 83-98. https://doi.org/10.1111/j.1469-7998.2000.tb00823.x

Mori, A. (1993). Does feeding experience with different size of prey influence the subsequent prey-handling behavior in *Elaphe climacophora*? *J. Ethol. 11*, 153–156. https://doi.org/10.1007/BF02350050

Nafus, M.G., Xiong P. X., Paxton, E.H., Yackel Adams A.A. & Goetz, S. M. (2021). Foraging behavior in a generalist snake (brown treesnake, *Boiga irregularis*) with implications for avian reintroduction and recovery. *Appl. Anim. Behav. Sci. 243*, 0168-1591. https://doi.org/10.1016/j.applanim.2021.105450

Ogle, D.H., Doll, J.C, Wheeler, A.P. & Dinno, A. (2025). *FSA: Simple fisheries stock assessment methods*. R package version 0.10.0, https://CRAN.R-project.org/package=FSA

RStudio Team. (2025). RStudio, 2025.05.1+513 "Mariposa Orchid" Release (ab7c1bc795c7dcff8f26215b832a3649a19fc16c, 2025-06-01) for windows

Ryerson, W.G., (2020) Ontogeny of strike performance in ball pythons (*Python regius*): A three-year longitudinal study. *Zool., 140*. https://doi.org/10.1016/j.zool.2020.125780

Sagan, C. (1977). The dragons of Eden: Speculations on the evolution of human intelligence. *Random House*, New York, USA. https://doi.org/10.1002/ajpa.1330500115

Suboski, M.D. (1992). Releaser-induced recognition learning by amphibians and reptiles. *Animal L&B 20*, 63–82. https://doi.org/10.3758/BF03199947

Szabo, B., Noble, D.W.A. & Whiting, M.J. (2021). Learning in non-avian reptiles 40 years on: advances and promising new directions. *Biol. Rev. 96*, 331-356. https://doi.org/10.1111/brv.12658

Turner, C.H. (1892). A few characteristics of the avian brain. *Science 19*, 16-17. https://doi.org/10.1126/science.ns-19.466.16

Westhoff, G. (2005). Expert report on the suitability of Geo Rack I systems (manufacturer: Lanzo Herp Cages) for species-appropriate husbandry and rearing of the ball python (*Python regius*). https://www.lanzo-herp.de/Gutachten/Expertises

Whiting, M.J. & Noble, D.W.A. (2018). Lizards - measuring cognition: practical challenges and the influence of ecology and social behaviour. In: *Field and laboratory methods in animal cognition* (eds N. Bueno-Guerra and F. Amici). 266–285. https://doi.org/10.1017/9781108333191.014

Wilkinson, A. & Huber, L. (2012). Cold-blooded cognition: reptilian cognitive abilities. In: *The Oxford handbook of comparative evolutionary psychology* (eds J. Vonk and T. K. Shackelford). 129–141. https://doi.org/10.1093/oxfordhb/9780199738182.013.0008

World Association of Zoos and Aquariums (WAZA). (2023). WAZA Code of Ethics [PDF document]. WAZA | World Association of Zoos and Aquariums.

STUDIA UNIVERSITATIS BABEŞ-BOLYAI BIOLOGIA, 70, 2, 2025 (p. 163-195)
doi:10.24193/subbbiol.2025.2.10

The diatom communities from Apuseni Mountains: a first approach on crenic diatom flora

Anca-Mihaela Şuteu[1,2,3,4] *, Laura Momeu[†,3], Mihai Puşcaş[1,2,3,4]

[1]*Doctoral School of Integrative Biology, "Babeş-Bolyai" University, Cluj-Napoca, Romania;*
[2]*A. Borza Botanic Garden, "Babeş-Bolyai" University, Cluj-Napoca, Romania;*
[3]*Faculty of Biology and Geology, "Babeş-Bolyai" University, Cluj-Napoca, Romania;*
[4]*Center for Systematic Biology, Biodiversity and Bioresources - 3B, Faculty of Biology and Geology, Babeş-Bolyai University, Cluj-Napoca, Romania*
* ***Corresponding author, E-mail: anca.ciorca@ubbcluj.ro.***

Article history: Received 26 November 2025; Revised 07 December 2025; Accepted 08 December 2025; Available online 20 December 2025

Abstract. The unique geomorphological and hydrological characteristics along with the stable abiotic parameters have shaped springs into suitable aquatic habitats for a high number of microorganisms. Increasing anthropogenic impact, such as groundwater pollution, alteration or destruction of the eucrenal spring area and high demand for pristine water, are affecting the crenic biodiversity. The present study is the first to focus on taxa belonging to the Bacillariophyta phylum and includes diatom samples taken from 30 karstic springs located in the Apuseni Mountains, Romania. Because diatoms often display distinct preferences for specific substrates, 15 samples were collected from each spring: five from each of the three substrate types (bryophytes, stones, and fine sediments) within the eucrenal area. For qualitative assessment, three mixed samples were subsequently prepared for each substrate type, resulting in a total of 99 analysed samples. A total of 216 taxa were identified in the analysed samples, with 16% found only on bryophytes and 15% occurring only on sand. Two groups of frequent taxa, distinguished by their preferred substrate type and present in at least 25 springs have been observed: *Caloneis fontinalis* (Grunow) A. Cleve, *Cocconeis lineata* Ehrenberg and *Meridion circulare* (Greville) C. Agardh

in epibryon, followed by *Gomphonema parvulum* (Kützing) Kützing and *Planothidium dubium* (Grunow) Round & Bukhtiyarova in epipsammon; three taxa *Achnanthidium minutissimum* (Kützing) Czarnecki, *Amphora pediculus* (Kützing) Grunow and *Cocconeis placentula* Ehrenberg stand out as a dominant group across all three types of substrates. Moreover, in the epilithon these were the only taxa present in all samples. Microhabitat-specific richness was shaped primarily by light conditions and canopy cover, with oxygen availability contributing as a secondary factor. *Gomphonema elegantissimum* E. Reichardt & Lange-Bertalot and *Caloneis fontinalis*, along with other 13 taxa have been identified for the first time in Romania.

Keywords: Bacillariophyta, Carpathian Mountains, epibryon, epilithon, epipsammon.

Introduction

The unique geomorphological and hydrological characteristics have shaped springs into being a suitable aquatic habitat for a high number of microorganisms. Compared to other aquatic habitats, springs are smaller in size, have high biodiversity and often serve as refuges for sensitive, rare or endangered species (Cantonati *et al*., 2006).

Springs provide several ecosystem services and play a key role in the conservation of aquatic biodiversity. The growing human demand for reliable drinking-water sources has threatened these habitats, degraded or even completely altered the eucrenal area through catchment development. These actions are carried out to the detriment of biodiversity, further intensifying the freshwater crisis. Moreover, in the European Water Directive (2000), springs are mentioned exclusively in the context of drinking water, without acknowledging the need to assess and monitor the ecological quality of spring ecosystems (vegetation near the springs, macroinvertebrates and phytobenthos).

The phytobenthos includes epiphytic (found on aquatic macrophytes), epilithic (growing on the surface of stones), epipsammic (living on fine sediments) diatoms. Being at the beginning of the food chain, diatoms are one of the key bioindicators of water quality and often display distinct preferences for a specific type of available substrate (Cantonati *et al*., 2007). As geographically isolated environments that support crenic organisms, springs represent more stable ecosystems compared to other freshwater habitats. Consequently, diatom communities act as sentinel organisms, responding rapidly to both long or short term, abiotic or biotic influences.

Studies conducted in the Alps and other regions have shown interdependence between some algal groups and a specific bryophyte or vascular plant species (Mogna *et al.* 2015, Cantonati *et al*., 2022), along with spring-type-specific benthic algal assemblages (Cantonati *et al*., 2012a).

The Romanian Carpathians are rich in crenic microhabitats, nonetheless a low number of studies have been published about the algal flora, especially diatoms inhabiting them. One of these studies included qualitative samples taken only from stones in the Cerna Karst Spring (Izbucul Cernei) in the Southern Carpathians (Sinitean *et al*., 2012), without addressing other substrate types. In contrast to karstic systems, another study investigated diatom assemblages in thermo-mineral springs at Băile Herculane (South-Western Romania), where preliminary qualitative and quantitative data were reported by Péterfi and Sinitean (2002). A more recent study investigates invertebrates alongside diatom communities in 5 limnocrene and rheocrene springs from the Transylvania region, central-western Romania (Micle *et al*., 2018). Although diatoms were sampled from bryophytes, above sand and from the surface of stones, the paper reports diatom data aggregated per spring, not separately per microhabitat. The focus was on frequent taxa identified in the quantitative approach of the study.

A different geographic setting was considered by Motaș *et al.* (1962) on springs and groundwater from the catchment area of The Neajlov River, approximately 50 km northwest of Bucharest. The study included several types of communities: algae, mosses, vascular plants and invertebrates. Two other studies investigate the diatom communities from mineral springs, being among the earliest detailed diatom studies on Romanian springs, widely cited in later Romanian diatom literature: Péterfi *et al.* (1983 and 1985). Comparative analyses of benthic diatom assemblages across several mineral springs in Romania, focusing on species composition, diversity and the role of ionic composition on community stability.

The aim of the present research is to provide a first insight into the crenic diatoms communities found in karstic spring habitats located in the Apuseni Mountains (South-Eastern Carpathians, Romania). Our objectives are: (i) to identify the diatom species composition in the studied springs and (ii) to characterize the karstic springs based on their biotic and physico-chemical attributes. Furthermore, we aim to contribute to the knowledge of crenic habitats by identifying diatom communities that may display preferences for specific microhabitats within the eucrenal area. Together with the existing studies on Carpathian springs (Fránková *et al*., 2009; Wojtal and Solak 2009; Wojtal and Sobczyk, 2012), our work provides new insights into crenic diatom distribution and substrate preference, contributing not only to the algal flora of Romania but also to the broader knowledge of Carpathian freshwater algal diversity.

Materials and methods

Study area

Crenic diatom communities were sampled during the summer of 2018 (May to August) from 30 springs located in different karstic regions of the Apuseni Mountains, South-Eastern Carpathians (Fig. 1). The investigated areas include the Pădurea Craiului Mountains, the Bihor-Vlădeasa Mountains, the Vaşcău Plateau and the Trascău Mountains, with altitudes ranging from 271 to 1229 m a.s.l. The studied springs belong to the main drainage basins of the rivers: Someşul Cald, Arieş, Crişul Repede, Crişul Alb and Crişul Negru. All sampled springs were known to have permanent discharge at the time of the sampling campaign, although their flow varies seasonally (Orăşeanu, 2016) and they do not undergo complete drought.

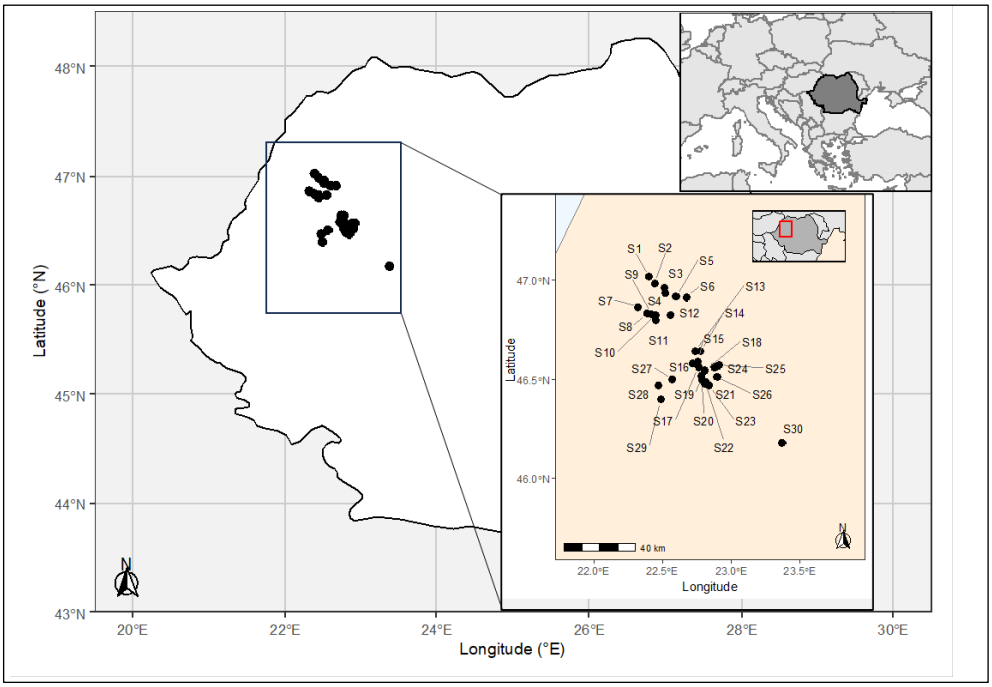

Figure 1. Map of the sampling sites (for spring codes see Table 1).

Spring classification

The different aquatic substrates, on which diatoms prefer to grow, occupy varying proportions of the eucrenal area and the specific hydrological characteristics of each spring justify a spring classification.

In this study, we adopted the spring classification proposed by Springer and Stevens (2009), Cantonati *et al.* (2007): limnocrene springs (L) characterized by the emergence of confined aquifers in a pool (2 springs); helocrene springs (H), which emerge from low-gradient wetlands, with multiple sources seeping from shallow, unconfined aquifers (2 springs); rheocrene springs (R) where water emerges into one or more stream channels (4 springs); and rheohelocrene (RH), emerging from low-gradient wetlands, typically with indistinct or multiple sources seeping from shallow, unconfined aquifers (6 springs). Fifteen springs were categorized as rheocrene cave (RC), where the water emerges from or within a cave through large conduits (Fig. 2). Finally, one rheocrene (RI) spring shows intermittent discharge throughout the year.

Figure 2. The three main types of springs: limnocrene (L), rheocrene cave (RC) and helocrene (H).

Sampling and processing methods

In order to be sampled, a spring had to fulfil the following criteria: karstic geological substrate, permanent discharge and three available microhabitats for diatoms – bryophytes, stones and sand. Only the eucrenal area was sampled from each spring included in this study.

For each sampling site, the following procedures were carried out. Firstly, a map was drawn for the eucrenal area and the percentage cover of each preferred substrate for diatoms was estimated. Only submerged habitats were taken into consideration when estimating the relative surface of every substrate type at the time of sampling. A set of physical and chemical parameters was measured once in the field using portable multimeters: Hanna HI98130, Hanna HI98194 and YSI-52 for water temperature, pH, conductivity, TDS and dissolved oxygen. The measured values are listed in the supplementary material in Cîmpean *et al.*, 2022.

Table 1. Spring codes and other characteristic considered for the present study (Br – epibryon; Sa – epipsammon; St – epilithon).

Spring codes	Name of the spring	Mountain groups	Altitude (m a.s.l)	Spring type	Canopy cover (%)	Number of diatom taxa			
						Total	Br	Sa	St
S1	Aştileu Cave	Pădurea Craiului	271	RC	65.08	69	44	44	20
S2	Moara Jurjii Cave	Pădurea Craiului	440	RC	64.78	34	15	28	9
S3	Vadul Crişului Cave	Pădurea Craiului	352	RC	81.13	39	26	23	17
S4	Izbucul Izbândiş	Pădurea Craiului	484	L	70.89	54	25	43	20
S5	Izbucul Bratcuţa Mare	Pădurea Craiului	384	RH	90.34	57	25	49	6
S6	Bulz Watery Cave	Pădurea Craiului	391	RC	71.39	56	26	48	16
S7	Topliţa de Vida Cave	Pădurea Craiului	303	RC	83.55	49	26	41	33
S8	Izbucul Toplita de Roşia	Pădurea Craiului	303	RC	84.81	36	26	19	4
S9	Izbucul Roşia Vally	Pădurea Craiului	363	RH	86.82	23	14	12	15
S10	Izbucul Toplicioara	Pădurea Craiului	436	R	62.05	35	21	25	6
S11	Izbucul Izbunească	Pădurea Craiului	335	R	65.67	19	18	10	5
S12	Valea Leşului Watery Cave	Pădurea Craiului	674	R	77.63	31	15	15	24
S13	Pepii Cave	Bihor-Vladeasa	1140	RC	61.41	39	24	25	19
S14	Izbucul Alunul Mic	Bihor-Vladeasa	1178	RC	62.09	45	30	37	18
S15	The Meadow of Karst Springs	Bihor-Vladeasa	1226	H	42.47	39	33	20	14
S16	Izbucul Ponor	Bihor-Vladeasa	1094	RC	45.43	52	38	37	13
S17	Gura Apei Cave	Bihor-Vladeasa	1225	RC	15.38	59	36	41	20
S18	Izbucul Vulturului	Bihor-Vladeasa	1063	RC	53.04	47	41	27	5
S19	Izbucul Tăuzului	Bihor-Vladeasa	923	L	65.24	41	33	22	8
S20	Corobană Cave	Bihor-Vladeasa	834	RC	68.88	28	15	24	13
S21	Izbucul Poliţei	Bihor-Vladeasa	874	RH	81.71	33	21	20	14

Spring codes	Name of the spring	Mountain groups	Altitude (m a.s.l)	Spring type	Canopy cover (%)	Number of diatom taxa			
						Total	Br	Sa	St
S22	Coteţul Dobreştilor Cave	Bihor-Vladeasa	840	RC	83.36	52	32	24	31
S23	Poarta lui Ionele Cave	Bihor-Vladeasa	850	RC	72.58	31	22	24	7
S24	Izbucul Lina Mare	Bihor-Vladeasa	1229	H	1	52	35	36	12
S25	Izbucul Apa Caldă	Bihor-Vladeasa	1106	R	77.6	37	33	13	13
S26	Izbucul Mătişeşti	Bihor-Vladeasa	966	RH	85.14	37	23	23	20
S27	Izbucul Bulzului	Bihor-Vladeasa	529	RC	66.98	54	35	33	13
S28	Izbucul Boiu	Platoul Vascau	321	RH	86.4	47	16	34	28
S29	Izbucul Călugări intermittent	Platoul Vascau	464	RI	21.9	41	34	21	9
S30	Izbucul Iezerului	Trascau	884	RH	62.12	36	22	24	10

Secondly, to avoid sample contamination, diatoms were surveyed in the following order: sand, stones and finally bryophytes. Five points were randomly selected for each preferred substrates, resulting in fifteen subsamples per spring. Within the eucrenal zone of each surveyed spring, one or two dominant bryophyte species were identified and sampled as substrates for the collection of epiphytic diatom communities. A bryophyte was considered dominant when it occupied at least five separate patches within the defined eucrenal sampling area, thereby qualifying it for sampling. Consequently, in several springs, multiple sets of epiphytic diatom samples were collected from each bryophyte taxa. In eight springs, two bryophyte species occurred in the eucrenal zone; consequently, five subsamples were collected for each bryophyte taxon. This resulted in a total number of 495 subsamples (150 for sand, 150 for stones and 195 for bryophytes).

For the qualitative assessment of crenic diatoms, mixed samples were prepared separately for each substrate type. From every sampling site, equal quantities of material (5 ml or a bryophyte tuft) were combined from the five subsamples to produce one mixed sample per substrate. Consequently, three mixed samples were prepared per spring (one for epipsammon, one for epilithon and one for each sampled bryophyte species), leading to a total of 99 Falcon tubes. All samples were preserved in ethanol.

Figure 3. Images with sampling methods applied in this study.

Using a 37 mm diameter tube fitted with a non-absorbent sponge at its end, a surface of 10.75cm^2 was scraped from the selected stones. The tube was pressed firmly against the stone surface, 25ml of spring water were added inside the tube and the biofilm was detached using a brush. The resulting suspension was extracted with a syringe and transferred into a Falcon tube (Fig. 3). Epipsammic diatoms were sampled by pipetting the surface layer of sediments 0,063 – 6,3mm in size (sand) from an area of 25-100 cm^2 or until 25ml were obtained. Epibryon samples consisted of tufts of the area-dominant bryophyte species present in the eucrenal area, placed in Falcon tubes with spring water. All samples were preserved in a known volume of ethanol.

From the middle of the eucrenal area of each spring, a photo was taken with a wide-angle camera, directed toward canopy above. Each photo was processed using an imaging software named Gap Light Analyzer (GLA), Version 2.0: to extract canopy structure and gap light transmission indices from photographs (Fig. 4) (Frazer *et al*., 1999). Afterwards, the images were analysed to calculate the percentage of shaded areas across each the sampled spring.

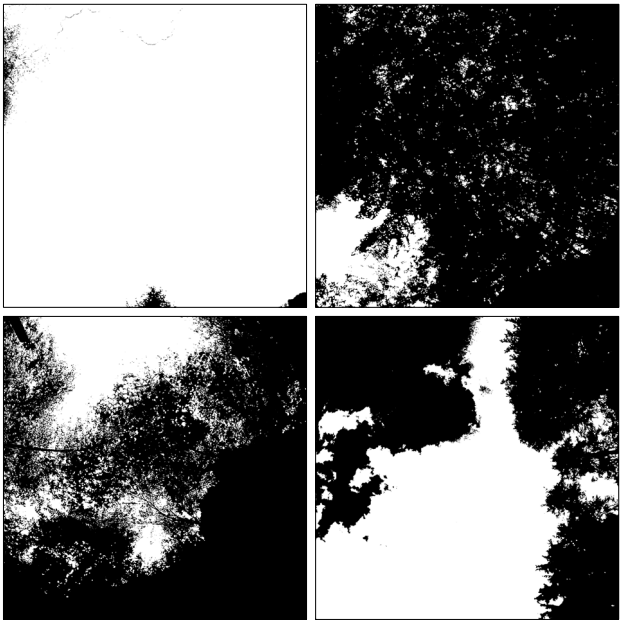

Figure 4. Examples of canopy cover above four of the sampled springs (S24, S05; S27, S15).

To obtain clean frustules, 10ml from each mixed sand and stone sample were added to approximately 20ml of hydrogen peroxide and left to react for at least five days or until the organic matter was removed. Because washing and squeezing the bryophytes in water does not fully remove the epiphytic diatoms, bryophyte tufts were treated with a mixture of H_2SO_4 and $KMnO_4$. After seven days of daily mixing, all samples were rinsed repeatedly with distillated water until the remaining diatom frustule sediment was clean.

Following standardized diatom slide preparation methods (Kelly *et al.*, 1998), a total of 198 slides (two for each mixed sample) were created. The entire coverslip area was examined during identification, with particular emphasis on detecting rare taxa. Identifications were made to species level using a Nikon Eclipse E400 optical microscope, with a few exceptions, where the ventral side of the valve was not visible. The following identification keys were used: Krammer and Lange-Bertalot 1986, 1988, 1991a, 1991b; Lange-Bertalot *et al.*, 2017.

Data analysis

The frequency of common taxa in the three types of samples was calculated as the percentage from the total number of samples discriminated between: rare species (those with less than 20% frequency, i.e., present in seven springs),

commonly occurring species (a frequency between 21% and 79%) and frequent species (a frequency above 80%, i.e., found in more than 25 springs).

Taxonomic occurrence, referred as number of taxa present in a sample, was arranged as a matrix with the value one for the species being present in a sample and the value zero representing its absence. Afterwards the matrix was used in software PAST version 4.14c (Hammer *et al*., 2001) to perform a multivariate analysis of clustering based on the Jaccard indices, a specific distance coefficient for presence/absence data. The similarity was indicated between the epiphytic, epilithic and epipsammic samples corresponding to each karstic spring.

To evaluate how each type of sampled microhabitat availability shapes diatom richness within karstic spring microhabitats, we analysed: the proportion (%) of each type of substrate in the eucrenal zone (epibryon – Br; epipsammon – Sa and epilithon – St) as explanatory variables and the number of taxa recorded on each corresponding substrate as biological response variables. Given that both variables comprise continuous values (expressed as percentages and richness counts, respectively) we employed two complementary correlation approaches: Pearson's correlation, which assumes linearity and approximate normality, and Spearman's rank correlation, which is non-parametric and detects monotonic trends irrespective of distribution form.

Prior to analysis, the frequency distribution of taxa richness values was inspected. Richness associated with bryophytes and sand substrates exhibited near-unimodal distributions with only slight skewness, whereas stone-associated richness showed moderate right-skew but no extreme outliers. On this basis, data transformation was not applied; richness values occurred within a comparable numeric range across springs, percentage predictors were already standardised on a 0–100 scale, thus transformation would risk obscuring ecological interpretability without improving model robustness. Furthermore, the application of Spearman correlation ensured methodological robustness in the presence of non-normal data distributions.

The Pearson's correlation and Spearman's rank correlation were performed using the PAST software. Correlation coefficients and p-values were analysed for both statistical measures. Patterns were interpreted as ecologically reliable only when correlation direction and significance were consistent between the two methods.

Multivariate analyses were used to visualize and interpret the data. Redundancy analysis (RDA) was used to project the data on a two-dimensional map and identify the relationship between environmental drivers and the biological communities. Two separate RDA analyses were performed and are presented as distinct figures. RDA-I examines how each type of sampled

microhabitat availability shapes diatom richness, whereas RDA-II illustrates the relationships between environmental variables and substrate-specific richness.

Given the linear and monotonic relationships between substrate cover and diatom richness confirmed by both Pearson and Spearman correlations, we used redundancy analysis (RDA I) to visualise how taxa richness on each microhabitat responds to different substrate availability. Prior to performing the RDA analysis, environmental predictors were automatically centered by Canoco 5 version 5.15 (ter Braak *et al*., 2012), which is standard practice in linear ordination. No further standardisation or transformation was required because variables were already comparable in scale and ecologically interpretable. Moreover, the substrate cover data is compositional and has a gradient 1.1 SD units long, so a linear method is recommended.

Environmental and taxa richness relationships were analysed using two datasets: the diatom communities found on each sampled substrate (number of taxa recorded on bryophytes, sand and stones in each spring), and environmental variables measured in situ (altitude, pH, dissolved oxygen, conductivity, temperature, total dissolved solids, and canopy cover).

Prior to multivariate analysis, all environmental predictors were z-standardised (mean-centred and scaled by standard deviation) using the R function *scale()*. Response variables were not standardized for the reasons mentioned above, at the first RDA analysis data preparation.

Spearman rank correlations were calculated between each environmental variable and each taxa richness, because Spearman's ρ does not require normally distributed data and remains reliable for monotonic yet non-linear ecological relationships. Statistical significance was evaluated using *cor.test()* with two-tailed p-values, and the correlation matrices with corresponding probabilities were interpretated.

Multivariate relationships were subsequently tested by performing a Redundancy Analysis (RDA II) using the vegan package (function *rda*() with the software Rstudio version 2023.03.0). A response matrix was constructed from the three richness variables (NbBr, NbSa, NbSt), and the matrix of standardised environmental variables served as the explanatory dataset. Significance of the global RDA model, individual canonical axes, and individual environmental predictors was assessed using permutation tests (999 permutations; functions *anova(rda_rich)*, *anova(rda_rich, by = "axis")*, and *anova(rda_rich, by = "term")*). Ordination was visualised with scaling = 2, and species-response vectors were extracted using scores (*rda_rich, display="species", scaling=2*) to interpret substrate-specific richness patterns along environmental gradients.

To explore relationships among sampling sites based on multiple environmental parameters, a Hierarchical Cluster Analysis (HCA) was performed

using the *pvclust* function from the *pvclust* package (with Ward's linkage method and Euclidean distances) in RStudio. Prior to performing the HCA, conductivity and dissolved oxygen values were log10-transformed to reduce skewness and improve comparability with linear variables. All variables (including altitude and pH, which were not log-transformed) were then standardized using Z-scores normalization to ensure equal weighting.

A heatmap was generated to visualize the relative frequency of diatom taxa across the three sample types (Br, St and Sa). The dataset was imported into R and converted into a numeric matrix, and no data scaling was applied. We used the *viridis colour gradient*, which allows intuitive interpretation of abundance intensity, with lower values represented by darker shades and higher values by yellow.

Results

Species composition

Across the 198 slides of epiphytic, epilithic and epipsammic samples a total number of 216 taxa were identified. A large number of species (n=83) was found in only one of the studied springs, either as a few frustules (*Cyclotella bodanica* var. *lemanica* (O. Müller ex Schröter) Bachmann) or as a more abundant population (*Achnanthidium pyrenaicum* (Hustedt) H. Kobayasi, *Fragilaria pinnata* Ehrenberg cf). *Achnanthidium minutissimum*, *Amphora pediculus*, *Cocconeis lineata*, *C. placentula*, *Meridion circulare* and *Planothidium lanceolatum* are the six species found in all the 30 karstic springs. Another nine taxa were present in more than 75% of the springs, such as: *Cocconeis placentula* var. *euglypta* (Ehrenberg) Cleve, *Gomphonema parvulum*, *Navicula cryptotenella* Lange-Bertalot, *Caloneis fontinalis*, *Planothidium dubium*, *Odontidium mesodon* (Ehrenberg) Kützing, *Cocconeis pseudolineata* (Geitler) Lange-Bertalot and *Navicula tripunctata* (O.F.Müller) Bory (supplementary data).

The lowest number of taxa (n=19) was recorded in spring S11, with more than three quarters of them belonging to the most commonly occurring species found in the studied karstic springs (listed above). In contrast, spring S1 showed highest richness, with 69 taxa identified, of which only four were not present in the other springs (Fig. 5). The average number of taxa per spring was 42.

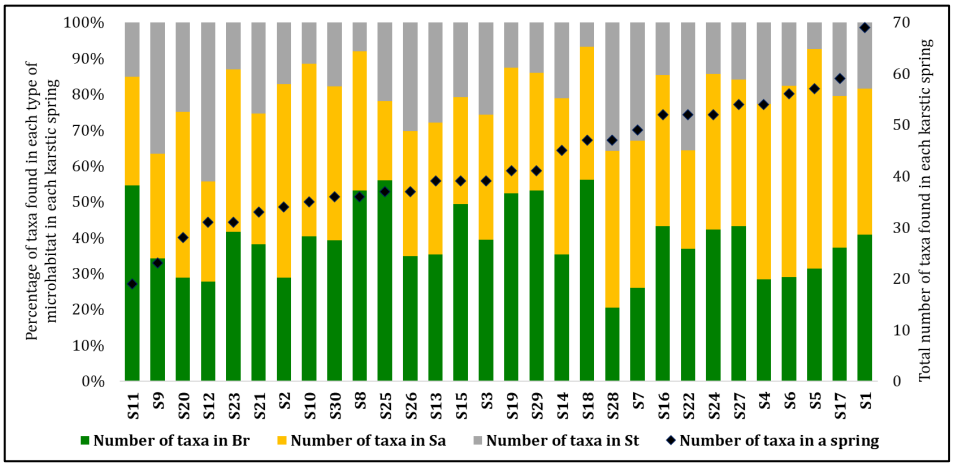

Figure 5. The number of taxa identified on bryophytes (Br), sand (Sa), and stones (St) shown as percentage bars, versus total number of taxa in a spring, represented by black rhombic symbols.

Epibryon diatom communities accounted for 66.6% of the species identified in the studied karstic springs. The number of taxa ranged from a minimum of 13 (in S9) to a maximum of 44 (in S1). In most springs, the number of taxa on bryophytes was relatively low; in twenty springs, richness ranged between 13–22 taxa, and in another group of springs it ranged between 23–32 taxa. Frequent species in the epiphytic samples were *Cocconeis placentula* and *Planothidium lanceolatum* (Fig. 6). Seven taxa were found in more than 75% of the bryophyte samples: *Meridion circulare*, *Cocconeis lineata*, *Achnanthidium minutissimum*, *Navicula cryptotenella*, *Amphora pediculus*, *Caloneis fontinalis* and *Cocconeis placentula* var. *euglypta*. In total, no more than 60 taxa occurred only once within the epibryon samples, of which 35 were found exclusively on bryophytes (i.e. *Amphora copulata* (Kützing) Schoeman & R.E.M. Archibald, *Cocconeis neothumensis* Krammer, *Gomphonema pumilum* (Grunow) E. Reichardt & Lange-Bertalot). The most species-rich genera were *Navicula* (20 taxa), *Gomphonema* (16 taxa), and *Nitzschia* (12 taxa), out of a total of 43 identified genera.

Of the total number of taxa identified in the karstic samples, fewer than half were present in the epilithic samples (n=102). Among these, 45 taxa occurred in only a single slide (i.e. *Cocconeis pediculus* Ehrenberg, *Cymbopleura subaequalis* (Grunow) Krammer, *Gomphonema acuminatum* Ehrenberg, *Hannaea arcus* (Ehrenberg) R.M.Patrick, *Navicula cari* Ehrenberg, *Placoneis elginensis* (W.Gregory) E.J.Cox). Seven taxa from this microhabitat had a frequency above 50%: *Achnanthidium minutissimum*, *Amphora pediculus*, *Cocconeis placentula*,

Navicula cryptotenella, *Meridion circulare*, *Planothidium lanceolatum* and *Gomphonema parvulum*. The number of taxa found on the surface of stones in a spring ranged from a minimum of 4 (in S8) to a maximum of 32 (S7). In half of the springs, taxa richness ranged between 12 and 21 taxa, and the average number of taxa in epilithic samples was 14.

The presence/absence rate was low in the epilithic samples, only one taxon, *Achnanthidium minutissimum*, was identified in almost all analysed slides (n=29). *Amphora pediculus* and *Cocconeis placentula* were the only two taxa found in more than 75% of the samples (Fig. 6). The genera *Gomphonema* and *Navicula* comprised the highest number of taxa in the samples collected from stones, out of a total of 40 identified genera.

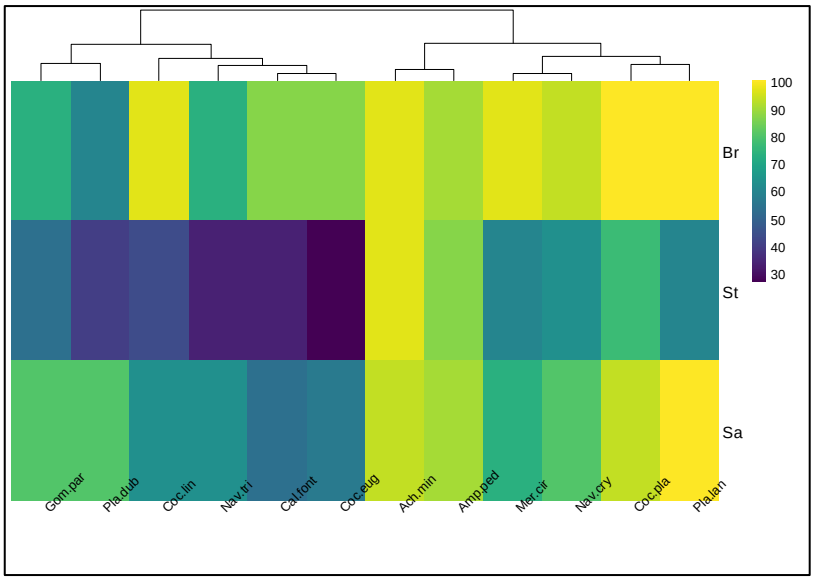

Figure 6. Heatmap showing taxa with frequencies above 50% across the three sampled substrates (Gom.par – *Gomphonema parvulum*; Pla.dub – *Planothidium dubium*; Coc.lin – *Cocconeis lineata*; Nav.tri – *Navicula trivialis*; Cal.font – *Caloneis fontinalis*; Coc.eug – *Cocconeis placentula* var. *euglypta*; Ach.min – *Achnanthidium minutissimum*; Amp.ped – *Amphora pediculus*; Mer.cir – *Meridion circulare*; Nav.cry – *Navicula cryptotenella*; Coc.pla – *Cocconeis placentula*; Pla.lan – *Planothidium lanceolatum*; Sa – sand; Br – bryophytes; St – stones).

A higher proportion of taxa (75% of the total number of identified taxa in this study) was present in the epipsammic samples. Moreover, approximately a quarter were found only once in the analysed slides. *Caloneis silicula* (Ehrenberg) Cleve, *Cyclotella bodanica* var. *lemanica* and *Tabellaria flocculosa* (Roth) Kützing

were among the 34 taxa identified exclusively on sand. The average number of taxa per spring was 27, ranging from a minimum of 10 (in S11) to a maximum of 48 (S5 and S6). *Planothidium lanceolatum* (Brébisson ex Kützing) Lange-Bertalot was observed in all analysed slides, with high number of individuals. *Achnanthidium minutissimum*, *Cocconeis placentula*, *Amphora pediculus*, *Gomphonema parvulum*, *Navicula cryptotenella*, and *Planothidium dubium* were present in 80% of the samples. The genus *Navicula* was the most species-rich (20 taxa), followed by *Nitzschia* (12 taxa) and *Gomphonema* (9 taxa). Overall, the sand samples displayed the highest genus-level diversity (55 genera).

The frequent species, occurring in the three substrate types and in all analysed slides were: *Achnanthidium minutissimum*, *Amphora pediculus* and *Cocconeis placentula*. *Planothidium lanceolatum*, *Navicula cryptotenella*, *Meridion circulare* and *Gomphonema parvulum* were commonly occurring taxa found in epipsammon and epibryon, usually with high number of individuals.

The highest similarity in the presence – absence patterns was observed among samples belonging to the same substrate type rather than between springs (using Jaccard index). Almost 70% of the taxa were shared between the sand samples from S18 and S20. In contrast, samples S8_St and S19_St showed the lowest similarity to all other samples, with fewer than 10% shared species. The bryophytes microhabitat showed the most homogeneous communities, with more than half of the samples clustering into two groups with similarity values of 40-55%. Epipsammic samples were more similar to the epibryon than to those collected from stones. Smaller clusters of epipsammic samples were also observed, and a general tendency was noted for samples from springs in the same area to cluster together. Seven epilithic samples formed a distinct cluster, sharing only 20% of their taxa (S5, S10, S11, S18, S23, S29, S30).

Karstic springs characteristics

The eucrenal area was assessed in order to estimate the proportion of each sampled substrate. Overall, the microhabitat offered by bryophytes was dominant in most of the karstic springs (Fig. 7), reaching up to 60% coverage of the eucrenal area.

Although rocks and boulders were a common feature in the rheocrene cave springs, the stone substrate formed a stable microhabitat in all karstic springs, covering 30–40% of the eucrenal area. Despite the wide percentage range of sand coverage (5–60%), in most springs it did not exceed 30% of the eucrenal area.

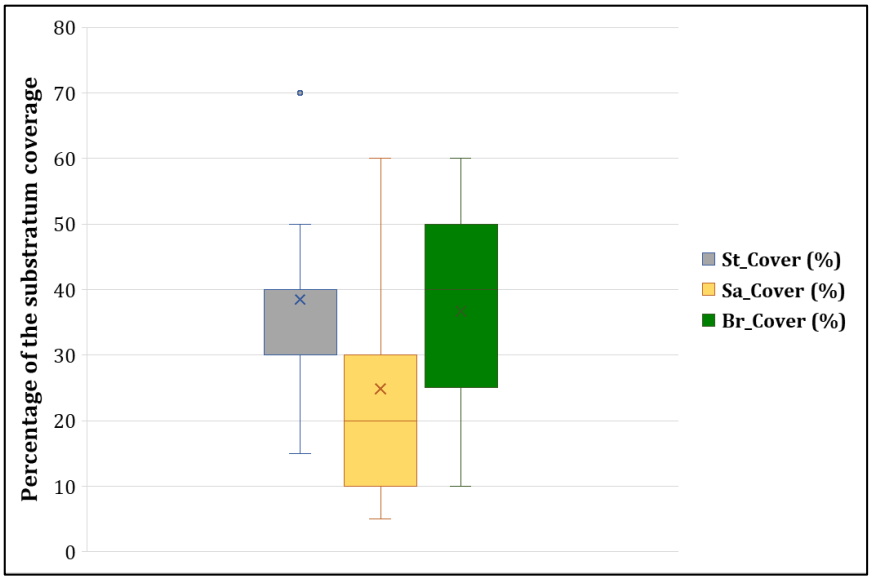

Figure 7. Boxplot with the percentage cover area of each microhabitat found in the eucrenal area of the sampled karstic springs.

The Spearman rank correlations and Pearson correlation matrix (Fig. 8) and associated p-values were calculated to assess the statistical significance of the relationships between substrate cover and taxonomic richness in the qualitative samples. In the eucrenal area, sites with higher coverage of stones (St%) supported fewer sand-associated taxa, likely reflecting reduced habitat availability for epipsammic colonisation. This observation is supported by a statistically significant negative correlation (Pearson $r = –0.47$, $p = 0.0082$; Spearman $\rho = –0.48$, $p = 0.0071$) between number of taxa in epipsammic samples and the percentage cover of stones (St%).

Similarly, sand cover was negatively correlated with stone-associated taxa ($r = –0.36$, $p = 0.0476$; $\rho = –0.43$, $p = 0.0185$). It demonstrates a pattern of mutual exclusion between these two types of substrates.

In contrast, bryophyte cover displayed the strongest significant positive relationship, correlating with increased richness of epilithic taxa ($r = +0.48$, $p = 0.0067$; $\rho = +0.47$, $p = 0.0081$). The observed pattern implies that bryophyte patches with greater structural complexity could enhance surface heterogeneity, consequently facilitating the increase in epilithic species.

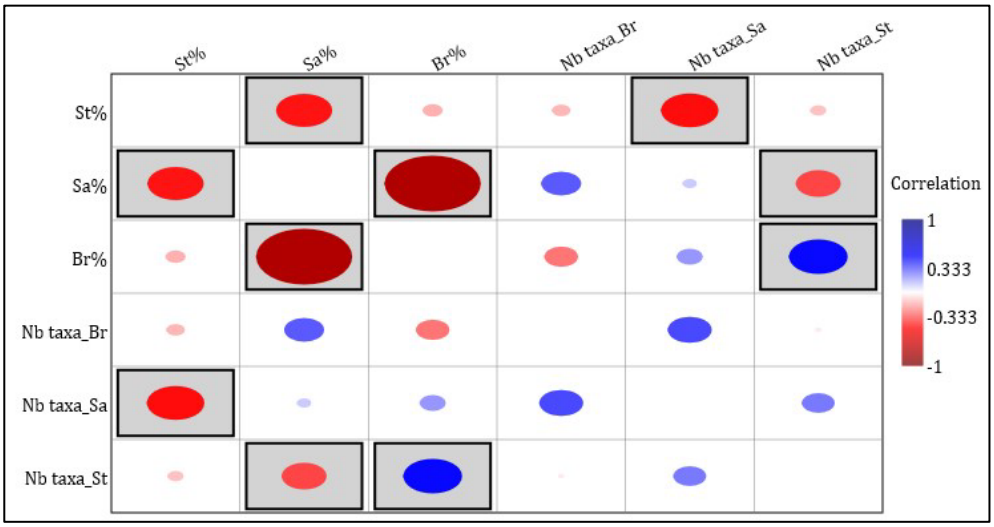

Figure 8. Pearson correlation matrix of the variables: percentages of each substrate type and the number of taxa found in each one (Nb taxa – number of taxa identified in the samples, St – epilithon, Sa – epipsammon, Br – epibryon).

A weaker positive association was observed between sand cover and bryophyte taxa in the Spearman analysis ($\rho = +0.36$, $p = 0.0487$), although not supported by Pearson correlation. All other relationships between substrate cover and taxa richness were weak and non-significant ($|r| < 0.32$, $p > 0.05$). Indicating that substrate abundance may not consistently predict diatom richness in the respective microhabitat.

Redundancy analysis (RDA I) showed that substrate cover remains an important driver of richness when considered across the entire eucrenal zone, not just at a microhabitat scale (Fig. 9). The analysis explained 27.12% of total variation in the dataset. Cumulatively, the first two axes captured 100% of the fitted variation, confirming that substrate gradients adequately describe the major richness shifts observed among springs. Permutation tests for the full model were significant (pseudo-$F = 3.2$, $p = 0.016$), demonstrating that substrate composition has a non-random, directional influence on diatom assemblage richness.

Structurally, the RDA analysis reflected the correlation patterns described previously: stone-dwelling taxa aligned positively with bryophyte cover and opposite the sand vector, indicating that bryophyte-rich microhabitats facilitate bigger lithic communities, while sand-dominated substrates suppress them.

Overall, the RDA highlights cross-microhabitat effects as key drivers of diatom assemblage structure in karstic eucrenal springs, with the strongest variance associated with gradients between bryophyte-enhanced and sand-suppressed lithic diversity.

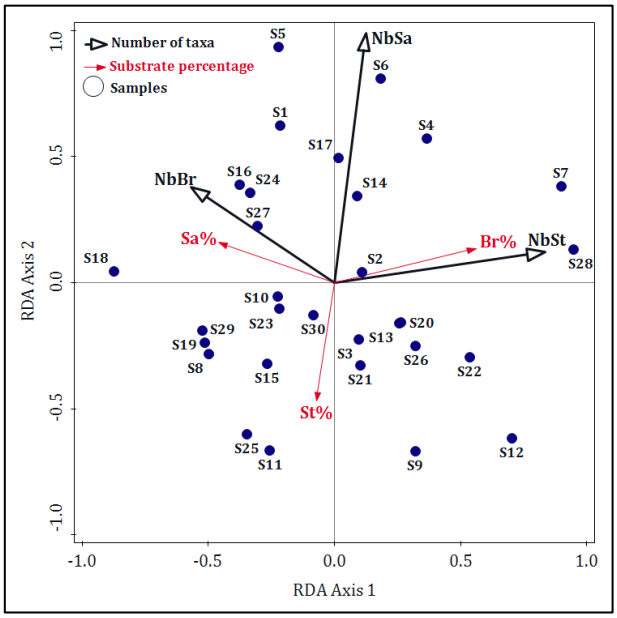

Figure 9. Redundancy analysis (RDA I) biplot (explained variation: 21.65% on Axis 1; 5,47% on Axis 2, p=0,016) showing substrate percentage cover in relation to taxa richness (NbSt – number of taxa in epilithon; NbSa - number of taxa in epipsammon; NbBr - number of taxa in epibryon).

Diatoms, as ecological bioindicators, reflect the physical and chemical characteristics of the aquatic habitat they inhabit. The 1000 m difference in elevation between the S1 and S24 springs provided a wide altitudinal range (Tab. 1), which may influence the structure of crenic diatom communities. Water temperature showed little variation among the studied springs, ranging from a minimum of 6°C and a maximum of 11.79°C in S30. Field measurements indicated circumneutral to slightly alkaline pH values, with a maximum of 9.68 recorded in S5, and 58% of the total identified diatoms indicate the same trend, reflecting their preference for alkaline environments.

Dissolved oxygen concentrations were consistently high (>8 mg/L) in most karst springs, which is supported by the fact that 40% of the crenic diatom community consisted of taxa preferring elevated oxygen levels; however, lower values were measured in the eucrenal zone of a few springs, likely reflecting drier sampling periods when reduced flow and stagnation may have decreased oxygen levels. Half of the diatom communities identified in this study thrive on wet and moist habitats or mainly occur in water bodies, however 10% of the taxa could survive when spring flow is significantly reduced. Information on ecological indicator values of diatoms and bioindicating characteristics was sourced from the framework presented by Van Dam *et al.* (1994).

Most springs exhibited conductivity values typical of waters flowing on calcareous substrate, between 300-500 µS/cm (Pricope, 1999). The only exception was S1, which recorded a maximum conductivity of 894 µS/cm.

To explore the relationships among sampling sites based on multiple environmental parameters, a Hierarchical Cluster Analysis (HCA) was performed. This method grouped the sites according to their overall similarity, and the resulting dendrogram (Fig. 10) identifies clusters of environmentally similar springs. Based on the environmental data, four different clusters were formed. The red rectangular clusters shown below have approximately unbiased values (AU) ≥95% and p-values < 0.05.

The first hierarchical cluster comprises a large group of 14 high elevated karstic springs located in the Bihor-Vlădeasa Mountains and characterized by cold and high-oxygenated waters, moderate pH and conductivity (from S13 to S26).

The second largest group of sampling sites which form a cluster are mid-altitude springs: S2, S3, S6, S8, S9, S10, S11 and S12 (located in the Pădurea Craiului Mountains), S27 (from the Bihor-Vlădeasa Mountains), S28 and S29 (from Platoul Vaşcău) and S30 (in the Trascău Mountains). Moderate mineral content and good oxygenation are dominant in this group, with more stable environmental parameters.

A smaller cluster (S1, S4 and S7) forms a group of low altitudes sampling sites from the Pădurea Craiului Mountains, with low oxygenated waters, high values of conductivity. A single outlier can be observed in the dendrogram, the rheohelocrene karstic spring Izbucul Brătcuţa Mare(S5), due to its highly alkaline water (pH=9.68). The value measured on the field was correct, as it has been confirmed by the Administration of the Valea Groşilor Nature Reserve.

From the eucrenal area of each karst spring, an upward-facing photograph of the canopy was taken to estimate the proportion of light passing through the cormophyte foliage. Of all studied springs, 48% were half-shaded; in some rheocrene cave springs, shading was caused by the cave walls. A total of 36% of the springs were almost completely shaded during the spring–summer season (Fig. 11). Springs S15 and S16 were partially sunny, S17 and S29 were fully sun-exposed, and S24 was the only spring in complete sunlight, situated in a meadow at 1229 m.

The RDA term-by-term permutation test showed that shade was the only significant predictor of diatom richness across the sampled substrates ($F = 2.94$, $p = 0.044$) (Fig. 11), while dissolved oxygen exhibited a marginal trend ($F = 2.44$, $p = 0.077$). Conductivity, pH, and altitude showed no significant effect after accounting for the influence of shade ($p > 0.25$). These results suggest that light availability and canopy cover play the primary role in structuring microhabitat-specific richness, with oxygen availability exerting a secondary influence.

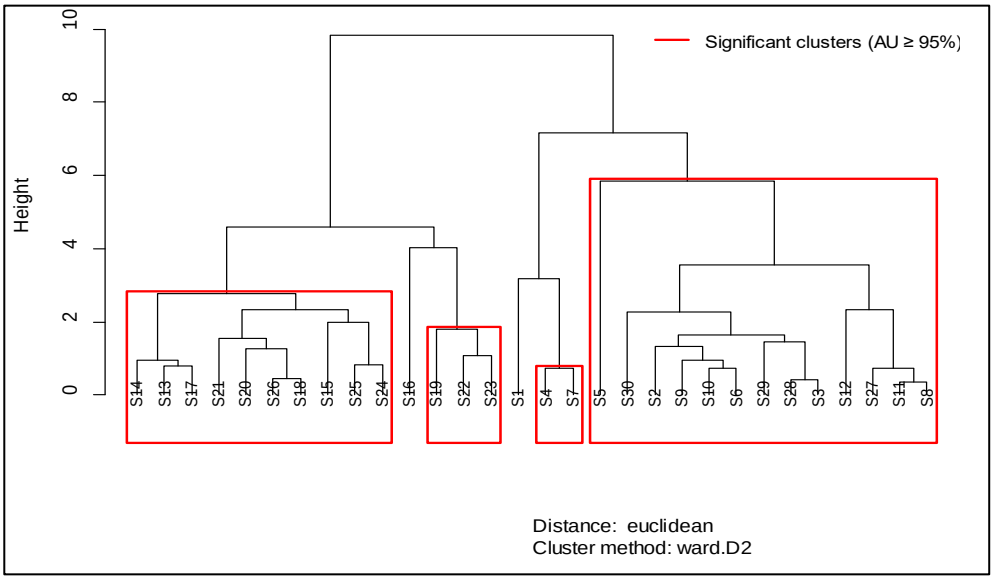

Figure 10. Hierarchical Cluster Analysis (HCA) dendrogram showing the clustering of the 30 springs based on their measured physico-chemical characteristics.

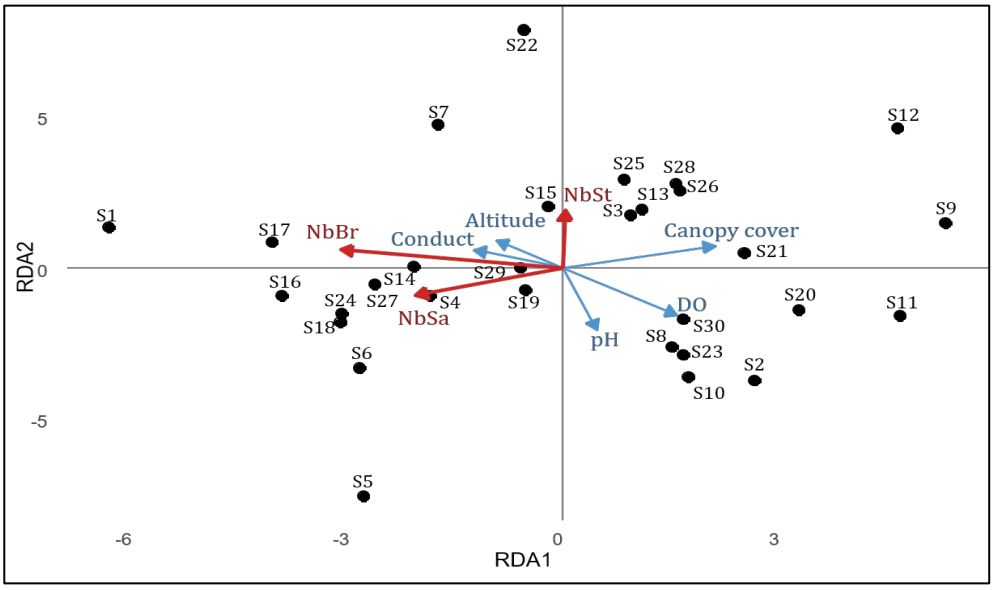

Figure 11. Redundancy analysis (RDA II) biplot (explained variation: 16.25% on Axis 1; 5.78% on Axis 2, p=0,002) illustrating the relationship between environmental variables (Altitude (m a.s.l.); Conduct – conductivity (µS/cm); DO – dissolved oxygen (mg/l); Canopy cover (%)) and diatom communities (NbSt – number of taxa in epilithon; NbSa - number of taxa in epipsammon; NbBr - number of taxa in epibryon).

New cited taxa and endangered species

In the present study 13 taxa were cited for the first time in Romania: *Amphora minutissima* W.Smith, *Caloneis fontinalis*, *Diploneis fontanella* Lange-Bertalot cf, *Diploneis krammeri* Lange-Bertalot & E. Reichardt cf, *Gomphonema elegantissimum*, *Gomphonema lateripunctatum E. Reichardt & Lange-Bertalot*, *Gomphonema procerum* E. Reichardt & Lange-Bertalot, *Gomphonema holmquistii* Foged, *Gomphonema minusculum* A. Cleve, *Gyrosigma obtusatum* (Sullivant & Wormley) C. S. Boyer, *Kolbesia gessneri* (Hustedt) Aboal, *Neidium cuneatiforme* Levkov, *Stauroneis reichardtii* Lange-Bertalot, Cavacini, Tagliaventi & Alfinito, *Surirella bohemica* (G. W. Maly) Schönfeldt and *Surirella birostrata* Hustedt. According to the Algae of Romania: a distributional checklist of actual algae (Cărăuș, 2017), these 13 taxa were not cited in Romania.

A group of 62 taxa from our study were identified in the Red List of diatoms (Hofmann *et al*., 2018) which included: species from the category early warning list (*Achnanthidium subatomus* (Hustedt) Lange-Bertalot, *Diploneis elliptica* (Kützing) Cleve, *Diploneis krammeri*, *Eunotia arcus* Ehrenberg, *Eunotia minor* (Kützing) Grunow, *Eunotia paludosa* Grunow, *Gomphonella calcarea* (Cleve) R. Jahn & N. Abarca, *Gomphonema lateripunctatum*, *Gomphonema sarcophagus* W. Gregory, *Halamphora normanii* (Rabenhorst) Levkov, *Nitzschia dissipata* var. *media* (Hantzsch) Grunow, *Nitzschia acidoclinata* Lange-Bertalot, *Pinnularia microstauron* C. A. Agardh, P. T. Cleve, and C. G. Ehrenberg, *Psammothidium subatomoides* (Hustedt) Bukhtiyarova & Round, *Stauroneis phoenicenteron* (Nitzsch) Ehrenberg and *Surirella spiralis* Kützing); extremely rare (*Diploneis pseudovalis* Hustedt, *Gomphonema subtile* Ehrenberg, *Pinnularia subrostrate* Lohman & G.W. Andrews, *Surirella bohemica* (G.W. Maly) Schönfeldt, *Surirella birostrata* Hustedt); 15 taxa with a status "hazard of unknown magnitude"(); endangered taxa like *Achnanthidium petersenii* (Hustedt) C.E. Wetzel, Ector, D.M. Williams & Jüttner, *Amphora aequalis* Krammer, *Caloneis tenuis* (W. Gregory) Krammer, *Caloneis schumanniana* (Grunow) Cleve, *Cymbella helvetica* Kützing, *Cymbella laevis* Nägeli, *Cymbopleura subaequalis* (Grunow) Krammer, *Delicatophycus delicatulus* (Kützing) M.J.Wynne, *Encyonema vulgare* Krammer, *Eunotia trinacria* Krasske, *Frustulia erifuga* Lange-Bertalot & Krammer, *Gomphonema procerum* E.Reichardt & Lange-Bertalot; highly endangered species: *Cymbella affinis* Kützing, *Eucocconeis flexella* (Kützing) F.Meister, *Eunotia praerupta* Ehrenberg, *Navicula angusta* Grunow, *Navicula densilineolata* (Lange-Bertalot) Lange-Bertalot, *Navicula gottlandica* Grunow, *Navicula wildii* Lange-Bertalot and *Neidium iridis* (Ehrenberg) Cleve. In springs S4 and S8 two threatened with extinction species were identified: *Cyclotella bodanica* var. *lemanica* and *Cyclotella planctonica* Brunnthaler, but only as a few frustules.

Discussion

Our study describes the diatom communities found on different microhabitats, such as bryophytes, stones and small sediments. It provides a first insight into the high taxa richness found in the eucrenal area of karstic springs in the Apuseni Mountains. The identifications and resulting data offer new information on the diatom communities inhabiting the karst crenic habitats located in the South-Eastern Carpathians, Romania.

We propose a straight-forward and easy to reproduce diatom sampling protocol which could be applied to many types of aquatic habitats and help with the monitoring of the diatom communities in all protected areas of the Carpathian Mountains.

In the present study, the three frequently occurring taxa were: *Achnanthidium minutissimum*, *Amphora pediculus* and *Cocconeis placentula*. Similar findings were cited from south-eastern Alps (Angeli *et al*., 2010), listed as the most frequent and abundant taxa, with a frequency of 92.6% in epibryon and epilithon samples. The first two species mentioned above were found also as frequent taxa in epilithic samples in another study (Delgado *et al*., 2013).

In the epipsammon and epibryon samples *Planothidium lanceolatum*, *Navicula cryptotenella*, *Meridion circulare* and *Gomphonema parvulum* were typically present in high numbers.

The percentage of the species identified only once in the analysed samples was 38%, a high number of taxa with one occurrence being common in spring habitats from southeastern Alps (Cantonati *et al*., 2012b). Moreover, both in epibryon and epipsammic samples the percentage of these taxa was high, even though in other studies the epilithon samples had the highest number of single occurrence species (Cantonati *et al*., 2012b; Wojtal and Sobczyk, 2012). The low number of the epilithic taxa may be attributed to the smaller sampling surface or to the carbonate substrate as a similar phenomenon was observed in another study (Cantonati *et al*., 2022).

A high number of diatom taxa associated with bryophytes has been reported in other studies (Mogna *et al*., 2015). Our results indicate that bryophyte-associated diatoms do not increase proportionally with bryophyte cover; instead, richness was highest where bryophyte growth occurred in smaller, compact patches rather than large bryophyte mats.

Corroborating the physico-chemical data with the biotic one, several trends could be identified in case of studied karstic springs: although 48% of the sampling sites are half-shaded springs, taxon richness appears to be unaffected, similar findings were presented in a study from Italy (Cantonati, 1998); oxygen availability represents an important driver of the taxa richness.

Higher richness in shaded springs suggests that crenic diatom assemblages benefit from the moderated temperature regime, reduced UV exposure, and sustained moisture typical of well-canopied headwaters. Consistent findings could be observed in 16 springs in the Northern Apennines (Cantonati *et al*., 2020). Conductivity and pH of the spring waters did not appear to affect taxa richness at the spring scale, but may still influence compositional turnover.

As the altitude increases, the occurrence of taxa listed in Red List of diatoms (Hofmann *et al*., 2018) may also increase. High numbers of species included in Red List of diatoms were also found in the following studies: Sherwood and Sheath (1999), Cantonati *et al*. (2010).

Conclusions

The present study illustrates for the first time the composition of crenic diatom assemblages sampled from the eucrenal area of 30 karstic springs located in the South-Eastern Carpathians, Romania. We investigated three eucrenal microhabitats and qualitatively characterized their diatom assemblages.

Diatom communities in the karstic springs of the Apuseni Mountains are characterized by: (1) high taxon richness within a small sampling area; (2) a high percentage of the canopy cover and elevated dissolved oxygen levels are significant predictors of diatom richness across substrates; (3) the presence of taxa newly reported for the Romanian algal flora; (4) numerous threatened species presented in the Red List(s).

Acknowledgements. Acknowledgments: The Apuseni Nature Park Administration are acknowledged for authorizing access to the springs located in protected areas. We sincerely thank Karina Paula Battes and Mirela Cîmpean for providing the necessary equipment for this study and Pavel Dan Turtureanu for his help in improving the experimental design and for providing constructive suggestions for the data analyses.

Funding: This research was partially funded by the PhD scholarship 19100/13388/04.10.2017.

Conflicts of Interest: The authors declare no competing interests.

Ethics declarations: not applicable.

References

Angeli, N., Cantonati, M., Spitale, D., & Lange-Bertalot, H. (2010). A comparison between diatom assemblages in two groups of carbonate, low-altitude springs with different levels of anthropogenic disturbances. *Fottea 10(1)*, 115-128. https://doi.org/10.5507/FOT.2010.006

Cantonati, M. (1998). Diatom communities of springs in the Southern Alps. *Diatom Res. 13(2)*, 201-220. https://doi.org/10.1080/0269249X.1998.9705449

Cantonati, M., Gerecke, R., & Bertuzzi, E. (2006). Springs of the Alps–sensitive ecosystems to environmental change: from biodiversity assessments to long-term studies. *Hydrobiologia 562(1)*, 59-96. https://doi.org/10.1007/s10750-005-1806-9

Cantonati M., Rott E., Pfister P. & Bertuzzi E. (2007). Benthic algae in springs: biodiversity and sampling methods. In: Cantonati M., Bertuzzi E. & Spitale D. (eds), The spring habitat: biota and sampling methods. Ed. *Museo Tridentino di Scienze Naturali*, Trento: 77-112 (Monografi e del Museo Tridentino di Scienze Naturali, 4).

Cantonati, M., & Lange-Bertalot, H. (2010). Diatom biodiversity of springs in the Berchtesgaden National Park (north-eastern Alps, Germany), with the ecological and morphological characterization of two species new to science. *Diatom Res. 25(2)*, 251-280. https://doi.org/10.1080/0269249X.2010.9705849

Cantonati, M., Rott, E., Spitale, D., Angeli, N., & Komárek, J. (2012a). Are benthic algae related to spring types? *Freshw. Sci. 31(2)*, 481-498. https://doi.org/10.1899/11-048.1

Cantonati, M., Angeli, N., Bertuzzi, E., Spitale, D., & Lange-Bertalot, H. (2012b). Diatoms in springs of the Alps: spring types, environmental determinants, and substratum. *Freshw. Sci. 31(2)*, 499-524. https://doi.org/10.1899/11-065.1

Cantonati, M., Segadelli, S., Spitale, D., Gabrieli, J., Gerecke, R., Angeli, N., Wehr, J. D. (2020). Geological and hydrochemical prerequisites of unexpectedly high biodiversity in spring ecosystems at the landscape level. *Sci Total Environ 740*, 140157. https://doi.org/10.1007/s10750-019-04167-2

Cantonati, M., Bilous, O., Spitale, D., Angeli, N., Segadelli, S., Bernabè, D., Lichtenwöhrer, K., Gerecke, R. and Saber, A.A. (2022). Diatoms from the spring ecosystems selected for the long-term monitoring of climate-change effects in the Berchtesgaden National Park (Germany). *Water*, *14*(3), 381. https://doi.org/10.3390/w14030381

Cărăuş, I. (2017). Algae of Romania: a distributional checklist of actual algae, Version 2.4, *Stud. Cerc. Biol.*, Bacău, pp. 1002.

Cîmpean, M., Şuteu, A. M., Berindean, A., & Battes, K. P. (2022). Diversity of spring invertebrates and their habitats: a story of preferences. *Diversity 14*(*5*), 367. https://doi.org/10.3390/d14050367

Delgado, C., Ector, L., Novais, M. H., Blanco, S., Hoffmann, L., & Pardo, I. (2013). Epilithic diatoms of springs and spring–fed streams in Majorca Island (Spain) with the description of a new diatom species *Cymbopleura margalefii* sp. nov.. *Fottea 13*(*2*): 87–104. https://doi.org/10.1007/s10750-012-1215-4

European Parliament and Council of the European Union (2000). Directive 2000/60/EC establishing a framework for Community action in the field of water policy. Official Journal of the European Communities, L327, 1–73.

Fránková, M., Bojková, J., Poulíčková, A., & Hájek, M. (2009). The structure and species richness of the diatom assemblages of the Western Carpathian Spring fens along the gradient of mineral richness, *Fottea 9*(*2*), 355-368. https://doi.org/10.1007/s10750-009-9725-0

Frazer, G.W., Canham, C.D., & Lertzman, K.P. (1999). Gap Light Analyzer (GLA), Version 2.0: Imaging software to extract canopy structure and gap light transmission indices from true-colour fisheye photographs. Simon Fraser University, Burnaby, British Columbia, and the Institute of Ecosystem Studies, Millbrook, New York.

Hammer, Ø., Harper, D.A.T., & Ryan, P.D. (2001). PAST: Paleontological Statistics software package for education and data analysis. *Palaeontol. Electron. 4*(*1*): 9.

Hofmann, G.; Lange-Bertalot, H.; Werum, M. & Klee, R. (2018). Rote Liste und Gesamtartenliste der limnischen Kieselalgen (Bacillariophyta) Deutschlands, In: *Rote Liste der gefährdeten Tiere, Pflanzen und Pilze Deutschlands. Band 7: Pflanzen,* Metzing, D., Hofbauer, N., Ludwig, G. & Matzke-Hajek, G. (Bearb.), Bonn (Bundesamt für Naturschutz). *Landwirtschaftsverlag* in Naturschutz und Biologische Vielfalt 70 (7), pp. 601–708.

Kelly, M.G., Cazaubon, A., Coring, E., Dell'Uomo, A., Ector, L., Goldsmith, B., Guasch, H., Hürlimann, J., Jarlman, A., Kawecka, B., Kwandrans, J. (1998). Recommendations for the routine sampling of diatoms for water quality assessments in Europe. *J. Appl. Phycol.*, *10*(*2*), 215-224. https://doi.org/10.1023/A:1008033201227

Krammer, K., Lange-Bertalot, H. (1986). Bacillariophyceae, 1. Teil: Naviculaceae, In: Ettl H, Gerloff, J., Heynig, H., Mollenhauer, D. (eds), Süßwasserflora von Mitteleuropa 2/1. Ed. *Gustav Fischer Verlag*, Stuttgart & New York, pp. 876.

Krammer, K., Lange-Bertalot, H. (1988). Bacillariophyceae, 2. Teil: Bacillariaceae, Epithemiaceae, Surirellaceae, In: Ettl, H., Gerloff, J., Heynig, H., Mollenhauer, D. (eds), Süßwasserflora von Mitteleuropa 2/2. Ed. *Gustav Fischer Verlag*, Stuttgart & New York, pp. 596.

Krammer, K., Lange-Bertalot, H. (1991a). Bacillariophyceae, 3. Teil: Centrales, Fragilariaceae, Eunotiaceae, In: In: Ettl, H., Gerloff, J., Heynig, H., Mollenhauer, D. (eds), Süßwasserflora von Mitteleuropa 2/3. Ed. *Gustav Fischer Verlag*, Stuttgart, Jena, pp. 598.

Krammer, K., Lange-Bertalot, H. (1991b). Bacillariophyceae, 4. Teil: Achnanthaceae. Kritische Ergänzungen zu Navicula (Lineolatae) und Gomphonema, In: Ettl, H., Gärtner, G., Gerloff, J., Heynig, H., Mollenhauer, D. (eds), Süßwasserflora von Mitteleuropa 2/4. Ed. *Gustav Fischer Verlag*, Stuttgart & New York, pp. 437.

Lai, G. G., Padedda, B. M., Wetzel, C. E., Lugliè, A., Sechi, N., & Ector, L. (2016). Epilithic diatom assemblages and environmental quality of the Su Gologone karst spring (centraleastern Sardinia, Italy). *Acta Bot. Croat. 75*(*1*), 129-143. https://doi.org/10.1515/botcro-2016-0008

Lange-Bertalot, H., Hofmann, G., Werum, M., Cantonati, M., & Kelly, M. G. (2017). Freshwater benthic diatoms of Central Europe: over 800 common species used in ecological assessment, Vol. 942, Ed. *Koeltz Botanical Books*, Schmitten-Oberreifenberg, pp. 908.

Micle, M., Şuteu, A. M., Momeu, L., Coman, P., Battes, K. P., & Cîmpean, M. (2018). Seasonal dynamics of biota from several springs located in the Apuseni Mountains, Romania. *Scientific Studies & Research. Series Biology/Studii si Cercetari Stiintifice. Seria Biologie*, *27*(2).

Mogna, M., Cantonati, M., Andreucci, F., Angeli, N., Berta, G., & Miserere, L. (2015). Diatom communities and vegetation of springs in the south-western Alps. *Acta Bot. Croat. 74*(2), 265-285. https://doi.org/10.1515/botcro-2015-0010

Springer, A. E., & Stevens, L. E. (2009). Spheres of discharge of springs. *Hydrogeol. J. 17*(1), 83-93. https://doi.org/10.1007/s10040-008-0381-0

Motaş, c., Botoşăneanu, l. & Negrea, Ş., (1962). Cercetări asupra biologiei izvoarelor şi apelor freatice din partea centrală a Cîmpiei Romîne, Ed. *Acad. R.P.R.*, pp. 366.

Orăşeanu, I. (2016). Hidrogeologia carstului din Muntii Apuseni. 1st Ed. *Belvedere*, Oradea, pp. 289.

Péterfi, L. Şt., Momeu, L., Veres, M. (1983) Efectul concentraţiei ionice asupra stabilităţii comunităţilor de diatomee din câteva izvoare minerale din România [The effect of ion concentration on the stability of diatom communities of some mineral springs in Romania]. *Evolution and Adaptation I*, 119-128.

Péterfi, L. Şt., Veres, M., Momeu, L. (1985) Composition and structure of benthic diatom communities from some Romanian mineral springs. *Evolution and Adaptation II*, 187-199.

Péterfi, L. Ş., & Sinitean, A. (2002). Preliminary studies on diatoms in thermo-mineral springs from Băile Herculane (Caraş–Severin District). *In Studies of Biodiversity, West Romanian Protected Areas* (Proc. Symp., USAMVBT, Timişoara) (pp. 25–28). USAMVBT.

Pricope, F. (1999) Hidrobiologie, Ed. *Ion Borcea*, Bacău, pp. 208.

Sherwood, A. R., & Sheath, R. G. (1998). Seasonality of macroalgae and epilithic diatoms in spring-fed streams in Texas, USA. *Hydrobiologia*, *390*(1), 73-82. https://doi.org/10.1023/A:1003514405082

Sinitean, A., Ianovici, N., & Petrovici, M. (2012). Composition and structure of the epilithic diatom communities from Izbucul Cernei, Cernişoara and the confluence area (Gorj County). *AES Bioflux 4*(2):37-49.

Teittinen, A., & Soininen, J. (2015). Testing the theory of island biogeography for microorganisms patterns for spring diatoms. *Aquat. Microb. Ecol. 75*(3), 239-250. https://doi.org/10.3354/ame01759

ter Braak, C. J. F., & Smilauer, P. (2012). Canoco reference manual and user's guide: software for ordination, version 5.0. Microcomputer Power.

Van Dam, H., Mertens, A., & Sinkeldam, J. (1994). A coded checklist and ecological indicator values of freshwater diatoms from the Netherlands. *Neth. J. Aquat. Ecol. 28*(1), 117-133.

Wojtal, A.Z. & Solak, C.N. (2009). Diatom assemblages in calcareous springs in Poland and Turkey, In: The joint 40th Meeting of the Dutch–Flemish Society of Diatomists (NVKD) and 3rd Central European Diatom Meeting (CE-DiatoM), Utrecht, The Netherlands, 26–29 March 2009. *Diatomemededelingen 33*: 130.

Wojtal, A. Z., & Sobczyk, Ł. (2012). The influence of substrates and physicochemical factors on the composition of diatom assemblages in karst springs and their applicability in water-quality assessment. *Hydrobiologia 695*(1), 97-108. https://doi.org/10.1016/j.ecolind.2011.07.002

Name of diatom taxa and author	S1	S2	S3	S4	S5	S6	S7	S8	S9	S10	S11	S12	S13	S14	S15	S16	S17	S18	S19	S20	S21	S22	S23	S24	S25	S26	S27	S28	S29	S30
Achnanthidium biasolettianum (Grunow) Lange-Bertalot	-	1	1	1	-	-	1	-	-	-	-	1	1	-	-	-	-	-	-	-	-	-	-	1	-	-	-	-	-	-
Achnanthidium minutissimum var. *jackii* (Rabenhorst) Lange-Bertalot	1	-	-	-	-	-	-	1	-	-	-	-	1	1	1	1	1	-	1	-	-	-	-	1	1	1	-	1	1	1
Achnanthidium minutissimum (Kützing) Czarnecki	1	1	1	1	1	1	1	1	1	1	1	1	1	1	1	1	1	1	1	1	1	1	1	1	1	1	1	1	1	1
Achnanthidium petersenii (Hustedt) C.E.Wetzel, Ector, D.M.Williams & Jüttner	-	-	-	-	-	-	-	-	1	-	-	-	-	-	-	-	-	-	-	-	-	-	-	1	-	-	-	-	-	-
Achnanthidium pyrenaicum (Hustedt) H.Kobayasi	-	-	-	-	-	-	-	-	-	-	-	-	-	-	-	-	-	-	-	-	-	-	-	-	-	-	-	1	-	-
Achnanthidium subatomus (Hustedt) Lange-Bertalot	-	-	-	1	-	-	-	-	-	-	-	-	-	-	-	-	-	-	-	-	-	-	-	-	-	-	-	-	-	-
Amphipleura pellucida (Kützing) Kützing	1	1	-	-	-	-	1	-	-	-	-	-	-	-	1	1	-	-	-	-	-	-	-	-	-	-	-	-	-	-
Amphora aequalis Krammer	-	1	-	1	1	-	-	-	-	-	-	-	-	-	-	-	-	1	-	-	-	-	-	-	-	-	-	-	-	-
Amphora copulate (Kützing) Schoeman & R.E.M.Archibald	-	-	-	-	-	-	-	-	-	-	-	-	-	-	-	-	-	1	-	-	-	-	-	-	-	-	-	-	-	-
Amphora inariensis Krammer	-	-	-	-	1	-	-	-	-	-	-	-	-	-	-	-	-	-	-	-	-	-	-	-	-	-	-	-	-	-
Amphora libyca Ehrenberg	1	-	-	-	-	-	1	-	-	1	-	-	-	1	-	-	1	1	1	1	1	-	-	1	-	-	1	-	-	-
Amphora minutissima W.Smith	1	-	-	1	1	-	-	1	-	-	-	-	-	-	-	-	-	-	-	-	-	-	-	1	-	-	-	-	1	-
Amphora ovalis (Kützing) Kützing	1	1	-	1	-	1	1	1	-	-	-	1	-	-	1	-	1	-	-	-	-	-	-	1	-	-	1	-	-	-
Amphora pediculus (Kützing) Grunow	1	1	1	1	1	1	1	1	1	1	1	1	1	1	1	1	1	1	1	1	1	1	1	1	1	1	1	1	1	1
Caloneis bacillum (Grunow) Cleve	-	-	-	-	-	-	-	-	-	-	-	-	-	-	-	-	1	-	-	-	-	-	-	1	-	-	-	1	-	-
Caloneis schumanniana (Grunow) Cleve	-	-	-	-	-	1	-	-	-	-	-	-	-	-	-	-	-	-	-	-	-	-	-	-	-	-	-	-	-	-
Caloneis silicula (Ehrenberg) Cleve	-	-	-	-	-	-	-	-	-	-	-	-	-	-	-	1	-	-	-	-	-	-	-	-	-	-	-	-	-	-
Caloneis tenuis (W.Gregory) Krammer	-	-	-	-	-	-	-	-	-	-	-	-	-	-	-	-	1	-	-	-	-	-	-	-	-	-	-	-	-	-
Caloneis fontinalis (Grunow) A.Cleve	-	1	1	1	1	1	1	1	1	1	1	1	1	1	1	1	1	1	1	1	1	1	1	1	1	1	1	-	1	1
Caloneis molaris (Grunow) Krammer	-	-	-	-	-	-	-	-	-	-	-	-	-	-	-	-	-	-	-	-	-	-	-	-	-	-	-	-	1	-
Cocconeis placentula Ehrenberg	1	1	1	1	1	1	1	1	1	1	1	1	1	1	1	1	1	1	1	1	1	1	1	1	1	1	1	1	1	1
Cocconeis placentula var. *euglypta* (Ehrenberg) Cleve	1	1	1	1	1	1	1	1	1	1	1	1	1	1	1	1	1	1	1	1	1	-	1	1	1	1	1	1	1	1
Cocconeis lineata Ehrenberg	1	1	1	1	1	1	1	1	1	1	1	1	1	1	1	1	1	1	1	1	1	1	1	1	1	1	1	1	1	1
Cocconeis neothumensis Krammer	-	-	-	-	-	-	-	-	-	-	-	-	-	-	-	-	-	-	-	-	-	-	-	-	-	-	1	-	-	-
Cocconeis pediculus Ehrenberg	1	1	-	-	-	-	-	-	-	-	-	-	-	1	-	1	1	1	1	-	1	1	-	-	1	-	-	1	-	-
Cocconeis pseudolineata (Geitler) Lange-Bertalot	1	1	1	1	1	1	1	1	-	1	1	1	-	1	1	1	-	1	1	1	1	-	1	-	-	1	1	-	1	1
Cyclotella bodanica var. *lemanica* (O.Müller ex Schröter) Bachmann	-	-	-	1	-	-	-	-	-	-	-	-	-	-	-	-	-	-	-	-	-	-	-	-	-	-	-	-	-	-
Cyclotella meneghiniana Kützing [1]	-	-	-	-	-	-	-	-	-	-	-	-	-	-	-	-	-	-	-	-	-	-	-	-	-	-	-	1	-	-
Cyclotella iris Brun & Héribaud	1	-	-	-	-	-	-	-	-	-	-	-	-	-	-	-	-	-	-	-	-	-	-	-	-	-	-	-	-	1
Cyclotella planctonica Brunnthaler	-	-	-	-	-	-	-	1	-	-	-	-	-	-	-	-	-	-	-	-	-	-	-	-	-	-	-	-	-	-
Cymatopleura apiculata W. Smith[2]	-	-	-	-	1	1	1	-	-	-	-	-	1	1	-	-	-	-	-	-	-	-	1	-	-	-	1	-	-	-

Cymatopleura elliptica W.Smith	1	-	-	-	-	-	-	-	-	1	-	-	-	-	-	-	-	-	-	-	-	-	-	-	-	-	-	-	-	-	-
Cymbella affinis Kützing	-	-	-	-	-	-	-	-	-	-	-	-	1	-	1	-	-	-	-	-	-	-	-	-	-	-	-	-	-	-	-
Cymbella aspera (Ehrenberg) Cleve	1	1	-	-	1	1	-	-	-	-	-	-	-	-	1	-	1	-	-	-	-	-	-	-	-	1	-	-	-	-	-
Cymbella cistula (Ehrenberg) O.Kirchner	-	-	-	-	-	-	-	-	-	-	-	-	-	-	-	-	-	-	-	-	-	1	-	-	-	-	-	-	1	-	-
Cymbella helvetica Kützing	1	-	-	1	-	-	-	-	-	-	-	-	-	1	-	-	-	-	1	-	-	1	-	-	-	-	-	-	-	-	-
Cymbella laevis Nägeli	-	-	-	-	-	-	-	-	-	-	-	-	-	-	-	-	-	-	-	-	-	1	-	-	-	-	-	-	-	-	-
Cymbella naviculiformis Auerswald ex Heiberg[3]	1	-	-	1	-	-	-	-	-	-	-	-	-	-	-	-	-	-	-	-	-	-	-	-	-	-	-	1	-	-	-
Cymbella tumidula Grunow	-	-	-	-	-	1	-	-	-	-	-	-	-	-	-	-	-	-	-	-	-	-	-	-	-	-	-	-	-	-	-
Cymbopleura subaequalis (Grunow) Krammer	-	-	-	-	-	-	-	-	-	-	-	-	-	1	-	-	-	-	-	-	-	-	-	-	-	-	-	-	-	-	-
Cymbopleura amphicephala (Nägeli ex Kützing) Krammer	-	-	-	-	-	-	-	-	-	-	-	-	-	-	-	-	-	-	-	-	-	-	-	1	-	-	-	-	-	-	-
Delicatophycus delicatulus (Kützing) M.J.Wynne	-	-	-	-	-	-	-	-	-	-	-	-	1	-	-	-	-	-	-	-	-	-	-	-	-	-	-	-	-	-	-
Denticula tenuis Kützing	1	1	1	1	1	-	1	-	-	1	-	-	1	1	1	-	1	1	1	-	-	-	1	1	1	1	1	-	1	1	
Diatoma moniliformis (Kützing) D.M.Williams	-	-	-	-	-	-	-	-	-	-	-	-	1	-	-	-	-	1	-	-	-	1	-	-	-	-	-	-	-	-	-
Diatoma ehrenbergii Kützing	1	-	-	-	-	-	-	-	-	-	-	-	-	-	-	-	-	-	-	-	-	1	-	-	-	-	-	-	-	-	-
Diatoma vulgaris Bory	1	-	-	-	-	-	-	-	-	-	-	-	-	1	-	-	-	1	1	1	-	1	-	-	-	-	-	-	-	-	-
Diploneis elliptica (Kützing) Cleve	-	-	-	-	-	-	1	-	-	-	-	-	-	-	-	-	1	-	-	-	-	-	1	-	-	1	-	-	1	-	
Diploneis fontanella Lange-Bertalot	-	1	-	-	-	-	-	-	-	-	-	-	-	-	-	-	-	-	-	-	-	-	-	-	-	-	-	-	-	-	-
Diploneis krammeri Lange-Bertalot & E.Reichardt	-	1	-	-	-	-	-	-	-	-	-	-	-	-	-	-	-	-	-	-	-	-	-	-	-	-	-	-	-	-	-
Diploneis oblongella (Nägeli ex Kützing) A.Cleve	1	1	1	-	1	1	1	-	-	-	-	-	-	-	-	-	-	1	-	-	-	-	-	-	-	-	1	-	-	-	-
Diploneis oblongellopsis Lange-Bertalot & Fuhrmann	-	-	-	-	-	-	-	-	-	-	-	-	-	-	-	-	-	-	-	-	-	-	-	1	-	-	-	-	-	-	-
Ellerbeckia arenaria (D.Moore ex Ralfs) Dorofeyuk & Kulikovskiy	-	-	1	-	-	-	1	-	-	-	-	-	-	-	-	-	-	-	-	-	-	-	-	-	-	-	-	-	-	-	-
Encyonema cespitosum Kützing	1	-	-	-	-	-	-	-	-	-	-	-	-	-	-	-	1	-	-	-	-	-	-	-	-	-	-	-	-	-	-
Encyonema mesianum (Cholnoky) D.G.Mann	-	-	-	-	-	-	-	-	-	-	-	-	-	-	-	-	-	-	-	-	1	-	-	-	-	-	-	-	-	-	-
Encyonema minutum (Hilse) D.G.Mann	1	1	-	1	1	1	-	-	-	1	-	-	1	1	1	1	1	1	1	1	1	1	-	1	1	1	1	-	1	1	
Encyonema silesiacum (Bleisch) D.G.Mann	1	-	1	-	-	1	1	-	-	-	-	-	1	-	1	1	1	1	1	1	-	1	-	1	-	-	1	-	-	-	
Encyonema vulgare Krammer	-	-	-	-	-	-	-	-	-	-	-	-	-	-	-	1	-	-	-	-	-	-	-	-	-	-	-	-	-	-	-
Eucocconeis flexella (Kützing) F.Meister	-	-	-	-	-	-	1	-	-	-	-	-	-	-	-	1	1	-	-	-	-	-	-	-	-	-	-	-	-	-	-
Eunotia arcus Ehrenberg	-	1	-	-	-	-	-	-	-	-	-	-	-	-	-	-	-	-	-	-	-	-	-	-	-	-	-	-	-	-	1
Eunotia bilunaris (Ehrenberg) Schaarschmidt	-	-	-	-	-	-	-	1	-	-	-	-	-	-	-	1	-	-	1	-	1	-	-	-	-	-	-	-	-	-	-
Eunotia boreoalpina Lange-Bertalot & Nörpel-Schempp	-	-	-	1	-	-	-	-	-	-	-	-	-	-	-	-	-	-	-	-	-	-	-	-	-	-	-	-	-	-	-
Eunotia exigua (Brébisson ex Kützing) Rabenhorst	-	-	-	-	-	-	-	-	-	-	-	-	-	-	-	1	-	-	-	-	-	-	-	-	-	-	-	-	-	-	-
Eunotia minor (Kützing) Grunow	1	-	-	-	1	-	-	-	-	-	-	-	-	-	-	-	1	-	1	-	-	-	-	-	-	-	-	-	-	-	-
Eunotia mucophila (Lange-Bertalot, Nörpel-Schempp & Alles) Lange-Bertalot	-	-	-	-	-	1	-	-	-	-	-	-	-	-	-	-	-	-	-	-	-	-	-	-	-	-	-	-	-	-	-
Eunotia paludosa Grunow	-	-	1	-	-	-	1	-	-	-	-	-	-	-	-	-	-	-	-	-	-	-	-	-	-	-	-	-	-	-	-

Eunotia praerupta Ehrenberg	-	-	-	-	-	1	-	-	-	-	-	-	-	-	-	-	-	-	-	-	-	-	-	-	-	-	-	-	-	-	-
Eunotia soleirolii (Kützing) Rabenhorst	-	-	-	-	-	-	-	-	-	-	-	1	-	-	-	-	-	-	-	-	-	-	-	-	-	-	-	-	-	-	-
Eunotia tenella (Grunow) Hustedt	-	-	-	-	-	-	-	-	-	-	-	1	-	-	-	-	-	-	-	-	-	1	-	-	-	-	-	-	-	-	-
Eunotia trinacria Krasske	-	-	-	-	-	-	-	-	-	-	-	-	-	-	-	-	1	-	-	-	-	1	-	-	-	-	-	-	-	-	-
Fragilaria biceps Ehrenberg	-	-	-	-	-	-	1	-	-	-	-	-	-	-	-	-	-	-	-	-	-	-	-	-	-	-	-	-	-	-	-
Fragilaria capucina Desmazières	-	-	-	-	-	-	-	-	-	-	1	-	-	1	-	1	1	-	1	-	-	1	-	-	-	-	1	1	-	-	-
Fragilaria capucina var. *capitellata* (Grunow) Lange-Bertalot	1	-	-	-	-	-	-	-	-	-	-	-	-	-	-	-	1	-	-	-	-	-	-	-	-	-	-	1	-	-	-
Fragilaria pinnata Ehrenberg[6]	-	-	-	-	-	-	-	-	-	-	-	-	-	-	-	-	-	-	1	-	-	-	-	-	-	-	-	-	-	-	-
Fragilaria vaucheriae (Kützing) J.B.Petersen	-	-	-	1	-	-	-	-	-	-	-	-	-	1	-	1	-	-	1	-	-	1	-	-	-	-	-	-	-	-	-
Frustulia erifuga Lange-Bertalot & Krammer	-	-	-	-	-	-	-	-	-	-	-	-	-	-	-	1	1	-	-	-	-	-	-	-	-	-	-	-	-	-	-
Frustulia rhomboides (Ehrenberg) De Toni	-	-	-	-	-	-	-	-	-	-	-	-	-	-	-	-	-	-	-	-	-	-	-	-	-	-	1	-	-	-	-
Frustulia vulgaris (Thwaites) De Toni	1	-	1	1	1	1	1	-	-	-	-	-	-	-	-	1	-	-	-	-	-	-	-	1	-	-	1	1	1	1	
Gogorevia exilis (Kützing) Kulikovskiy & Kociolek	-	-	1	-	-	-	1	-	-	1	-	-	1	-	-	-	-	-	-	-	-	-	1	1	1	1	1	-	1	-	
Gomphonella calcarea (Cleve) R.Jahn & N.Abarca	-	-	-	-	-	-	-	-	-	1	-	-	-	-	-	-	-	-	-	-	-	-	-	-	-	-	-	-	-	-	
Gomphonella olivacea (Hornemann) Rabenhorst	-	-	-	-	-	1	-	-	-	-	-	-	1	1	-	-	-	-	-	-	-	-	-	-	-	-	-	-	-	-	
Gomphonema acuminatum Ehrenberg	1	-	-	-	-	-	-	-	-	-	-	-	-	1	-	-	1	-	-	-	-	-	-	-	-	-	-	-	-	-	
Gomphonema angustatum (Kützing) Rabenhorst	-	-	-	1	-	-	-	-	1	-	-	-	-	1	1	1	1	1	-	1	1	1	1	1	1	1	-	1	-	1	
Gomphonema angustum C.Agardh	-	1	1	-	-	-	1	-	-	1	1	-	1	1	1	1	1	1	1	1	1	-	1	1	1	1	-	-	-	-	
Gomphonema elegantissimum E.Reichardt & Lange-Bertalot	-	-	1	-	-	-	1	-	1	1	1	1	1	1	1	1	-	-	1	-	-	1	1	1	1	1	1	1	-	-	
Gomphonema gracile Ehrenberg	-	-	-	-	-	-	-	-	-	-	-	-	-	-	1	-	1	1	-	-	-	-	1	-	1	-	1	-	-	-	
Gomphonema lateripunctatum E.Reichardt & Lange-Bertalot	-	-	-	1	1	-	-	1	-	-	-	1	-	-	-	-	-	-	-	-	-	-	-	-	1	-	-	-	-	1	
Gomphonema minusculum A.Cleve	-	-	-	1	1	-	-	-	-	-	-	1	-	-	1	-	-	-	-	-	-	-	-	-	-	-	-	-	-	-	1
Gomphonema minutum (C.Agardh) C.Agardh	1	1	-	-	1	-	-	1	-	-	-	-	1	-	1	1	1	1	1	-	-	-	-	1	1	-	1	-	1	1	
Gomphonema parvulum (Kützing) Kützing	1	1	1	1	1	1	1	1	1	1	1	1	1	1	1	1	1	1	1	-	1	1	1	1	1	1	1	1	1	1	
Gomphonema procerum E.Reichardt & Lange-Bertalot	-	-	-	-	-	-	-	-	-	-	-	-	1	-	-	-	-	-	-	-	-	-	-	-	-	-	-	-	-	-	-
Gomphonema pseudotenellum Lange-Bertalot	-	-	-	-	-	1	-	-	-	-	-	-	-	-	-	-	1	1	-	-	-	1	-	-	-	-	1	1	-	-	
Gomphonema pumilum (Grunow) E.Reichardt & Lange-Bertalot	-	-	-	-	-	-	-	-	-	-	-	-	-	-	-	-	-	-	-	-	-	-	-	-	1	-	-	-	-	-	
Gomphonema pumilum var. *rigidum* E.Reichardt & Lange-Bertalot	-	-	-	-	-	-	-	-	-	-	-	-	-	-	-	-	-	-	-	-	-	-	-	-	1	-	-	-	-	-	
Gomphonema subclavatum (Grunow) Grunow	-	-	-	-	-	-	-	-	-	-	-	-	-	-	-	-	-	-	-	-	-	-	-	-	-	-	-	-	1	-	
Gomphonema subtile Ehrenberg	-	-	-	-	-	-	1	-	1	-	-	-	-	-	-	-	-	-	-	-	-	-	-	-	1	-	-	-	-	1	
Gomphonema truncatum Ehrenberg	-	-	-	-	-	-	-	-	-	-	-	-	-	-	-	-	-	-	-	-	-	1	-	-	-	-	-	-	-	-	
Gomphonema sarcophagus W.Gregory	-	-	-	1	-	-	-	-	-	-	-	-	-	-	-	-	-	-	-	-	-	-	-	-	-	-	-	-	-	-	
Gomphosphenia holmquistiae (Foged) Lange-Bertalot	1	-	-	-	1	-	-	1	-	-	-	-	-	-	-	-	-	-	-	-	-	-	-	-	-	-	-	-	1	-	

Gyrosigma acuminatum (Kützing) Rabenhorst	1	-	-	-	-	1	1	-	-	-	-	-	-	-	-	-	-	-	-	-	-	-	-	-	-	-	-	-	-	-	-
Gyrosigma scalproides (Rabenhorst) Cleve	1	-	-	-	-	1	-	-	-	-	-	-	-	-	-	-	-	-	-	-	-	-	-	-	-	-	1	-	1	-
Gyrosigma attenuatum (Kützing) Rabenhorst	-	-	-	-	-	1	-	-	-	-	-	-	-	-	-	-	-	-	-	-	-	-	-	-	-	-	-	-	-	-
Gyrosigma obtusatum (Sullivant & Wormley) C.S.Boyer	-	-	-	1	-	-	-	-	-	-	-	-	-	-	-	-	-	-	-	-	-	-	-	-	-	-	-	-	-	-
Halamphora montana (Krasske) Levkov	-	-	1	-	-	-	-	-	-	1	-	-	-	-	-	-	-	-	-	-	-	-	-	-	-	1	1	1	-
Halamphora normanii (Rabenhorst) Levkov	1	-	-	-	-	-	-	1	-	-	-	-	-	-	-	-	-	-	-	-	-	-	-	-	-	1	-	1	-
Hannaea arcus (Ehrenberg) R.M.Patrick	1	-	-	-	-	-	-	-	-	-	-	-	-	-	-	-	-	-	-	-	1	1	-	-	-	-	-	1	-	-
Hantzschia amphioxys (Ehrenberg) Grunow	1	-	-	-	1	-	1	-	-	-	-	-	-	-	-	-	-	-	-	-	-	-	-	-	-	1	1	1	-	1
Hippodonta costulata (Grunow) Lange-Bertalot, Metzeltin & Witkowsk	-	-	-	-	-	-	-	-	-	1	-	-	-	-	-	-	-	-	-	-	-	-	-	-	-	-	-	-	-	-
Humidophila contenta (Grunow) R.L.Lowe, Kociolek, Johansen, Van de Vijver, Lange-Bertalot & Kopalová	-	-	-	-	-	-	-	1	-	-	-	-	-	-	1	-	-	-	-	-	-	1	-	-	-	1	-	-	1	-
Humidophila perpusilla (Grunow) R.L.Lowe, Kociolek, J.R.Johansen, Van de Vijver, Lange-Bertalot & Kopalová	1	-	-	-	-	-	-	-	-	-	-	1	-	-	-	-	1	-	-	-	-	1	-	-	-	1	-	-	-	-
Iconella linearis (W.Smith) Ruck & Nakov	1	-	1	-	-	-	1	-	1	-	-	1	-	1	-	1	1	-	-	-	1	-	-	1	-	-	1	-	-	-
Iconella hibernica (Ehrenberg) Ruck & Nakov	1	-	-	-	-	-	-	-	-	-	-	-	-	-	-	-	-	-	-	-	-	-	-	-	-	-	-	-	-	-
Kolbesia gessneri (Hustedt) Aboal	-	-	-	-	-	-	-	-	-	-	-	-	-	-	-	-	-	1	-	1	-	-	-	-	-	-	-	-	-	-
Luticola goeppertiana (Bleisch) D.G.Mann ex Rarick, S.Wu, S.S.Lee & Edlund	-	-	-	-	-	-	-	-	-	-	-	-	-	-	-	-	-	-	-	-	-	1	-	-	-	-	-	1	-	-
Luticola mutica (Kützing) D.G.Mann	-	-	-	-	-	-	-	-	1	-	-	-	-	1	-	1	-	-	-	-	-	1	1	-	-	-	-	1	-	-
Luticola nivalis (Ehrenberg) D.G.Mann	-	-	-	-	-	-	-	-	-	-	-	-	-	-	-	-	-	-	-	-	-	-	-	-	-	-	-	1	1	-
Melosira varians C.Agardh	1	-	-	-	1	1	1	-	-	-	-	-	1	-	-	-	-	-	-	-	-	-	-	-	1	-	-	1	-	-
Meridion circulare (Greville) C.Agardh	1	1	1	1	1	1	1	1	1	1	1	1	1	1	1	1	1	1	1	1	1	1	1	1	1	1	1	1	1	1
Meridion constrictum Ralfs	-	-	-	-	-	-	-	-	-	-	-	-	-	1	-	-	-	-	-	-	-	1	-	-	-	-	-	-	-	-
Navicula angusta Grunow	-	-	1	-	1	-	-	-	-	-	-	-	-	1	-	-	-	-	-	-	-	-	-	-	-	-	-	-	-	-
Navicula arenaria Donkin	-	-	-	-	-	-	-	-	-	1	-	-	-	-	-	-	-	-	-	-	-	-	-	-	-	-	-	-	-	-
Navicula capitatoradiata H.Germain ex Gasse	1	-	-	-	1	1	-	1	-	-	-	-	-	-	-	-	-	-	-	-	-	-	-	-	-	-	-	1	-	-
Navicula cari Ehrenberg	-	-	-	-	1	1	-	-	-	-	-	-	-	-	1	-	-	-	-	-	-	-	-	-	-	1	-	-	-	-
Navicula cincta (Ehrenberg) Ralfs	-	-	-	-	1	1	1	-	-	-	-	-	1	-	-	1	1	1	1	1	-	1	1	1	-	-	-	1	-	-
Navicula crucifera Grunow	-	-	-	-	1	-	-	-	-	-	-	-	-	-	-	-	-	-	-	-	-	-	-	-	-	-	-	-	-	-
Navicula cryptocephala Kützing	-	-	-	-	1	1	1	-	-	-	-	-	-	1	-	-	-	-	-	-	-	1	-	-	-	-	1	-	-	-
Navicula cryptotenella Lange-Bertalot	1	1	1	1	1	1	1	1	1	-	1	1	1	1	1	1	1	1	1	1	1	1	1	1	1	1	1	1	1	1
Navicula densilineolata (Lange-Bertalot) Lange-Bertalot	-	-	-	-	-	-	-	-	-	-	-	-	-	-	-	-	1	-	-	-	1	-	-	-	-	-	-	-	-	-
Navicula digitoradiata (W.Gregory) Ralfs	-	-	-	-	-	-	-	-	-	-	-	-	-	-	-	-	-	-	-	-	-	1	-	-	-	-	-	-	-	-
Navicula gottlandica Grunow	-	-	-	-	-	-	-	-	-	-	-	-	-	-	-	-	1	-	-	-	-	-	-	-	-	-	-	-	-	-
Navicula gregaria Donkin	-	-	-	-	1	1	-	-	-	1	-	-	-	-	-	1	1	-	1	-	-	-	-	-	-	-	-	-	-	-
Navicula lanceolata Ehrenberg	1	-	1	1	1	1	1	-	-	-	-	-	-	-	1	-	-	-	-	-	-	-	-	-	-	-	-	-	-	1

Navicula menisculus Schumann	-	-	-	-	-	-	1	-	-	-	-	-	1	-	1	1	1	1	-	-	-	1	-	-	-	-	-	1	-	-
Navicula metareichardtiana Lange-Bertalot & Kusber	-	-	-	-	1	-	-	-	-	-	-	-	-	-	-	-	-	-	-	-	-	-	-	-	-	-	-	-	-	-
Navicula perminuta Grunow	-	-	-	-	-	-	-	-	-	1	-	-	-	-	-	-	-	-	-	-	-	-	-	-	-	-	-	-	-	-
Navicula phyllepta Kützing	-	-	-	-	-	-	-	-	-	-	-	-	-	-	-	-	-	-	-	-	-	-	-	-	-	1	-	-	-	-
Navicula radiosa Kützing	1	1	1	-	1	1	1	1	-	-	-	1	1	1	1	1	1	1	1	-	-	-	1	1	1	-	-	-	1	1
Navicula recens (Lange-Bertalot) Lange-Bertalot	-	-	-	-	-	-	-	-	-	-	-	-	-	-	-	-	1	-	-	-	-	-	-	-	-	-	-	-	-	-
Navicula reinhardtii (Grunow) Grunow	-	-	-	-	-	-	-	-	-	-	-	-	1	1	-	-	1	-	1	1	-	-	-	-	-	-	-	-	-	-
Navicula rostellata Kützing	-	-	-	-	1	-	-	-	-	-	-	-	-	-	-	-	-	-	-	-	-	-	-	-	-	-	-	-	-	-
Navicula tenelloides Hustedt	-	-	-	-	-	-	-	-	-	-	-	-	-	-	-	-	-	-	-	-	-	-	-	-	1	-	-	-	-	-
Navicula tripunctata (O.F.Müller) Bory	1	-	1	1	1	1	1	1	1	1	1	1	-	1	-	-	-	1	1	1	1	1	1	-	-	1	1	1	1	1
Navicula trivialis Lange-Bertalot	-	-	-	-	-	-	-	-	-	-	-	-	-	-	-	1	-	-	-	-	-	-	-	-	-	-	-	1	-	1
Navicula viridul (Kützing) Ehrenberg	1	-	-	1	-	-	-	1	-	1	-	-	-	-	-	-	-	1	-	-	-	-	-	-	-	-	-	-	-	-
Navicula wildii Lange-Bertalot	-	-	-	1	-	-	-	-	-	-	-	-	-	-	-	-	-	-	-	-	-	-	-	-	-	-	-	-	-	-
Navicula cryptotenelloides Lange-Bertalot	-	-	-	1	1	-	-	-	-	-	-	-	-	-	-	-	-	1	-	-	-	1	-	-	-	-	1	-	-	-
Neidiomorpha binodiformis (Krammer) M.Cantonati, Lange-Bertalot & N.Angeli	-	-	-	-	1	-	-	-	1	-	-	-	-	-	-	-	-	-	-	-	1	-	-	1	-	1	1	-	-	-
Neidium dubium (Ehrenberg) Cleve	1	-	-	-	-	1	-	-	-	-	-	-	-	-	-	1	1	-	-	-	-	-	-	-	-	-	-	-	-	-
Neidium iridis (Ehrenberg) Cleve	-	-	-	-	-	1	-	-	-	-	-	-	-	-	-	-	-	-	-	-	-	-	-	-	-	-	-	-	-	-
Neidium cuneatiforme Levkov	1	-	-	-	-	-	-	-	-	-	-	-	-	-	-	-	-	-	-	-	-	-	-	-	-	-	-	-	-	-
Nitzschia capitellata Hustedt	-	-	1	-	-	-	-	-	-	-	-	-	-	-	-	-	-	-	-	-	-	-	-	-	-	-	-	-	-	-
Nitzschia dissipata (Kützing) Rabenhorst	1	-	-	1	1	1	1	1	-	1	-	-	1	1	1	1	1	1	1	1	1	1	-	1	1	-	-	1	1	-
Nitzschia dissipata var. *media* (Hantzsch) Grunow	-	-	-	-	-	-	-	-	-	-	-	-	-	-	-	-	-	-	-	-	-	1	-	-	1	1	-	1	-	-
Nitzschia frustulum (Kützing) Grunow	-	-	-	-	-	-	-	-	-	-	-	-	-	-	-	-	-	-	-	-	-	-	-	-	-	-	1	-	1	-
Nitzschia gracilis Hantzsch	-	-	-	-	-	-	-	-	-	-	-	-	-	-	-	-	-	-	1	-	-	-	-	-	-	-	-	-	-	-
Nitzschia heufleriana Grunow	-	-	-	-	-	-	-	-	-	-	-	-	-	-	-	-	-	-	-	-	-	-	-	1	-	-	-	1	-	-
Nitzschia intermedia Hantzsch ex Cleve & Grunow	-	-	-	-	1	-	-	-	-	-	-	-	-	-	-	-	-	-	1	-	-	-	-	-	-	-	-	-	-	-
Nitzschia linearis W.Smith	1	-	1	1	1	1	1	-	1	-	-	1	-	1	-	1	1	-	-	-	-	1	1	1	-	-	-	1	-	1
Nitzschia linearis var. *tenuis* (W.Smith) Grunow	-	-	-	1	1	-	-	-	-	-	-	-	-	-	-	1	-	-	-	-	-	-	-	-	-	-	-	-	-	-
Nitzschia palea (Kützing) W.Smith	1	1	1	1	-	-	1	-	-	1	1	1	-	1	1	1	1	-	-	-	-	1	-	1	1	1	1	1	-	-
Nitzschia paleaeformis Hustedt	-	-	1	-	-	-	-	-	-	-	-	-	-	-	-	-	-	-	-	-	-	-	-	1	-	-	-	-	-	-
Nitzschia pellucida Grunow	-	-	-	-	-	1	-	-	-	-	-	-	-	-	-	-	-	-	-	-	-	-	-	-	-	-	-	-	-	-
Nitzschia perminuta Grunow	-	-	-	-	-	-	-	-	-	-	-	-	1	-	-	-	-	-	-	-	-	-	-	-	-	-	-	-	-	-
Nitzschia recta Hantzsch	1	-	-	-	-	-	-	-	-	-	-	-	-	-	-	-	-	-	-	-	-	-	-	-	-	-	1	-	-	-
Nitzschia sigmoidea (Nitzsch) W.Smith	-	-	-	-	-	1	-	-	-	-	-	-	-	-	1	-	-	-	-	-	1	-	-	-	-	-	-	-	-	-
Nitzschia acidoclinata Lange-Bertalot	-	-	-	-	-	-	-	1	-	-	-	-	-	-	-	-	-	-	-	-	-	-	-	-	-	-	-	-	-	-
Nitzschia paleacea (Grunow) Grunow	1	-	-	-	-	-	-	-	-	-	-	-	-	-	-	-	-	-	-	-	-	-	-	-	-	-	-	-	-	-
Nitzschia tubicola Grunow	-	-	-	-	-	-	-	-	-	-	-	-	-	-	-	-	-	-	-	-	-	-	-	-	-	-	-	-	1	-

Nupela lapidosa (Krasske) Lange-Bertalot	-	-	-	-	-	-	-	-	-	-	-	-	-	-	-	-	-	-	-	-	-	-	-	-	-	-	-	-	1	-
Odontidium hyemale (Roth) Kützing	-	-	-	-	1	-	-	-	-	-	-	-	1	1	-	1	1	1	1	1	-	1	-	1	1	1	1	-	-	-
Odontidium mesodon (Ehrenberg) Kützing	-	1	1	1	1	1	1	-	1	1	1	1	1	1	-	1	-	1	-	1	1	1	1	1	1	1	1	-	1	1
Orthoseira roeseana (Rabenhorst) Pfitzer[5]	-	-	-	-	1	-	-	-	-	-	-	-	-	-	-	-	-	-	-	-	-	-	-	-	-	-	-	-	-	-
Pantocsekiella ocellata (Pantocsek) K.T.Kiss & Ács	-	-	-	-	-	-	-	-	-	-	-	-	1	-	-	-	-	-	-	-	-	-	-	-	-	-	-	-	-	1
Pinnularia borealis Ehrenberg	-	-	-	-	-	-	-	-	-	-	-	-	-	-	-	-	-	-	-	-	-	-	-	-	-	1	-	-	-	-
Pinnularia divergentissima (Grunow) Cleve	-	-	-	-	-	-	-	-	-	-	-	-	-	-	-	-	-	-	-	-	-	-	-	-	-	1	-	-	-	-
Pinnularia gibba (Ehrenberg) Ehrenberg[4]	-	-	-	-	-	-	-	-	-	-	-	-	-	-	-	-	-	-	1	-	-	-	-	-	-	-	-	-	-	-
Pinnularia microstauron (Ehrenberg) Cleve	-	-	-	-	-	-	-	-	-	-	-	-	-	-	1	-	-	-	-	-	-	-	-	-	-	-	-	-	-	-
Pinnularia obscura Krasske	-	-	-	-	-	-	-	1	-	-	-	-	-	-	-	-	1	1	-	-	-	-	-	-	-	-	-	-	-	-
Pinnularia subrostrata (A.Cleve) A.Cleve	-	-	-	-	-	-	-	-	-	-	-	-	-	-	-	1	-	-	-	-	-	-	-	-	-	-	-	-	-	-
Pinnularia brebissonii (Kützing) Rabenhorst	-	-	-	-	-	1	-	-	-	-	-	-	-	-	-	-	-	-	-	-	-	-	-	-	-	-	1	-	-	-
Pinnularia rupestris Hantzsch	-	-	-	-	-	1	-	-	-	-	-	-	-	-	-	-	-	-	-	-	-	-	-	-	-	-	-	-	-	-
Pinnularia viridis (Nitzsch) Ehrenberg	-	-	-	-	-	-	-	-	-	-	-	-	-	-	-	-	-	-	-	-	-	-	-	1	-	-	-	-	-	-
Placoneis elginensis (W.Gregory) E.J.Cox	-	-	-	-	-	-	-	1	-	-	-	-	-	-	-	-	-	-	-	-	-	-	-	-	-	-	-	1	-	-
Planothidium boyei (Østrup) Van de Vijver, Coomans, Pottiez & C.E.Wetzel	1	1	-	1	1	1	-	1	-	-	-	1	1	-	1	-	1	1	1	-	1	1	-	-	-	1	1	1	1	1
Planothidium dubium (Grunow) Round & Bukhtiyarova	1	1	1	1	1	1	1	1	1	1	1	1	1	1	1	-	1	1	1	1	-	1	1	1	1	1	1	-	1	-
Planothidium frequentissimum (Lange-Bertalot) Lange-Bertalot	1	1	-	1	-	-	-	1	-	-	-	1	-	-	-	-	1	-	-	1	1	-	1	1	1	1	-	1	1	1
Planothidium lanceolatum (Brébisson ex Kützing) Lange-Bertalot	1	1	1	1	1	1	1	1	1	1	1	1	1	1	1	1	1	1	1	1	1	1	1	1	1	1	1	1	1	1
Planothidium rostratum (Østrup) Lange-Bertalot	-	-	1	-	-	1	-	-	-	-	1	-	-	-	-	-	-	-	-	-	-	-	-	-	-	-	1	1	-	-
Prestauroneis integra (W.Smith) Bruder	-	-	-	-	-	-	-	-	-	-	-	-	-	-	-	-	-	-	-	-	1	-	-	-	-	-	-	-	-	-
Psammothidium helveticum (Hustedt) Bukhtiyarova & Round	-	-	-	1	-	-	-	-	-	-	-	-	-	-	1	1	-	1	1	-	1	1	-	1	1	1	-	-	-	-
Psammothidium marginulatum (Grunow) Bukhtiyarova & Round	-	-	-	-	-	-	-	-	-	-	-	-	-	-	-	-	-	-	-	-	1	-	-	-	-	-	-	-	-	-
Psammothidium subatomoides (Hustedt) Bukhtiyarova & Round	-	-	-	-	-	-	-	-	-	-	-	-	-	-	-	-	-	-	-	-	-	1	-	-	-	-	-	-	-	-
Psammothidium bioretii (H.Germain) Bukhtiyarova & Round	-	-	-	-	-	-	-	-	-	-	-	1	-	-	-	-	-	-	-	-	-	-	-	-	-	-	-	-	-	-
Pseudostaurosira parasitica (W.Smith) E.Morales	-	-	-	-	-	-	1	-	-	-	-	-	-	-	-	-	1	-	-	-	-	-	-	-	-	-	-	-	-	-
Reimeria sinuate (W.Gregory) Kociolek & Stoermer	1	-	-	-	-	-	-	1	-	-	-	-	-	1	-	1	1	1	-	-	1	-	-	1	-	-	1	1	1	-
Rhoicosphenia abbreviata (C.Agardh) Lange-Bertalot	1	1	1	-	1	1	-	1	-	1	-	-	-	1	-	-	-	-	-	-	-	-	-	1	-	1	-	1	-	1
Rossithidium pusillum (Grunow) Round & Bukhtiyarova	-	-	-	1	-	-	-	-	-	-	-	-	-	-	-	-	-	-	-	-	-	-	-	-	-	-	-	-	-	-
Sellaphora pupula (Kützing) Mereschkovsky	1	-	-	1	1	1	-	1	-	1	-	-	-	-	-	-	-	-	-	-	1	-	-	1	-	-	-	-	-	-
Stauroneis acidoclinata Lange-Bertalot & Werum	-	-	-	-	-	-	-	-	-	-	-	-	-	-	-	1	-	-	-	-	-	-	-	-	-	-	-	-	-	-
Stauroneis gracillima Hustedt	-	-	-	-	-	-	-	-	-	-	-	-	1	-	-	-	-	-	-	-	-	-	-	-	-	-	-	-	-	-

Stauroneis phoenicenteron (Nitzsch) Ehrenberg	-	-	-	1	-	-	-	-	-	1	-	-	-	-	-	-	-	-	-	-	-	-	-	1	-	-	-	-	-	1
Stauroneis reichardtii Lange-Bertalot, Cavacini, Tagliaventi & Alfinito	-	-	-	-	-	-	-	-	-	-	-	-	-	-	-	-	-	-	-	-	-	-	-	1	-	-	-	-	-	-
Stauroneis smithii Grunow	1	1	-	1	-	1	-	-	-	1	-	-	-	-	-	1	-	-	-	-	-	-	-	1	-	-	1	-	-	-
Staurosira venter (Ehrenberg) Cleve & J.D.Möller	-	-	-	-	-	-	-	-	-	1	-	-	-	-	-	-	-	-	-	-	-	-	-	-	-	-	-	-	-	-
Staurosirella pinnata (Ehrenberg) D.M.Williams & Round	-	-	-	1	-	-	-	-	-	1	-	-	-	-	-	-	1	-	-	-	-	-	-	1	-	-	-	-	-	1
Surirella angusta Kützing	1	-	1	1	1	1	1	-	-	-	-	-	-	-	1	1	1	1	-	-	-	1	1	1	1	-	1	1	-	-
Surirella bohemica (G.W.Maly) Schönfeldt	-	-	-	-	-	-	-	-	-	-	-	-	-	-	-	-	-	1	-	-	-	-	-	-	-	-	-	-	-	-
Surirella brebissonii Krammer & Lange-Bertalot	-	-	-	-	1	-	-	-	-	-	-	-	-	-	-	-	-	-	-	-	-	-	-	-	-	-	1	-	-	-
Surirella brebissonii var. *kuetzingii* Krammer & Lange-Bertalot	1	-	1	-	-	1	-	-	-	-	-	-	-	-	-	-	-	1	-	-	-	-	-	-	-	-	1	1	-	-
Surirella librile (Ehrenberg) Ehrenberg	1	-	-	-	1	1	-	-	-	-	-	-	-	1	-	-	1	-	-	-	-	-	1	-	-	-	-	-	-	-
Surirella spiralis Kützing	-	-	-	-	-	-	-	-	-	-	-	1	-	-	-	-	-	-	-	-	-	-	-	-	-	-	1	-	-	-
Surirella birostrata Hustedt	1	-	-	-	-	-	-	-	-	-	-	-	-	-	-	-	-	-	-	-	-	-	-	-	-	-	-	-	-	-
Surirella minuta Brébisson ex Kützing	1	-	-	1	-	-	-	-	-	-	-	-	-	-	-	1	-	-	-	-	-	-	-	1	-	-	1	-	1	1
Tabellaria ventricosa Kützing	-	-	-	-	-	-	-	-	-	-	-	-	-	-	-	1	-	-	-	-	-	-	-	-	-	-	-	-	-	-
Tabellaria flocculosa (Roth) Kützing	-	-	-	-	1	-	-	-	-	-	-	-	-	-	-	-	-	-	-	-	-	-	-	-	-	-	-	-	-	-
Ulnaria acus (Kützing) Aboal	1	-	-	1	-	1	1	-	-	-	-	1	-	-	-	-	-	-	-	-	-	-	-	-	-	-	-	-	-	-
Ulnaria ulna (Nitzsch) Compère	1	1	1	1	-	1	1	1	1	-	-	-	-	-	-	1	-	1	1	1	-	1	-	-	-	-	1	1	-	-

Currently accepted names:

[1] *Stephanocyclus meneghinianus* (Kützing) Kulikovskiy, Genkal & Kociolek 2022

[2] *Surirella microlibrile* Van de Vijver, Pottiez & Jüttner 2024

[3] *Cymbopleura naviculiformis* (Auerswald ex Heiberg) Krammer 2003

[4] *Rhopalodia gibba* (Ehrenberg) O.Müller 1895

[5] *Aerophilia roeseana* (Rabenhorst) Danz, Van de Vijver & Kociolek 2024

[6] *Staurosirella pinnata* (Ehrenberg) D.M.Williams & Round 1988